

Derivation of Metocean Design and Operating Conditions

**ANSI/API RECOMMENDED PRACTICE 2MET
SECOND EDITION, JANUARY 2021**

**ISO 19901-1:2015 (Modified), Petroleum and natural gas industries—
Specific requirements for offshore structures—Part 1: Metocean
design and operating considerations**



Special Notes

API publications necessarily address problems of a general nature. With respect to particular circumstances, local, state, and federal laws and regulations should be reviewed.

Neither API nor any of API's employees, subcontractors, consultants, committees, or other assignees make any warranty or representation, either express or implied, with respect to the accuracy, completeness, or usefulness of the information contained herein, or assume any liability or responsibility for any use, or the results of such use, of any information or process disclosed in this publication. Neither API nor any of API's employees, subcontractors, consultants, or other assignees represent that use of this publication would not infringe upon privately owned rights.

API publications may be used by anyone desiring to do so. Every effort has been made by the Institute to ensure the accuracy and reliability of the data contained in them; however, the Institute makes no representation, warranty, or guarantee in connection with this publication and hereby expressly disclaims any liability or responsibility for loss or damage resulting from its use or for the violation of any authorities having jurisdiction with which this publication may conflict.

API publications are published to facilitate the broad availability of proven, sound engineering and operating practices. These publications are not intended to obviate the need for applying sound engineering judgment regarding when and where these publications should be utilized. The formulation and publication of API publications is not intended in any way to inhibit anyone from using any other practices.

Any manufacturer marking equipment or materials in conformance with the marking requirements of an API standard is solely responsible for complying with all the applicable requirements of that standard. API does not represent, warrant, or guarantee that such products do in fact conform to the applicable API standard.

All rights reserved. No part of this work may be reproduced, translated, stored in a retrieval system, or transmitted by any means, electronic, mechanical, photocopying, recording, or otherwise, without prior written permission from the publisher. Contact the publisher, API Publishing Services, 200 Massachusetts Avenue, Suite 1100, Washington, DC.

Copyright © 2019 American Petroleum Institute

API Foreword

Nothing contained in any API publication is to be construed as granting any right, by implication or otherwise, for the manufacture, sale, or use of any method, apparatus, or product covered by letters patent. Neither should anything contained in the publication be construed as insuring anyone against liability for infringement of letters patent.

The verbal forms used to express the provisions in this document are as follows.

Shall: As used in a standard, "shall" denotes a minimum requirement in order to conform to the standard.

Should: As used in a standard, "should" denotes a recommendation or that which is advised but not required in order to conform to the standard.

May: As used in a standard, "may" denotes a course of action permissible within the limits of a standard.

Can: As used in a standard, "can" denotes a statement of possibility or capability.

This document was produced under API standardization procedures that ensure appropriate notification and participation in the developmental process and is designated as an API standard. Questions concerning the interpretation of the content of this publication or comments and questions concerning the procedures under which this publication was developed should be directed in writing to the Director of Standards, American Petroleum Institute, 200 Massachusetts Avenue, Suite 1100, Washington, DC 20001. Requests for permission to reproduce or translate all or any part of the material published herein should also be addressed to the director.

Generally, API standards are reviewed and revised, reaffirmed, or withdrawn at least every five years. A one-time extension of up to two years may be added to this review cycle. Status of the publication can be ascertained from the API Standards Department, telephone (202) 682-8000. A catalog of API publications and materials is published annually by API, 200 Massachusetts Avenue, Suite 1100, Washington, DC 20001.

Suggested revisions are invited and should be submitted to the Standards Department, API, 200 Massachusetts Avenue, Suite 1100, Washington, DC 20001, standards@api.org.

Foreword

ISO (the International Organization for Standardization) is a worldwide federation of national standards bodies (ISO member bodies). The work of preparing International Standards is normally carried out through ISO technical committees. Each member body interested in a subject for which a technical committee has been established has the right to be represented on that committee. International organizations, governmental and nongovernmental, in liaison with ISO, also take part in the work. ISO collaborates closely with the International Electrotechnical Commission (IEC) on all matters of electrotechnical standardization.

The procedures used to develop this document and those intended for its further maintenance are described in the ISO/IEC Directives, Part 1. In particular, the different approval criteria needed for the different types of ISO documents should be noted. This document was drafted in accordance with the editorial rules of the ISO/IEC Directives, Part 2 (see www.iso.org/directives).

Attention is drawn to the possibility that some of the elements of this document may be the subject of patent rights. ISO shall not be held responsible for identifying any or all such patent rights. Details of any patent rights identified during the development of the document will be in the Introduction and/or on the ISO list of patent declarations received (see www.iso.org/patents).

Any trade name used in this document is information given for the convenience of users and does not constitute an endorsement.

For an explanation on the meaning of ISO specific terms and expressions related to conformity assessment, as well as information about ISO's adherence to the World Trade Organization (WTO) principles in the Technical Barriers to Trade (TBT), see Foreword – Supplementary Information at the following URL: www.iso.org/iso/foreword.html.

The committee responsible for this document is ISO/TC 67, *Materials, equipment and offshore structures for petroleum, petrochemical and natural gas industries*, Subcommittee SC 7, *Offshore structures*.

This second edition cancels and replaces the first edition (ISO 19901-1:2005), which has been technically revised.

ISO 19901 consists of the following parts, under the general title *Petroleum and natural gas industries—Specific requirements for offshore structures*:

- *Part 1: Metocean design and operating considerations*
- *Part 2: Seismic design procedures and criteria*
- *Part 3: Topsides structure*
- *Part 4: Geotechnical and foundation design considerations*
- *Part 5: Weight control during engineering and construction*
- *Part 7: Stationkeeping systems for floating offshore structures and mobile offshore units*
- *Part 8: Marine soil investigations*

The following parts are under preparation:

- *Part 6: Marine operations*
- *Part 9: Structural integrity management*

ISO 19901 is one of a series of standards for offshore structures. The full series consists of the following International Standards:

- ISO 19900, *Petroleum and natural gas industries—General requirements for offshore structures*
- ISO 19901 (all parts), *Petroleum and natural gas industries—Specific requirements for offshore structures*
- ISO 19902, *Petroleum and natural gas industries—Fixed steel offshore structures*
- ISO 19903, *Petroleum and natural gas industries—Fixed concrete offshore structures*
- ISO 19904-1, *Petroleum and natural gas industries—Floating offshore structures—Part 1: Monohulls, semi-submersibles and spars*
- ISO 19905-1, *Petroleum and natural gas industries—Site-specific assessment of mobile offshore units—Part 1: Jack-ups*
- ISO/TR 19905-2, *Petroleum and natural gas industries—Site-specific assessment of mobile offshore units—Part 2: Jack-ups commentary*
- ISO 19905-3, *Petroleum and natural gas industries—Site-specific assessment of mobile offshore units—Part 3: Floating unit*
- ISO 19906, *Petroleum and natural gas industries—Arctic offshore structures*

Contents

1	Scope.....	1
2	Normative References	1
3	Terms and Definitions	2
4	Symbols and Abbreviated Terms	10
4.1	Symbols	10
4.2	Abbreviated Terms.....	12
5	Determining the Relevant Metocean Parameters	12
5.1	General	12
5.2	Expert Development of Metocean Criteria.....	13
5.3	Selecting Appropriate Parameters for Determining Design Actions and Action Effects	14
5.4	The Metocean Database	15
5.5	Storm Types in a Region	15
5.6	Directionality	15
5.7	Extrapolation to Extreme and Abnormal Conditions	16
5.8	Metocean Parameters for Fatigue Assessments	16
5.9	Metocean Parameters for Short-term Activities	17
5.10	Metocean Parameters for Medium-term Activities	18
6	Water Depth, Tides, and Storm Surges	18
6.1	General	18
6.2	Tides	19
6.3	Storm Surges.....	19
6.4	Extreme Water Level.....	19
7	Wind.....	20
7.1	General	20
7.2	Wind Actions and Action Effects	21
7.3	Wind Profile and Time-averaged Wind Speed	22
7.4	Wind Spectra	22
8	Waves	22
8.1	General	22
8.2	Wave Actions and Action Effects	24
8.3	Sea States—Spectral Waves.....	24
8.4	Regular (Periodic) Waves.....	25
8.5	Maximum Height of an Individual Wave for Long Return Periods.....	26
8.6	Nonlinear Wave Models.....	26
8.7	Wave Crest Elevation.....	27
9	Currents	27
9.1	General	27
9.2	Current Velocities	27
9.3	Current Profile	28
9.4	Current Profile Stretching	28
9.5	Current Blockage	28
10	Other Environmental Factors	29
10.1	Marine Growth	29
10.2	Tsunamis	29
10.3	Seiches.....	30
10.4	Sea Ice and Icebergs.....	30
10.5	Snow and Ice Accretion.....	30
10.6	Miscellaneous.....	30

11	Collection of Metocean Data	31
11.1	General	31
11.2	Common Requirements	31
11.3	Meteorology	32
11.4	Oceanography	33
11.5	Data Quality Control	34
12	Information Concerning the Annexes	34
12.1	Information Concerning Annex A	34
12.2	Information Concerning the Regional Annexes	34
Annex A (informative) Additional Information and Guidance	35	
Annex B (informative) Northwest Europe	88	
Annex C (informative) West Coast of Africa	98	
Annex D (informative) Offshore Canada	109	
Annex E (informative) Sakhalin/Sea of Okhotsk.....	137	
Annex F (informative) Caspian Sea	160	
Annex G (informative) Southern East Asian Sea	178	
Annex H (informative) US Gulf of Mexico.....	197	
Annex I (informative) US Coast of California	240	
Annex J (informative) Other US Waters	245	
Annex K (informative) Identification and Explanation of Deviations	249	
Bibliography	251	
Figures		
1	Water Depth, Tides, and Storm Surges.....	20
A.1	Overview of the Process of Producing Metocean Parameters	37
A.2	Examples of Wind Spectra	52
A.3	Regions of Convergence of Alternative Wave Theories	67
A.4	Doppler Shift in Wave Period due to Steady Current—Relationship between Intrinsic and Apparent Periods	70
A.5	Linear and Nonlinear Stretching of Current Profiles	77
B.1	Map of Northwest Europe Region	95
B.2	Water Depths—Northwest Europe Region	96
B.3	Limit of Sea Ice—Northwest Europe Region—Annual Probabilities of Exceedance of 10^{-2} and 10^{-4}	97
B.4	Limit for Collision with Icebergs—Northwest Europe Region—Probabilities of Exceedance of 10^{-2} and 10^{-4}	97
C.1	Map of West Coast of Africa Region: Locations of Example Metocean Parameters	108
D.1	Map of Canada	110
D.2	East Coast of Canada Current Regions of Oil and Gas Production Operations—Near Sable Island Offshore Nova Scotia and on the Grand Banks Offshore Newfoundland and Labrador	111
D.3	Canadian East Coast Ocean Current Regime	114
D.4	Map of the Gulf of St. Lawrence Showing the General Circulation Pattern	116
D.5	Mean General Summer Circulation of the Surface Water in the Beaufort and Chukchi Seas ¹	117
D.6	Surface Circulation in the Southeastern Beaufort Sea for Northwest and East Winds from Surface Drift Studies	118
D.7	30-Year Frequency of Sea Ice Offshore the Canadian East Coast for the Last Week of March (1981–2010)	119
D.8	Map Showing the Three Beaufort Sea Ice Zones in the Arctic	123
D.9	Probability of Finding Pressure Ridge Keels in the Polar Ice Pack	124
D.10	Extent of the Landfast Ice from 1977 to 1980	125

D.11	Ice Thickness in the Beaufort Sea from 1991 to 2002, Including the Canadian Ice Service Mean Curve and the EIS min. and max. Curves	125
D.12	Historical Yearly Mean Iceberg Distribution Offshore Newfoundland, Based on Data from 1981 to 2003	127
D.13	Amount of Daylight Hours as a Function of Latitude	130
E.1	Map of Sakhalin Showing Locations of Example Metocean Parameters	137
E.2	Probability of Any Ice in an Average Year per Given 10-day Period	142
E.3	Probability of Any Ice in the Tartar Strait in an Average Year	149
F.1	Map of the Caspian Sea, Showing Four Designated Regions: Northern, Central, Apsheron, and Southern Caspian	161
F.2	Positions of the Ice Edge in the Caspian Sea by Month and by Winter Severity	162
F.3	Long-term Variation in Caspian Sea MSL	165
F.4	Seasonal Fluctuations in Caspian Sea MSL	165
F.5	Storm Surges in the Northern Caspian Sea	166
F.6	Generalized Current Flows in the Caspian Sea	167
F.7	Precipitation (mm) Over Winter Season in Atyrau, Northern Caspian Sea	169
F.8	Region of the Caspian Sea Where Historical Tsunamis or Anomalous Sea Levels Were Observed	173
G.1	Geography of the Southern East Asian Sea	179
G.2	Bathymetry of the East Asia Sea	181
G.3	Spatial Representation of Maximum Significant Wave Height for January, February, March, and April	183
G.4	Spatial Representation of Maximum Significant Wave Height for May, June, July, and August	184
G.5	Spatial Representation of Maximum Significant Wave Height for September, October, November, and December	185
H.1	Gulf of Mexico (Bathymetry in m)	197
H.2	US Outer Continental Shelf and Deep Water Lease Areas	198
H.3	US Inner Continental Shelf Lease Areas	199
H.4	Tracks of Tropical Cyclones, 2005	201
H.5	Circulation in the Gulf of Mexico	202
H.6	Maximum Sustained Wind Speed—Hurricane Katrina (2005)	204
H.7	Annual Sea Temperature Range—Western Gulf of Mexico	206
H.8	Full Population Hurricane Areas of the Gulf	208
H.9	N -year H_{max} —Western Gulf of Mexico	210
H.10	N -year Extreme Water Level—Western Gulf of Mexico	210
H.11	Associated Surge with Tide—Western Gulf of Mexico	211
H.12	N -year H_{max} —Central Gulf of Mexico	211
H.13	N -year Extreme Water Level—Central Gulf of Mexico	213
H.14	Associated Surge with Tide—Central Gulf of Mexico	213
H.15	N -year H_{max} —Eastern Gulf of Mexico	215
H.16	N -year Extreme Water Level—Eastern Gulf of Mexico	215
H.17	Associated Surge with Tide—Eastern Gulf of Mexico	216
H.18	Direction Factor for Wave Heights North of 26° N, West of 84° W, Depths ≥ 30 m, Return Periods > 10 Years	219
H.19	Current Heading, Depth ≤ 50 m	220
H.20	N -year H_{max} —All Regions	224
H.21	N -year Extreme Water Level—All Regions	224
H.22	Associated Surge with Tide—All Regions	225
H.23	N -year Winter Storm H_{max} , West of 86° W	230
H.24	10-year Loop Current/Eddy Surface Speeds (m/s)	232
H.25	100-year Loop Current/Eddy Surface Speeds (m/s)	233
H.26	June/December Wind Roses—Northwest Gulf of Mexico	236
I.1	Map of California Offshore Region	244
J.1	Other US Waters	246

Tables

A.1	Coefficients in Equation (A.21) for Points P_1 and P_2	54
A.2	Directional Spreading Factors for Open Water Conditions	63
A.3	Relationship between Spreading Factor ϕ and Exponents n and s for Directional Spreading Functions $D_1(\theta)$ and $D_2(\theta)$	64
A.4	Potential Application of Metocean Information.....	80
A.5	Recommended Instrument Accuracy and Typical Operational Performance	81
B.1	Terminal Thickness of Marine Growth—UK Sector	90
B.2	Estimated Maximum Thickness of Marine Growth—Areas Offshore Norway	90
B.3	Accumulation of Ice: Offshore Structures in UK Sector	91
B.4	Ice Accretions: Annual Probability of Exceedance of 10^{-2}	92
B.5	Indicative Values of Metocean Parameters—Sites in Celtic Sea.....	93
B.6	Indicative Values of Metocean Parameters—Sites in Southern North Sea	93
B.7	Indicative Values of Metocean Parameters—Sites in Central North Sea	93
B.8	Indicative Values of Metocean Parameters—Sites in Northern North Sea	93
B.9	Indicative Values of Metocean Parameters—Sites West of Shetland.....	94
B.10	Indicative Values of Metocean Parameters—Sites at the Haltenbank.....	94
B.11	Indicative Values of Metocean Parameters—Sites in Barents Sea	94
B.12	Temperature Ranges—Sites in North Sea, Eastern North Atlantic, and Norwegian Sea	94
C.1	Indicative Wind, Wave, and Current Parameters—Shallow Water Sites off Nigeria	103
C.2	Indicative Wind, Wave, and Current Parameters—Deep Water Sites off Nigeria	104
C.3	Indicative Wind, Wave, and Current Parameters—Sites off Northern Angola.....	104
C.4	Indicative Wind, Wave, and Current Parameters—Sites off Southern Namibia	105
C.5	Indicative Extreme Values for Other Metocean Parameters	105
C.6	Percentage Occurrence of Total Significant Wave Height vs. Spectral Peak Period—Offshore Nigeria Location	106
C.7	Percentage Occurrence of Total Significant Wave Height vs. Spectral Peak Period—Offshore Angola Location	106
C.8	Example of Wind Sea States Used for Combined Wind Sea/Swell Bimodal Sea States—Offshore Angola	107
D.1	Ice Tendencies in the Gulf of St. Lawrence	121
D.2	Statistics for Ice Scours in the Beaufort Sea	129
D.3	Seabed Scour Statistics for the Beaufort Sea.....	129
D.4	Extreme Air and Water Temperatures for Canadian Offshore Areas	131
D.5	Extreme Metocean Parameters for Canadian Offshore Areas.....	132
E.1	Summary of Ice Conditions	141
E.2	Indicative Values of Metocean Parameters—Sakhalin East Coast (52.5° N to 55° N and Water Depths from 30 m to 100 m)	157
E.3	Indicative Values of Metocean Parameters—Sakhalin East Coast (51° N to 52.5° N and Water Depths from 30 m to 100 m)	157
E.4	Indicative Values of Metocean Parameters—Aniva Bay (Central, Northern Half)	157
E.5	Indicative Values of Metocean Parameters—Tartar Strait (51° N to 52° N and Water Depth of About 30 m).....	158
E.6	Monthly Air Temperature in Korsakov ($46^\circ 37' N$, $142^\circ 47' E$) from 1966 to 2000	158
E.7	Monthly Air Temperature in Odoptu ($53^\circ 22' N$, $143^\circ 10' E$) from 1975 to 2000.....	158
E.8	Sea Temperature Ranges—Indicative Monthly-mean Values.....	158
E.9	Percentage Occurrence of Total Significant Wave Height vs. Spectral Peak Period Offshore Sakhalin NE Coast (52.50° N, 143.66° E)	159
E.10	Percentage Occurrence of Total Significant Wave Height vs. Spectral Peak Period in Aniva Bay (46.45° N, 142.75° E)	159
E.11	Percentage Occurrence of Total Significant Wave Height vs. Spectral Peak Period in Northern Tartar Strait (51.48° N, 141.44° E)	159
F.1	Number of Events per Year with Winds > 15 m/s.....	167
F.2	Average Number of Days per Month with Dust Storms at Fort Shevchenko.....	170
F.3	Summary of Ice Conditions in the Northern Caspian Sea	171

F.4	Historical Tsunamis and Tsunami-like Events Observed in the Caspian Sea.....	172
F.5	Indicative Values of Metocean Parameters for the Northern Caspian Sea Region	174
F.6	Indicative Values of Metocean Parameters for the Central Caspian Sea Region	174
F.7	Indicative Values of Metocean Parameters for the Apsheron Ridge Area of the Caspian Sea	175
F.8	Indicative Values of Metocean Parameters for the Southern Caspian	175
F.9	Indicative Temperatures Ranges for the Caspian Sea	176
F.10	Percentage Occurrence of Total Significant Wave Height vs. Spectral Peak Period for a Location in the Northern Caspian Sea	176
F.11	Percentage Occurrence of Total Significant Wave Height vs. Spectral Peak Period for a Location on the Apsheron Ridge Area of the Caspian Sea	177
G.1	Offshore Vietnam—Shallow Water	189
G.2	Offshore Vietnam—Deep Water	190
G.3	Gulf of Thailand—North	190
G.4	Gulf of Thailand—South	191
G.5	Offshore Peninsular Malaysia	191
G.6	Offshore Natuna Island (South Natuna Sea)	192
G.7	Offshore Natuna Island (North Natuna Sea)	192
G.8	Offshore Borneo—Sarawak Shallows	193
G.9	Offshore Borneo—Sarawak Shelf Edge	193
G.10	Offshore Borneo—Sabah Shallows	194
G.11	Offshore Borneo—Sabah Shelf Edge	194
G.12	Offshore Borneo—Sabah Deepwater	195
G.13	Offshore Philippines—Palawan Area	195
G.14	Indicative Extreme Values for Other Metocean Parameters	196
H.1	Compressed Marine Growth Thickness.....	206
H.2	Hurricane Winds, Waves, Currents, and Surge in Deep Water—Western Gulf of Mexico (92° W to 98° W)	209
H.3	Hurricane Winds, Waves, Currents, and Surge in Deep Water—Central Gulf of Mexico (84° W to 92° W) ...	212
H.4	Hurricane Winds, Waves, Currents, and Surge in Deep Water—Eastern Gulf of Mexico (82° W to 84° W)...	214
H.5	Recommended Adjustments to “Surge + Tide” and $T_{H\max}$ for Gulf of Mexico Conditions	218
H.6	Factors for Combining Independent Extremes into Load Cases in Shallow Water (10 m ≤ Depth ≤ 50 m) ..	221
H.7	Factors for Combining Independent Extremes into Load Cases in Deep Water (Depth > 50 m) ...	222
H.8	Sudden Hurricane Winds, Waves, Currents, and Surge (All Regions, Depth ≤ 120 m)	223
H.9	Early Season (June 1 to August 1) Hurricane Winds, Waves, Currents, and Surge—Central and Western Gulf of Mexico (88° W to 98° W), Depth ≥ 120 m	226
H.10	Late Season (October 21 through November 30) Hurricane Winds, Waves, Currents, and Surge—Central and Western Gulf of Mexico (88° W to 98° W), Depth ≥ 120 m	227
H.11	Early Season (June 1 to August 1) Hurricane Winds, Waves, Currents, and Surge—Eastern and Central Gulf of Mexico (82° W to 88° W), Depth ≥ 120 m	227
H.12	Late Season (October 21 through November 30) Hurricane Winds, Waves, Currents, and Surge—Eastern and Central Gulf of Mexico (82° W to 88° W), Depth ≥ 120 m	228
H.13	Winter Storm Winds, Waves, Currents, and Surge, Depth ≥ 120 m	229
H.14	Factors for Combing Independent Extremes into Load Cases	230
H.15	Squall Gust Extremes and Associated Sea State and Current	231
H.16	Loop Current Profile and Associated Wind, Waves, and Surge.....	233
H.17	N -Year Current from TRW, 3 m above Bottom	234
H.18	Indicative Extreme Air and Sea Temperatures.....	234
H.19	Percentage Occurrence of Total Significant Wave Height and Spectral Peak Period Combinations—Deep Water Location—Gulf of Mexico	235
I.1	Indicative Independent Extreme Values for Winds, Waves, and Hurricane-driven Currents for Southern California (Santa Barbara and San Pedro Channels)	243
I.2	Indicative Independent Extreme Values for Central California	243
I.3	Indicative Extreme Values for Other Metocean Parameters	244
J.1	Nominal 100-year Extreme Wave with Associated Current and Storm Tide for Other US Waters (Depths > 90 m Unless Otherwise Noted).....	247
J.2	100-year Extreme Wind Speeds for Other US Waters	248

Introduction

The series of International Standards applicable to types of offshore structure, ISO 19900 to ISO 19906, constitutes a common basis covering those aspects that address design requirements and assessments of all offshore structures used by the petroleum and natural gas industries worldwide. Through their application the intention is to achieve reliability levels appropriate for manned and unmanned offshore structures, whatever the type of structure and the nature or combination of the materials used.

It is important to recognize that structural integrity is an overall concept comprising models for describing actions, structural analyses, design rules, safety elements, workmanship, quality control procedures, and national requirements, all of which are mutually dependent. The modification of one aspect of design in isolation can disturb the balance of reliability inherent in the overall concept or structural system. The implications involved in modifications, therefore, need to be considered in relation to the overall reliability of all offshore structural systems.

The series of International Standards applicable to types of offshore structure is intended to provide a wide latitude in the choice of structural configurations, materials, and techniques without hindering innovation. Sound engineering judgement is therefore necessary in the use of these International Standards.

The overall concept of structural integrity is described above. Some additional considerations apply for metocean design and operating conditions. The term "metocean" is short for "meteorological and oceanographic" and refers to the discipline concerned with the establishment of relevant environmental conditions for the design and operation of offshore structures. A major consideration in the design and operation of such a structure is the determination of actions on, and the behavior of, the structure as a result of winds, waves, and currents.

Environmental conditions vary widely around the world. For the majority of offshore locations, there are few measured data from historic conditions; comprehensive data often only start being collected when there is a specific need, for example, when exploration for hydrocarbons is being considered. Despite the usually short duration for which data are available, designers of offshore structures need estimates of extreme and abnormal environmental conditions (with an individual or joint probability of the order of $1 \times 10^{-2}/\text{year}$ and 1×10^{-3} to $1 \times 10^{-4}/\text{year}$, respectively).

Even for areas such as the Gulf of Mexico, offshore Indonesia, and the North Sea, where there are up to 30 years of fairly reliable measurements available, the data are insufficient for rigorous statistical determination of appropriate extreme and abnormal environmental conditions. The determination of relevant design parameters has therefore to rely on the interpretation of the available data by experts, together with an assessment of any other information, such as prevailing weather systems, ocean wave creation, and regional and local bathymetry, coupled with consideration of data from comparable locations. In particular, due account needs to be taken of the uncertainties that arise from the analyses of limited data sets. It is hence important to employ experts from both the metocean and the structural communities in the determination of design parameters for offshore structures, particularly since setting of appropriate environmental conditions depends on the chosen option for the offshore structure.

This part of ISO 19901 provides procedures and guidance for the determination of environmental conditions and their relevant parameters. Requirements for the determination of the actions on, and the behavior of, a structure in these environmental conditions are given in ISO 19901-3, ISO 19901-6, ISO 19901-7, ISO 19902, ISO 19903, ISO 19904-1, ISO 19905-1, and ISO 19906.

Some background to, and guidance on, the use of this standard is provided in informative Annex A. The clause numbering in Annex A is the same as in the main text to facilitate cross-referencing.

Regional information, where available, is provided in the Regional Annexes B to J. This information has been developed by experts from the region or country concerned to supplement the guidance provided in this standard. Each Regional Annex provides regional or national data on environmental conditions for the area concerned.

Annex K highlights the areas where this adoption of ISO 19901-1 as the second edition of API RP 2MET differs from ISO 19901-1:2015.

Derivation of Metocean Design and Operating Conditions

1 Scope

This standard gives general requirements for the determination and use of meteorological and oceanographic (metocean) conditions for the design, construction, and operation of offshore structures of all types used in the petroleum and natural gas industries.

The requirements are divided into two broad types:

- those that relate to the determination of environmental conditions in general, together with the metocean parameters that are required to adequately describe them;
- those that relate to the characterization and use of metocean parameters for the design, the construction activities, or the operation of offshore structures.

The environmental conditions and metocean parameters discussed are as follows:

- extreme and abnormal values of metocean parameters that recur with given return periods that are considerably longer than the design service life of the structure;
- long-term distributions of metocean parameters, in the form of cumulative, conditional, marginal, or joint statistics of metocean parameters; and
- normal environmental conditions that are expected to occur frequently during the design service life of the structure.

Metocean parameters are applicable to:

- the determination of actions for the design of new structures;
- the determination of actions for the assessment of existing structures;
- the site-specific assessment of mobile offshore units;
- the determination of limiting environmental conditions, weather windows, actions and action effects for pre-service and post-service situations (i.e. fabrication, transportation and installation, or decommissioning and removal of a structure); and
- facility operations, where appropriate.

NOTE Specific metocean requirements for site-specific assessment of jack-ups are contained in ISO 19905-1, for arctic offshore structures in ISO 19906, and for topside structures in ISO 19901-3.

2 Normative References

The following documents, in whole or in part, are normatively referenced in this document and are indispensable for its application. For dated references, only the edition cited applies. For undated references, the latest edition of the referenced document (including any amendments) applies.

ISO 19900¹, *Petroleum and natural gas industries—General requirements for offshore structures*

ISO 19906, *Petroleum and natural gas industries—Arctic offshore structures*

WMO-No. 306², *Manual on Codes*

3 Terms and Definitions

For the purpose of this document, the terms and definitions given in ISO 19900 and the following apply.

3.1

abnormal value

Design value of a parameter of abnormal severity used in accidental limit state checks in which a structure is intended not to suffer complete loss of integrity.

NOTE Abnormal events are typically accidental and environmental (including seismic) events having probabilities of exceedance of the order of 10^{-3} to 10^{-4} per annum.

3.2

chart datum

Local datum used to fix water depths on a chart or tidal heights over an area.

NOTE Chart datum is usually an approximation to the level of the lowest astronomical tide.

3.3

conditional probability

conditional distribution

Statistical distribution (probability) of the occurrence of a variable *A*, given that other variables *B*, *C*, ... have certain assigned values.

NOTE The conditional probability of *A* given that *B*, *C*, ... occur is written as $P(A|B,C,\dots)$. The concept is applicable to metocean parameters, as well as to actions and action effects.

EXAMPLE When considering wave parameters, *A* can be the individual crest elevation, *B* the water depth, and *C* the significant wave height, and so on.

3.4

design crest elevation

Extreme crest elevation measured relative to still water level.

NOTE The design crest elevation is used in combination with information on astronomical tide, storm surge, platform settlement, reservoir subsidence, and water depth uncertainty and is derived using extreme value analysis. Where simplified models are used to estimate the kinematics of the design wave, the design crest elevation can be different from (usually somewhat greater than) the crest elevation of the design wave used to calculate actions on the structure. In reality, the wave with the greatest trough-to-crest height and the wave with the highest crest will be different waves.

¹ International Organization for Standardization, Chemin de Blandonnet 8, CP 401, 1214 Vernier, Geneva, Switzerland, www.iso.org.

² World Meteorological Organization, 7bis, Avenue de la Paix, Case Postale 2300, CH-1211 Geneva 2, Switzerland.

3.5**design wave**

Deterministic wave used for the design of an offshore structure.

NOTE 1 The design wave is an engineering abstraction. Most often it is a periodic wave with suitable characteristics (e.g. height H , period T , steepness, crest elevation). The choice of a design wave depends on:

- the design purpose(s) considered;
- the wave environment;
- the geometry of the structure;
- the type of action(s) or action effect(s) pursued.

NOTE 2 Normally, a design wave is only compatible with design situations in which the action effect(s) are quasi-statically related to the associated wave actions on the structure.

3.6**expert**

<Metocean> individual who through training and experience is competent to provide metocean advice specific to the area or topic in question.

3.7**extreme water level****EWL**

Combination of design crest elevation, astronomical tide, and storm surge referenced to either LAT or MSL.

3.8**extreme value**

Representative value of a parameter used in ultimate limit state checks.

NOTE Extreme events have probabilities of the order of 10^{-2} per annum.

3.9**gravity wave**

Wave in a fluid or in the interface between two fluids for which the predominant restoring forces are gravity and buoyancy.

NOTE Wind-generated surface waves are an example of gravity waves.

3.10**gust**

Brief rise and fall in wind speed lasting less than 1 min.

NOTE In some countries, gusts are reported in meteorological observations if the maximum wind speed exceeds approximately 8 m/s.

3.11**gust wind speed**

Maximum value of the wind speed of a gust averaged over a short (3 s to 60 s) specified duration within a longer (1 min to 1 h) specified duration.

NOTE 1 For design purposes, the specified duration depends on the dimensions and natural period of (part of) the structure being designed such that the structure is designed for the most onerous conditions; thus, a small part of a structure is designed for a shorter gust wind speed duration (and hence a higher gust wind speed) than a larger (part of a) structure.

NOTE 2 The elevation of the measured gust should also be specified.

3.12**highest astronomical tide****HAT**

Level of high tide when all harmonic components causing the tides are in phase.

NOTE The harmonic components are in phase approximately once every 19 years, but these conditions are approached several times each year.

3.13**hindcasting**

Method of simulating historical (metocean) data for a region through numerical modelling.

3.14**infra-gravity wave**

Surface gravity wave with a period in the range of approximately 25 s to 300 s.

NOTE In principle, an infra-gravity wave is generated by different physical processes but is most commonly associated with waves generated by nonlinear second-order difference frequency interactions between different swell wave components.

3.15**internal wave**

Gravity wave that propagates within a stratified water column.

3.16**long-term distribution**

Probability distribution of a variable over a long time scale.

NOTE The time scale exceeds the duration of a sea state, in which the statistics are assumed constant (see 3.34 "short-term distribution"). The time scale is hence comparable to a season or to the design service life of a structure.

EXAMPLE Long-term distributions of:

- significant wave height (based on, for example, storm peaks or all sea states);
- significant wave height in the months May to September;
- individual wave heights;
- current speeds (such as for use in assessing vortex-induced vibrations of drilling risers);
- scatter diagrams with the joint distribution of significant wave height and wave period (such as for use in a fatigue analysis);
- a particular action effect;
- sea ice types and thickness;
- iceberg mass and velocity;
- storm maximum significant wave height.

3.17**lowest astronomical tide****LAT**

Level of low tide when all harmonic components causing the tides are in phase.

NOTE The harmonic components are in phase approximately once every 19 years, but these conditions are approached several times each year.

3.18**marginal distribution****marginal probability**

Statistical distribution (probability) of the occurrence of a variable A independent of any other variable.

NOTE The marginal distribution is obtained by integrating the full distribution over all values of the other variables B , C , ... and is written as $P(A)$. The concept is applicable to metocean parameters, as well as to actions and action effects.

EXAMPLE When considering wave conditions, A can be the individual crest elevation for all mean zero-crossing periods B and all significant wave heights C , occurring at a particular site.

3.19**marine growth**

Living organisms attached to an offshore structure.

3.20**mean sea level****MSL**

Arithmetic mean of all sea levels measured over a long period.

NOTE Seasonal changes in mean level can be expected in some regions, and over many years the mean sea level can change.

3.21**mean wind speed**

Time-averaged wind speed, averaged over a specified time interval and at a specified elevation.

NOTE The mean wind speed varies with elevation above mean sea level and the averaging time interval; a standard reference elevation is 10 m and a standard time interval is 1 h. See also 3.11 "gust wind speed" and 3.43 "sustained wind speed."

3.22**mean zero-crossing period**

Average period between (up or down) zero-crossing waves in a sea state.

NOTE In practice the mean zero-crossing period is often estimated from the zeroth and second moments of the wave spectrum as $T_z = T_2 = \sqrt{m_0(f)/m_2(f)} = 2\pi\sqrt{m_0(\omega)/m_2(\omega)}$.

3.23**monsoon**

Seasonally reversing wind pattern, with associated pattern of rainfall.

NOTE The term was first applied to the winds over the Arabian Sea which blow for six months from northeast and for six months from southwest, but it has been extended to similar winds in other parts of the world.

3.24**most probable maximum**

Value of the maximum of a variable with the highest probability of occurring.

NOTE The most probable maximum is the value for which the probability density function of the maxima of the variable has its peak. It is also called the mode or modus of the statistical distribution.

3.25**operating conditions**

Most severe combination of environmental conditions under which a given operation is permitted to proceed.

NOTE Operating conditions are determined for operations that exert a significant action on the structure. Operating conditions are usually a compromise: they are sufficiently severe that the operation can generally be performed without excessive downtime, but they are not so severe that they have an undue impact on design.

3.26**polar low**

Depression that forms in polar air, often near a boundary between ice and sea.

3.27**residual current**

Part of the total current that is not constituted from harmonic tidal components (i.e. the tidal stream).

NOTE Residual currents are caused by a variety of physical mechanisms and comprise a large range of natural frequencies and magnitudes in different parts of the world.

3.28**return period**

Average period between occurrences of an event or of a particular value being exceeded.

NOTE The offshore industry commonly uses a return period measured in years for environmental events. For a rare event, the return period in years is equal to the reciprocal of the annual probability of exceedance of the event.

3.29**scatter diagram**

Joint probability of two or more (metocean) parameters.

NOTE A scatter diagram is especially used with wave parameters in the metocean context (for example, in fatigue assessments). The wave scatter diagram is commonly understood to be the probability of the joint occurrence of the significant wave height (H_s) and a representative period (T_z or T_p).

3.30**sea floor**

Interface between the sea and the seabed and referring to the upper surface of all unconsolidated material.

3.31**sea state**

Condition of the sea during a period in which its statistics remain approximately stationary.

NOTE In a statistical sense the sea state does not change markedly within the period. The period during which this condition exists is often assumed to be 3 h, although it depends on the particular weather situation at any given time.

3.32**seabed**

Materials below the sea in which a structure is founded, whether of soils such as sand, silt or clay, cemented material, or of rock.

3.33**seiche**

Oscillation of a body of water at its natural period.

3.34**short-term distribution**

Probability distribution of a variable within a short interval of time during which conditions are assumed to be statistically stationary.

NOTE The interval chosen is most often the duration of a sea state.

3.35**significant wave height**

Statistical measure of the height of waves in a sea state.

NOTE The significant wave height was originally defined as the mean height of the highest one-third of the zero up-crossing waves in a sea state. In most offshore data acquisition systems, the significant wave height is currently taken as $4\sqrt{m_0}$, (where m_0 is the zeroth spectral moment; see 3.37 "spectral moment") or 4σ , where σ is the standard deviation of the time series of water surface elevation over the duration of the measurement, typically a period of approximately 30 min.

3.36**soliton**

Solitary wave or wave packet travelling on an internal density discontinuity that, as a result of the cancellation of nonlinear and dispersive effects, maintains its shape and speed over extended distances.

EXAMPLE Internal tides that form on the density gradient within the water column can interact with the continental slope and form internal solitary wave packets. Offshore Northwest Australia breaking internal solitons have been noted to generate elevated seabed currents.

3.37**spectral moment** **n th spectral moment**

Integral over frequency of the spectral density function multiplied by the n th power of the frequency, either expressed in hertz (cycles per second) as $m_n(f) = \int_0^\infty f^n S(f) df$ expressed in circular frequency (radians/second) as $m_n(\omega) = \int_0^\infty \omega^n S(\omega) d\omega$.

NOTE 1 As $\omega = 2\pi f$, the relationship between the two moment expressions is: $m_n(\omega) = (2\pi)^n m_n(f)$.

NOTE 2 The integration extends over the entire frequency range from zero to infinity. In practice the integration is often truncated at a frequency beyond which the contribution to the integral is negligible and/or the sensor no longer responds accurately. Care should be taken when utilizing moments of order higher than 2, as for standard spectral models, the 4th moment will not converge; the value is in effect determined by the choice of truncation.

3.38**spectral peak period**

Period of the maximum (peak) energy density in the spectrum.

NOTE In practice there is often more than one peak in a spectrum.

3.39**spectral density function****energy density function****spectrum**

Measure of the variance associated with a time-varying variable per unit frequency band and per unit directional sector.

NOTE 1 Spectrum is a shorter expression for the full and formal name of spectral density function or energy density function.

NOTE 2 The spectral density function is the variance (the mean square) of the time-varying variable concerned in each frequency band and directional sector. Therefore, the spectrum is in general written with two arguments: one for the frequency variable and one for a direction variable.

NOTE 3 Within this standard, the concept of a spectrum applies to waves, wind turbulence, and action effects (responses) that are caused by waves or wind turbulence. For waves, the spectrum is a measure of the energy traversing a given space.

3.40**squall**

Strong wind event characterized by a sudden onset, a duration of the order of minutes, and a rather sudden decrease in speed.

NOTE 1 A squall is often accompanied by a change in wind direction, a drop in air temperature and heavy precipitation.

NOTE 2 The WMO classification of a squall requires the wind speed to increase by at least 8 m/s and attain a top speed of at least 11 m/s, lasting at least 1 min in duration.

3.41**still water level**

Abstract water level used in the calculation of elevations at which actions are applied.

NOTE 1 Still water level is typically used for the calculation of:

- wave kinematics for global actions;
- wave crest elevation for minimum deck elevations;
- maximum elevation of ice actions.

NOTE 2 Still water level, also referred to as storm water level, is an engineering abstraction calculated by adding the effects of tides and storm surge to the water depth but excluding variations due to waves (see Figure 1). It can be above or below mean sea level.

3.42**storm surge**

Change in sea level (either positive or negative) that is due to meteorological (rather than tidal) forcing.

3.43**sustained wind speed**

Time-averaged wind speed with an averaging duration of 10 min or longer at a specified elevation.

3.44**swell**

Wave that was wind-generated but has travelled out of its generation area and has no relationship with the local wind.

3.45**tropical cyclone**

Closed atmospheric circulation around a zone of low pressure that originates over the tropical oceans.

NOTE 1 The circulation is counter-clockwise in the northern hemisphere and clockwise in the southern hemisphere.

NOTE 2 At maturity, the tropical cyclone can be one of the most intense storms in the world, with wind speeds exceeding 90 m/s and accompanied by torrential rain.

NOTE 3 In some areas, local terms for tropical cyclones are used. For example, tropical cyclones are typically referred to as hurricanes in the Gulf of Mexico and North Atlantic, whereas in the East Asian Sea and Pacific Northwest, they are called typhoons. In the South Pacific and South Indian Ocean, however, they are commonly referred to as cyclones.

NOTE 4 The term "cyclone" is also used to refer to a tropical storm with sustained wind speeds in excess of 32 m/s (Beaufort Force 12).

.....

3.46**tsunami**

Long period surface waves caused by displacement of a large volume of a body of water, normally an ocean.

NOTE The vertical movement of the sea floor is often associated with fault rupture during earthquakes or with seabed mud slides.

3.47**water depth**

Vertical distance between the sea floor and still water level.

NOTE 1 As there are several options for the still water level, there can be several water depth values. Generally, design water depth is determined to LAT or to mean sea level.

NOTE 2 The water depth used for calculating wave kinematics varies between the maximum water depth of the highest astronomical tide plus a positive storm surge, and the minimum water depth of the lowest astronomical tide less a negative storm surge, where applicable. The same maximum and minimum water depths are applicable to bottom-founded and floating structures, although water depth is usually a much less important parameter for floating structures. Water depth is, however, important for the design and analysis of the mooring system and risers for floating structures.

3.48**wave spectrum**

Measure of the amount of energy associated with the fluctuation of the sea surface elevation per unit frequency band and per unit directional sector.

NOTE 1 The wave frequency spectrum (integrated over all directions) is often described by use of some parametric form such as the Pierson-Moskowitz or JONSWAP wave spectrum.

NOTE 2 The area under the wave spectrum is the zeroth spectral moment m_0 , which is a measure of the total energy in the sea state; m_0 is used in contemporary definitions of the significant wave height.

3.49**wave steepness**

Characteristic of individual waves defined as wave height divided by wave length.

NOTE For periodic waves, the concept is straightforward as H/λ . For random waves, the definition is normally used with the significant wave height (H_s) and the wavelength that corresponds with the mean zero-crossing period (T_z) of the wave spectrum in deep water. The significant wave steepness is then defined as $H_s / \lambda_z = H_s / [(g/2\pi) T_z^2]$.

3.50**wind spectrum**

Measure of the variance associated with the fluctuating wind speed per unit frequency band.

NOTE 1 The wind spectrum is an expression of the dynamic properties of the wind (turbulence). It reflects the fluctuations about and in the same direction as a certain mean wind speed, usually the 1 h sustained wind speed. There is hence no direction variable associated with the wind spectrum within this standard.

NOTE 2 As the sustained wind speed varies with elevation, the wind spectrum is a function of elevation.

4 Symbols and Abbreviated Terms

4.1 Symbols

$D(\theta)$	wave directional spreading function
$D(f, \theta)$	general form of the wave directional spreading function
d	water depth
$F_{coh}(f; P_1, P_2)$	coherence function between turbulence fluctuations at $P_1(x_1, y_1, z_1)$ and at $P_2(x_2, y_2, z_2)$
f	frequency in cycles per second (hertz)
f_1	mean wave frequency of the wave spectrum [$f_1 = 1/T_1 = \omega_1 / (2\pi)$]
f_a	apparent wave frequency [$f_a = 1/T_a = \omega_a / (2\pi)$]
f_e	encounter wave frequency [$f_e = 1/T_e = \omega_e / (2\pi)$]
f_i	intrinsic wave frequency [$f_i = 1/T_i = \omega_i / (2\pi)$]
f_p	peak or modal frequency at the peak of the spectrum [$f_p = 1/T_p = \omega_p / (2\pi)$]
f_z	average zero-crossing frequency of the water surface elevation [$f_z = 1/T_z = \omega_z / (2\pi)$]
g	acceleration due to gravity
H	height of an individual wave
H_b	breaking wave height
H_N	maximum height of an individual wave having a return period of N years. Both H_{max} and H_{mp} are also used in this context
H_s	significant wave height
$I_u(z)$	wind turbulence intensity at z m above mean sea level
k	wave number = $2\pi/\lambda$
m_n	n th spectral moment (either in terms of f or ω). In particular, m_0 is the zeroth spectral moment and is equivalent to σ^2 , the variance of the corresponding time series
S	spectral density function, energy density function
$S(f), S(\omega)$	wave frequency spectrum
$S(f, \theta), S(\omega, \theta)$	directional wave spectrum
S_{JS}	JONSWAP spectrum for a sea state
S_{PM}	Pierson-Moskowitz spectrum for a sea state
S_{OH}	Ochi-Hubble spectrum for a total sea state consisting of a combination of two sea states with a general formulation

T	wave period; also period in general
T_0	standard reference time-averaging interval for wind speed of 1 h = 3600 s
T_a	apparent period of a periodic wave (to an observer in an earth-bound reference frame)
T_e	encounter period of a periodic wave (to an observer in a reference frame that moves with respect to earth as well as the wave; the frame is usually fixed to a moving vessel)
T_i	intrinsic period of a periodic wave (in a reference frame that is stationary with respect to the wave, i.e. with no current present)
T_p	modal or peak period of the spectrum
T_z	mean zero-crossing period of the water surface elevation in a sea state
T_1	mean period of the water surface elevation in a sea state, defined by the zero and first-order spectral moments
t	time
U_c	free stream current velocity
U_{co}	surface current speed at $z = 0$
U_{ref}	reference wind speed, $U_{ref} = 10$ m/s
$U_c(z)$	current speed at elevation z ($z < 0$)
$U_w(z,t)$	spatially and temporally varying wind speed at elevation z above mean sea level and at time instant t
$U_w(z)$	mean wind speed at elevation z above mean sea level averaged over a specified time period
$U_{w,1h}(z)$	1 h sustained wind speed at elevation z above mean sea level
$U_{w,T}(z)$	sustained wind speed at elevation z above mean sea level, averaged over time interval $T < 1$ h
U_{w0}	1 h sustained wind speed at 10 m above mean sea level (the standard reference speed for sustained winds)
$u_w(z,t)$	fluctuating wind speed at elevation z around $U_w(z)$ and in the same direction as the mean wind
$V_{\text{in-line}}$	component of the current velocity in-line with the direction of wave propagation
x,y,z	coordinates of a right-handed orthogonal coordinate system with the xy -plane at the undisturbed still water level (for waves and currents) or mean sea level (for winds) and the z -axis positive upwards
z	vertical coordinate [measured upwards from the still water level (for waves and currents) or mean sea level (for winds)]
z_r	reference elevation for winds above the mean sea level, $z_r = 10$ m

z_s	stretched vertical coordinate for waves and currents (measured upwards from the still water level)
γ	shape parameter of the peak enhancement factor in the JONSWAP spectrum
η	water surface elevation above still water level as a function of time and location
θ	wave direction angle
$\bar{\theta}$	mean wave direction
θ_c	direction of the current velocity relative to the wave direction
λ	wavelength or Ochi-Hubble spectrum peak enhancement factor
σ	standard deviation of the water surface elevation in a sea state
σ_a, σ_b	parameters in the peak enhancement factor of the JONSWAP spectrum
σ_g	parameter defining the width of the symmetric swell spectrum (equals the standard deviation of the Gaussian function)
ϕ	directional spreading factor
ω	angular frequency (radians per second $\omega = 2\pi f$)

4.2 Abbreviated Terms

CTD	conductivity-temperature-depth
HAT	highest astronomical tide
ITCZ	intertropical convergence zone
LAT	lowest astronomical tide
MHHW	mean higher high water
MLLW	mean lower low water
MOR	meteorological optical range
MSL	mean sea level
PSU	practical salinity unit
RVR	runway visual range
VIV	vortex-induced vibration

5 Determining the Relevant Metocean Parameters

5.1 General

The owner or operator of an offshore installation is responsible for the selection of the environmental conditions applicable to specific design situations or for particular operations.

The selection shall include:

- the type of structure being designed or assessed;
- the nature of the operation to be undertaken (e.g. construction, transportation, installation, drilling, production, etc.);
- the limit state considered (e.g. ultimate, fatigue, accidental);
- any additional company or regulatory requirements.

NOTE In addition to accidental events, the accidental limit states relate to abnormal environmental events, including abnormal level earthquakes.

The type of metocean information that can be required include the following:

- a) extreme and abnormal metocean parameters, which are required to develop extreme and abnormal environmental actions and/or action effects; these parameters are used to define design situation(s), whereas the extreme and abnormal environmental actions and/or action effects are used to perform design checks for ultimate limit states and accidental limit states, respectively;
- b) long-term distributions of metocean parameters in the form of cumulative conditional or marginal statistics; these parameters are used:
 - to define design situation(s) and to perform design checks for the fatigue limit state, or
 - to make evaluations of downtime/workability/operability during a certain period of time, for the structure or for associated items of equipment;
- c) long-term time series of metocean parameters for use in response-based analyses;
- d) short-term environmental conditions that are required:
 - for carrying out checks for serviceability limit states,
 - for developing actions and action effects to determine when particular operations can safely take place, and
 - for planning construction activities (fabrication, transportation, or installation) or field operations (e.g. drilling, production, offloading, underwater activities).

Depending on the geographical region and the offshore operations involved, other environmental conditions can be required for specific design situations or for particular operations.

5.2 Expert Development of Metocean Criteria

Reliable estimates of (very) low probability environmental events can be made using a number of different approaches, including analysis of all data values, annual or monthly maxima, or peak-over-threshold events. Implicit in the use of each approach are assumptions about the data used, the statistical procedures applied, and the interpretation of the results.

The appropriate design parameters are also dependent on the structural form chosen; for example, different design parameters can be appropriate to fixed or floating structures.

Experts in meteorology and oceanography are needed to obtain reliable and appropriate design parameters. The experts should be involved in the analyses of the data and their interpretation into design criteria. They should be integral members of design teams, particularly when the environmental

conditions and associated metocean parameters used for the design of proposed structures are based on design criteria for actions (action effects) with long return periods.

For regions subject to continuous, seasonal, or periodic ice events such as sea ice and icebergs, metocean experts should be supplemented by experts in the relevant ice hazards.

5.3 Selecting Appropriate Parameters for Determining Design Actions and Action Effects

Environmental actions and associated action effects used in the design and assessment of offshore structures are dominated by one or more metocean parameters depending on factors including:

- the structural form (e.g. fixed jacket, semisubmersible or monohull);
- the geographical location (e.g. regions where strong currents can be present);
- the exposure of individual structural elements to wind, wave, current, or ice action;
- the limit state being addressed.

Information on the metocean parameters appropriate to each structural form is presented in the relevant structure-specific standards in the ISO 19900 series of publications. The final choice of metocean parameters to be used to determine design actions or action effects should be carried out in consultation with structural engineers.

Where wave actions dominate, the wave condition(s) that shall be assessed for a particular design situation can be specified through the following.

- a) Long-term statistical distributions of the oceanographic parameters describing the wave climate at the location of interest over many years.

Where adequate data are available, the statistical distributions can reflect the joint occurrences of oceanographic parameters. Alternatively, only marginal distributions are provided. From these long-term distributions, appropriate oceanographic design parameters should be derived that are compatible with the design situations involved.

- b) Short-term descriptions of one or more design sea states, in conjunction with one or more design values of winds and currents.

A design sea state should be described by a wave spectrum in terms of a significant wave height, a representative frequency or period, and a mean wave direction. Where appropriate, the wave spectrum may be supplemented with a directional spreading function (see 8.3). A design current is specified by a surface velocity and its velocity profile over the water column, including its direction (see Clause 9).

- c) One or more individual design waves, in conjunction with one or more design winds and currents.

A design wave shall be specified by its height and period, together with an appropriate wave theory from which the wave kinematics can be derived, as well as (an) associated direction(s) (see Clause 8). A design current is specified by a surface velocity and its velocity profile over the water column including its direction (see Clause 9).

The above descriptions shall be supplemented by associated meteorological conditions that are relevant for the particular design situation considered.

The selection of the most appropriate specification a), b), or c) above depends on the data that are available for the location of interest, the type of structure concerned, the design situation involved, and

the limit state considered. It is entirely appropriate that a different selection is made to suit different structure types, different design situations, and different limit states.

If the current is known to dominate design actions on the structure, the selection of associated wave heights and wind speeds for a given current velocity should be considered.

If ice in the form of sea ice, icebergs, etc. could occur, relevant design situations shall be defined and environmental parameters shall be developed in accordance with ISO 19906. ISO 19906 also includes provisions for other environmental phenomena encountered in arctic and cold regions, such as snow and ice accretion, and ice encroachment.

Where environmental actions for structural design are not dominated by wave, current, or ice conditions (but, for example, by wind or earthquakes), special consideration shall be given to the selection of the relevant metocean parameters in combination with those other events.

5.4 The Metocean Database

A site-specific metocean database shall be established containing information on:

- sea state parameters such as significant and maximum wave heights, periods, directions, and spreading;
- current speeds and directions at a number of depths throughout the water column;
- wind speeds and directions;
- sea ice, icebergs, snow, and ice accretion;
- water levels; and
- other relevant metocean parameters (air and water temperatures, water salinity, etc.).

The database may be established either by site-specific measurements over a period of years or by numerical modelling (hindcasts) of historical events. If numerical simulations are used, the simulated results shall be calibrated (or verified) against appropriate measurements.

Where possible, the database should be sufficiently long to encompass all the physical processes that can be encountered during the lifetime of the structure. Where this is not possible, the metocean criteria derived directly from the database should be modified appropriately.

5.5 Storm Types in a Region

General information on the various types of storms that can affect the structure shall be used to supplement available data.

When determining the appropriate environmental conditions, it is important to separate storms of different types, for example, monsoons and typhoons, before performing an extreme value analysis. Furthermore, it can be necessary to set operating limits for a particular structure for particular storm types and seasons.

5.6 Directionality

In some locations, representative storm tracks and topographic features can provide fetch limitations on wave heights from specific directions, or tidal or general circulation currents can be in a predominant direction. For design in such situations, different wave, wind, and/or current magnitudes may be used for different approach directions, provided that sufficient reliable data are available to derive them. However,

the owner of the structure shall ensure that the overall reliability of the structure is not compromised by the use of such lower directional environmental conditions.

If reliable directional information is not available, conservative assumptions shall be made with respect to relative directions of winds, waves, and current.

5.7 Extrapolation to Extreme and Abnormal Conditions

Designers require metocean parameters at (very) low probabilities or recurrence rates, e.g. with a return period of 100, 1000, or 10,000 years. Where data covering such long periods are not available, an extrapolation of existing data is necessary. Many extrapolation methods are used, and there is no universally accepted method; expert advice shall be sought. In general, the longer the data set the more accurate the extrapolation will be. In some relatively homogeneous areas, site-pooling of hindcast data sets can be used to extend the time basis for estimating return period values at a particular site, thereby reducing the uncertainty of the extrapolation. Important considerations in site-pooling are to choose sites that are far enough apart such that they provide independent realizations of the local conditions, but not to choose sites that are so far apart that true spatial variations in extremes are smoothed over. However, even with long data sets, estimates of (very) low probability parameters can still depend to a considerable degree on the extrapolation method and sampling variability. Confidence intervals can be estimated to assess the uncertainty due to sampling variability.

5.8 Metocean Parameters for Fatigue Assessments

The fatigue limit state can govern the design of individual structural components in fixed and floating offshore structures in several parts of the world.

Fatigue is an accumulation of damage caused by the repeated application of time-varying stresses that can result from the environmental actions to which the structure is exposed.

Fatigue limit state assessment of a structure requires specification of all environmental conditions that are expected to occur during the entire period of the structure's exposure, i.e. its construction phase, including transportation, and its design service life. The specification of the environment is given by the long-term distribution(s) of one or more metocean parameters. The metocean parameters relevant for the fatigue assessment depend on the type of structure and the location under consideration. The distribution(s) of the relevant parameter(s) shall be determined from the metocean database, taking due account of the requirements for the structure being considered.

When computing the cumulative fatigue damage over the life of the structure using the distribution of relevant parameters, it should be kept in mind that this is an estimate of the expected long-term fatigue damage. In such assessments, by their very nature, rare events are weighted with a low probability of occurrence. In some cases, however, it should be considered how much damage a structure may accumulate during a rare event that imposes a relatively low number of very large amplitude stress cycles. Such "low-cycle fatigue assessments" ensure that the occurrence of a single extreme or abnormal event does not consume a significant proportion of the overall fatigue life of a structural system.

For some components and types of structures, cyclic stresses due to vortex-induced vibrations (VIV) in steady currents or winds should also be considered.

Structures in ice environments can experience dynamic ice actions and ice-induced vibrations that should be considered in accordance with ISO 19906.

Information on the metocean parameters appropriate to the fatigue assessment of different forms of offshore structure is presented in the relevant structure-specific standard in the ISO 19900 series of publications.

5.9 Metocean Parameters for Short-term Activities

Transportation, installation, maintenance, and removal of a structure are scheduled activities that are weather-sensitive. Operation of a structure includes regular and routine activities that are also weather-sensitive. Some of these activities are sensitive to high winds, whereas others are sensitive to currents, swell, wave heights, wave periods, wave directions, or combinations thereof.

Examples of weather-sensitive scheduled short-term activities are:

- a) transportation of the structure over a relatively short distance;
- b) installation of fixed steel offshore structures, including:
 - 1) lifting, launching, upending, and placement on the seabed,
 - 2) the period following placement but prior to and during piling, and
 - 3) the period following piling but prior to and during pile grouting and until the grout sets;
- c) installation of fixed concrete offshore structures, including:
 - 1) placement on the seabed, and
 - 2) the period following placement but prior to and during any grouting and until grout setting;
- d) establishment/re-establishment of a floating structure at the operating location, including the setting of mooring systems;
- e) installation and foundation pre-loading for jack-ups;
- f) topsides installation;
- g) underwater operations, including inspection and repair; and
- h) removal for decommissioning or reuse.

As well as being critical and expensive, these activities usually require a weather window with low environmental conditions for significant durations, e.g. sufficient to allow for all piling and pile fixing. Consequently, the accuracy of short-term forecasting can be as important as the values of the metocean parameters.

Examples of routine activities that are weather-sensitive are as follows:

- use of cranes for lifting to and from supply boats;
- use of cranes for moving items around decks;
- under-deck access;
- use of drilling derrick, particularly derrick movements;
- helicopter movements;
- personnel transfer operations by boat.

These activities generally have different weather sensitivities.

Limiting criteria shall be established for each activity. In many cases the limitations are established by considering the safety of personnel.

It is useful in the planning of a development or the planning of a specific activity to know that the probability of the metocean parameters exceeding the criteria for particular activities is sufficiently low for sufficient time to complete these activities. The probability of sufficiently calm conditions for a given location typically varies on a seasonal basis.

Predictions of the variation in the relevant metocean parameters should be made from the metocean database. Predictions should provide either the proportion of time and the durations for which metocean parameters are expected to remain within limiting criteria, or the probability of the values of certain metocean parameters being exceeded. Seasonal variations (by month or by quarter) should be reported if these are significant. In addition, it should be considered and made clear to users of such criteria that in addition to seasonal variations in operational conditions, there can be significant year-to-year variations.

5.10 Metocean Parameters for Medium-term Activities

Medium-term activities such as transportation of a structure or structural members, particularly when involving long exposed tows, are scheduled activities that are weather-sensitive but which have durations significantly longer than the length of the available weather forecast. For such activities, certain design criteria can be required, such as sea-fastening load criteria.

For transportation, the design criteria should be defined, consisting of the design wave, design wind, and, if relevant, design current. Where the transportation transits through different geographical areas, the maximum wave and maximum wind may not occur in the same area, in which case it is necessary to check the extremes in each area, to establish governing load cases.

6 Water Depth, Tides, and Storm Surges

6.1 General

The water depth at the site, including variations in the water depth, shall be determined where significant for the type of structure being considered.

The range of water depths at a particular site is important for the design of structures as it affects several parameters, including:

- environmental actions on the structure;
- elevations of boat landings, fenders, and cellar deck on bottom-founded structures;
- riser length/stroke on floating structures; and
- mooring forces for taut or vertically moored floating structures.

For the purpose of design or assessment, the water depth can be considered to consist of a more or less stationary component, this being the water depth to a reference chart datum (e.g. LAT or MSL), and variations with time relative to this level (see Figure 1). The variations are due to the astronomical tide (see 6.2) and to the wind and atmospheric pressure, which can create storm surges (which can be positive or negative) (see 6.3). Other variations in water level can result from long-term climatic variations, sea floor subsidence, or episodic events such as tsunamis. Water level variations can have a relatively minor impact in deep water, but can be considerably more important in shallow water.



It is important for the design of all structures (and in particular bottom-founded structures in shallow water) to have a good knowledge of the joint distribution of the tide, the storm surge height, and the crest and trough elevations of the waves.

6.2 Tides

Tidal variations are the result of the gravitational and rotational interaction between the sun, moon, and earth and are regular and largely predictable; they are bounded by the highest astronomical tide (HAT) and the lowest astronomical tide (LAT) at the site.

The variations in elevation of the daily astronomical tides determine the elevations of boat landings, fenders, splash-zone treatment, conductors and risers, and the upper limits of marine growth for bottom-founded structures.

6.3 Storm Surges

Storm surges are meteorologically generated. Since the generation of surges is unrelated to tides, their occurrences are randomly superimposed on tidal variations. In deep and modest water depths, tidal and storm surge elevations can be arithmetically added to good approximation. In shallow water, tide and surge can interact due to nonlinear bottom friction effects. Since surges cause water level variations additional to tides, total still water levels above HAT and below LAT can occur.

6.4 Extreme Water Level

The extreme water level is derived through a combination of design crest elevation, astronomical tide, and storm surge referenced to either LAT or MSL.

The combination can be either a straight summation of the design crest elevation and the still water level, or it can be developed taking into account the joint probability of occurrence of crest, tide, and surge.

Extreme water level is a starting point for ascertaining the minimum height of the main deck of a bottom-founded structure. Allowance should also be made for platform settlement, reservoir subsidence, and water depth uncertainty.

Structures with large diameter columns can modify the incident wave field, resulting in changes to the extreme water level (and other wave properties) estimated in the absence of wave/structure interactions. Such changes may need to be addressed as part of the design process.

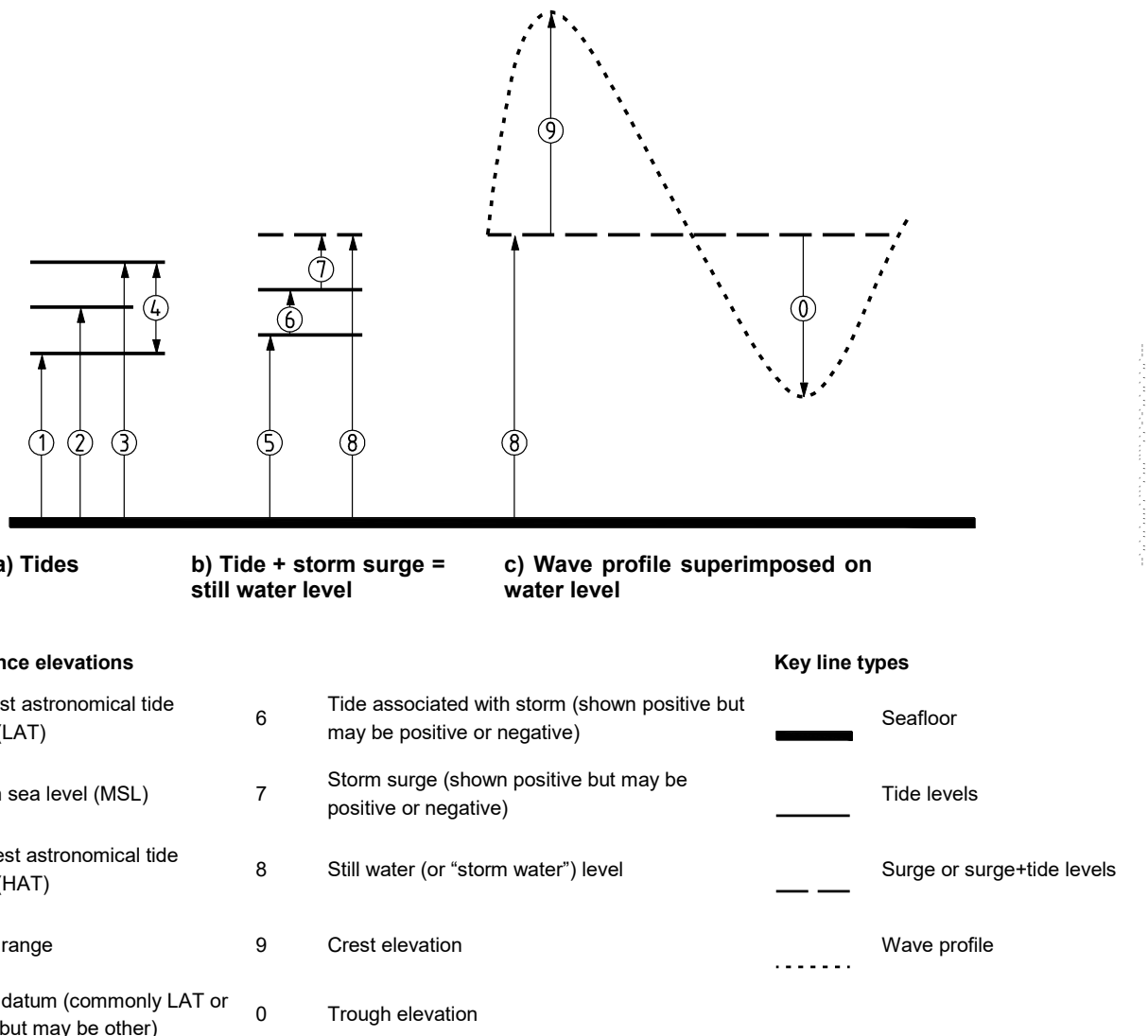


Figure 1—Water Depth, Tides, and Storm Surges

7 Wind

7.1 General

Wind speed and direction vary in space and time. Normally, wind speed time-series data at a site are only available at a single elevation. It is unusual to have multiple measurements on the tens to hundreds of meters horizontal-length scales relevant to offshore structures. Furthermore, time series are often only available at time scales much longer (e.g. 10 min to 3 h) than the natural response periods of most structures. On length scales typical of even the largest offshore structures, the mean and standard deviation of the wind speed, averaged over durations of the order of an hour, do not vary horizontally, but they do change with elevation (wind profile). For averaging durations shorter than 1 h, there will be periods with higher mean speeds and increased spatial variation. As such, typical practice is to specify wind criteria at a clearly specified averaging interval and reference elevation. The most commonly used reference elevation is 10 m above mean sea level (MSL). Wind profile factors, gust factors, auto- or coherence spectra appropriate to the local wind regime can then be applied in conjunction with the reference winds to appropriately account for fine-scale spatial and temporal effects.

Wind speeds are classified as either:

- sustained wind speeds, or
- gust wind speeds.

The elevation and averaging interval of any wind speed or gust should always be reported.

Extreme gusts occur due to a variety of phenomena. These include squalls, thunderstorms, downbursts, tornados, water spouts, all of which are relatively short-lived. The ratio of maximum gust wind speed to hourly mean wind speed at any one location in these examples can be large.

However, gusts also occur during periods of high hourly mean wind speed due simply to turbulence, but in this case the ratio of maximum gust wind speed to hourly mean wind speed over the sea is typically less than about 1.5.

Wind conditions shall be determined by proper analysis of wind data. Guidance on collecting wind data is given in A.7.1.

To determine appropriate design situations for offshore structures with regard to wind, the extreme, abnormal and operationally relevant wind conditions shall be specified in accordance with the type of structure and the nature of the structure's response. Wind turbulence in gusts has three-dimensional spatial scales related to their duration. For example, 3 s gusts are coherent over shorter distances and therefore affect smaller components of a structure than 15 s gusts. For structures (structural components) that are subject to appreciable dynamic response, it can be necessary to take the time variation of actions caused by wind into account.

Further guidance is provided below, whereas procedures for determining actions and action effects caused by wind for different types of structure shall be in accordance with the relevant structure-specific standard in the ISO 19900 series of publications.

7.2 Wind Actions and Action Effects

Wind acts on the topsides and that portion of the structure that is above the water, as well as upon any equipment, deck houses, bridges, flare-booms, and derricks that are located on the topsides. As the wind speed varies with elevation, the height of the component shall be taken into account. A vertical wind profile that can be used is discussed in 7.3 and provided in A.7.3.

For the design of offshore structures that respond globally in a nearly static fashion, global actions caused by wind are generally much less important than those caused by waves and currents. However, for the local response of certain parts or of individual components of these structures, the action effects caused by wind can be significant. Global actions on structures shall be determined using a time-averaged design speed in the form of a sustained wind speed. For the design of individual structural components, a time-averaged wind speed can also be adequate, but the averaging duration shall be reduced to allow for the smaller turbulence scale that can affect individual components. Local actions on individual components shall therefore be determined using a gust wind speed. Guidance on the selection of appropriate averaging times is given in A.7.2.

For the design of offshore structures (or structural components) that are subject to appreciable dynamic response, the time and spatial variation of the wind speed shall be accounted for. A dynamic analysis of a structure (or structural components) is generally necessary when the wind field contains energy at frequencies near the natural frequencies of the structure (structural components). Such analyses require detailed knowledge of the wind turbulence intensity, the wind frequency spectrum, and its spatial coherence (see 7.4).

A special case of dynamic response is the VIV of relatively slender structures subjected to steady winds in which alternate vortex shedding excites components. Components of fixed steel offshore structures can be exposed to VIV during construction and transportation. Flare structures and telecommunication towers can also be susceptible to VIV throughout their lives.

Wind should be considered in detail for compliant bottom-founded structures and floating structures.

7.3 Wind Profile and Time-averaged Wind Speed

The vertical profile of the mean wind speed in storms is usually expressed by a logarithmic function. Adjustments to the wind profile at a particular location or under certain conditions may be made when appropriate measured data from an offshore location are available (i.e. measured data for the kind of event used in design).

7.4 Wind Spectra

If a structure (or a structural component) exhibits appreciable dynamic response due to wind action, the temporal and spatial variations of the wind speed shall be assessed. Turbulent wind may be viewed as an evolving field of vortices being swept past the structure. Additional turbulence is generated by the structure itself. The most accurate wind actions are derived from physical testing in a boundary-layer wind tunnel, or by using computational fluid dynamics. Useable results can be obtained from a time series of wind velocity generated by adding spectral frequency components (mathematically as described below for waves) to the mean wind speed. In the absence of three-dimensional wind modelling, only the speed fluctuations in the mean wind direction can be described. An appropriate form of the frequency spectrum for wind speeds in the mean direction is given in A.7.4. The spatial variation of the wind speed in the mean direction between two points in space is expressed by means of a coherence function (see A.7.4).

The concept of a wind spectrum is only applicable to stationary wind conditions. As squalls are transient (nonstationary), the temporal and spatial variations of the wind speed in a squall cannot be described by a wind spectrum. Analysis of actions and action effects caused by squalls requires the specification of a time series of wind velocity, which captures the transient squall peak.

8 Waves

8.1 General

Surface waves are generally very important for the design of offshore and coastal structures. Facility design requires the specification of the operational wave statistics and extreme and abnormal return-period wave conditions comprising spectral and/or deterministic wave height and period parameters, direction of wave propagation, and the spread of the directions.

Ocean waves are irregular in shape; vary in height, length, and speed of propagation; and travel in many directions. In general, small waves in deep water may be regarded as the linear superimposition of many small individual sinusoidal components, each of which is a periodic wave with its own amplitude, frequency, and direction of propagation; with linear waves the components have random phase relationships with respect to each other. Linear superposition of waves can be described as a wave spectrum defining the amplitude of waves for frequencies and directions.

For larger waves, generally occurring at low probabilities (long return periods), waves are not linear. Interactions of wave components of differing frequencies and directions change the shape of the waves, an effect being that higher wave crests occur compared to those estimated using linear wave assumptions. In intermediate and shallow water depths, the nonlinearity of the waves increases and becomes very important.

Waves can be described as either:

- a sea state, defined by either the frequency-direction wave spectrum or the frequency spectrum (see 8.3) or
- an individual wave, defined by wave height (or crest height), period, and water depth (this wave is also called a deterministic or single wave) (see 8.4).

In a sea state, the wave energy can be distinguished into two broad classes: wind-seas and swells. Wind-seas are generated by the local wind, whereas swells consist of wind-driven waves that have travelled out of the generation area and have no relationship with the local wind.

The range of wave conditions that can occur at the site of the structure shall be specified. For operational conditions, details of the occurrence and joint occurrence of wave heights, periods, directions, spectral shape, and spreading of waves shall be specified. For extreme or abnormal conditions, the return-period values of waves shall be specified. Associated values and ranges of wave periods and water depths shall also be specified.

It can be required to partition the wave energy spectrum into swell and wind sea components.

In determining the operational, extreme, or abnormal wave conditions, the physical processes that lead to the wave forms at the site shall be assessed. In this respect, nonlinear effects can be significant (e.g. breaking).

The response of a structure to waves depends on, among other things, its dynamic response characteristics. Structures with significant dynamic response (i.e. natural periods around the wave frequencies or their second-order components) require wave energy spectra or time series of the surface elevation for their analysis. These can be specified in a number of ways; a common approach is to use a sea state defined by a standard wave frequency spectrum, with a given significant wave height, a representative frequency/period, a mean wave direction, and, sometimes, a directional spreading function. It is important to define the range of wave conditions that can be experienced at the facility site.

For structures that only respond in a quasi-static manner, it can be sufficient to use individual periodic waves. The most important wave parameters required to describe a single, periodic design wave are its height, crest elevation above still water level, period, and direction of travel. The wave kinematics properties can then be estimated using the local still water depth. The distribution of individual waves in a given sea state can be estimated from statistical wave parameters, such as the significant wave height and the mean zero-crossing period.

In some applications, periodic or regular waves may be used as an adequate abstraction of a real sea for design purposes. Periodic waves are also the building blocks for the linear random wave model. Where closer agreement to real waves is required, fully nonlinear wave models are available for use, but require careful calibration for application to design conditions to ensure that consistent structural reliability levels are achieved.

It is often desirable to specify the duration associated with sea states. Traditionally, 3 h durations are often specified. However, durations actually depend on the particular weather situation and how the criteria will be applied to design. In differing parts of the world, significant wave heights near the peak of a storm can be nearly constant over durations that could either be significantly shorter or significantly longer than 3 h. Furthermore, if the intention of specifying a duration is to design to a response at a given N -year target return period level, then the duration necessary to achieve this response shall be carefully determined. The N -year response is not necessarily achieved during the peak of the N -year sea state. The most rigorous way to ensure that the N -year response is achieved is through a response-based design approach.

8.2 Wave Actions and Action Effects

Wave conditions shall be specified in an appropriate way for the type of structure under consideration, for extreme, abnormal, and normal (operating) conditions.

The linear spectral model for waves is presented in 8.3. Regular periodic wave models are presented in 8.4. The height of the highest wave crests in extreme and abnormal metocean conditions can be of special significance (see 8.7).

Procedures for determining actions and action effects caused by waves for different types of structure shall be in accordance with the relevant structure-specific standard in the ISO 19900 series of publications.

8.3 Sea States—Spectral Waves

8.3.1 Wave Spectrum

The sea state can be described in terms of the linear random wave model by specifying a wave spectrum that defines the energy in different frequency and/or direction bands. In most cases, the wave spectrum is represented by empirical equations defining the distribution of energy over frequency and/or direction. Parameters typically required for defining a wave spectrum for design are the significant wave height and a representative frequency or period. For many applications, wave direction, wave spreading, and peakedness of the wave spectrum are also required.

There are several standard wave-frequency spectra in use; the most appropriate spectral form depends on the geographical area, the severity of the sea state, and the application concerned.

Wave spectra may be determined from site-specific measurements and numerical wave modelling. Use of wave spectra from measurements generally provides the more accurate description of the spectral content of the sea state and should be used in preference to numerical models to define ambient spectral shapes and extreme spectral shapes. Spectral fitting to measured spectra is generally required for application to design, although in some cases this will not be adequate and measured spectra should be recommended for direct application to design (e.g. where the wave spectrum is used to drive response models within a response-based approach).

Spectral fitting should be used to define spectral shapes with parametric forms of wave spectrum, and the parameters of the selected spectral shape should be defined as part of the ambient and extreme design metocean conditions.

Further discussion and guidance on wave spectra and the most common parametric forms for the wave spectrum are given in A.8.3.1.

8.3.2 Directional Spreading

As the water surface elevation in a sea state is in reality three-dimensional (short-crested), the wave frequency spectrum may be supplemented by a directional spreading function. Parametric forms for the wave directional spreading function are given in A.8.3.

The wave directional spreading factor can be modified, if justified, to account for spatial effects.

8.3.3 Wave Periods

The spectral description of waves requires specification of a representative wave period, for example, the peak spectral wave period. For consistency, other wave periods such as the average zero-crossing period should be computed from the spectrum.

8.3.4 Wave Kinematics—Velocities and Accelerations

Linear (or Airy) theory is a first-order approximation for real waves. It is based on a linearization of the free-surface boundary conditions and as such is only valid for waves of low steepness.

Wave kinematics may be determined from a wave spectrum by linear superposition of the individual components of wave velocity and acceleration. However, extrapolation of the kinematics associated with the higher frequency components into the crest of a wave can lead to significant errors. This is often referred to as “high frequency” contamination. Commonly applied engineering approximations avoid this by stretching the kinematics to the instantaneous free surface; for example, using linear stretching [also known as Wheeler stretching (see A.9.4.1) or Delta stretching (see A.8.4)]. These approximations can be nonconservative and so should only be used where their application can be shown to be justified.

Better approximations are recommended and are provided by nonlinear wave models (see 8.6).

8.4 Regular (Periodic) Waves

8.4.1 General

A single regular (periodic) wave can be defined by characteristic parameters, for example, height and period. Water depth is also required. The characteristic parameters should be chosen to suit both the wave theory to be applied and the loading recipe. For example, when applying a “Stokes’ fifth wave theory” approach within the context of the API 2A-WSD loading recipe (for fixed jacket platform design), the height and period should be the zero-downcrossing height and period.

For determination of actions by individual waves on structures, a nonlinear periodic wave theory may be used with a calibrated loading recipe. Calibrated loading recipes for drag-dominated structures are coded in typical loading software. Stokes’ fifth wave theory is commonly used for these types of structure. Other wave theories, such as Extended Velocity Potential and Chappelar theory, may also be used, if used with a loading recipe calibrated for these wave theories. An appropriate order of numerical solution shall be selected as appropriate to the water depth, wave height, and wavelength.

As an alternative to periodic wave theories, representative waves from a random sea derived with wave theories such as New-wave theory may be used. The New-wave is a representation of the most probable waveform of an extreme wave in a linear random sea. To ensure approximate parity of actions caused by different design waves, the crest elevation in New-wave shall then be taken as 5/9 times the wave height used in Stokes’ fifth-order or stream function theory. Experience has shown that Delta stretching should be used with New-wave.

In addition, realistic representation of ocean waves is possible with fully nonlinear numerical wave models, but their use in the calculation of design actions shall be calibrated.

8.4.2 Wave Period

The period of the regular (periodic) wave should be established to be consistent with the sea state(s) in which the wave is likely to exist.

8.4.3 Wave Kinematics—Velocities and Accelerations

Wave particle velocities and accelerations for periodic waves may be calculated using an appropriately selected wave theory.

Discussion on the wave theories, range of convergence, and references is given in A.8.4.

Most periodic wave theories do not account for wave directional spreading in their kinematics. Where appropriate, directional spreading can be approximately modelled in periodic waves by multiplying the horizontal velocities and accelerations by a wave directional spreading factor ϕ (see A.8.3).

8.4.4 Intrinsic, Apparent, and Encounter Wave Periods

Wave periods appear to differ depending on the relative velocities of wave propagation and the reference frame of an observer. This is due to the Doppler effect. For example, an observer moving against the direction of the waves encounters successive wave crests more quickly than an observer travelling in the same direction as the waves.

When waves are superimposed on a (uniform) current, the intrinsic reference frame for the waves travels at the speed and in the direction of the underlying current.

Three particular situations are as follows.

- An observer travelling at the same speed and in the same direction as the current is stationary with respect to the intrinsic reference frame and will therefore measure the intrinsic wave period T_i .
- An observer on a fixed structure is stationary relative to the seabed and measures the apparent wave period, T_a . If the waves are travelling in the same direction as the current, approaching wave crests pass the structure more quickly than if there was no current and consequently the apparent period is shorter than the intrinsic period. Similarly, if the waves are travelling against the current, the apparent period is longer than the intrinsic period. If there is no current, the fixed structure is stationary with respect to the intrinsic reference frame and hence $T_a = T_i$.
- An observer on a moving vessel (having a velocity relative to the seabed) measures the encounter wave period, T_e . The difference between T_e and T_i depends on the relative speeds and directions of the moving vessel and of the current. If the moving vessel is travelling at the same speed and in the same direction as the current, then $T_e = T_i$.

See A.8.4 for the relationship between T_i , T_a , and T_e .

Wave kinematics for the calculation of actions caused by waves shall be derived from the intrinsic wave period (or the intrinsic wave frequency).

8.5 Maximum Height of an Individual Wave for Long Return Periods

If regular (periodic) waves are adequate for use as a design wave for an offshore structure, the height of an individual wave with the specified return period, H_N (e.g. H_{100} for a 100-year return period and 0.01 annual probability of exceedance) shall be used. The data derived from measurement programmes or provided directly from hindcasts are time series of significant wave height and mean zero-crossing period (or spectral peak period). The required long-term individual wave height, H_N , (or crest height) shall be established by convolution of long-term distributions derived from these data with a short-term distribution that accounts for the distribution of individual wave heights in a sea state. Calculation of the wave in this manner differs from the calculation of the expected maximum wave in a sea state, which normally results in a nonconservative wave height (or crest elevation).

8.6 Nonlinear Wave Models

Either linear spectral waves or periodic waves are commonly applied in the design of offshore and coastal facilities. However, these representations are an abstraction of real ocean waves. Linear spectral representations ignore the nonlinear interactions between waves of different frequencies and directions, whereas periodic waves ignore the irregular nature of waves. The linear random wave models and

regular waves most often used for design and analysis are convenient approximations. However, they are not always very accurate in defining the position of the free surface, kinematics beneath the surface, or, in consequence, local or global actions. Neither regular nor linear random wave theories give the correct elevation of the wave crest or kinematics over the water column.

Real ocean surface waves are random, broad-banded, directionally spread, and nonlinear. Thus, for many purposes, a more accurate nonlinear carefully calibrated random wave model can be helpful, or even essential.

In practice, the extension of spectral representations to second order provides an adequate approximation of the surface profile and kinematics of moderately steep waves. Examples of where a second-order spectral model can be inaccurate and where a fully nonlinear model is a better choice include the calculation of loads during the inundation of the deck of a platform by green water and the calculation of wave forces on a fixed structure in very steep waves.

8.7 Wave Crest Elevation

Distributions of extreme and abnormal crest elevations that account for the nonlinear nature of large-amplitude waves are required for setting minimum deck heights on bottom-founded structures and for assessing the probability of green water intruding onto the topsides of all types of structures, decks, and hulls that are intended to be kept above the waves.

For structures where there can be significant wave-structure interaction (e.g. for structures with a caisson or with very large diameter legs), the possible enhancement of the crest elevation due to the presence of the structure shall be determined. This enhancement often does not lead to large increases in the global actions on the structure, but can impose significant local pressures on the underside of the topsides. It can also impede operations (particularly under-deck), and local measures to reduce its effect can be necessary.

The statistics of wave crest elevation may be determined for a single point in space (i.e. point statistics). However, the elevations within finite areas (e.g. platform deck area) are exceeded at higher probability than provided by the point statistics. For structures that are sensitive to exceedance of airgap, consideration should be given to this increased probability of exceedance in assessing the structural reliability to be achieved or implied by the relevant code.

9 Currents

9.1 General

Currents affect the design, construction, and operation of offshore structures in various ways. In addition to their impact on the environmental actions and action effects on the structure, they affect the location and orientation of boat landings and fenders, can create sea floor scouring, and often have an adverse effect on operating practices. All of these factors can influence the structure's design.

The current velocity generally varies through the water column. Information on the vertical profile is given in 9.3. Where currents co-exist with waves, the current profile is stretched and compressed with the water surface elevation; guidance on current profile stretching is provided in 9.4. Currents can also be modified by partly transparent structures (see 9.5).

9.2 Current Velocities

Like wind, current speeds vary in space and time but at much lower rates. Therefore, currents may generally be considered as a steady-flow field in which velocity is only a function of depth.

The total current velocity is composed of tidal currents, resulting from astronomical forcing, and residual currents. The components of the residual current can include circulation and storm-generated currents, as

well as short- and long-period currents generated by various phenomena such as density gradients, wind stress, and internal waves.

Depth-averaged tidal currents are regular and predictable. Circulation currents are relatively steady, large-scale features of the general oceanic circulation. Examples include the Gulf Stream in the Atlantic Ocean and the Loop Current in the Gulf of Mexico, where surface velocities can be in the range of approximately 1 m/s to 2 m/s. While relatively steady, these circulation features can meander and intermittently break off from the main circulation feature to become large-scale eddies or rings, which then drift at a speed of a few kilometers per day. Velocities in such eddies or rings can approach or exceed that of the main circulation feature. These circulation features and associated eddies occur in deep water beyond the shelf break, but in some areas of the world they can affect shallow water sites.

Storm-generated currents are caused by the wind stress and atmospheric pressure gradient throughout a storm. Storm current velocities are a complex function of the storm intensity and meteorological characteristics, bathymetry and shoreline configuration, and water density profile. In deep water along open coastlines, surface storm currents can be roughly estimated to have velocities up to 3 % of the 1 h-sustained wind speed during storms. As a storm approaches the coastline and shallower water, the storm surge and current can increase, and after a storm has passed inertial currents can persist for some time.

Sources of information about the statistical distribution of currents and their variation with depth through the water column are generally scarce in most areas of the world. To avoid encountering problems during early phases such as exploration drilling, concerted measurement campaigns are required to acquire the data, particularly in remote, deep water areas near the edges of continental shelves. In deep water areas (water depths typically greater than 200 m) such as in the Gulf of Mexico and along the northern and eastern coasts of South America, currents are a major consideration in carrying out offshore operations and in the design of structures.

The variation of current velocity with depth shall be determined by an experienced metocean expert.

9.3 Current Profile

The variation of current speeds and directions through the water column shall be determined for the specific location of the structure, taking into account all available information. In general, current profiles vary in strength and direction through the water column. Where the density does not vary significantly through the water column, the direction of the current velocities over the full water column is usually relatively uniform and simple profiles are appropriate; guidance is provided in A.9.3. Where the density varies through the water column, or different water masses flow into the region, more complex current profiles are common.

9.4 Current Profile Stretching

Current speeds and current profiles are determined for still water conditions, although in some situations they are applicable to storm conditions. The current profile is modified by the presence of waves, with a component of the current being present throughout the water column from sea floor to free water surface (between wave crest and wave trough).

Wave kinematics, adjusted for directional spreading where appropriate, shall be vectorially combined with the current velocities and adjusted for blockage where appropriate (see 9.5). As the current profile used in design is specified only up to the storm still water level, the profile to the local instantaneous wave surface shall be modified by some means (see A.9.4).

9.5 Current Blockage

The current velocity around and through a structure is modified by blockage. The presence of the structure causes the incident flow to diverge, with some of the flow going around the structure rather than through it. For structures that are more or less transparent, the current velocities within the structure are reduced from the free-stream values.

The degree of blockage depends on the type of structure. For dense, fixed-space frame structures, it will be large, whereas for some types of transparent floaters it will be very small. More specific advice for the treatment of current blockage for different types of structure is given in the relevant structure-specific standard in the ISO 19900 series of publications.

10 Other Environmental Factors

10.1 Marine Growth

Marine growth on submerged structural components and other parts of a structure can have a significant influence on the hydrodynamic actions to which the structure is exposed.

The influence of marine growth on hydrodynamic actions is due to increased dimensions and increased drag coefficients due to roughness, as well as to the increased mass and its influence on dynamic response and the associated mass inertial forces. Where sufficient information is available, the loading coefficients may be selected based on the nature of the marine growth.

Structural components can be considered hydrodynamically smooth if they are either above HAT or sufficiently deep such that marine growth is sparse enough to allow its effect on roughness to be ignored. However, caution should be exercised, as a small increase in roughness can cause an increase in the drag coefficient to a level similar to that corresponding to a rough surface.

The type and thickness of marine growth varies with depth and depends on location, the age of the structure, and the maintenance regime. Experience in one area of the world cannot necessarily be applied to another. Where necessary, site-specific studies shall be conducted to establish its likely type, thickness, and depth dependence.

More specific advice for the different types of structure is given in the relevant structure-specific standard in the ISO 19900 series of publications.

10.2 Tsunamis

Tsunamis are water waves caused by impulsive disturbances that displace a large water mass in the sea. The main disturbances causing tsunamis are earthquakes, but they can also be generated by seabed subsidence, landslides, underwater volcanic eruptions, nuclear explosions, and even impacts from objects from outer space (meteorites, asteroids, and comets). Their wavelength is several tens of kilometers and they have periods in the range of 5 min to 100 min. Their speed of propagation across the ocean is a function primarily of water depth; in the deepest oceans tsunami waves can travel at speeds of several hundred kilometers per hour.

In deep water, tsunamis have a low height and very long period and pose little hazard to floating or fixed offshore structures. Tsunamis contain more energy when they are generated in deeper water, and can be extremely destructive when they impact the coast. When they reach shallow water, the wave form pushes upward from the bottom to create a rise and fall of water that can break in shallow water and wash inland with great power.

The greatest hazard to offshore structures from tsunamis results from inflow and outflow of water in the form of waves and currents. These waves can be significant in shallow water, causing substantial actions on structures. Currents caused by the inflow and outflow of water can cause excessive scour problems.

Tsunamis travel great distances very quickly and can affect regions that are not normally associated with the disturbances that cause them. The likelihood of tsunamis affecting the location of the structure shall be determined.

10.3 Seiches

Coastal measurements of sea level in semi-enclosed bodies of water often show seiches with amplitudes of a few centimeters and periods of a few minutes due to oscillations of the local harbor, estuary, or bay, superimposed on the normal tidal changes. Normally, variations are small enough offshore that they can be ignored, but if a structure is located in shallow partly enclosed seas, the effect of seiches should be considered.

10.4 Sea Ice and Icebergs

Sea ice and icebergs can affect the design and operation of structures. Before commencing design for, construction of, or operations on structures in areas that are likely to be affected by sea ice and icebergs, adequate data shall be collected in accordance with ISO 19906 and may include:

- seasonal distribution of sea ice;
- distribution and probability of ice floes, pressure ridges, and/or icebergs;
- effect of ice-gouges on the seabed from icebergs or ice ridges;
- type, thickness, and representative features of sea ice;
- drift speed, direction, shape and mass of ice floes, pressure ridges and/or icebergs; and
- strength and other mechanical properties of the ice.

These data shall be used to determine design characteristics of the structure, as well as possible evacuation procedures.

For specific provisions for sea ice and icebergs, see ISO 19906.

10.5 Snow and Ice Accretion

Where relevant, snow accumulation and ice accretion shall be included in the design of structures.

An estimate shall be made of the extent to which snow can accumulate on the structure and topsides, and of its possible effect on the structure.

Topsides icing can increase the diameter of structural components and can lead to a substantial increase in actions caused by wind and gravity, particularly for long, slender structures such as flares. Topsides snow and icing can also adversely affect the stability of floating structures and the operation of emergency equipment.

Icing from sea spray, freezing rain or drizzle, freezing fog, or cloud droplets shall be included in the design.

For specific provisions for snow and ice accretion, see ISO 19906.

10.6 Miscellaneous

Depending on circumstances, other environmental factors can affect operations and can consequently influence the design of structures. Appropriate data shall be compiled, including, where appropriate, records and/or predictions of:



- air temperature (maximum and minimum where appropriate);
- barometric pressure;
- cloudiness and cloud base levels;
- humidity;
- lightning;
- precipitation;
- salinity;
- seawater composition;
- sea temperatures;
- solar radiation;
- visibility;
- wind chill;
- phenomena specific to arctic and cold regions (see ISO 19906).

11 Collection of Metocean Data

11.1 General

Offshore metocean monitoring systems can vary from simple weather stations for aviation purposes, to complete data acquisition systems incorporating a wide range of sensors and sophisticated data processing, display, storage, and transmission features. By providing real-time information for operational use and long-term records for engineering design purposes, offshore metocean monitoring systems play an important role in ensuring safe offshore operations.

This standard is intended as an initial reference for offshore operators when planning metocean monitoring equipment on offshore installations. It provides guidance on both possible statutory requirements and the operator's own requirements, spanning applications such as weather forecasting, climate statistics, helicopter traffic, tanker loading, marine operations, etc.

The collection of metocean data is normally the result of requirements imposed by a regulator or other authority, and the operator's own needs. When specifying a metocean data collection system, the operator shall cater for the requirements of each of these organizations where they differ from those presented herein.

11.2 Common Requirements

11.2.1 General

Procedures that ensure the proper functioning of the measuring and recording systems described herein, as well as instrument accuracy and calibration, shall be established and maintained.

Qualified personnel shall carry out observations, select, install, check, and maintain the equipment and repair any faults or malfunctions. Service and calibration intervals on equipment shall be a maximum of 1 year. When new types of instruments are introduced, notification shall be given to all regular receivers of data.

Time references given in local or UTC (universal time coordinate) shall be recorded together with the measured data or derived parameters. The time reference should not be dependent on a manual resetting following a temporary cessation in operation of the system. Local user interfaces should clearly show both UTC and local time.

11.2.2 Instrumentation

The accuracy, range, type, and location of the instruments should be determined with due regard to the purpose of the recordings.

11.3 Meteorology

11.3.1 General

Information concerning instrument accuracy and calibration requirements shall be established.

Data that cannot be measured by means of instruments shall be obtained by observation by qualified observers. Observers shall have completed relevant meteorological observer training. Consideration shall be given to suitable refresher training for observers to comply with local regulations.

11.3.2 Weather Observation and Reporting for Helicopter Operations

The specifications provided herein address only metocean conditions and do not constitute a complete system for offshore helicopter operations. The relevant local helicopter regulations shall be applied in order to ensure that all necessary aspects are covered.

A complete aviation routine weather report is specified in WMO-No. 306, under code FM 15-XV Ext. METAR. The data are transmitted in a "message" that consists of information derived from instrumental measurements and manual observations taken by a qualified observer.

The parameters included are as follows:

- wind direction;
- wind speed;
- visibility [according to METAR specifications, and runway visual range (RVR) if available];
- weather;
- cloud;
- dew-point temperature;
- air temperature;
- air pressure (QNH—barometric pressure adjusted to sea level);
- significant wave height;
- sea surface temperature.

The wind measurements from the top of derrick are normally not representative for the wind field at the helicopter deck. A separate wind sensor shall be installed near the helideck to measure values representative for the wind field at the helicopter deck. This requirement may be waived if it can be clearly demonstrated that this is not necessary.

11.3.3 Weather Observation and Reporting for Weather Forecasting Services

A complete weather observation report is specified in WMO-No. 306 under code FM 13-XIV Ext. SHIP. The message consists of information derived from instrumental measurements and manual observations taken by a qualified observer.

The parameters included are as follows:

- wind direction;
- wind speed;
- air pressure;
- air temperature;
- sea surface temperature;
- humidity;
- wave height;
- wave period;
- clouds;
- visibility [meteorological optical range (MOR)];
- weather;
- icing.

Observations shall be made at standard synoptic hours, expressed in terms of UTC at which, by international agreement, meteorological observations are made simultaneously throughout the globe. Standard synoptic hours are 00, 03, ... 21 UTC. The observations shall be recorded in accordance with WMO-No. 306, under code FM 13-XIV Ext. SHIP (Section A, pp. 7–24).

11.3.4 Weather Observation and Reporting for Climatological Purposes

In addition to the data collected for the weather report (SHIP format), the wave parameters of maximum wave height, peak period, and wave direction shall be included if available. The normal recording interval shall be 1 h as a minimum, although more frequent recording is recommended, and the resolution of the data shall be in accordance with the instrument accuracy.

11.4 Oceanography

11.4.1 General

In the context of this standard, the term “oceanography” shall encompass:

- ocean currents at specified depths;
- water level;
- sea temperature at specified depths;
- salt content (salinity) at specified depths;
- oxygen content at specified depths;
- icebergs, their size, and drift;
- sea ice.

Ocean waves and sea surface temperature are defined as part of meteorology and covered in 11.3.

Apart from ocean currents and water level, the measurements and observation of oceanographic parameters are not commonly included in platform metocean systems. The operators shall, however, consider their own need for collecting such data contingent upon the natural conditions at the location, the inadequacy of the database, the type of structure or installation, and the operational situation of the facility.

11.4.2 Measurements and Observations

Ocean currents should be measured at fixed depths (or bins) and include at least three depths in shallow waters: near-surface, mid-depth, and near-bottom. For measurements in deeper waters, more measurement depths are recommended to capture the spatial variability of currents with depth. The observation of sea ice and icebergs (size and drift), can be performed by combining, e.g. manual observations, instrument recordings, and remote sensing.

11.5 Data Quality Control

Procedures shall be established to ensure that collected data are processed and standard analyses carried out in such a way that the quality of the data can be verified. The analyses should be sufficiently extensive to allow all significant errors to be discovered. The data should be compared to other recorded data, to the extent this is practicable.

Local regulations can require the provision of metocean data and/or reports to a regulatory body or agency at regular intervals. Careful consideration shall be given to how these requirements will be met by the observation system and its operation.

12 Information Concerning the Annexes

12.1 Information Concerning Annex A

The clauses in Annex A provide additional information and guidance on clauses in the body of this standard. The same numbering system and heading titles have been used for this informative text for ease in identifying the subclause in the normative text to which it relates.

12.2 Information Concerning the Regional Annexes

The annexes subsequent to Annex A present an overview of various regions of the world for which information has been developed by experts on each region, and is intended to supplement the provisions, information, and guidance given in the main body and Annex A of this standard. They also provide some guidance relating to the particular region dealt with in each annex, as well as some indicative values for metocean parameters that can be suitable for conceptual studies. However, site- or project-specific metocean parameters shall be developed for structural design and/or assessment.

Annex A (informative)

Additional Information and Guidance

NOTE The clauses in this Annex provide additional information and guidance on the clauses in the body of this document. The same numbering system and heading titles have been used for ease in identifying the subclause in the body of this document to which it relates. Guidance is only offered on the identified clauses.

A.1 Scope

Environmental conditions generally have a significant influence on the design and the construction of offshore structures of all types. In some areas of the world, the prevailing environmental conditions can also have an influence on the operational aspects of a structure, which in turn can affect the design of the structure.

The environmental conditions and metocean parameters discussed herein relate to the pre-service, the in-service, and the removal phases of structures.

It is beyond the scope of this standard to provide detailed instructions that can be followed to produce reliable estimates of extreme or abnormal conditions in all areas and in all cases.

Requirements for the calculation of environmental actions on offshore structures and the resulting action effects are given in ISO 19902 for fixed steel structures, ISO 19903 for fixed concrete structures, ISO 19904-1 for floating structures (monohulls, semi-submersibles, and spars), ISO 19905-1 for site-specific assessments of jack-ups, ISO 19906 for arctic offshore structures, and ISO 19901-3 for topsides structures.

A.5 Determining the Relevant Metocean Parameters

A.5.1 General

The design parameters should be chosen after considering all of the relevant service and operating requirements for the particular type of structure.

Selection of environmental conditions and the values of the associated parameters should be made after consultation with both the structure designer and appropriate experts in oceanography, meteorology, and related fields. The sources of all data should be noted. The methods used to develop available data into the desired metocean parameters and their values should be defined.

General information on the various types of environmental conditions that can affect the site of the structure should be used to supplement data developed for normal conditions. Statistics can be compiled giving the expected occurrence of metocean parameters by season, direction of approach, etc.

Of special interest for the planning of construction activities, platform operations, and evacuation are the duration, the speed of development, the speed of movement, and the extent of storm conditions. The ability to forecast storms in the vicinity of a structure is very important.

If the amount of metocean data available is very limited (particularly in the early phases of a project), the extreme and abnormal metocean conditions should be derived conservatively. If, in the judgement of the metocean expert, there is considerable uncertainty in the data, the extremes should be set too high rather

than too low. A subsequent increase in extreme values later in a project can have both safety and economic consequences^[1].

Figure A.1 presents an overview of the process involved in developing metocean parameters.

A.5.2 Expert Development of Metocean Criteria

It is important to select a metocean expert(s) with experience in all facets of the process; this includes the hardware and software associated with data gathering (in situ or remote sensing), hindcasting procedures, data sampling and analysis procedures, and extreme statistical analysis techniques.

The approach used to determine metocean parameters is often dictated by the available data (measured, continuous, storm hindcasts, ship's visual observations, satellite, radar, etc.). Understanding of the methods used to record and analyze the data is critical, as is knowledge of how these methods and data can influence the selection of an analysis approach or possibly bias the result. A sound understanding of the data techniques is necessary in order to be able to account for them during interpretation of the data sets and to apply any corrections that could be necessary to the final estimates.

Given a suitable database of measured and/or hindcast data, it is important to investigate the sensitivity of estimates to the use of different data sets (measured or hindcast) and statistical analysis procedures. It is important that the design engineer who will use the metocean parameters is aware of the uncertainty (preferably by a quantitative assessment) in the parameters provided. Relatively small changes in design estimates can significantly affect the reliability of offshore structures. However, given reliable long-term data sets, the various statistical approaches should tend to similar results.

A.5.3 to A.5.9 provide brief general descriptions of the principal considerations for deriving safe, reliable metocean parameters to support the design and operation of different types of offshore structures.

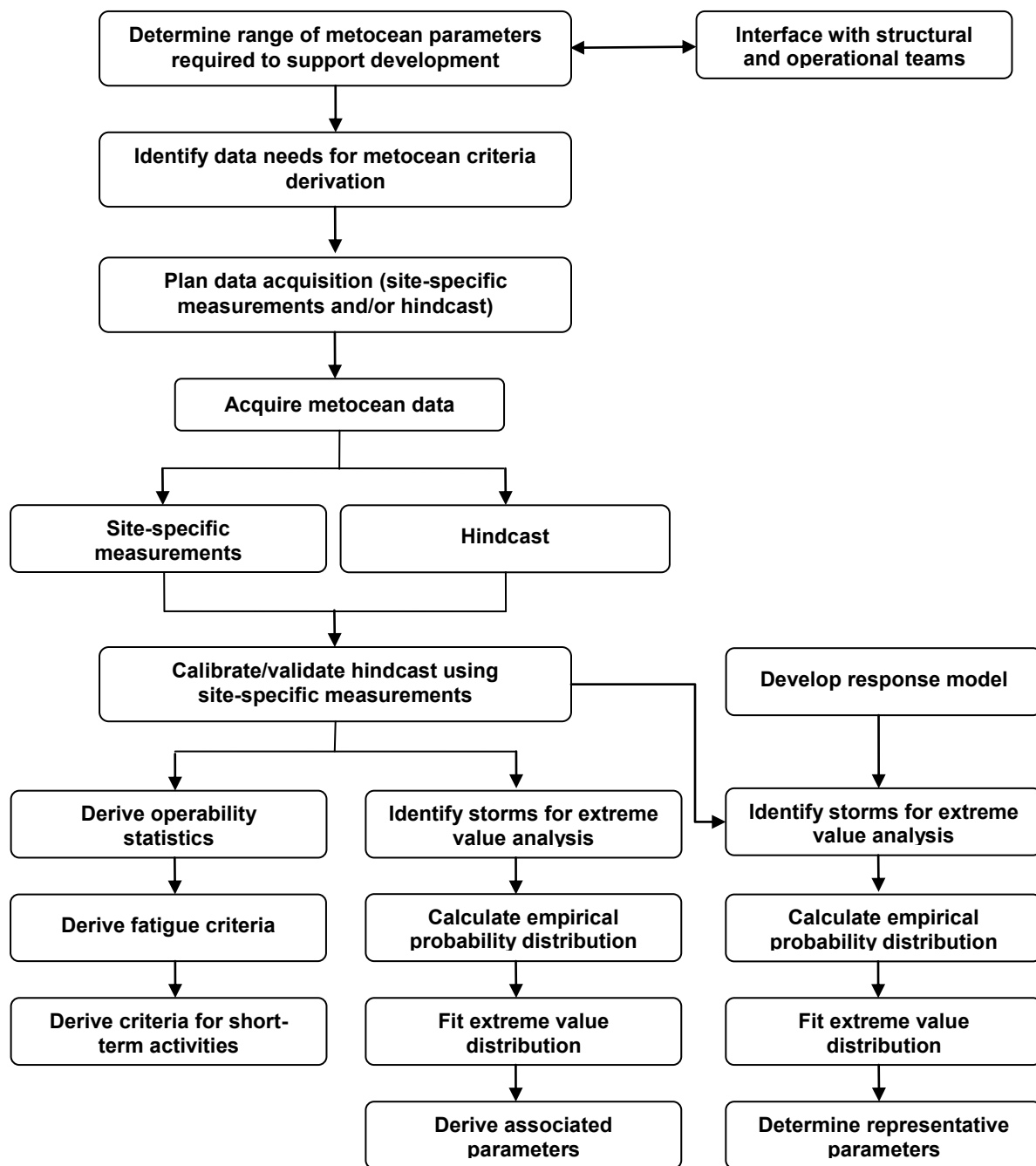


Figure A.1—Overview of the Process of Producing Metocean Parameters

A.5.3 Selecting Appropriate Parameters for Determining Design Actions or Action Effects

The design or site assessment of structures is often governed by extreme actions or extreme action effects caused by the local environment conditions. The conditions appropriate to design or site assessment are usually quantified in terms of the metocean parameters (e.g. a combination of extreme wave height, current, and wind velocity) or the action effect (e.g. global bending moment on a hull).

The traditional approach to offshore structural design and assessment required the use of a predetermined set of metocean parameters (e.g. 100-year wave plus associated current). This type of

approach is still widely used, its advantage being that the metocean parameters are well defined and understood, they can be determined prior to the detailed structural model being finalized, and the design process is simplified (in particular, the metocean parameters do not normally need to be revisited during detailed design). The disadvantages are that it does not tend to provide an optimized structure, nor does it facilitate the use of reliability- or risk-based approaches.

The shift in emphasis toward reliability-based approaches has led to the increased use of response-based methods. These require the determination of the N -year response or action effect (e.g. the 100-year overturning moment of a jacket structure or the bending moment of a drilling riser). An appropriate set of metocean conditions that result in the 100-year response can then be determined.

Reliability-based approaches provide a more rational basis on which to design or assess any structural form, in particular those that respond to complex combinations of metocean actions. However, they usually require a closer interaction between the metocean and structural models and experts, and if used to their full potential, the development of detailed structural response models.

The term “100-year storm” has no meaning except as an informal description of a set of conditions that introduce the parameter or action effect.

The return period in years, for larger values of return period, can be taken as the inverse of the annual probability of exceedance of a parameter (e.g. a wave height or wind speed).

Parameters appropriate to the design or assessment of different forms of offshore structure are provided in the relevant ISO publication:

- ISO 19901-3 for topside structure;
- ISO 19902 for fixed steel offshore structures;
- ISO 19903 for fixed concrete offshore structures;
- ISO 19904-1 for floating offshore structures;
- ISO 19905-1 for site-specific assessment of mobile offshore units;
- ISO 19906 for arctic offshore structures.

Three methods are discussed below for defining an environment that generates the extreme direct action and, generally, also the extreme action effect, caused by the combined extreme wind, wave, and current conditions. Other methods are possible.

- a) Specified return-period wave height (significant or individual) with “associated” wave period, wind, and current velocities. A similar methodology can be applied where a parameter other than wave height dominates the action effect.

This has been the established practice for deriving wind and current extremes occurring simultaneously with the wave height in some areas (e.g. USA). The specified return period is usually 100 years. It has also been used for deriving secondary parameters (such as wave periods) in the North Sea. The “associated” wave period, current, or wind is the value estimated to co-exist with the specified return-period wave height. The method is applicable if:

- there is a statistically significant correlation between the associated value and the specified return-period wave height, and
- the extreme global environmental action on the structure is dominated by waves.

In the case where a structure's responses are dominated by waves, one way of developing the associated value of a particular parameter is to find a (positive) correlation between the parameter and the wave height. For example, assume a model hindcast has been made in a region dominated by tropical storms. To find the associated current, one can develop a regression plot of the modelled significant wave height versus current velocity at or near the peak of each storm. To account for directionality, the current component in line with the significant wave height can be used. Assuming this plot shows that the current is statistically correlated with the wave, an equation can be developed for the in-line current as a function of significant wave height. The associated current is then the value given from the equation using the specified return-period significant wave height.

If there is not a strong correlation between waves and current or if the global environmental action is not wave-dominated, then there is no explicit confirmation in this method that the combination of the primary metocean parameter (here, wave height) and its associated parameters (here, current and wind velocities) will approximate to the return-period global environmental action on a structure. By contrast, method c) below, when correctly applied, will always provide a good estimate of the specified return-period global environmental action.

When the present method is used for structures that are sensitive to wave period, the most onerous combination of wave height and period can be at a different period from that associated with the maximum specified return period wave height. Consequently, a reasonable range of variations in both period and wave height should be investigated to determine the most onerous combination of wave height and period with the same, or higher probability of occurrence than the specified return period.

- b) Specified return-period wave height combined with the wind speed and the current velocity with the same specified return period, all determined by extrapolation of the individual parameters considered independently.

This method has been used in the North Sea and many other areas of the world, normally with a return period of 50 years or 100 years. A modified version, using the 100-year wave height and the 100-year wind speed combined with the 10-year current velocity, has been used in Norway.

The method is simple, independent of the structure, and can be determined from separate (marginal) statistics of waves, currents, and wind. It always yields results that are conservative compared to either of the two other methods for the same specified return period when used to determine design actions for fixed structures, but is not appropriate for floating and other types of structure with significant dynamic response.

- c) "Response-based analysis" that requires any "reasonable" combination of wave height and period, wind speed and current velocity that results in:
- the global extreme environmental action on the structure with the specified return period, or
 - a relevant action effect (global response) of the structure (base shear, overturning moment, floater displacement, etc.) with the specified return period.

This method involves calculating an associated current and wind speed using the wave height and one or several critical structural response functions (action effects), such as base shear or overturning moment on a fixed structure or horizontal displacement of a floating structure^[2-4]. Directional effects of wind, wave and current, and water-depth fluctuation due to tide and surge, are fully accounted for. Storms are treated as independent events, and short-term variability is taken into account. The long-term distribution of the structural response is then determined and from this its extreme and abnormal values. The same structural response function can be used to determine combinations of metocean parameters leading to the desired return-period extreme and abnormal responses. It should be noted that a set of parameters is not unique: several other related sets will produce the same result. In addition, the statistics can be used in the development of partial factors for environmental actions (action effects) as described below. Reference [2] describes the procedure in some detail.

Although this method can involve time and cost in developing software, it can provide a realistic set of design parameters—even if there is little correlation between waves, winds, and currents. Thus, defining the specified return-period action or action effect has a significant advantage over defining

the specified return-period wave height, either with associated or with specified return-period values of wind and current. The definition of the action or action effect should not use an arbitrary set of related wave, wind, and current values that satisfies the specified return-period global environmental action or action effect, but should make a “reasonable” (expected) choice so as to correctly model the probable spatial distribution of global hydrodynamic actions over the structure. Reasonably accurate combinations of metocean parameters can be deduced from observing the combinations that cause the greatest responses in the storms used in developing response statistics.

Care should be taken in the application of a response-based approach where the final concept remains to be fully defined.

Additional consideration should be given to obtaining extreme direct actions (action effects) for locations where there are strong currents that are not driven by local storms. Such currents can be driven by tides or deep-water currents, such as the Loop Current in the Gulf of Mexico or the Gulf Stream. In this case, method a) can be acceptable if the storm-generated conditions are the predominant contributors to the extreme global environmental action (action effect) and if the appropriate “associated” value of tidal and circulation currents can be determined. However, method c) is conceptually more straightforward and preferable. Method b) is the simplest method and ensures an adequate design environmental action (action effect); however, this can be very conservative compared to the true global environmental action (action effect) of the required return period.

For many areas, substantial databases are becoming available with which it is possible to establish statistics of joint occurrence of wind, wave, and current magnitudes and directions. When sufficient data are available, method c) above provides the most rigorous basis for estimating extreme action effects. The corresponding partial factors to be used in conjunction with the global environmental action (action effect) should be determined using reliability analysis principles, in order to ensure that an appropriate safety level is achieved. This approach provides more consistent reliability (safety) for different geographic areas than has been achieved by the practice of using separate (marginal) statistics of winds, currents, and waves.

A.5.4 The Metocean Database

There are various circumstances in which site-specific data from measurements or hindcasts should be analyzed in order to produce metocean parameters, including the following:

- where regulatory requirements insist on the use of site-specific data;
- where the operator has field data in addition to the data used in producing the environmental conditions presented in standard guidance documents;
- where environmental conditions are not provided in standard guidance documents or are otherwise deemed by an operator to be inappropriate;
- where an operator wishes to produce metocean parameters for return periods other than those available in standard guidance documents;
- where the structure’s response is such that available metocean data do not provide the basis for deriving appropriate metocean parameters (e.g. data to be used in the response-based analysis of a floating system).

A well-controlled series of measurements at the location of an offshore structure is a valuable reference source for establishing design situations as well as operating conditions and associated criteria. Because measurements taken over a short duration can give misleading estimates of long-term extremes, measurements are more often used to validate a hindcast over a longer period. However, care should be taken in comparing measured and hindcast data, in particular to address differences in:

- temporal averaging (e.g. 3 h hindcast H_s versus H_s derived from a 20 min measurement);
- spatial averaging (e.g. hindcast may deliver H_s over a 10 km × 10 km grid vs. a measured “spot” value).

The hindcast should be for as long a period as possible in order to capture the effects of climate variability—typically 20 years, ideally longer.

Producing long-period hindcast data sets of current can be difficult due to a lack of measured data, a lack of reliable data to drive the current models, or the inability of models to faithfully reproduce important dynamic processes in a region. In such cases, alternative means of addressing the impact of longer-term climatic variations should be considered. From a practical standpoint, this can require multi-year measurement campaigns to capture a sufficient number of severe current event episodes necessary for developing estimates of extremes.

Extremes derived from short-term site-specific measurements should be used in preference to any indicative values presented in standard guidance documents only if care is taken to adjust the records to reflect long-term variability.

Climatic variations during the design service life of structures can result in changes in:

- water level (mean, tide, and/or surge);
- frequency of severe storms;
- intensity of severe storms; and
- associated changes in the magnitude and frequency of extreme winds, waves, and currents.

Wave height depends on wind speed, direction, fetch, and duration, all of which are potentially affected by changes in intensity, frequency, and track of weather systems. The analysis of meteorological observations is affected by homogeneity problems in historical weather maps and data.

The various application(s) for the database should be considered when determining the type(s) of wave hindcast model calibrations that are most appropriate. For example, if a primary concern is to derive downtime estimates for tanker-offloading operations in a mild climate (e.g. through the use of persistence analyses), it is important to verify the accuracy of the database for low sea states with a broad range of wave periods and directions. If the database is also used for deriving fatigue estimates on deep-water fixed or on bottom-founded compliant structures, the database should be verified for the full dynamic range of significant wave heights (H_s) and wave periods (T_p or T_2) in order to derive representative directional wave scatter diagrams—perhaps together with estimates of directional associated current profiles.

If the database is used for establishing extreme design parameters, it is important to establish that the database is as long and as accurate as possible. A judgement should be made on the suitability of the design parameters that have been developed, e.g. with respect to how climatologically representative the available database is. Factors that should be considered include the time over which the data have been collected, and whether this time was climatologically normal in terms of the frequency and strength of storms.

When extrapolating metocean databases to low probabilities of exceedance, it is assumed that the database is representative of long-term conditions. This hypothesis should continue to be tested, and, if necessary, suitable allowances should be made to incorporate any residual uncertainty.

Reference [5] contains guidelines for safe practice for undertaking metocean and arctic surveys.

A.5.5 Storm Types in a Region

The definition of environmental conditions and the associated metocean parameters that can occur in different storm types is an important part of understanding the workability of various offshore operations, as well as determining the processes that will be needed to define the extreme and abnormal metocean parameters. For some areas, the definition of storm types is problematic, in particular in regions where tropical cyclones lose their identity and metamorphose into extra-tropical storms. Such storms can become very severe, and their characteristics during the transition are not yet well understood^[6]; the derivation of extreme and abnormal metocean parameters in such areas requires additional care.

A.5.6 Directionality

In locations where storm tracks, storm types, bathymetry, or surrounding coastal morphology lead to significant variations in the strength of winds, waves, and currents as a function of direction, it is often desirable to provide criteria by directional sectors. This can allow designers to optimize structures to local conditions. This can occur as structures are designed for strength but can also be important when specifying operational criteria so that flare tower and boat landings can be placed to optimize safe operation.

One common approach to providing directional criteria is to specify conditions in 45° sectors. Alternatively, sectors may be “naturally” defined based on the directionality inherent in measured or hindcast data. When this is done, criteria can be specified in as few as four or five sectors. The sectors do not need to be of uniform size, and in general none should be smaller than 45° to avoid “over-optimization.”

When directional criteria are specified, it is important to ensure that the overall reliability of the structure is not compromised by the use of such criteria. The metocean specialist can aid in this effort by discussing the assumptions, limitations, and appropriate use of directional criteria with the structural design team.

See Reference [7].

A.5.7 Extrapolation to Extreme or Abnormal Conditions

The problem of determining low probability values of metocean parameters has become even more important because of the recent trend to use very rare events to directly calculate the failure probability of a structure. It is becoming increasingly common for owners and regulators to require consideration of the 1000-year to 10,000-year events, i.e. the 10^{-3} and 10^{-4} annual nonexceedance probability, respectively. Great caution should be used in extrapolating data to such extremely low probabilities.

There are two basic methods for calculating low probability values: the historical method and the deductive method. Both have their strengths and weaknesses.

The historical method takes data, either from measurements or model hindcasts, and fits the tail (low probability region) of the probability distribution with appropriate extreme value distributions. This method is well documented in Reference [8].

The historical method is easy to apply. It requires simply using a curve-fitting routine (e.g. least squares or maximum likelihood) to fit an analytical expression (e.g. Gumbel, Weibull) to data originating from measurements or from a hindcast model. A disadvantage is that the statistical confidence in the extrapolated value rapidly decreases for return periods greater than two or three times the length of the database. It follows that extrapolations to very rare recurrence intervals of 1000 years or greater are speculative, given the length of commonly available data sets.

The deductive method begins by breaking the regional storm type into parameters whose probability can be determined from historical data, e.g. in the case of a hurricane this could be the radius to maximum wind, pressure deficit and forward speed. Synthetic storms are generated by combining the parameters accounting for their joint probability of occurrence. In the simplest case, where the parameters are statistically independent, the probability of a synthetic storm simply becomes the product of the probabilities of each of the storm’s parameters. In this way, very rare synthetic storms can be constructed using storm parameters with relatively high and statistically confident probabilities. Parameters that are statistically correlated complicate the analysis, but can be handled provided that the joint probability distributions can be deduced from the historical data. The main disadvantage of the deductive method is that it is time-consuming to apply, and in regions where storms are physically complicated it can be impossible to derive parameters that adequately describe the storms. The deductive method is applicable only if the extreme event is due to a rare combination of parameters that occur reasonably frequently within their individual distributions. Modelling such regions is a topic of ongoing research in the oil and gas industry.

Since the deductive method is relatively uncommon and its application in the oil and gas industry is still in its infancy, the remainder of this subclause relates to the historical method. Reference [8] provides a detailed discussion of how to apply the historical method.

When extrapolating data sets, the following recommendations and considerations are relevant:

- It has been argued that some distributions are theoretically superior to others. However, experience has shown that the most robust extreme estimates are obtained by finding the distribution that fits a subset of a reasonable number of the more extreme data points most closely, using an error-minimizing algorithm (e.g. maximum likelihood method).
- When fitting data, care should be taken not to mix data from one type of storm event (e.g. winter storms) with data from another type of storm event (e.g. hurricanes). The probability distributions of the two types of extreme event are often a strong function of the storm physics (storm type), and mixing storm types can lead to nonconservative estimates of the extremes; each storm type should be fitted separately and then the combined statistics computed.
- Fitting should include a sufficient number of storms to achieve statistical confidence in the fit.
- The statistical uncertainty in estimated extreme parameters increases as the extrapolation extends beyond the length of the data set. Metocean parameters with return periods up to a factor of three beyond the length of a statistically stationary data set can be estimated with some confidence. Where more extreme extrapolation is required, care should be taken to account for the increased level of uncertainty by, for example, providing a range of possible values and an indication of the confidence levels associated with each.
- Bias should be removed from the data, whether the data are from measurements or from hindcast modelling. Biased data can lead to substantial offsets in the estimates of rare events that can be nonconservative because of the extrapolation process. Scatter (noise) increases the confidence limits on the extrapolations and can introduce positive bias. The bias tends to increase as one extrapolates further beyond the data.
- Generally, it is preferable to extrapolate a noisy data set of longer duration rather than a shorter-duration cleaner data set. For example, a 50-year model hindcast data set to estimate the 100-year storm is preferred to a few years of measurements, even though the hindcast results can have more scatter than the measurements. This assumes that bias has been removed from both data sources. It is emphasized that any model used to extrapolate data should be carefully validated against available measurements.
- A variety of different techniques should be considered before deciding on an extreme value, e.g. the use of different thresholds, different distributions, annual maxima, peak-over-threshold and cumulative frequency distribution analyses.
- Estimates of rare events should be checked to make sure they do not exceed some limiting state imposed by physical constraints, e.g. the wave-breaking limit in shallow water.
- Confidence in estimates of rare events can often be improved by pooling data from nearby sites, especially in places where storms are sparse. Pooling is straightforward if the data source is a gridded hindcast model. There are other methods of reducing statistical uncertainty, such as averaging extreme estimates from adjacent sites, but research suggests that these can introduce bias and are inferior to pooling. Regardless of the method used, one should take great care to exclude sites that can be expected to be different from the site of interest because of a differing physical environment. For example, wave data from shallow-water sites should not be pooled with wave data from a substantially different water depth. The other concern with pooling is that if sites too close to one another are used, they will not provide independent realizations of the environment. Use of highly correlated nearby sites cannot only give a false sense of confidence in extremes, but the concern has also been expressed that use of correlated points can lead to a low bias in the tail of

the distribution. The optimal pooling distance depends on the storm type, storm length scale, and local physical constraints (e.g. fetch limits in the case of waves, proximity to slope for deepwater currents), so that optimal separation distances for site pooling need to be carefully considered on a case-by-case basis.

A.5.8 Metocean Parameters for Fatigue Assessments

A.5.8.1 General

Time-varying stresses in an offshore structure are due to time-varying actions caused by waves (with or without currents), gust winds, and combinations thereof. Time-varying stresses for a fatigue assessment are characterized by the number of occurrences of various magnitudes of stress range (maximum stress minus preceding or following minimum stress), in some cases supplemented by the mean value of the stress range. Determination of the relevant metocean parameters should take due account of the required characterization for each case.

A.5.8.2 Fixed Structures

Variable stresses during the in-place situation of fixed structures (either steel or concrete) are due to gust winds and waves, with or without the simultaneous presence of a current. The variable stresses caused by gust winds are normally small and, except for the design of some topsides components, can be neglected.

The effect of current is normally not taken into account, for the following reasons:

- current velocities co-existing with waves in other than extreme or abnormal environmental conditions are usually small and not in the same direction as the waves;
- the influence of current on stress ranges is generally much smaller than the influence on the maximum stress experienced.

The minimum requirement for the fatigue assessment of a fixed structure during the in-place situation is therefore an appropriate description of the site-specific wave environment during its design service life. This is ideally provided by the long-term joint distribution of the significant wave height (H_s), a representative wave period (T_z or T_p), the mean wave direction ($\bar{\theta}$), and the directional spreading around the mean wave direction. Wave-directional spreading is usually neglected or accounted for by a standard spreading function independent of the other three parameters (see A.8.3.2).

The long-term distribution should cover either the full duration of the design service life or the duration of a typical year. If annual distributions are used, it is assumed that the conditions during the typical year repeat themselves each year during the design service life. Seasonal distributions are not appropriate for fatigue assessments.

Where a deterministic fatigue assessment can be used for quasi-statically responding structures, the site-specific wave environment during the structure's design service life may be specified by the long-term marginal distribution of individual wave heights. This distribution can be derived from the wave scatter diagram.

Where VIV due to currents in the in-place situation are important, the long-term marginal distribution of site-specific current speeds should also be determined.

For VIV due to wind action in the pre-service condition, the long-term marginal distribution of sustained wind speeds during the construction period should be made available.

Where variable stresses due to gust winds cannot be disregarded (e.g. for separate support structures for vent stacks or flare towers), the two- or three-parameter wave scatter diagram should be replaced by a three- or four-parameter scatter diagram of the joint occurrence of waves and winds. In such special

cases, the waves are as usual specified by H_s and T_z or T_p , supplemented if possible by $\bar{\theta}$, whereas the wind is normally specified by the sustained wind speed U_{w0} as being the parameter representative of gust winds (see A.7.4).

For slender structural components above water (e.g. drilling derricks, flare towers), the long-term marginal distribution of sustained wind speeds should suffice for a fatigue assessment due to excitation by both gust winds and vortex-induced vibrations.

Requirements and guidance for the fatigue assessment of fixed steel and fixed concrete structures are given in ISO 19902 and ISO 19903, respectively.

A.5.8.3 Floating Structures

In principle, the specification of all environmental conditions that are expected to occur during the floating structure's period of exposure is along similar lines as that for fixed structures. However, the behavior of a floating structure under environmental actions is normally more complex than that of a fixed structure. Therefore, the long-term joint distribution of relevant metocean parameters should comprise more parameters than for fixed structures.

Floating structures experience oscillatory motions in six degrees-of-freedom due to wave action. Additionally, floating structures are subjected to slow variations in their position and their orientation, as a result of the simultaneous effects of wind, current, and waves. The relevant metocean parameters and the way in which these are specified should suit the procedure being used. For requirements and guidance for the fatigue assessment of floating structures, see ISO 19904-1 for monohulls, semi-submersibles, and spars.

A.5.8.4 Jack-ups

For requirements and guidance for the fatigue assessment of a jack-up during a site-specific application, see ISO 19905-1.

A.5.9 Metocean Parameters for Short-term Activities

A.5.9.1 General

Almost all short-term offshore operations, and some offshore-related aviation operations, are sensitive to the accuracy, reliability, and timeliness of weather forecasts. Planning prior to the operation is essential to enable safety plans to be properly completed, cost estimates to be accurately determined, and any capacity limits on accommodation or transport to be defined.

The most common technique used in such planning exercises is the so-called "persistence" or "weather-window" analysis. This analysis is typically applied to a long-time series (e.g. with a duration of 10 years) of a metocean variable such as significant wave height, mean wind speed or current speed. More sophisticated analyses of multiple parameters (including wave period) can be necessary, in particular for operations involving floating systems.

EXAMPLE In order to plan a required operation at an installation safely, the average number of occasions in the months June to August when the significant wave height at a specific location can be expected to be below 1.5 m for a period of 36 h or more, when at the same time the wind speed should be less than 10 m/s, and the spectral peak wave period is less than 9 s, can be evaluated. It can be necessary to modify an operation to allow the limiting criteria to be relaxed.

In all cases, weather forecasts are likely to be needed both before and during the operations, and it is often worthwhile to collect real-time data on critical metocean parameters (such as wind speed and wave height/period) during the operation in order to assist with the accuracy and timing of the forecasts.

References [1] and [9] provide examples of applications of operations requiring metocean data, and Reference [10] describes the types of metocean analyses that are often needed in studies to support the planning of floating systems operations.

A.5.9.2 Metocean Parameters for Medium-term Activities

For medium-term activities such as transportation, the risk of encounter of extreme conditions is dependent on the length of time that the transport spends in those route sectors where extreme conditions are possible. If the length of time is reduced, then the probability of encountering extreme conditions is similarly reduced.

It is generally accepted that for a prolonged ocean transport the wind and wave design criteria should be those with a probability of exceedence per voyage in the range of 0.01 to 0.1. The exceedence level provided by the metocean expert should be matched to the design procedure being used and the requirements of the marine warranty surveyor to ensure that an overall target reliability is achieved. The exceedence per voyage refers to the probability of a parameter (e.g. significant wave height) being exceeded over the course of a voyage. This should not be confused with percent exceedence values computed on the basis of exposure during a voyage, which refer to the percentage of time that a parameter will exceed given levels (and which can be of interest in estimating fatigue damage). In areas affected by tropical cyclones, slow tows that cannot avoid cyclones may need to meet an additional requirement of satisfying a seasonal cyclone condition (e.g. 10-year monthly extreme). In addition, for short tows where the exceedence per voyage values may be low, it may be appropriate to design to the 1-year monthly extremes if they are higher.

A.6 Water Depth, Tides, and Storm Surges

A.6.1 General

Changes in relative still water level comprise several components, including atmospheric tides, storm surge effects, changes in MSL, vertical movement of the earth's crust, settlement, and subsidence. Records in areas such as northern Europe over the past 100 years show a downward trend in relative still water level, because the crust in this area is lifting at a faster rate than the rise in actual sea level. Apart from sudden tectonic movements, such as earthquakes, changes in relative sea level from tectonics and isostasy are unlikely to be significant during the design service life of a structure. However, there can be significant local crustal movements over periods of decades or so caused by local effects, such as sediment compaction and subsidence, including the effects of reservoir compaction.

Global sea level, and hence still water level, has been rising and is expected to continue to rise with climate change through the 21st century and beyond; the magnitude of the increase is not expected to be uniform over the globe. See Reference [11].

Changes in water depth due to changes in still water level cause little change in tide and surge elevations unless depths are modified by many meters.

A.6.2 Tides

The best estimates of the water depth and of the fluctuations in water level (HAT, LAT, extreme surge elevation, and extreme total still water level) are derived from site-specific measurements with an offshore tide gauge measuring pressure from the sea floor. If the tidal signal is dominant, adequate estimates of the tidal range at a given site can be obtained from one month of measured data. However, accurate estimates of extreme tides, including HAT and LAT, require at least one complete year of high-quality data from one location.

A method of analyzing water level data requires:

- conversion of pressure measurements to equivalent depths, using density/temperature/atmospheric pressure corrections;
- harmonic tidal analysis, giving values of all significant tidal constituents and the mean water level;
- prediction of tides over 19 years (to account for the 18.6-year precession of the lunar nodes) and extraction of HAT and LAT;
- subtraction of predicted tides from measured levels, giving time series of storm surge elevations;
- separate statistical analyses of the tidal and storm surge elevations; and
- combination of the frequency distribution of tidal and surge elevations to give the required probabilities of total still water level.

When tide gauge measurements have not been made and water depth has been determined by local soundings, corrections should be made for the state of the tide by reference to published tide tables, co-tidal charts, or the nearest available tide gauge.

A.6.3 Storm Surge

Accurate estimates of the storm surge require a long data set (at least 10 years), either measured or from a suitable hindcast.

A.7 Wind

A.7.1 General

When making wind measurements, it is recommended that:

- the height of the wind measurement above MSL be known and be sufficiently high to be clear of disturbances to the airflow from the wave surface or from the structure;
- the averaging time of the wind speed measurement be known;
- the air and sea temperatures be measured to enable an evaluation of the atmospheric stability that can affect the wind profile and the wind spectrum (see A.7.3 and A.7.4) in low wind conditions;
- the anemometer not be aerodynamically shielded.

Reference [12] contains guidance on suitable measuring instruments and their use.

Measurements at a location away from the site of interest can be misleading, e.g. because of a sharp gradient in wind speed near a coastline. If it is decided to use such measurements because site-specific measurements are not available, allowance should be made (e.g. by the use of numerical models) for such effects. Wind measurements made over land should be corrected to reflect over-water conditions.

Wind data should be adjusted to a standard elevation of 10 m above MSL (the reference elevation z_r) with a specified averaging time such as 1 h. Wind data can be adjusted to any specified elevation different from the base value by using the wind profile given in A.7.3^[13].

A.7.2 Wind Actions and Action Effects

When determining appropriate design wind speeds for extreme and abnormal conditions, the projected extreme wind speeds in specified directions and with specified reference elevations and averaging times should be developed as a function of their recurrence interval.

For most offshore locations, long enough records of in situ wind data will not be available to establish reliable estimates of extreme and abnormal wind speeds. In such cases, hindcast data are extremely useful. Even when hindcast data are available, calibration of the hindcast against measurements should be carried out if possible.

Important aspects of measurements to note (whether for direct use or as calibration data) are:

- the measurement site, date of occurrence, magnitude of measured sustained wind speeds, wind directions, and gust wind speeds for the recorded data that were used during the development of extreme and abnormal winds;
- the type of storm causing high winds, which is significant when more than one type of storm can be present in the region.

When determining appropriate design wind speeds for normal and short-term conditions, criteria of the following types can be desired:

- the frequency of occurrence of specified sustained wind speeds from various directions for each month or season;
- the persistence of sustained wind speeds above specified thresholds for each month or season;
- the probable gust wind speed associated with sustained wind speeds.

In some instances, the spectrum of wind speed fluctuations about the mean should be specified. For example, floating and other compliant structures in deep water can have natural sway periods in the range of a minute or more, a period at which there is significant energy in the wind speed fluctuations. Data on wind spectra are given in A.7.4.

For most purposes a relatively simple wind model, consisting of the scalar Formula (A.1) in the mean wind direction θ_w , suffices:

$$U_w(z,t) = U_w(z) + u_w(z,t) \quad (\text{A.1})$$

where

$U_w(z,t)$ is the spatially and temporally varying wind speed at elevation z above MSL and at time instant t ;

$U_w(z)$ is the mean wind speed at elevation z above MSL, averaged over a specified time interval;

$u_w(z,t)$ is the fluctuating wind speed at elevation z around $U_w(z)$ and in the same direction as the mean wind.

The wind speed in a 3 s gust is appropriate for determining the maximum quasi-static local actions caused by wind on individual components of the structure, whereas 5 s gusts are appropriate for maximum quasi-static local or global actions on structures whose maximum horizontal dimension is less than 50 m, and 15 s gusts are appropriate for the maximum quasi-static global actions on larger structures.

When design actions due to wind need to be combined with actions due to waves and current, the following are appropriate:

- for structures with negligible dynamic response, the 1 h mean wind can be used to determine quasi-static global actions caused by wind in conjunction with extreme or abnormal quasi-static actions due to waves and currents;
- for structures that are moderately dynamically sensitive, but do not require a full dynamic analysis, the 1 min mean wind can be used to determine quasi-static global actions caused by wind, again for wind in conjunction with extreme or abnormal quasi-static actions due to waves and currents;
- for structures with significant dynamic response to excitation with periods longer than 20 s, a full dynamic response analysis to fluctuating winds should be considered.

A.7.3 Wind Profile and Time-averaged Wind Speed

A.7.3.1 Relationships for Different Storm Types

The most general formulations for wind profile and gust factors take into account atmospheric stability. The fairly simple relations presented here have implicitly taken stability into account by fitting to data in specific storm types. The relations are appropriate for engineering purposes in relevant storm types. For “extratropical storms,” it is recommended to use the profile and gust factors based on the Frøya measurements made offshore Norway^[13]. It is presently recommended to apply these relations in A.7.3.2 to all storm types except tropical cyclones and convective storms (such as squalls). For tropical cyclones, the set of profiles and gust factors in A.7.3.3, based on the ESDU relations, are recommended^[234,235]. Analysis of measurements made in squalls offshore the Congo has found that profile and gust factors (A.7.3.4) seem to show a somewhat different nature than these other storm types^[236].

A.7.3.2 Extratropical Storm Wind Profile and Time-averaged Wind Speed

Measurements of representative offshore conditions, in strong, nearly neutrally stable atmospheric wind conditions, suggest that the mean wind speed profile $U_w(z)$ in storm conditions can be more accurately described by a logarithmic profile as given in Equation (A.2) than by the power law profile traditionally used:

$$U_{w,1h}(z) = U_{w0} [1 + C \ln(z/z_r)] \quad (\text{A.2})$$

where

$U_{w,1h}(z)$ is the 1 h sustained wind speed at a height z above MSL;

U_{w0} is the 1 h sustained wind speed at the reference elevation z_r and is the standard reference speed for sustained winds;

C is a dimensionally dependent coefficient, the value of which is dependent on the reference elevation and the wind speed, U_{w0} . For $z_r = 10$ m, $C = (0.0573)(1 + 0.15 U_{w0})^{1/2}$ where U_{w0} is expressed in meters per second;

z is the height above MSL;

z_r is the reference elevation above MSL ($z_r = 10$ m).

For the same storm conditions, the mean wind speed for averaging times shorter than 1 h may be expressed by Equation (A.3) using the 1 h sustained wind speed $U_{w,1h}(z)$ of Equation (A.2):

$$U_{w,T}(z) = U_{w,1h}(z) [1 - 0.41 I_u(z) \ln(T/T_0)] \quad (\text{A.3})$$

where additionally

- $U_{w,T}(z)$ is the sustained wind speed at height z above MSL, averaged over a time interval $T < 3600$ s;

$U_{w,1h}(z)$ is the 1 h sustained wind speed at height z above MSL [see Equation (A.2)];

T is the time-averaging interval with $T < T_0$;

T_0 is the standard reference time averaging interval for wind speed of 1 h = 3600 s;

$I_u(z)$ is the dimensionally dependent wind turbulence intensity at a height z above MSL, given by Equation (A.4), where U_{w0} is expressed in meters per second:

$$I_u(z) = (0.06) \left[1 + 0.043 U_{w0} \right] \left(\frac{z}{z_f} \right)^{-0.22} \quad (\text{A.4})$$

The equations in this subclause are typical engineering equations derived from curve-fitting through available data^[13] and contain numerical constants that are valid only in the SI units of meters and seconds.

NOTE 1 Approximations to Equations (A.2) and (A.3) using a power law can be adequate.

NOTE 2 For tropical cyclone winds, equations in A.7.3.3 are recommended, and for squalls, equations in A.7.3.4 are recommended.

NOTE 3 The above equations are not valid for the description of squall winds, since the duration of the squall is often less than 1 h.

A.7.3.3 Tropical Cyclone Storm Wind Profile and Time-averaged Wind Speed

Within 100 m elevation of the sea surface, boundary layer corrections are insignificant and an ESDU-based mean profile for tropical cyclone conditions can be simplified to a basic log-law profile. For tropical cyclone conditions the 1 h sustained wind speed at a height z above MSL is:

$$U_{w,1h}(z) = \frac{u_*}{0.4} \ln \left(\frac{z}{z_0} \right), \quad \text{for } z \leq 100 \text{ m} \quad (\text{A.5})$$

where u_* is the friction velocity and z_0 is the boundary-layer scaling parameter given by:

$$u_* = \sqrt{C_{d_{10}}} U_{w0} \quad (\text{A.6})$$

$$z_0 = 10 \exp \left| -0.4 / \sqrt{C_{d_{10}}} \right| \quad (\text{A.7})$$

For tropical storms, the drag coefficient C_{d10} is capped at higher wind speeds:

$$C_{d_{10}} = \begin{cases} (0.49 + 0.065U_{w0})10^{-3}, & \text{for } U_{w0} < 27.85 \text{ m/s} \\ 0.0023, & \text{for } U_{w0} \geq 27.85 \text{ m/s} \end{cases} \quad (\text{A.8})$$

The T -second gust at any elevation z is found by applying the peak gust factor $g_T(z)$ and turbulence intensity $I_u(z)$ to the 1 h wind at the given elevation as:

$$U_{w,T}(z) = U_{w,ih}(z) \left[1 + g_T(z) I_u(z) \right] \quad (A.9)$$

The gust factor and turbulence intensity are given by:

$$g_T(z) = \left| \sqrt{2\ln(T_0\nu)} + \frac{0.577}{\sqrt{2\ln(T_0\nu)}} \left[1 - 0.193 \left(\frac{T_u}{T} + 0.1 \right)^{-0.68} \right] \right|, \quad \text{for } T \leq 600 \text{ s} \quad (\text{A.10})$$

$$I_u(z) = \frac{u_* 7.5 \eta [0.538 + 0.09 \ln(z/z_0)]^{\eta^{16}}}{1 + 0.156 \ln\left(\frac{u_*}{f_C z_0}\right)} \frac{1}{U_{w,1h}(z)} \quad (\text{A.11})$$

The gust factor depends on the standard reference time $T_0 = 3600$ s, the zero-upcrossing frequency ν , the integral time scale T_u and the scaling parameter η , which are described by:

$$\nu = \frac{0.007 + 0.213 \left[\frac{T_u}{T} \right]^{0.654}}{T_u}$$

$$T_u = 3.12 z^{0.2}$$

$$\eta = 1 - 6 f_C z / u_*$$
(A.12)

The scaling parameter η and turbulence intensity have an additional dependence on site latitude ψ (in decimal degrees) through the absolute value of the Coriolis parameter f_C :

$$f_C = 2\Omega \sin|\psi| = 2(7.29 \times 10^{-5}) \sin|\psi| \quad (\text{A.13})$$

where Ω is the rotation of the earth in radians per second.

The equations in this subclause are typical engineering equations derived from curve-fitting through available data and contain numerical constants that are valid only in the SI units of meters and seconds.

NOTE 1 The equations in this subclause are intended specifically for tropical cyclones. For other storm types, the equations in subclause A.7.3.2 or A.7.3.4 are recommended.

NOTE 2 In the original References [234,235], Equation (A.5) contains a boundary layer correction term, which is insignificant over the lower 100 m of the atmosphere.

NOTE 3 In the limit, the gust factor in Equation (A.10) does not reduce to 1.0 for $T = 3600$ s. For $T = 3600$ s, Equation (A.5) may be used directly.

A.7.3.4 Squall Wind Profile and Time-averaged Wind Speed

Because squalls are transient wind events in which peak winds may be sustained for durations of less than 10 min, the reference wind speed for squall events is defined as the peak 1 min average wind speed at 10 m elevation. The peak 1 min wind speed at elevations other than 10 m may be estimated using a log-layer profile in the form:

$$U_{w,1min}(z) = \frac{\ln(z/z_0)}{\ln(10m/z_0)} U_{w,1min}(10m) \quad (\text{A.14})$$

where

$$z_0 = 7.0 \times 10^{-10} \text{ m} \quad (\text{A.15})$$

The peak 3 s gust at a given elevation may be estimated from the peak 1 min wind at the same elevation by applying a gust factor:

$$U_{w,3\text{sec}}(z) = g_{3\text{sec}}(z) U_{w,1\text{min}}(z) \quad (\text{A.16})$$

where

$$g_{3\text{sec}}(z) = 1.06 + 0.0491 \exp\{-0.0514(z-10)\} \quad (\text{A.17})$$

The equations in this subclause are typical engineering equations derived from curve-fitting through available data and contain numerical constants that are valid only in the SI units of meters and seconds.

NOTE 1 The equations in this subclause are intended specifically for squall events. For other storm types, the equations in subclause A.7.3.2 or A.7.3.3 are recommended.

NOTE 2 The basis ^[236] for the squall elevation and gust factors presented here are measurements made offshore the Congo at elevations between 10 m and 37.5 m above sea level.

A.7.4 Wind Spectra

A.7.4.1 Spectra for Different Storm Types

Separate spectral forms are recommended for extratropical storms (see A.7.4.2) and tropical cyclones (see A.7.4.3). Squalls are inherently transient phenomena and therefore dynamic responses to squall events would most appropriately be analyzed in the time domain using realistic event histories. Figure A.2 shows wind spectra using both the recommended forms for extratropical storms and tropical cyclones for 1 h sustained wind speeds of 20 m/s, and 40 m/s at elevations of $z = 10$ m and $z = 50$ m.

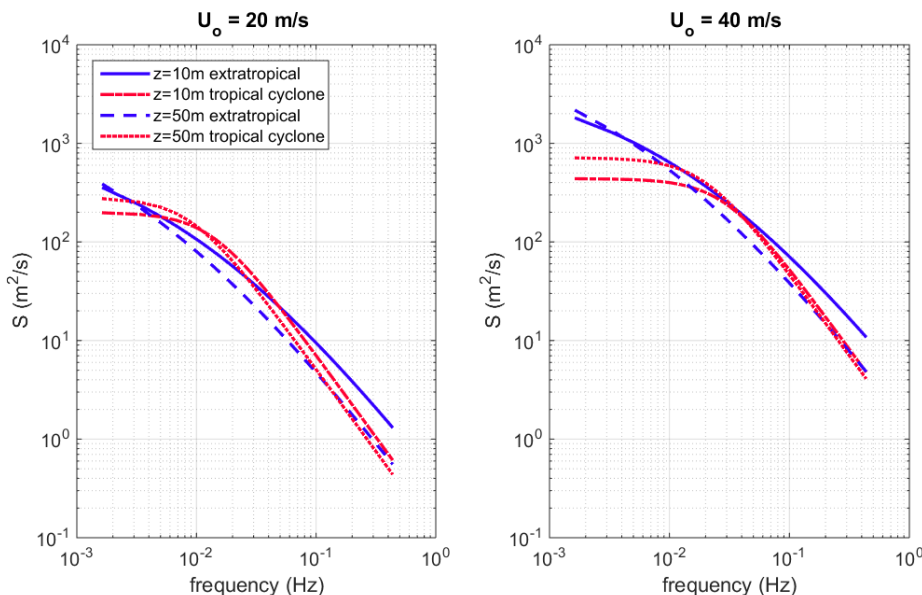


Figure A.2—Examples of Wind Spectra

A.7.4.2 Extratropical Storm Wind Spectra

Wind turbulence, i.e. the dynamic properties of the wind, depends on the stability of the atmospheric boundary layer. Stability, in turn, depends on the temperature difference between air and sea and on the mean wind speed. The equations in this subclause for the dynamic wind properties are appropriate for nearly neutral (slightly unstable) atmospheric stability in storm conditions [13]. For general atmospheric conditions where (in)stability is important, and for weaker wind conditions, a more complex formulation that allows deviations from neutral stability is more appropriate.

The fluctuating wind speed $u_w(z,t)$ (turbulence) can be described in the frequency domain by a wind spectrum, analogous to the way in which the wave spectrum describes the water surface elevation (see A.8.3). The spectral density function of the longitudinal wind-speed fluctuations at a particular point in space can be described by the one-point turbulence spectrum of Equation (A.18):

$$S(f,z) = \frac{(320 \text{ m}^2/\text{s}) \times \left(\frac{U_{w0}}{U_{\text{ref}}}\right)^2 \times \left(\frac{z}{z_r}\right)^{0.45}}{\left(1 + \tilde{f}^n\right)^{5/(3n)}} \quad (\text{A.18})$$

where

- $S(f,z)$ is the wind spectrum (spectral or energy density function) at frequency f and elevation z ;
- U_{w0} is the 1 h sustained wind speed at the reference elevation z_r (the standard reference speed for sustained winds);
- U_{ref} is the reference wind speed, $U_{\text{ref}} = 10 \text{ m/s}$;
- f is the frequency in cycles per second (hertz) over the range $0.00167 \text{ Hz} < f < 0.5 \text{ Hz}$;
- z is the height above MSL;
- z_r is the reference elevation above MSL ($z_r = 10 \text{ m}$);
- \tilde{f} is a nondimensional frequency defined by Equation (A.19) where the numerical factor 172 has the dimension of seconds:

$$\tilde{f} = (172 \text{ s}) f \left(\frac{z}{z_r}\right)^{2/3} \left(\frac{U_{w0}}{U_{\text{ref}}}\right)^{-0.75} \quad (\text{A.19})$$

- n is a coefficient equal to 0.468.

The variance (i.e. the square of the standard deviation) of the wind speed fluctuations about the mean wind speed is by definition equal to the integral of the spectral density function over the entire frequency range from $f = 0$ to $f = \infty$. However, the data from Reference [13], from which the spectral formulation in Equations (A.18) and (A.19) has been derived, extend from $f = 1/600 = 0.00167 \text{ Hz}$ to $f = 0.43 \text{ Hz} \approx 0.50 \text{ Hz}$. The integral of the spectrum over frequency can thus only reflect wind speed fluctuations within this frequency range. Therefore, the integral of the spectrum will only correspond with a part of the total variance of the wind speed, and so caution should be exercised when relating the integral to available measurements to ensure that comparable frequency ranges are compared. It should further be noted that $S(f,z)$ from Equation (A.18) does not go to zero below the lowest frequency of $f = 1/600 \text{ Hz}$ considered in the measurements.

For practical applications, the wind spectrum at a point should be supplemented by a description of the spatial coherence of the fluctuating longitudinal wind speeds over the exposed surface of the structure or

the structural component. In frequency domain analyses, it can be conservatively assumed that all scales of turbulence are fully coherent over the entire topsides. However, for some structures, it can be advantageous to account in the dynamic analysis for the less-than-full coherence at higher frequencies. The correlation between the spectral energy densities of the longitudinal wind speed fluctuations at frequency f between two points in space can be described in terms of the two-point coherence function. The recommended coherence function between two points $P_1(x_1, y_1, z_1)$ and $P_2(x_2, y_2, z_2)$, with along-wind positions x_1 and x_2 , across-wind positions y_1 and y_2 , and elevations z_1 and z_2 , is given by Equation (A.20):

$$F_{\text{Coh}}(f, P_1, P_2) = \exp \left\{ -\frac{1}{U_{w0}} \left[\sum_{i=1}^3 (A_i)^2 \right]^{1/2} \right\} \quad (\text{A.20})$$

where

$F_{\text{Coh}}(f, P_1, P_2)$ is the coherence function between turbulence fluctuations at $P_1(x_1, y_1, z_1)$ and at $P_2(x_2, y_2, z_2)$;

U_{w0} is the 1 h sustained wind speed at 10 m above MSL, in meters per second;

A_i is a function of frequency and the position of the two points P_1 and P_2 .

A_i is calculated from Equation (A.21):

$$A_i = \alpha_i f^{r_i} (D_i)^{q_i} \left(\frac{z_g}{z_r} \right)^{-p_i} \quad \text{in meters per second} \quad (\text{A.21})$$

where

f is the frequency, in hertz;

D_i is the distance, expressed in meters, between points P_1 and P_2 in the x , y , and z directions for $i = 1, 2$, and 3 , respectively (see Table A.1);

z_g is the geometrical mean height of the two points, $z_g = (z_1 \times z_2)^{1/2}$;

z_r is the reference elevation above MSL, $z_r = 10$ m;

α_i , p_i , q_i , and r_i are coefficients given in Table A.1.

Table A.1—Coefficients in Equation (A.21) for Points P_1 and P_2

i	D_i	α_i	p_i	q_i	r_i
1	$ x_1 - x_2 $	2.9	0.4	1.00	0.92
2	$ y_1 - y_2 $	45.0	0.4	1.00	0.92
3	$ z_1 - z_2 $	13.0	0.5	1.25	0.85

A.7.4.3 Tropical Cyclone Wind Spectra

For tropical storms the representation of velocity spectrum at a given elevation z is as follows:

$$S(f,z) = \frac{4 I_u^2 U_{w,ih}(z) L_{u,x}(z)}{\left[1 + 70.8(f L_{u,x}(z)/U_{w,ih}(z))^2\right]^{5/6}} \quad (\text{A.22})$$

where f is the frequency in hertz and $L_{u,x}$ is the integral length scale and is a measure of the effective size of the turbulent eddies within the atmospheric boundary layer. It is a function of z and z_0 in the form:

$$L_{u,x}(z) = \frac{50 z^{0.35}}{z_0^{0.063}} \quad (\text{A.23})$$

where z_0 is the boundary-layer scaling parameter for tropical cyclone winds defined by Equation (A.7).

Corresponding coherence functions have not been derived for the tropical cyclone spectrum.

A.8 Waves

A.8.1 General

The main factors to be considered when assessing the properties of waves at a particular site and their influence on the design, construction, and operation of structures are described below.

- Fetch limitations

Wave growth is restricted by fetch length and width if the waves are generated by local winds. Reference [14] provides simple parametric expressions quantifying these effects, whereas more complete numerical models referenced below include these processes for much more general geometries.

- Nonlinear wave effects

In extreme storms, even in deep water, individual waves exhibit nonlinear behavior. In shallow water, even under normal conditions, waves also exhibit nonlinear behavior, as they are affected by the sea floor. In deep water, for waves that are not too high or too steep, linear wave theory (Airy) is adequate for describing the kinematics of the waves, but for higher or steeper waves in deep water and in shallow water, higher-order theories are more appropriate to describe wave properties, such as the crest elevation and kinematics. Water can be taken as shallow when the water depth/deep water wavelength of the spectral peak frequency is less than approximately 0.13^[8].

- Refraction

As waves propagate into shallow water, their speed (which depends on their period and the local water depth) is reduced and they are refracted. For simple bathymetry and single wave periods, refraction can be estimated using Snell's Law or by ray plotting techniques as described in Reference [14]. For more complex bathymetry and short-crested waves, a numerical method is more appropriate. Refraction can result in both increases and decreases in wave energy/heights as well as in changes in direction between adjacent sites within a shallow water area, depending on the bathymetric configuration. Currents can also cause refraction and should be considered, particularly where tides or rivers create strong currents.

- Diffraction and reflection

These processes can be important when waves encounter a protruding object, such as a breakwater or an island. The potential for focal points of wave energy occurring behind nearby islands or seamounts should be considered.

- Shoaling and wave breaking

As a periodic wave propagates into shallower water, its length is reduced but its period remains the same. For random waves, it may be assumed that the spectral peak period remains the same. This process is known as shoaling. As the wave continues to propagate into shallow water, the wave steepens until the particle velocity at the crest exceeds the speed of the wave and breaking results. In shallow water with a flat seabed, the empirical limit of the wave height is approximately 0.78 times the local water depth for waves that are long-crested. The wave height of short-crested waves can approach 0.9 times the local water depth. The breaker height also depends on beach slope. In deep water, waves can break with a theoretical limiting steepness of 1/7. In addition, nonlinearity in the sea state can increase the wave height due to nonlinear shoaling.

— Crest elevations

An accurate description of the distribution of extreme crest elevations at the site is needed to establish the minimum deck elevation of bottom-founded structures and to establish the likelihood of wave impact on the underside or deck of semi-submersibles. Wave-structure interactions can affect crest elevations, in particular where structures have large diameter columns. Shoaling and nonlinear processes affect crest elevations as waves move into shallow water. The proportion of the wave height above nominal still water increases as the water becomes shallower.

— Bottom dissipation

As waves move into shallow water, the horizontal oscillatory velocities at the bottom become large and turbulent dissipation results. This process can be modelled in present-day hindcast models, as shown in Reference [15].

— Wave-wave interaction

Detailed directional wave spectra at several sites were examined in Reference [16]. It was found that the evolution of the wave spectrum could be parameterized as a function of local water depth. It was proposed that this was due to the nonlinear wave-wave interactions between different wave frequency components.

— Infra-gravity waves

These are surface gravity waves with periods in the range of roughly 25 s to 300 s. In principle, they can be generated by different physical processes, but are most commonly associated with waves generated by nonlinear second-order difference frequency interactions between different swell wave components. As swells propagate over shallow water, forced infra-gravity wave energy associated with swell wave interactions can be released and propagate freely. Forced and free infra-gravity wave energy can be reflected from shore and can become trapped in shallow water due to refraction (edge-waves) or can propagate back out into deep water (leaky waves). Except in the surf zone, amplitudes are normally on the order of tens of centimeters. They are of particular importance when their periods match those of shallow-water moored vessels with lightly damped surge responses, and dynamic responses result.

In view of the complexity of shallow-water processes, the best method of calculating wave height is usually through a comprehensive numerical wave model that includes the relevant processes outlined above. Reference [17] shows how accurate wave models have become.

Estimates from many locations around the world indicate that the following accuracies can be achieved with hindcast models in either deep or shallow water:

- mean error (bias) in H_s of 0.1 m;
- coefficient of variation of 10 % to 15 % for storm peak H_s ;
- coefficient of variation of approximately 20 % for all H_s over long continuous periods (e.g. 10-year hindcasts).

No wave sensor or wave model is ideal in its ability to accurately measure waves or reproduce still water level as a reference base. For example, operating constraints on bottom-founded offshore structures frequently mean that platform-mounted sensors do not measure the undisturbed sea surface. Similarly, wave buoys do not respond ideally in high sea states, in particular they underestimate large crest heights. Wave models are only as good as the physics that are incorporated in them and the description of the input wind fields used to drive them. The strengths and weaknesses of any particular data set should be recognized throughout the process of its analysis and interpretation.

When using hindcast data, care should be taken to ensure that hindcast waves are consistent with site-specific and reliable measured data recorded over the same period. In particular, the spatially and temporally averaged nature of hindcast data and the sampling noise inherent in many measurement data sets should be taken into account, and one or both data sets should be factored if necessary.

Reference [18] provides a description of a recording philosophy for waves. A description of methods for analyzing wave data and calculating extremes can be found in References [8] and [2].

Experienced experts, knowledgeable in the fields of meteorology, oceanography, and hydrodynamics, should be consulted when developing wave-dependent environmental conditions and associated metocean parameters. In developing sea state data, either in the form of statistical parameters characterizing the sea state or in the form of representative individual waves occurring within the sea state, consideration should be given to the following.

a) For normal conditions and short-term activities (for both seas and swells):

- 1) the probability of occurrence and the average persistence of various sea states for each month and/or season (e.g. environmental conditions with waves higher than 3 m from specified directions in terms of general sea state parameters, such as the significant wave height and the mean zero-crossing wave period);
- 2) the wind speeds, tides, and currents occurring simultaneously with the above sea states;
- 3) the percentage of significant or individual wave heights, directions, and periods within specified ranges (e.g. 3 m to 4 m high waves from the SE quadrant during each month and/or season).

b) For extreme and abnormal conditions:

Estimated extreme and abnormal wave heights from specified directions should be developed and presented as a function of their return periods. Other data that should be developed include:

- 1) the probable range and distribution of wave periods associated with extreme and abnormal wave heights, for the specification of individual design waves;
- 2) the distribution of maximum crest elevations, and the wave energy spectrum in the sea state producing extreme and abnormal wave heights;
- 3) the tides, currents, winds, and marine growth likely to occur simultaneously with the sea state producing the extreme and abnormal waves.

A.8.2 Wave Actions and Action Effects

When considering extreme and abnormal conditions for design situations, the following points should be considered.

- The maximum height of an individual wave with a given return period is, in general, higher than the most probable maximum wave height of a 1 h or 3 h sea state with the same return period.
- The highest action on, or the largest action effect in, a structure is not necessarily induced by the highest sea state or the highest wave in a sea state. This is due to the sensitivity of structures to the frequency content of waves in a sea state, and the geometric particulars of the structure concerned.
- Waves and currents can create seabed scour around objects on or near the sea floor that obstruct free flow conditions. Examples where scour can occur are around the legs of structures and jack-ups, around subsea templates, and underneath pipelines.
- Loads on submarine pipelines are complicated, because drag and lift loads are functions of the ratio of steady current to wave orbital velocity and the Keulegan-Carpenter number.

A.8.3 Sea States—Spectral Waves

A.8.3.1 Wave Spectrum

A.8.3.1.1 General

The shape of wave spectra varies widely. The two broad classifications of sea state are:

- Wind seas: Generated by the local wind; the corresponding shape of the wave spectrum will thus depend on the wind speed, the fetch length of the wind over open water, and the duration during which the wind has been blowing. Within wind seas, there is a further distinction between wave conditions that are fully developed and wave conditions that are still developing. In the first case, the sea is in a state of equilibrium: the energy input by the wind and the energy dissipation in the wave processes are in balance. In the second case, there is net energy input and the waves are consequently still growing.
- Swells: These are wind-generated waves that have travelled far from the generation region. Swell waves have no relationship with the local wind regime.

Spectral fitting is used to determine the parameters of parametric wave spectral shapes. In addition, for design it is sometimes required to separate the swell components of the wave spectrum from the wind sea components of the wave spectrum. To achieve this, spectral splitting and fitting is required. There are various methods of spectral splitting, from simple frequency division at a nominated frequency (such as 0.1 Hz/10 s) to complex wave-train tracking algorithms. Spectral splitting is used to provide a swell and/or wind sea spectral description that can be associated with ambient conditions (as required for fatigue and operability assessments) and for extreme design conditions.

Some of the parametric formulations of the wave frequency spectrum $S(f)$ most frequently used in the offshore industry are presented below.

A.8.3.1.2 The JONSWAP Spectrum and Pierson-Moskowitz Spectrum

The JONSWAP (Joint North Sea Wave Project) wave frequency spectrum is a modification of the Pierson-Moskowitz spectrum. The JONSWAP wave spectrum was originally formulated in terms of wind speed and nondimensional fetch. A form such as the one proposed by Goda^[19], which is expressed in terms of significant wave height, peak spectral period, and peak enhancement factor γ , is much more convenient for engineering purposes:

$$S(f) = \infty H_s^2 T_p^{-4} f^{-5} \exp\left\{-1.25(T_p f)^{-4}\right\} \gamma^\beta \quad (\text{A.24})$$

where

$$\alpha \approx \frac{0.0624}{0.230 + 0.0336\gamma - 0.185(1.9 + \gamma)^{-1}} \quad (\text{A.25})$$

$$\beta = \exp \left\{ -\frac{(T_p f - 1)^2}{2\sigma^2} \right\} \quad (\text{A.26})$$

$$\sigma = \begin{cases} \sigma_a & \text{when } f \leq f_p \\ \sigma_a & \text{when } f > f_p \end{cases} \quad \begin{aligned} \text{and } \sigma_a &= 0.07 \\ \sigma_b &= 0.09 \end{aligned} \quad (\text{A.27})$$

In the above expressions:

- γ is a nondimensional peakedness parameter (when $\gamma = 1$, the JONSWAP spectrum reverts to the Pierson-Moskowitz spectrum);
- f_p is the peak frequency;
- σ is the spectral width either side of the spectral peak.

The values of σ above and below the peak frequency of 0.07 and 0.09 used in the Goda formulation correspond to the mean values measured in the original JONSWAP formulation. It is common to use these values in the absence of other derived values. However, the values for σ and γ can vary widely between different times during the development of the sea and between different sites around the world. Therefore, when fitting measured spectra, the values of α , σ , and γ may be varied to optimize the fit.

A.8.3.1.3 Swell Gaussian Spectra

Wave frequency spectra for swells are generally much narrower in frequency content than spectra for wind seas. Long-period swells from distant storms are more or less symmetrical in shape around the swell peak frequency. Even so, the swell spectrum is frequently described using a JONSWAP function with a large peak enhancement factor. Use of the JONSWAP function has the advantage that the spectral shape of shorter-period swells, which tend to have broader spectra particularly above the peak frequency, can be described well. In addition, the JONSWAP spectrum does not leak energy below zero frequency. Nevertheless, the symmetric normal or Gaussian function is generally considered to be a better descriptor of swell, particularly long-period swell.

A symmetric swell spectrum can be defined in complete analogy with the normal or Gaussian probability density function as:

$$S(f) = \frac{H_s^2}{16} \frac{1}{\sigma_g \sqrt{2\pi}} \exp \left(-\frac{1}{2} \left[\frac{f - f_p}{\sigma_g} \right]^2 \right) \quad (\text{A.28})$$

where

- f_p is the peak frequency;
- σ_g is the parameter defining the width of the symmetric swell spectrum (equals the standard deviation of the Gaussian function).

Typical values of σ_g vary from 0.05 to 0.015. In application, spectral fitting should generally be undertaken to determine the range of values of the standard deviation.

In applying a Gaussian spectrum to design, care should be taken with the low frequency side of the spectrum, since values of the standard deviation (higher than ~0.01) can introduce energy at very low frequencies, including the zero frequency. For dynamically sensitive facilities, this can cause excessive and unrealistic responses.

A.8.3.1.4 The Ochi-Hubble Form for Bimodal Sea States

The Ochi-Hubble spectral form^[20] was developed for the purpose of describing dual-peaked (bimodal) wave spectra. The full bimodal spectrum is formed by combining two sea state partitions as:

$$S_{\text{total}}(f) = S_1(f) + S_2(f) \quad (\text{A.29})$$

Typically, one of these partitions describes a longer period swell component, and the other partition describes shorter period seas. Each partition of the spectrum is defined as:

$$S_i(f) = \frac{\pi}{2} \left[\frac{\{4(4\lambda_i+1)\pi^4 f_{p,i}^4\}^{\lambda_i}}{\Gamma(\lambda_i)} \frac{H_{s,i}^2}{(2\pi f)^{4\lambda_i+1}} \exp \left\{ -\left(\frac{4\lambda_i+1}{4} \right) \left(\frac{f_{p,i}}{f} \right)^4 \right\} \right] \quad (\text{A.30})$$

where

$H_{s,i}$ is the significant wave height of the i th partition of the spectrum;

$f_{p,i}$ ($= 1/T_{p,i}$) is the peak spectral frequency of the i th partition;

λ_i is the spectral peak enhancement factor of the i th partition;

Γ is the mathematical gamma function.

Note that since spectral energy is proportional to wave height-squared, the significant wave heights of the two spectral partitions do not add linearly. Rather, the overall significant wave height in a bimodal Ochi-Hubble spectrum is given by:

$$H_{s,\text{total}} = \sqrt{H_{s,1}^2 + H_{s,2}^2} \quad (\text{A.31})$$

A.8.3.1.5 General Multi-modal Spectra

The Ochi-Hubble spectrum is just one multi-modal spectral form. In general, multi-peaked spectra can be formed simply by adding spectral partitions as:

$$S_{\text{total}}(f) = \sum_{i=1}^N S_i(f) \quad (\text{A.32})$$

If multi-peaked spectra are specified, the overall significant wave height is:

$$H_{s,\text{total}} = \sqrt{\sum_{i=1}^n H_{s,i}^2} \quad (\text{A.33})$$

Torsethaugen [21] developed sets of bimodal spectra typical of the northern North Sea by combining pairs of JONSWAP spectra. In regions where the Gaussian spectrum is used to describe long-period swells (e.g. Nigeria), the Gaussian swells might be combined with a JONSWAP partition to describe local seas. In swell-dominated regions, it can also be advantageous to specify multiple-swell partitions as well as a sea. In such cases, n is three or higher. In principle n can be arbitrarily high, but in practice if n is higher than three it can be more straightforward to use a discrete numerical description of the spectrum rather than using a parameterized form.

A.8.3.1.6 Applications

The most appropriate form of the wave frequency spectrum for an offshore structure depends on the geographical area, the severity of the sea state, whether the sea state is fully developed or is still growing, and the application concerned. For example, for a short-term North Sea design storm condition, a unidirectional JONSWAP spectrum can be most appropriate, whereas for the modelling of a series of sea states for a long-term fatigue analysis directionally spread, Pierson-Moskowitz spectra are often more appropriate. Similarly, for vessel downtime studies offshore West Africa, the use of a bimodal spectrum composed of a low-frequency swell spectrum from one direction and a high-frequency wind sea spectrum from a different direction could be appropriate.

Wave spectral shapes in shallow water do not generally conform to either the Pierson-Moskowitz or the JONSWAP forms, although a modified version of the JONSWAP spectrum is sometimes used (see Reference [16]).

A.8.3.1.7 Definition of Frequency

The wave frequency can either be expressed in terms of ω in radians per second (rad/s) or in terms of f in cycles per second or hertz. The relationship between these two frequencies is as follows:

$$\omega = 2\pi f = \frac{2\pi}{T} \quad (\text{A.34})$$

Since the energy per frequency band remains the same, i.e.:

$$S(\omega)d\omega = S(f)df$$

the relationship between the two alternative expressions of the wave frequency spectrum is given by Equation (A.35):

$$S(f) = 2\pi S(\omega) \quad (\text{A.35})$$

A.8.3.2 Directional Spreading

A.8.3.2.1 General

The directional characteristics of wave spectra are often assumed to be independent of frequency, allowing a separation of variables so that the directional wave spectrum can be expressed as the product of a wave directional spreading function $D(\theta)$ (see A.8.3.2.2), independent of frequency, and a wave frequency spectrum $S(f)$, which is independent of direction. The general relationship in Equation (A.36):

$$S(f, \theta) = D(f, \theta)S(f) \quad (\text{A.36})$$

is then replaced by Equation (A.37):

$$S(f, \theta) = D(\theta) \times S(f) \quad (\text{A.37})$$

where the directional spreading function by definition satisfies the relationship:

$$\int_{-\pi}^{\pi} D(\theta) d\theta = 1 \quad (\text{A.38})$$

Standard formulations for the directional spreading function can be found in the literature, for example in Reference [8]. However, detailed directional wave information is not always available. In practical applications, unidirectional sea states are often taken as a modelling assumption. However, if the influence of directional wave spreading is expected to be significant, sensitivity analyses should be performed to investigate the effect. In such cases, one of the distributions shown in Equation (A.39) can be used.

The directional spreading function $D(\theta)$ is a symmetric function around the mean direction $\bar{\theta}$. In the absence of information to the contrary, the mean wave direction can be assumed to coincide with the mean wind direction. There are three expressions for $D(\theta)$ in common use:

$$\begin{aligned} D_1(\theta) &= C_1(n) \times \left(\cos(\theta - \bar{\theta}) \right)^n && \text{for } -\frac{1}{2}\pi \leq (\theta - \bar{\theta}) \leq +\frac{1}{2}\pi \\ D_2(\theta) &= C_2(s) \times \left[\cos\left(\frac{\theta - \bar{\theta}}{2}\right) \right]^{2s} && \text{for } -\pi \leq (\theta - \bar{\theta}) \leq +\pi \\ D_3(\theta) &= C_3(\sigma) \times \frac{1}{\sigma\sqrt{2\pi}} \times \exp\left[-\frac{(\theta - \bar{\theta})^2}{2\sigma^2}\right] && \text{for } -\frac{1}{2}\pi \leq (\theta - \bar{\theta}) \leq +\frac{1}{2}\pi \\ D_1(\theta) = D_2(\theta) = D_3(\theta) &= 0 && \text{for all other } (\theta - \bar{\theta}) \end{aligned} \quad (\text{A.39})$$

where

$$C_1(n) = \frac{\Gamma(n/2 + 1)}{\sqrt{\pi} \Gamma(n/2 + 1/2)}$$

$$C_2(s) = \frac{\Gamma(s + 1)}{2\sqrt{\pi} \Gamma(s + 1/2)}$$

$$C_3(\sigma) = 1$$

The functions all have a peak at $\theta = \bar{\theta}$, the sharpness of which depends on the exponent n in $D_1(\theta)$ or s in $D_2(\theta)$, or the standard deviation σ of the normal distribution $D_3(\theta)$. The coefficients C are normalizing factors dependent on n , s , or σ , which are determined such that the integral of $D(\theta)$ over all θ is equal to 1.0. For appropriately chosen values of the parameters, the functions $D_1(\theta)$ and $D_2(\theta)$ are virtually indistinguishable.

In engineering applications, $D_1(\theta)$ is often used with $n = 2$ to $n = 4$ for wind seas; for $n = 2$, the corresponding factor $C_1(2) = 2/\pi$. For swells, the value $n = 6$ or higher is more appropriate.

If $D_2(\theta)$ is used, typical values of s are $s = 6$ to 15 for wind seas and $s = 15$ to 75 for swells.

A.8.3.2.2 Directional Spreading Factor

For engineering applications, the sea state is often represented by a long crested wave, assuming the wave energy only propagates in a single direction. This is an abstraction of a real sea. The directional spreading factor ϕ is used to reduce the kinematics (velocities and accelerations) of unidirectional wave theories to account for directionality.

Design wave procedures typically apply unidirectional waves. This is especially common practice for the static design of fixed steel structures of space-frame configuration. In a real sea, the directional spreading of the wave energy tends to result in peak global actions that are somewhat smaller than those predicted for unidirectional seas. As such, design recipes often allow a reduction in the horizontal velocity and acceleration obtained from unidirectional wave theories by the spreading factor.

Only the wave energy that travels in the principal wave direction contributes to the wave kinematics in that direction. The ratio of the in-line energy to the total wave energy is the “in-line variance ratio.” Since the kinematics are proportional to the square root of the wave energy, the directional spreading reduces the in-line kinematics under the highest point of the crest by a spreading factor that is equal to the square root of the in-line variance ratio. All of the energy in the wave spectrum contributes to the kinematics, so that the spreading factor is calculated by integrating the entire wave spectrum over frequency and direction.

The directional spreading factor ϕ is dependent on the type of storm in the area concerned and the distance of the site of interest from the storm centre. Although reference may be made to site-specific directional spreading data where these are available, caution should be exercised since such data are difficult to interpret. In addition, it should be noted that spreading data derived from hindcasts often lead to an underestimate of ϕ . In general, the values in Table A.2 from Reference [41] are appropriate for open water, where refraction and diffraction effects do not modify spreading.

Table A.2—Directional Spreading Factors for Open Water Conditions

Type of Storm or Region	Directional Spreading Factor ϕ
Low-latitude monsoons typically $ \psi < 15^\circ$	0.88
Tropical cyclones below approximately 40°	0.87
Extra-tropical storms for the range of latitudes $36^\circ < \psi < 72^\circ$	$1.0193 - 0.00208 \psi $

NOTE 1 ψ is the geographical latitude in degrees. Additional information on directional spreading factors for other storm types and locations may be provided in the relevant regional annex.

NOTE 2 In Reference [41], it is noted that in extra-tropical storms there may be a trend of decreasing spreading with increasing storm severity. In extreme or abnormal extra-tropical storm events, it can be advisable to consider specifying a lower degree of spreading (where this would be conservative).

The wave directional spreading factor may be applied to kinematics that neglect the directionality of the sea state.

The relationship between the spreading factor ϕ and the exponents n and s in the two formulations $D_1(\theta)$ and $D_2(\theta)$ in Equation (A.39) is given in Table A.3.

Table A.3—Relationship between Spreading Factor ϕ and Exponents n and s for Directional Spreading Functions $D_1(\theta)$ and $D_2(\theta)$

Variable	$D_1(\theta)$	$D_2(\theta)$
Directional spreading factor ϕ in terms of n or s	$\phi^2 = \left[\frac{(n+1)}{(n+2)} \right]$	$\phi^2 = 0.5 \left[1 + \frac{s(s-1)}{(s+1)(s+2)} \right]$
Exponent n or s in terms of directional spreading factor ϕ	$n = \frac{2\phi^2 - 1}{1 - \phi^2}$	$s = \frac{3\phi^2 - 1 + \sqrt{(\phi^4 + 6\phi^2 - 3)}}{(2 - 2\phi^2)}$

The spreading factor for low-latitude monsoons of $\phi = 0.88$ in Table A.2 corresponds with $n = 2.43$ and $s = 6.25$. The factor given in Table A.2 for tropical cyclones of $\phi = 0.87$ similarly corresponds with $n = 2.11$ and $s = 5.60$. For extra-tropical storms at a latitude $|\psi| = 60^\circ$, Table A.2 provides a spreading factor of $\phi = 0.895$ that corresponds with $n = 3.00$ and $s = 7.41$.

A.8.3.3 Wave Periods

In order to fully define a wave spectrum, a peak spectral wave period (T_p) or range of representative wave periods should be given (note that in some formulations T_z may be needed instead). Values of peak spectral periods associated with given H_s values are often determined through a regression analysis. Regression analyses can be performed on storm peak data or on all available data. The form of the regression can be linear, or sometimes nonlinear forms such as $T_p = aH_s^b$ allow a better fit to the underlying data. Since use of spectral data implies analysis of a structure with a dynamic response, strong consideration should be given to specifying a range of periods about the best fit values determined by regression. Alternatively, contours of H_s and T_p can be provided. Contours are usually used to capture the fact that, for a given value of significant wave height, wave periods much shorter or longer than the best fit value can occur, although they represent less likely H_s and T_p combinations.

In wave spectra formulations, the frequency parameter is the intrinsic frequency. However, a stationary structure (fixed or floating) in a wave field with current responds to the apparent frequency f_a . To be able to perform the response calculations, the wave frequency spectrum formulation should therefore be transformed into the apparent frequency. As the wave energy per frequency band is independent of the reference frame, $S(f_i)df_i = S(f_a)df_a$ and hence the wave spectrum in the apparent frequency becomes $S(f_a) = S(f_i)df_i/df_a$.

The coordinate transformations are carried out using Equation (A.43), taking due account of the fact that the wave number k is a function of the intrinsic wave frequency f_i through Equation (A.44). However the wave actions on a spatially distributed structure cannot be determined accurately using this spectrum as both the wavelength and the kinematics are a function of the intrinsic period and not the apparent period.

Prior to undertaking any spectral conversion, it is important to establish the extent to which the wave spectra derived directly from either measured or hindcast data are likely to be representative of the apparent or intrinsic frequency spectra (or something in between).

The correct treatment of intrinsic and apparent wave periods is of particular relevance for structures whose design and/or assessment are sensitive to dynamic effects or the phasing of the wave loads as the wave progresses through the structure (e.g. certain jack-up units). In such circumstances an alternative approach can be more appropriate (e.g. one based on the modification of the wave particle kinematics to account directly for the current velocity). For further details, see A.8.4.3.

A.8.4 Regular (Periodic) Waves

A.8.4.1 Wave Period

The wave period $T_{H_{\max}}$ associated with the maximum wave height can be estimated based on wave measurements or simulations of waves in extreme sea states. Time series measurements of individual waves in extreme sea states are rare and therefore site-specific measurement-based estimates are often not possible. The ratio of $T_{H_{\max}} / T_p$ in large sea states typically varies between 0.8 and 1.0. Reference [23] presents ratios of $T_{H_{\max}} / T_p$ based on measurements made in different areas of the world that agree with this range, and further suggest that the ratio varies with spectral bandwidth. Simulation of extreme JONSWAP spectra with varying peak enhancement factors confirms this basic trend. For a JONSWAP spectrum with $\gamma = 1$ the expected ratio of $T_{H_{\max}} / T_p$ is 0.9; as γ increases beyond a value of 5, the expected ratio approaches unity. Simulation of extreme sea states using a spectral model (first- or second-order) can lead to refined estimates of $T_{H_{\max}}$ and insight into the range of values that can be associated with large individual waves. Whether measured or simulated data are considered, it is sometimes insightful to consider looking at wave heights versus some measure of steepness rather than only considering H versus T .

As a practical matter, for shallow-water jacket structures where the response is not overly dynamic, approximate ratios of the period of maximum wave to the peak spectral period associated with the same return period significant wave height are often used. For tropical cyclones, a ratio of 0.90 to 0.92 is commonly assumed. In North Sea storm conditions, ratios from 0.88 to 0.96 are commonly used. For dynamic structures (fixed or floating), specifying a wide range or performing simulations in order to determine a range is prudent. Of course, if a structure has a significant dynamic response, the use of a design wave approach using H_{\max} and $T_{H_{\max}}$ might itself be questioned. In such cases, designers may need to consider a spectral approach in order to capture dynamic effects.

A.8.4.2 Wave Kinematics—Velocities and Accelerations

Several periodic wave theories can be used to predict the kinematics of two-dimensional regular waves. The different theories all provide approximate solutions to the same differential equations with appropriate boundary conditions. All compute a waveform that is symmetric about the crest and propagates without changing shape. The theories differ in their functional formulation and in the degree to which they satisfy the nonlinear kinematic and dynamic boundary conditions at the wave surface.

Linear wave theory^[8] is applicable only when the linearization of the free surface boundary conditions is reasonable, i.e. strictly speaking only when the wave amplitude and steepness are infinitesimally small. Stokes' fifth-order theory^[24] is a fifth-order expansion in the wave steepness about mean water level that satisfies the free surface boundary conditions with acceptable accuracy over a fairly broad range of applications, as shown in Figure A.3, which is adapted from Reference [10]. Chappelear's theory^[25] is similar to Stokes' fifth-order theory, but determines the coefficients in the expansion numerically through a least squares minimization of errors in the free surface boundary conditions, rather than analytically. Extended velocity potential theory (EXVP-D)^[26] satisfies the dynamic boundary condition exactly and minimizes the errors in the kinematic boundary condition. Stream function theory^[27] satisfies the kinematic boundary condition exactly and minimizes the errors in the dynamic boundary condition.

When Stokes' fifth-order theory is not applicable, stream function theory can be used. Selection of the appropriate solution order can be based either on the percentage error in the dynamic and kinematic boundary conditions, or on the percentage error in the velocity or acceleration compared with the next higher order. These two methods provide comparable solution orders over most of the feasible domain, but differ in the extremes for $H > 0.9 H_b$ (where H_b is the breaking wave height) and $d / gT_i^2 < 0.003$. In

these extremes, the theories have not been well substantiated with laboratory measurements and should therefore be used with caution. In particular, the curve for long-crested breaking wave height H_b shown in Figure A.3 is not universally accepted.

New-wave theory (see, for example, Reference [28]) is based on a mathematical derivation of the characteristics of the most probable maximum wave in a sea state. The New-wave surface has the shape of the autocorrelation function. New-wave includes the continuous spectrum of wave frequencies in a random sea; it is not based on discrete harmonics of the fundamental frequency. The kinematics of each wave frequency are computed using linear wave theory, summed and subsequently delta-stretched.

Delta stretching^[29] provides a simple empirical correction to extend the kinematics obtained from linear theory into the wave crest above the still water level. When the local water surface elevation is above still water level and the vertical coordinate being considered, z , is above the stretching depth, d_s (the distance below the still water level at which the stretching process begins), then z in the equations for linear wave kinematics should be replaced by the stretched vertical coordinate z_s :

$$z_s = F_s (d_s + z) - d_s = (F_s - 1) d_s + F_s z \quad (\text{A.40})$$

where

z is defined as the vertical coordinate with $z = 0$ at the still water level;

F_s is a stretching factor defined by:

$$F_s = \frac{d_s + a\eta}{d_s + \eta} \quad (\text{A.41})$$

where

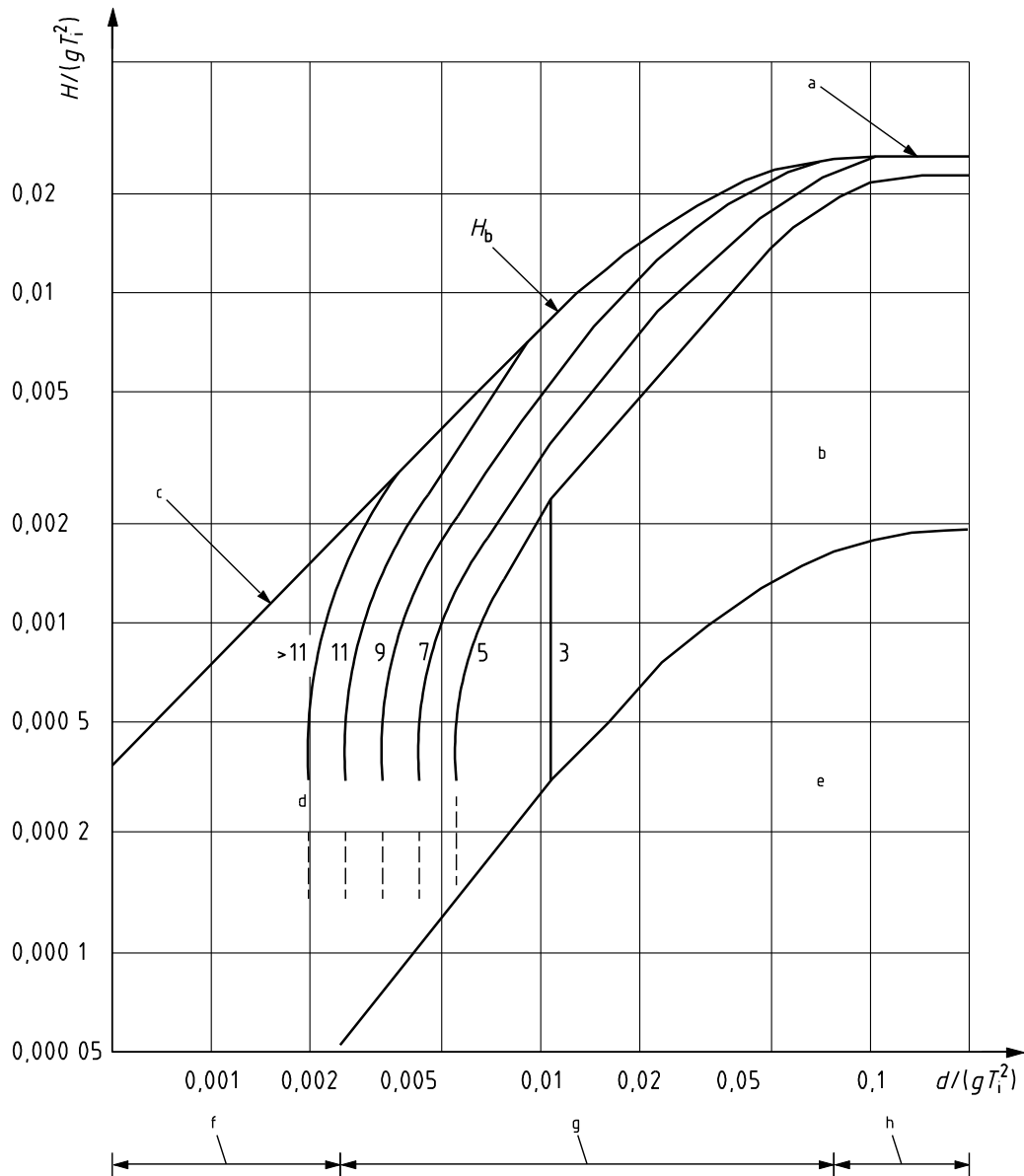
a is a stretching parameter ($0 < a < 1.0$);

η is the water surface elevation at the horizontal location of interest.

The stretching depth (d_s) is typically set to one-half of the significant wave height or half of the crest elevation, and the stretching parameter a typically equals 0.3. The stretching factor F_s is always smaller than 1.0 and consequently $z_s < z$.

In the use of New-wave theory, the kinematics are evaluated at only one instant during the wave evolution and are kept constant as the wave propagates through the structure. New-wave is compatible with random directional wave models and produces results for global direct actions on fixed steel structures similar to those calculated by time-domain simulations.

Another form of stretching is linear or Wheeler stretching (see A.9.4.1).

**Key**

- | | |
|---|--|
| a Deep water breaking limit $H / \lambda = 0.14$ | e Linear/Airy or third-order stream function |
| b Stokes' fifth-order, New-wave, or third-order stream function | f Shallow water |
| c Shallow water breaking limit $H / d = 0.78$ | g Intermediate depth |
| d Stream function (showing order number) | h Deep water |

Figure A.3—Regions of Convergence of Alternative Wave Theories**A.8.4.3 Intrinsic, Apparent, and Encounter Wave Periods**

The correct period to be used in all periodic wave theories to determine the wavelength and all wave kinematics is the intrinsic period. If the wave period is derived from measurements taken by fixed (rather than drifting) instruments, the measurements are of the apparent wave period. If the wave period is based on hindcasts of waves with a model that is calibrated to measurements taken by fixed instruments, and no adjustments are made to the model to account for the presence of current, then again the wave period

represents the apparent wave period. In both cases, the intrinsic wave period should be calculated from the apparent wave period. These are the usual cases for offshore structures covered by this standard. If the wave hindcast model already accounts for the Doppler effect on the wave periods due to currents, no adjustment is required.

In calculating wave particle kinematics, some computer programs adjust the wave period/length internally to account for currents. Other programs require the user to manually adjust the wave period before using it to compute kinematics. The user should ensure that the correct procedure is applied.

For a uniform current profile over the water depth, the basic problem is formulated by the relationship between speeds in the apparent and the intrinsic coordinate systems:

$$\begin{aligned} c_a &= c_i + V_{\text{in-line}} \\ c_a &= \frac{\lambda}{T_a} \\ c_i &= \frac{\lambda}{T_i} \\ V_{\text{in-line}} &= U_c \cos \theta_c \end{aligned} \tag{A.42}$$

where

- a is a subscript for an apparent property;
- i is a subscript for an intrinsic property;
- c is the wave celerity (the wave phase speed);
- λ is the wavelength;
- T is the wave period;
- $V_{\text{in-line}}$ is the component of the current velocity in-line with the direction of wave propagation;
- U_c is the free-stream steady current velocity, not reduced by structure blockage;
- θ_c is the direction of the current velocity with respect to the direction of wave propagation.

This results in the relationship between the apparent and intrinsic periods:

$$\frac{\lambda}{T_a} = \frac{\lambda}{T_i} + V_{\text{in-line}} \tag{A.43}$$

Through multiplication by the wave number $k = 2\pi/\lambda$, Equation (A.43) can be rewritten in terms of the apparent and intrinsic frequencies:

$$\omega_a = \omega_i + k V_{\text{in-line}} \tag{A.44}$$

where ω is the wave circular frequency, $\omega = 2\pi/T$.

The wavelength, which is unaffected by the frame of reference, and the intrinsic period are coupled through the dispersion equation, which for first- and second-order waves is as follows:

$$T_i^2 = \frac{2\pi\lambda}{gtanh(2\pi d/\lambda)} = \frac{4\pi^2}{kgtanh(kd)} \quad (\text{A.45})$$

where

- d is the water depth;
- g is the acceleration due to gravity.

For higher-order waves, the dispersion relationship is determined through numerical simulations.

$V_{\text{in-line}}$ is positive when wave propagation and the in-line component of the current velocity are in the same direction ($-90^\circ < \theta_c < +90^\circ$); in these cases the apparent frequency is higher than the intrinsic frequency.

Conversely, $V_{\text{in-line}}$ is negative when wave propagation and the in-line component of the current velocity are in opposite directions ($\theta_c > +90^\circ$ or $\theta_c < -90^\circ$) and the apparent frequency is lower than the intrinsic frequency. For negative values of $V_{\text{in-line}}$ (opposing currents), the condition $c_i + V_{\text{in-line}} > 0$ should be satisfied—otherwise, the waves move faster downstream by the current than they can propagate forward. For the special case of $c_i + V_{\text{in-line}} = 0$ and $\theta_c = 0$, standing waves occur.

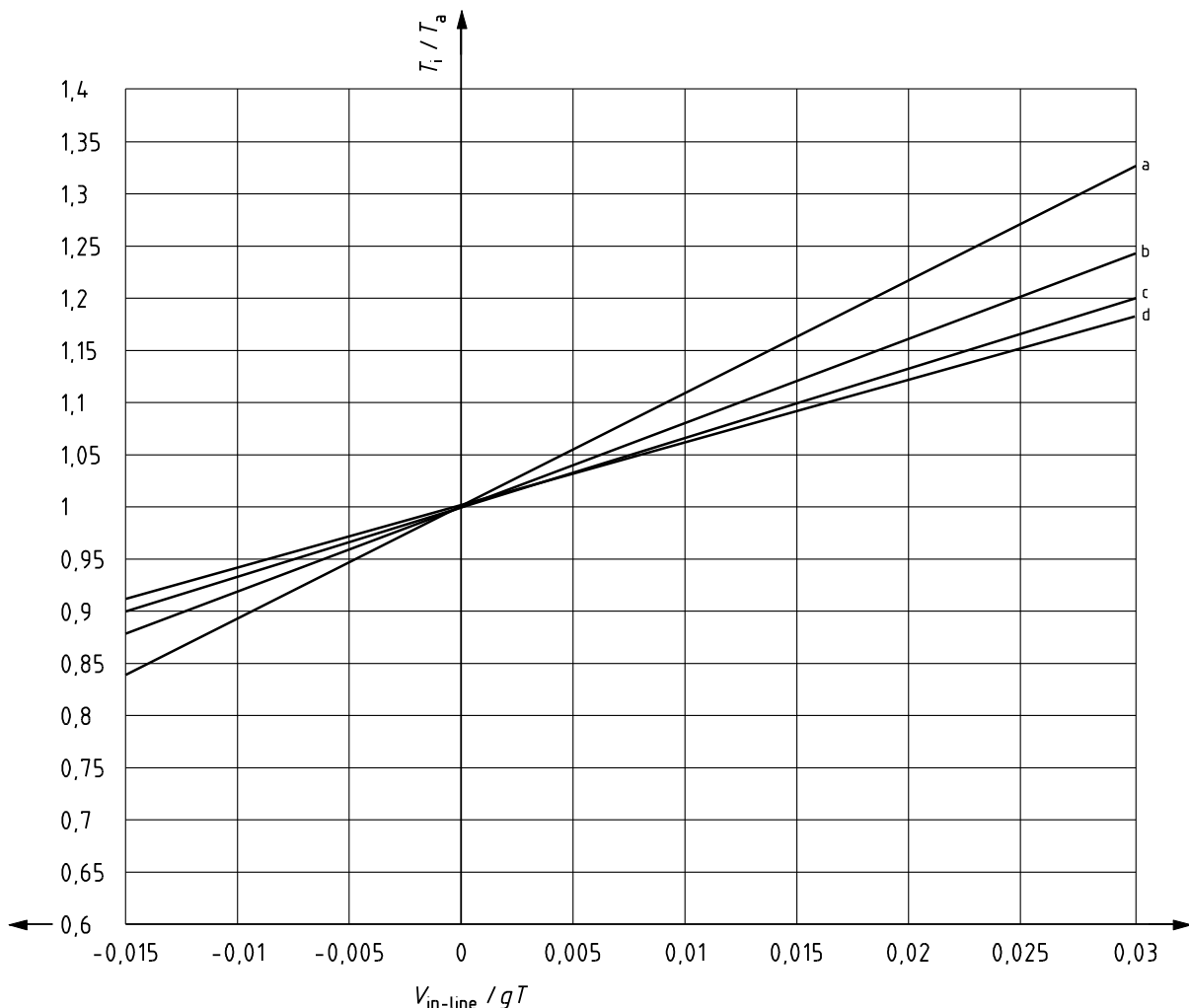
When the intrinsic period T_i [or frequency ω_i] is known, the wavelength λ and the wave number k are also known [see Equation (A.45)], and there is a unique apparent period T_a [or frequency ω_a] associated with T_i [ω_i] for each current velocity. When the apparent wave period T_a [ω_a] is known, there is only a unique intrinsic period T_i [ω_i] associated with T_a [ω_a] when the current velocity is in the direction of wave propagation ($V_{\text{in-line}} > 0$). For opposing current velocities, i.e. $-c_i < V_{\text{in-line}} < 0$, there are in principle two values of T_i [ω_i] that correspond with each T_a [ω_a]. However, the second solution is associated with excessively short, unrealistic waves and can be ignored.

Equations (A.42) to (A.45) directly provide T_a from a given T_i , but should be solved iteratively to determine T_i from a given T_a . For the special case of a uniform current profile, the solution to these equations is provided in nondimensional form in Figure A.4. This figure gives the ratio of T_i to T_a as a function of $V_{\text{in-line}}/gT$ for constant values of $d/gT^2 > 0.01$. Figure A.4 may be used with $T = T_a$ to determine T_i or with $T = T_i$ to determine T_a . For smaller values of d/gT^2 , shallow-water depth approximations apply and the equation

$$\frac{T_i}{T_a} = 1 + \frac{V_{\text{in-line}}}{\sqrt{gd}} \quad \text{can be used.}$$

While strictly applicable only to a current that is uniform over the full water depth, Figure A.4 provides acceptable estimates of T_i/T_a for “slab” current profiles that are uniform over the top 50 m or more of the water column. For nonuniform current profiles a weighted, depth-averaged in-line current speed may be used, as shown in Reference [22]:

$$V_{\text{in-line}} = \frac{2k}{\sinh(2kd)} \int_{-d}^0 U_c(z) \cos \theta(z) \cosh[2k(z+d)] dz \quad (\text{A.46})$$

**Key**

a	$d/(gT^2) = 0.01$	c	$d/(gT^2) = 0.04$
b	$d/(gT^2) = 0.02$	d	$d/(gT^2) = 0.10$

NOTE Either $T = T_a$ or $T = T_i$ can be used to calculate $d/(gT^2)$ and $V_{\text{in-line}} / gT$.

Figure A.4—Doppler Shift in Wave Period due to Steady Current—Relationship between Intrinsic and Apparent Periods

Spatial relationships change in a similar manner as the temporal relationships. The relationship between the coordinate (x) in the direction of wave propagation in the apparent reference frame and the intrinsic reference frame is as follows:

$$x_a = x_i + V_{\text{in-line}} t \quad (\text{A.47})$$

so that the space- and time-dependent argument ($kx_i - \omega_i$) of the harmonic function in all wave equations transforms, using Equations (A.47) and (A.44), into:

$$kx_i - \omega_i t = kx_a - (\omega_i + kV_{\text{in-line}}) t = kx_a - \omega_a t \quad (\text{A.48})$$

The transformation between encounter periods as measured from a moving vessel and intrinsic periods follows similar principles.

In wave spectra formulations (see A.8.3), the frequency parameter is the intrinsic frequency. However, a stationary structure (fixed or floating) in a wave field with current responds to the apparent frequency. To be able to perform the response calculations, the wave frequency spectrum formulation should therefore be transformed into the apparent frequency. As the wave energy per frequency band is independent of the reference frame, $S(\omega_i)d\omega_i = S(\omega_a)d\omega_a$ and hence the wave spectrum in the apparent frequency becomes $S(\omega_a) = S(\omega_i)d\omega_i/d\omega_a$. The coordinate transformations are carried out using Equation (A.44), taking due account of the fact that the wave number k is a function of the intrinsic wave frequency ω_i through Equation (A.45). However, the wave actions on a spatially distributed structure cannot be determined accurately using this spectrum as both the wavelength and the kinematics are a function of the intrinsic period, not the apparent period. An approach to addressing this issue is presented in Reference [64].

A.8.5 Maximum Height of an Individual Wave for Long Return Periods

The long-term maximum height H_N of an individual wave with a return period of N years can be estimated in several ways. The method used should account for the long-term uncertainty in the severity of the environment and the short-term uncertainty in the severity of the maximum wave of a given sea state or storm.

The statistically correct methods are based on storms. Storms are obtained from a time series of significant wave height by breaking it into events that have a peak significant wave height (H_{sp}) above some threshold.

The long-term uncertainty in the severity of the environment is treated using the probability distribution of the severity of the storm, measured in terms of either its peak significant wave height or the most probable maximum value of the individual waves in the storm (H_{mp}). The uncertainty in the height of the maximum wave of any storm is estimated as a probability distribution conditional on H_{sp} or H_{mp} . Convolution of the two distributions gives the distribution for any random storm and, thereby, the complete long-term distribution for the heights of individual waves. For further information, see Reference [2].

A similar method has been applied using sea states rather than storms as the independent variable. It is recognized that this method is not statistically robust because successive sea states are not independent. It involves analysis of many sea states that do not contribute to the final result and can give a false confidence in the results, as the amount of independent input data are much less than it appears. Despite these known flaws, this method often provides a useful first estimate of conditions in an area when only a short (e.g. 1 year to 2 years) measured data set of H_s is available (see, for example, Reference [30]).

An approximation that is sometimes used to generate H_N is to multiply H_{sN} , an estimate of the N -year return period H_s , by a factor that relates to the ratio of the most-probable highest wave in a sea state to the significant wave height H_{sN} . However, this method underestimates H_N because it ignores the contribution from sea states that are lower but more frequent than H_{sN} , as well as sea states that are higher but less frequent than H_{sN} . The accuracy of the method also depends on the mutual cancellation of errors in all the steps leading to the final answer. When this method is used, the individual wave heights are generally assumed to obey a Rayleigh or Forristall^[31] distribution (see below), and the sea state is assumed to have a duration of 3 h. Although the method has been applied in the past with some success, its use demands extreme care and should be avoided as better methods are now available (see, for example, References [2] and [8] for a discussion of various methods).

The classical description of the distribution of crest to trough heights (H) in narrow-banded seas is the Rayleigh distribution^[32], which in its cumulative probability form is given by:

$$P(H \leq H^*) = 1 - \exp \left[\frac{-2(H^*)^2}{(H_s)^2} \right] \quad (\text{A.49})$$

where H^* is any desired value of the significant wave height.

In practice, most seas are not narrow-banded and using the Rayleigh distribution would tend to over-predict the height of waves. To take account of the finite bandwidth, a number of empirically derived distributions have been proposed. The distribution proposed by Forristall [31], which was empirically derived using hurricane wave data from the Gulf of Mexico, is often used:

$$P(H \leq H^*) = 1 - \exp \left[\frac{-(4H^*/H_s)^\alpha}{\beta} \right] \quad (\text{A.50})$$

where

$$\alpha = 2.126;$$

$$\beta = 8.42.$$

NOTE 1 When $\alpha = 2$ and $\beta = 8$, the Forristall distribution reverts to the Rayleigh form.

NOTE 2 Though the above coefficients were developed using hurricane data, Krogstad's distribution based on North Sea storms is virtually the same [33].

The probability distributions for the maximum individual wave height in a stationary sea state can be established by raising Equation (A.49) or Equation (A.50) to a power equal to the number of waves in the interval. The probability distribution for the maximum individual wave height conditional on H_{sp} or H_{mp} can be determined by combining the distributions for each of the stationary sea states of which the storm is composed.

A.8.6 Nonlinear Wave Models

The fully nonlinear modelling of random, directional waves has been an active area of research for several years and some methods are now applicable for realistic sea states. Examples that might be considered for engineering application are those in References [34] to [38]. Though the methods offer the advantages of realism, there are the following difficulties and limitations:

- a) The models are slow even on the fastest computers. Computational effort can be significantly reduced by calculating New-waves rather than complete, random sea states.
- b) Some of the methods use Fourier models to describe the free-surface. This limits the validity of results as waves become steep-fronted at the crest at the onset of breaking. Others can restrict the freedom of motion of surface particles, with similar consequences.
- c) The overall recipe for calculation of actions based on regular wave or linear, random theory may have been subject to calibration against offshore measurements. When this is the case, actions calculated from the fully nonlinear methods should be tested either against the measurements or against the conventional method in the regime of the measurements.

Wave models based on expansions in wave slope might also be considered, although, as perturbation methods, they are not fully nonlinear [38, 39]. There is some indication that schemes valid to third-order, including quartet resonance effects, capture much of the important nonlinearity. However, as a wave slope expansion, they can fail, at least locally, as a wave becomes steep-fronted.

Linear spectral representations ignore the nonlinear interactions between waves of different frequencies and directions, whereas periodic wave representations ignore the irregular nature of waves. Extension of spectral representations to second-order has been used in practice (see Reference [40]).

A.8.7 Wave Crest Elevation

The long-term distribution of extreme and abnormal crest elevations can be established from a long time series of significant wave heights (H_s) and a short-term distribution of crest elevations conditional on H_s , $P(\eta > \eta^* | H_s)$. The statistically correct approach would use storms as the independent variable^[2]. The methods described in A.8.5 for wave height are equally useful for obtaining design values of crest elevation and total surface elevation.

Recent research suggests that crest elevations for seas with typical directional spreading of wave energy are satisfactorily predicted by second-order, random, directional wave theory. The short-term distribution of $P(\eta > \eta^* | H_s)$ can be obtained directly from theory or from a model distribution calibrated to fit the results of the theory. In Reference [42], a Weibull model has been matched to the theory over a range of water depths and wave steepnesses. The Weibull expression is:

$$P(\eta > \eta^* | H_s) = \exp \left[-\left(\frac{\eta}{\alpha H_s} \right)^\beta \right] \quad (\text{A.51})$$

where α and β are empirical functions of the wave steepness (S_1) and the Ursell number (U_r). S_1 and U_r are given by:

$$S_1 = 2 \pi H_s / g T_1^2 \quad (\text{A.52})$$

$$U_r = H_s / (k_1^2 d^3) \quad (\text{A.53})$$

where

- T_1 is the mean wave period calculated from the ratio of the first two moments of the wave spectrum, m_0/m_1 ;
- k_1 is the local wave number for a wave frequency $2\pi/T_1$;
- d is the water depth.

For a spread sea, the expressions for α and β are given by:

$$\alpha = 0.3536 + 0.2568 S_1 + 0.0800 U_r \quad (\text{A.54})$$

$$\beta = 2 - 1.7912 S_1 - 0.5302 U_r + 0.2824 U_r^2 \quad (\text{A.55})$$

It should be noted that the crest elevation estimates derived using distributions derived from measurements at a single point effectively only reflect the risk of exceedance at a single point. However, as described by Forristall^[103], when the true area of exposure to wave crests is considered (i.e. the full platform-deck area), the probability of having the point estimate exceeded somewhere locally within the deck is naturally higher than the probability of having it exceeded just at one point, since the potential crest encounter area is larger than one point. When the entire deck area is considered, a local crest height occurring somewhere in the deck area can exceed the point-estimated crest height by as much as 15 % for the same probability level. The local crest height in shallow water will, however, be limited due to wave breaking effects.

A.9 Currents

A.9.1 General

For bottom-founded structures, the total current profile associated with the sea state producing extreme or abnormal waves should be specified for the design of the structure. For floating structures, the selection of an appropriate combination of currents, waves and winds is often less obvious and needs careful consideration.

A.9.2 Current Velocities

The current flow at a particular site varies both in time and with depth below the mean sea surface. The characteristics of the extreme or abnormal current profile that need to be estimated for the design of offshore structures are particularly difficult to determine, since current measurement surveys are relatively expensive and consequently it is unlikely that any measurement program will be sufficiently long to capture a representative number of severe events. Furthermore, current (hindcast) modelling is not as advanced as wind and wave modelling. Also, extrapolation of any data set demands that account be taken of the three-dimensional nature of the flow.

Site-specific measurements of currents at the location of a structure can be used either as the basis for independent estimates of likely extremes or to check the indicative values of the various components of the total current.

Information on the frequency of occurrence of total current speed and direction at different depths for each month and/or each season is normally useful for planning operations. For most design situations in which waves are dominant, estimates of the extreme or abnormal residual current and total current can be obtained from high-quality site-specific measurements; these should extend over the water profile and over a period that captures several major storm events that generated large sea states. Current models may be used in lieu of site-specific measured data. The period over which the current model is run should be adequate to allow tidal decomposition to be carried out and the residual current to be separated out of the total current where appropriate. Consideration should be given to long-period, large-scale environmental fluctuations, which can affect the residual current climate. Efforts should be made to ensure that if a current model is used it is validated against nearby measured data.

A.9.3 Current Profile

The characteristics of the current profile over depth in different parts of the world depend on the regional oceanographic climate, in particular the vertical density distribution and the flow of water into or out of the area. Both of these controlling aspects vary from season to season. Typically, shallow-water current profiles in which tides are dominant can often be characterized by simple power laws of velocity versus depth, whereas deep-water profiles are more complex and can even show reversals of the current direction with depth. Such characteristics of the current flow can be particularly important to consider in the design of deep-water structures and parts of the system such as risers and mooring systems.

The power law current profile given in Equation (A.56) can be used where appropriate (e.g. in areas dominated by tidal currents in relatively shallow water, such as the southern North Sea):

$$U_C(z) = U_{C0} \left(\frac{z+d}{d} \right)^\alpha \quad (A.56)$$

where

- $U_c(z)$ is the current speed at elevation z ($z \leq 0$);
- U_{c0} is the surface current speed (at $z = 0$);
- z is the vertical coordinate, measured positively upwards from still water level;
- d is the still water depth;
- α is an exponent (typically 1/7).

Other current profiles in common use are as follows:

- a linear distribution between the surface current U_{c0} and a bottom current of half the surface current ($U_{c0}/2$),
- a bilinear distribution with parameters that are determined for the location concerned, and
- a slab profile [see Figure A.5 b)] where a uniform current occurs over the upper part of the water column with zero current over the lower part.

For deep water, design current profiles can be derived from long-term measured current-profile data sets through a two-stage process. In the first stage, the data are parameterized using empirical orthogonal functions; in the second stage, the design current profile with the required return period is selected through a process involving an inverse first-order reliability method (FORM) procedure. The method is described in Reference [43].

When a sufficiently long data series is available, with simultaneous data at different water depths, an alternative approach to deriving an N -year current profile commences with the estimation of the N -year current speed at a given reference depth. The conditional mean speed (given the extreme speed at the reference depth) is then selected for other depths. The process is repeated for differing reference depths, with the most onerous profile (for the particular application) being selected.

For some applications, an approach using a response function such as the integrated drag loading on a vertical cylinder can be used, as described in A.5.3 c).

A.9.4 Current Profile Stretching

A.9.4.1 General

References [44] and [45] show that waves alternately stretch and compress the current profile under crests and troughs, respectively. Stretching means that, in the presence of waves, the instantaneous current speed $U_c(z)$ of a water particle calculated at depth z (measured positively upwards from still water level for $-d \leq z \leq 0$) is effective at a stretched vertical coordinate z_s . In the design data, the current profile $U_c(z)$ is specified over the full water column between the sea floor at $z = -d$ and the still water level at $z = 0$. Both linear and nonlinear stretching methods are used.

In linear stretching, the relationship between z_s and z is proportional to the ratio of the instantaneous height of the water surface elevation and the still water depth. A stretching factor F_s can be introduced, in a manner analogous to the Delta stretching procedure for wave kinematics. For current stretching, F_s is defined as:

$$F_s = \frac{d + \eta}{d} \quad (\text{A.57})$$

where

- η is the instantaneous height of the water surface elevation (measured upwards from still water level);
- d is the still water depth.

The stretched vertical coordinate can then be expressed as:

$$z_s = F_s (d + z) - d \quad (\text{A.58})$$

where

- z_s is the stretched elevation (measured upwards from still water level);
- z is the original elevation (measured upwards from still water level).

For current stretching, the stretching factor F_s is larger than 1.0 and consequently $z_s > z$.

In nonlinear stretching, the elevations z_s and z are related through linear (Airy) wave theory as:

$$z_s = z + \eta \frac{\sinh [k_{nl}(z + d)]}{\sinh(k_{nl}d)} \quad (\text{A.59})$$

where, additionally,

- k_{nl} is the nonlinear wave number:

$$k_{nl} = \frac{2\pi}{\lambda_{nl}}$$

- λ_{nl} is the wavelength for the regular wave under consideration for water depth d and wave height H (calculated using nonlinear wave theory and the intrinsic wave period).

Equation (A.59) provides a nonlinear stretching of the current, with the greatest stretching occurring high in the water column, where the particle orbits have the greatest radii. Figure A.5 illustrates a comparison of linear and nonlinear stretching for sheared and slab current profiles.

Nonlinear stretching is the preferred method. For slab or power-law current profiles, simple vertical extension of the current profile from the still water level to the instantaneous wave surface is a good approximation to nonlinear stretching. For other current profiles, linear stretching is an acceptable approximation.

Another approximate model is the linearly stretched model described by Equation (A.59), adjusted such that the total momentum in the stretched profile from the sea floor to the wave surface equals that in the specified profile from the sea floor to the still water level. However, this procedure is not supported by the theoretical analyses in References [44] and [45].

If the current is not in the same direction as the wave, the methods discussed above can still be used, with one modification: both the in-line and the normal components of the current need to be stretched, but only the in-line component used to estimate T_i for the Doppler-shifted wave.

While no exact solution has been developed for irregular waves, the wave/current solution for regular waves can be logically extended. In the two approximations described above for regular waves, the period and length of the regular wave are replaced by the period and length corresponding to the spectral peak frequency.

A linearly stretched current profile is an acceptable approximate model for many applications. The method is exactly analogous to the stretching of linear wave kinematics as applied by Wheeler^[46].

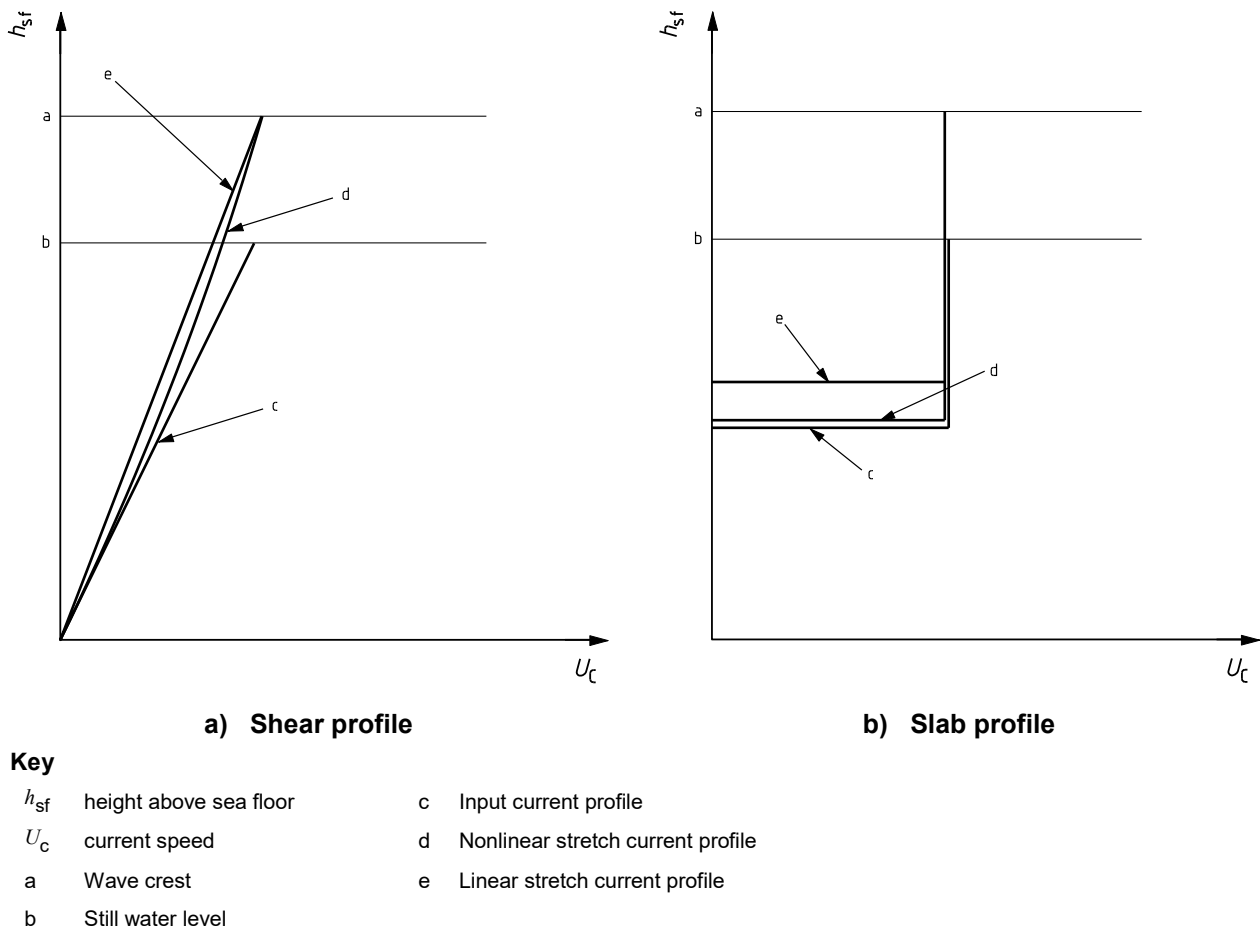


Figure A.5—Linear and Nonlinear Stretching of Current Profiles

A.9.4.2 Effect of Current Profile Stretching on Hydrodynamic Actions

Reference [44] reports that a model that combined Doppler-shifted wave kinematics with a nonlinearly stretched current profile gave the best estimate of global hydrodynamic actions on a space-frame structure. These are within a few percent of those produced by the exact solution on a typical drag-dominant fixed structure subjected to representative waves and current profiles.

In most cases, simple vertical extrapolation of the input current profile above mean water level produces reasonably accurate estimates of global hydrodynamic actions on drag-dominated fixed structures. In particular, for a slab profile thicker than approximately 50 m, vertical extrapolation produces nearly the same result as nonlinear stretching, as illustrated in Figure A.5. However, if the specified profile $U_c(z)$ has

a very high speed at the still water level, sheared to much lower speeds just below still water level, the global action can be overestimated (by approximately 8 % in a typical application).

A.9.5 Current Blockage

Current blockage refers to the global distortion of the current field in and around nonsolid structures. These are structures with a configuration that is to some extent transparent to the current and which thus allow partial flow at a reduced velocity through the structure. Taking account of current blockage can be of interest for the design of space-frame-type structures, both fixed and floating (e.g. semi-submersibles and TLPs), especially when they accommodate a large number of conductors or risers.

For fixed steel structures, reference should be made to ISO 19902.

A.10 Other Environmental Factors

A.10.1 Marine Growth

No guidance is offered. Some information is included within regional annexes. See Reference [47].

A.10.2 Tsunamis

For a given location, the frequency of earthquake events is generally very low and in particular the frequency of occurrence of a tsunami at a site is even lower, since only a very few earthquakes give rise to tsunamis. In comparison to earthquake data, the data on tsunamis are limited. Historical records should be examined to see if any tsunamis have occurred at or near a particular location, and consideration should also be given to possible source events and possible magnitudes. Tsunami waves undergo strong refraction, so consideration should be given to the exposure of a site to the possible directions of tsunami wave approach and the resulting associated currents. Detailed tsunami studies consider potential source zones that can generate tsunami waves, model transoceanic propagation and local refraction. Historic run-up events can be used for model validation, and modelling potential source zone events can lead to extreme-value estimates.

For the majority of offshore structures, the environmental actions are dominated by extreme wind waves. Most structures are effectively in deep water with regard to tsunami wave physics, which are at most a few tens of centimeters in height. While tsunami waves do not generally govern the design of fixed offshore structures, their very long periods can result in substantial actions on moored floating structures in water shallower than 100 m. It is prudent to be aware of the potential impact of tsunamis on moored floating structures that form part of an offshore field development.

Tsunami heights can radically increase due to shoaling and refraction, so special care should be taken at shallow-water sites near complicated bathymetry that can lead to a caustic (focal point for wave energy) or near semi-enclosed features such as bays. Coastal facilities are likely to be at the greatest risk due to the run-up of the tsunami and the potential for inundation of the facility and processing plant. Tsunamis approaching the coastline often scour the seabed, transporting large amounts of sediment shoreward and dumping it onshore, thereby increasing their destructiveness. It is prudent to perform an inspection if a tsunami passes over a pipeline.

Where tsunamis have a high probability of occurrence and significance (exceeding the generally accepted risk level in the design), the effects on structures should be assessed. Where possible, offshore structures should be designed against potential tsunamis or they should be located to minimize the consequences of impact.

Detailed procedures for seismic design are described in ISO 19901-2, which provides guidance and methods for determining the magnitude and probability of earthquake events.

A.10.3 Seiches

The effect of seiches can be important to consider for the design of loading and offloading facilities, as well as for operations (e.g. of tankers) in relatively shallow water locations.

A.10.4 Sea Ice and Icebergs

Where data are being collected on sea ice and icebergs, the following should be considered.

- The type of sea ice expected to occur is a measure of its age, whether first-year, multi-year, or of glacial origin. Distribution statistics reflect the variations that occur in the thickness, consolidation, and concentration of ice types during a season, both seasonally and from year to year.
- Sea-ice keels can create gouges in the seabed in relatively shallow or intermediate water depths (typically less than 25 m water depth).
- Characterization of year-round regional ice cover includes the occurrence and distribution of ice concentrations, thicknesses, floe sizes, and types present during freeze-up, winter, break-up, and open water seasons.
- Probability of occurrence of specific ice features, such as multi-year hummock fields and ice islands. In areas where ice of glacial origin is to be expected, the annual and seasonal variation in the flux, concentration, and size of icebergs is relevant.
- The probability distributions or extreme values of the velocity of pack ice, ice floes, and discrete ice features (such as icebergs, "bergy bits," "growlers," and ice islands) and seasonal variations of these distributions are relevant.

If sea ice or icebergs are possible and could be in excess of that which can be accommodated in a structure's design, an emergency preparedness system should be established. Solutions based on the relocation of the structure or the towing away of the ice feature may be chosen; in such cases, the emergency preparedness should be reliable and planned in relation to the time required to relocate the structure or to tow the ice feature away.

A.10.5 Snow and Ice Accretion

Snow can settle on both horizontal surfaces and, if the snow is sufficiently wet, on nonhorizontal windward parts of a structure. On vertical surfaces, it is only likely to stay in position as snow for a few hours, although it can freeze and remain as ice. It can therefore affect all exposed areas above the splash-zone. On horizontal surfaces, dry snow is blown off as soon as any thickness accumulates, whereas wet snow can remain in position for several hours.

In areas that are affected by icing, consideration should be given to the possibility of topsides icing from freezing sea-spray and freezing atmospheric vapour.

Ice can form on the topsides of a structure through a number of mechanisms:

- freezing of old wet snow;
- freezing sea spray;
- freezing fog and super-cooled cloud droplets;
- freezing rain.

In the absence of specific information, new snow can be assumed to have a density of 100 kg/m³ and the average density of ice formed on the structure can be taken to be 900 kg/m³.

A.11 Collection of Metocean Data

A.11.1 General

Table A.4 provides a range of potential applications of metocean information collected as part of a metocean data collection system.

Table A.4—Potential Application of Metocean Information

Application	Comments
Bridge and flotel disengagement	Bridge and/or flotel disengagement are required once predefined wind/wave criteria are exceeded.
Installation	Wind and wave data are usually needed for setting deck and modules, and currents can be important for running risers and stabbing tension leg platform tendons.
Crane operations	Wind and waves (or vessel heave) have an impact on safety margins for crane operations.
Diving operations	Can depend on a number of metocean parameters.
Evacuation	Meteorological and oceanographic data are vital for decisions regarding time of evacuation and selection of evacuation means.
Helicopter operations	Dependent on a number of metocean parameters, principally winds and visibility.
Maintenance	Maintenance operations, especially outdoor work above the open sea, are often subject to restrictions on weather and sea state.
Marine operations	Most marine operations need reliable metocean information.
Production shut-down	Can depend on a number of metocean parameters, mainly waves and wind.
Remotely operated vehicle operations	Can depend on a number of metocean parameters, mainly waves and ocean currents.
Search and rescue/man overboard (SAR/MOB)	Accurate metocean information can be crucial for effective and safe SAR and MOB operations.
Tanker loading	Tanker loading operations are sensitive to sea state and wind conditions, in particular during docking operations.
Verification studies	A number of long-term metocean parameters can be required for verification of offshore structures. Verification studies can depend on special metocean parameters or installation of standard instruments in special locations.

A.11.2 Common Requirements

A.11.2.2 Instrumentation

The required measurement uncertainty of metocean recordings should be chosen in accordance with Table A.5, which is based on information presented in Annex 1.B, pp. 19–24, Chapter 1, of WMO-No. 8:2008.

Table A.5—Recommended Instrument Accuracy and Typical Operational Performance

(1) Variable	(2) Range	(3) Reported Resolution	(4) Mode of Measurement/ Observation	(5) Required Measurement Uncertainty	(6) Sensor Time Constant	(7) Output Averaging Time	(8) Typical Operational Performance	(9) Remarks
1 Temperature								
1.1 Air temperature	-40 °C to +40 °C	0.1 K		0.1 K	20 s	1 min	0.2 K	Operational performance and effective time constant can be affected by the design of thermometer solar radiation screen.
1.2 Extremes of air temperature	-40 °C to +40 °C	0.1 K		0.1 K	20 s	1 min	0.2 K	
1.3 Sea-surface temperature	-2 °C to +40 °C	0.1 K		0.1 K	20 s	1 min	0.2 K	
2 Humidity								
2.1 Dewpoint temperature	< -60 °C to +35 °C	0.1 K		0.1 K	20 s	1 min	0.5 K	If measured directly. Tending to ± 0.1 °C when relative humidity nearing saturation.
2.2 Relative humidity	5 % to 100 %	1 %		+3 %	40 s	1 min	+3 % to 5 %	Solid state sensors can show significant temperature and humidity dependence. Humidity nearing saturation.
3 Atmospheric pressure								
3.1 Pressure	920 hPa to 1080 hPa	0.1 hPa		0.1 hPa	20 s	1 min	0.3 hPa	Range to sea level. Accuracy seriously affected by dynamic pressure due to wind and temperature co-efficient of transducer.
3.2 Tendency	Not specified	0.1 hPa		0.2 hPa			0.2 hPa	Difference between instantaneous values.

Table A.5—Recommended Instrument Accuracy and Typical Operational Performance (continued)

(1) Variable	(2) Range	(3) Reported Resolution	(4) Mode of Measurement/ Observation	(5) Required Measurement Uncertainty	(6) Sensor Time Constant	(7) Output Averaging Time	(8) Typical Operational Performance	(9) Remarks
4. Clouds								
4.1 Cloud amount	0/8 to 8/8	1/8	I	1/8	n/a		2/8	Period (30 s) clustering algorithms may be used to estimate low cloud amount automatically.
4.2 Height of cloud base	0 m to 30 km	10 m	I	10 m for \leq 100 m 10 % for > 100 m	n/a		\approx 10 m repeatability*	*Accuracy difficult to determine since no definition exists for instrumentally measured cloud base height.
5. Wind								
5.1 Speed	0 m/s to 60 m/s	0.5 m/s	A	0.5 m/s for \leq 5 m/s 10 % for > 5 m/s	Distance constant. 2 m to 5 m	2 min and/or 10 min	0.5 m/s for \leq 5 m/s 10 % for > 5 m/s	Average over 2 and /or 10 min. Nonlinear devices. Care needed in design of averaging process.
5.2 Direction	0° to 360°	1°	A	5°	1 s	2 min and/or 10 min	5°	
5.3 Gusts	0 m/s to 75 m/s	0.1 m/s	A	10 %		3 s	0.5 m/s for \leq 5 m/s 10 % for > 5 m/s	Highest 3 s average should be recorded.

Table A.5—Recommended Instrument Accuracy and Typical Operational Performance (continued)

(1) Variable	(2) Range	(3) Reported Resolution	(4) Mode of Measurement/ Observation	(5) Required Measurement Uncertainty	(6) Sensor Time Constant	(7) Output Averaging Time	(8) Typical Operational Performance	(9) Remarks
6. Visibility								
6.1 MOR	< 50 m to 70 km	10 m	I	50 m for ≤ 500 m 10 % for > 500 m and ≤ 1500 m 20 % > 1500 m	< 30 s	1 min and 10 min	The larger of 20 m or 20 %	Achievable instrumental accuracy can depend on the cause of obscuration. Quantity to be averaged: extinction coefficient (see WMO-No 8, Part III, Chapter 3, Section 3.6). Preference for averaging logarithmic values.
6.2 RVR	10 m to 1500 m	1 m	A	10 m for ≤ 400 m 25 m for > 400 m to ≤ 800 m 10% for > 800 m	< 30 s	1 min and 10 min	The larger of 20 m or 20 %	Should be in accordance with WMO-No.49, Volume II, Attachment A (2004 ed.) and ICAO Doc 9328-AN/908 (2nd ed., 2000).
7. Waves								
7.1 Time series of sea surface elevation	-15 m to +20 m	0.1 m	I		0.5 s	n/a	±0.2 m for ≤ 5 m ±4 % for > 5 m	Length of time series 17 min (typical). Sampling frequency 2 Hz.
7.2 Variables from time series (zero crossing analysis)							Depends on averaging time and sea regularity as well as intrinsic instrument accuracy.	Observed value at location of sensor. New value every 30 min (typical).
7.2.1 Significant wave height (H_s)	0 m to 20 m	0.1 m	A	0.5 m for ≤ 5 m 10 % for > 5 m	0.5 s	20 min (typical)		
7.2.2 Average zero crossing period (T_z)	3 s to 30 s	1 s	A	0.5 s	0.5 s	20 min (typical)		
7.2.3 Maximum wave height (H_{max})	0 m to 35 m		I		0.5 s	20 min (typical)		

Table A.5—Recommended Instrument Accuracy and Typical Operational Performance (continued)

(1) Variable	(2) Range	(3) Reported Resolution	(4) Mode of Measurement/ Observation	(5) Required Measurement Uncertainty	(6) Sensor Time Constant	(7) Output Averaging Time	(8) Typical Operational Performance	(9) Remarks
7.3 Wave spectrum						Minimum 17 min	Depends on averaging time and sea regularity as well as intrinsic instrument accuracy.	Instruments may include wave buoys, altimeter, microwave Doppler radar, HF radar, navigation radar etc. (1 Hz sampling frequency is sufficient.)
7.3.1 1-D spectral density		0.1 m ² ·Hz ⁻¹	I				Should be sufficient to achieve 7.4 requirements.	
Frequency	0.035 Hz to 0.3 Hz	< 0.01 Hz						
7.3.2 2-D spectral density		0.1 m ² ·Hz ⁻¹ ·rad ⁻¹						
Frequency	0.035 Hz to 0.3 Hz	< 0.01 Hz					Should be sufficient to achieve 7.4 requirements.	
Direction	0 ° to 360 °	10° (see remark)						2-D spectrum may be based on parameterized directional distribution and reported as direction and spread parameters.

Table A.5—Recommended Instrument Accuracy and Typical Operational Performance (continued)

(1) Variable	(2) Range	(3) Reported Resolution	(4) Mode of Measurement/ Observation	(5) Required Measurement Uncertainty	(6) Sensor Time Constant	(7) Output Averaging Time	(8) Typical Operational Performance	(9) Remarks
7.4 Variables from wave spectrum							Depends on averaging time and sea regularity as well as intrinsic instrument accuracy.	
7.4.1 Significant wave height (H_{mo})	0 m to 20 m	0.1 m	A		0.5 s	20 min	0.5 m for \leq 5 m; 10 % for $>$ 5 m	
7.4.2 Average period (T_{m02})	3 s to 30 s	0.1 s	A		0.5 s	20 min	0.5 s	
7.4.3 Peak period (T_p)	3 s to 30 s	0.1 s	A		0.5 s	20 min	0.5 s	Period of peak of frequency spectrum.
7.4.4 Mean direction	0 ° to 360 °	10°	A		0.5 s	20 min	20°	May be spectrally averaged or based on angular harmonics.
7.4.5 Direction spread	0 ° to 360 °	10°	A					
8 Ocean currents								
8.1 Current speed	0 cm·s⁻¹ to 250 cm·s⁻¹	1 cm·s⁻¹	A	1 cm·s⁻¹ to 10 cm·s⁻¹	1 s	5 min to 20 min	2 cm·s⁻¹ to 10 cm·s⁻¹	Achievable accuracy affected by type of measurement; direct or acoustic Doppler profilers.
8.2 Current direction	0° to 360°	1°	A	±5°	1 s	5 min to 20 min	±5°	
9 Water level	±3 m	1 cm	I	±1 cm		10 min	±5 cm	

Table A.5—Recommended Instrument Accuracy and Typical Operational Performance (continued)

(1) Variable	(2) Range	(3) Reported Resolution	(4) Mode of Measurement/ Observation	(5) Required Measurement Uncertainty	(6) Sensor Time Constant	(7) Output Averaging Time	(8) Typical Operational Performance	(9) Remarks
10 Temperature profile	-2 °C to +25 °C	0.1 K	I	0.01 K	0.5 s	1 s	0.05 K	Achievable accuracy according to commonly used CTD sensors.
11 Salinity profile	0 to 40 PSU	0.1	I	±0.01 PSU	0.5 s	1 s	±0.05 PSU	As per temperature profile unit: PSU (Practical Salinity Unit) according to PSS78.
12 Oxygen	0 ml/l to 15 ml/l	0.1 ml/l	I	±5 %	0.5 s	1 s	±5 %	

NOTE 1 Column 1 gives the basic variable.

NOTE 2 Column 2 gives the common range for most variables; limits depend on local climatological conditions.

NOTE 3 Column 3 gives the most stringent resolution as determined in WMO-No. 8.

NOTE 4 In column 4:

I: Instantaneous. In order to exclude the natural small-scale variability and the noise, an average value over a period of 1 min is considered as a minimum and most suitable; averages over periods of up to 10 min are acceptable.

A: Averaging. Average values over a fixed time period, as specified by the coding requirements.

A.11.3 Meteorology

A.11.3.1 General

Details on instrument accuracy and calibration are found in WMO-No. 8, Parts I and III.

A.11.3.2 Weather Observation and Reporting for Helicopter Operations

Experience has shown that the best quality wind measurements are achieved if the location of the wind sensor is selected to minimize the influence from the construction itself (living quarters, cranes, etc.). This means that the top of derrick or mast is the best choice in most cases.

The measurement of these parameters does not replace the need for an easily perceptible wind sock or cone.

The observations should be recorded in accordance with WMO-No. 306, Section A, pp. 25–36.

In addition to METAR, a code for special reports is specified in WMO-No. 306, under code FM 16-XV Ext. SPECI.

The criteria for, and frequency of, issue of METARs and SPECIs is the responsibility of the relevant aviation regulations. International recommendations may be found in WMO-No. 842 (Chapter 4).

A.11.4 Oceanography

A.11.4.2 Measurements and Observations

Ocean currents should be measured at fixed depths (or bins), and include at least three depths in shallow waters: near-surface, mid-depth, and near-bottom.

For measurements in deeper waters, the following depths should be considered in addition to near-surface and near-bottom: 50 m, 100 m, 150 m, 200 m, 300 m, and every 200 m thereafter to 3 m above the seabed.

The mean speed and direction of ocean currents should be recorded at least once per hour. Measurements of sea temperature and salinity should be performed as an integrated activity. If Nansen bottles or similar equipment are used, data should be recorded at standard depths: 0 m, 5 m, 10 m, 20 m, 30 m, 50 m, 75 m, 100 m, 125 m, 150 m, 200 m, 250 m, 300 m, 400 m, 500 m, 600 m, 800 m, etc.

If a conductivity-temperature-depth (CTD) sensor is used for measuring temperature and salinity, data should be stored for at least every 50 kPa (0.5 bar).

Oxygen content, if required, should be measured at a subset of the temperature/salinity depths given above. However, the number of depths may be considerably reduced.

The observation of sea ice and icebergs (dimensions and drift) can be performed by combining, e.g. manual observations, instrument recordings, and remote sensing.

Annex B (informative)

Northwest Europe

B.1 Description of Region

The geographical extent of the region of northwest Europe is bounded by the continental shelf margins of Europe, as shown in Figure B.1. The region is diverse, stretching from the sub-arctic waters off Norway and Iceland to the Atlantic seaboard of France and Ireland in the south, and includes:

- the waters off Norway, part of which are within the Arctic Circle;
- the Baltic Sea;
- the North Sea;
- the Irish Sea;
- the English Channel;
- the northern half of the Bay of Biscay;
- the waters off the west coasts of Ireland and Scotland; and
- the waters off the Faroe Islands.

B.2 Data Sources

Measured data are available from many stations throughout the area. Sources for measured data can be identified through the International Oceanographic Data and Information Exchange^[48], which is part of UNESCO (United Nations Educational, Scientific and Cultural Organization). Links will be found to national oceanographic data centres, which in turn provide links to specialist institutes and other organizations within each country. Data may also be obtained from commercial organizations. In addition to measured data, in recent years a number of joint industry-sponsored hindcast studies have been performed (see, for example, References [49] and [50]). These have resulted in extensive (but usually proprietary) data sets for the companies involved; however, a recently published report^[51] provides useful information derived from the NEXT hindcast study^[49].

B.3 Overview of Regional Climatology

The conditions experienced within the region vary from arctic to temperate. The north of Norway experiences very cold winters, with low temperatures and associated ice in various forms. However, ice occurs very rarely in the southwest of the region.

In all parts of the region, extremes of wind and wave are most likely to occur during the passage of a vigorous frontal depression. Depressions are areas of low atmospheric pressure and cyclonic airflow; they vary from nebulous, with light winds, to intense and stormy with a large area of strong winds. Together with associated frontal systems, they cross the area throughout the year, generally from west to east. They can move rapidly, with speeds of translation of 5 m/s to 15 m/s, and a wide range of conditions can be experienced at any one site. Depressions are larger than tropical cyclonic storms such as

hurricanes. Another type of depression is called a “polar low.” Such depressions do not have fronts and are less common than frontal depressions and generally less intense.

B.4 Water Depth, Tides, and Storm Surges

Water depths in the area are shown in Figure B.2. Much of the water around the British Isles and in the North Sea and Baltic Sea is less than 200 m deep. However, there is a deep trench adjacent to the southern coast of Norway where water depths in excess of 1000 m occur. Off the continental shelf, the Norwegian Sea is deep water, whereas the Barents Sea is approximately 500 m deep. The Faroe-Shetland Channel is approximately 1000 m deep.

Tides in the region are semi-diurnal, with two high and two low tides per day. Largest tidal ranges occur on the eastern side of the Irish Sea, the east coast of the UK, in the English Channel, and around the Brest Peninsula.

The highest storm surges occur in the southeastern part of the North Sea. Storm surges also affect areas with large tidal range.

B.5 Winds

The airflow in depressions is cyclonic, which is anti-clockwise in the northern hemisphere. The fronts associated with depressions occur in troughs of low pressure within the depression and are often marked by a change of wind direction and/or speed.

Intense depressions generate sustained winds with speeds in excess of 33 m/s, which is hurricane force. The strongest winds tend to blow from between southwest and northwest, with the lightest winds being those from the northeast. Topography and unstable atmospheric conditions can modify wind speed and direction. A warmer sea overlain with cooler air produces unstable atmospheric conditions conducive to squalls and turbulent airflow.

B.6 Waves

The region includes semi-enclosed seas, i.e. the Irish Sea, the English Channel, the North Sea, and the Baltic Sea, as well as areas of ocean. While strong winds can occur over the whole region, the nature of waves varies according to the water depth and fetch over which they have been generated. Where fetch is restricted, storm waves are shorter, steeper, and lower than in the deep ocean. The oceanic area is subject to swell waves that have moved out of the area in which they were generated. These swell waves can occur without any wind and can have wave periods of 20 s or more. Swell can penetrate to all but the most sheltered locations.

B.7 Currents

The seas of the region contain extensive areas of shallow water, channels, and headlands that experience strong tidal currents on a daily basis.

Periodically, strong currents can also occur in association with storm surge. This is water flow induced by meteorological forcing such as wind and atmospheric pressure.

Significant eddies occur in a permanent current along the coast of Norway.

In the oceans, the continental shelf edge is subject to particularly complex processes that have been the subject of extensive study. The area west of the Shetland Islands experiences strong currents at all depths, due to the topography of the sea floor and the interaction of water masses with differing characteristics. Other sections of the continental shelf edge have yet to be studied in detail. A comparison

of the area to the west of Shetland with the northern North Sea, together with a discussion of the background to the complex current regime in the area, can be found in Reference [52].

B.8 Other Environmental Factors

B.8.1 Marine Growth

Marine growth, or fouling, occurs in both hard and soft forms and also as seaweed or kelp. Hard fouling consists of mussels, barnacles and tubeworms, whereas soft fouling consists of organisms such as hydroids, anemones, and coral. Different types of marine growth occur at different water depths and in different parts of the region. An anti-fouling coating can delay marine growth, but significant fouling is likely within 2 years to 4 years.

Estimates of marine growth on offshore structures in UK waters are given in References [47] and [53]; the information from Reference [53] is summarized in Table B.1.

Table B.1—Terminal Thickness of Marine Growth—UK Sector

Depth	Type of Growth		
	Hard	Soft	Algae/Kelps
0 m to 15 m	0.2 m	0.07 m	3.0 m
15 m to 30 m	0.2 m	0.3 m	unknown
30 m to sea floor	0.01 m	0.3 m	no growth

Unless more accurate data are available, or if regular cleaning is not planned, the thickness of marine growth for areas offshore Norway may be assumed to be those shown in Table B.2 (Reference [54]). The thickness of marine growth may be assumed to increase linearly over a period of 2 years after the structure has been placed offshore.

Table B.2—Estimated Maximum Thickness of Marine Growth—Areas Offshore Norway

Depth from Mean Water Level m	Thickness of Marine Growth at Latitude	
	56° N to 59° N	59° N to 72° N
Above +2	0.00 m	0.00 m
+2 to -40	0.10 m	0.06 m
Below -40	0.05 m	0.03 m

B.8.2 Sea Ice and Icebergs

The Barents Sea is the most northerly sea in the region, and there is a large variation of ice conditions from year to year. The ice usually reaches its maximum extension in April, when in the eastern part it reaches the Russian mainland. The minimum extension is usually in August, when an ice border can typically be seen at 80° N. The icebergs that drift in the Barents Sea originate from the glaciers at Svalbard and Franz Joseph Land and Novaya Zemlya. Reference [55] provides a good general overview of the meteorological and oceanographic conditions pertaining to the Barents Sea area.

Actions from sea ice and icebergs should be taken into account when structures are located in areas near shore, in Skagerrak, in the northern and western parts of the Norwegian Sea, and in parts of the Barents Sea.

Figure B.3 shows the occurrence of first-year ice in the region, based on satellite observations, with an annual probability of exceedance of 10^{-2} . For planning of operations, the monthly extreme ice limit with annual probability of exceedance of 10^{-2} may be used; however, these data should be used with caution and allowance made for ice concentrations below some 10 % to 20 %, which cannot be detected by satellite. Monthly values for the extreme ice limit with an annual probability of exceedance of 10^{-2} can be found in Reference [55]. These values may be used in evaluations during an early phase of exploration.

To calculate the actions caused by ice, values for thickness and dimensions of ice floes that are representative of the area should be selected. The mechanical properties of the ice can be assumed to be similar to those in other arctic areas.

Regions where collision between icebergs and a structure can occur with an annual probability of exceedance of 10^{-2} and 10^{-4} in the Barents Sea are shown in Figure B.4. Icebergs were observed in considerable numbers off the East Finnmark coast in 1881 and in 1929.

B.8.3 Snow and Ice Accretion

The incidence of snow and ice varies considerably between the southwestern and northeastern limits of northwest Europe. In the southwest, snow and ice occur infrequently, whereas in the northeast, snow and ice are important design parameters.

Estimates of extreme snow accumulations on offshore structures in UK waters are given in Reference [53]; typical values are given in Table B.3. The pressure due to wet snow has been calculated as being in the range of 0.15 kPa to 0.24 kPa.

Table B.3—Accumulation of Ice: Offshore Structures in UK Sector

Cause of Ice	Thickness mm	Density kg/m ³
Wet snow	10 to 30	900
Sea spray	5 to 25	850

Useful information about the occurrence of snow and ice accretion off Norway can be found in Reference [54]. For areas on the Norwegian continental shelf where more accurate meteorological observations have not been made, the characteristic pressure due to snow may be assumed to be 0.5 kPa.

In the absence of a more detailed assessment, values for the thickness of ice accretion caused by sea spray and precipitation may be taken from Table B.4. The thicknesses and densities should be calculated separately for ice created from sea spray and ice created from precipitation, and both should be applied. When calculating wind, wave, and current actions, increases in dimensions and changes in the shape and surface roughness of the structure as a result of ice accretion should be considered by assuming that:

- ice from sea spray covers the whole circumference of the element, and
- ice from precipitation covers all surfaces facing upwards or against the wind (for tubular structures, it can be assumed that ice covers half the circumference).

An uneven distribution of ice should be considered for buoyancy-stabilized structures. The effects of ballast water, firewater, etc., which can freeze, should also be taken into account.

Table B.4—Ice Accretions: Annual Probability of Exceedance of 10⁻²

Height above Sea Level m	Ice Created from Sea Spray			Ice Created from Precipitation	
	Thickness mm		Density kg/m ³	Thickness mm	Density kg/m ³
	56° N to 68° N	North of 68° N		—	
5 to 10	80	150	850	10	900
10 to 25	Linear reduction from 80 to 0	Linear reduction from 150 to 0	Linear reduction from 850 to 500	10	900
Above 25	0	0	—	10	900

B.8.4 Air Temperature, Humidity, and Visibility

In winter, typical air temperatures range from -4°C in the Barents Sea to $+10^{\circ}\text{C}$ south of Ireland. Absolute minima are considerably lower. In summer, typical air temperatures range from 6°C in the Barents Sea to 18°C south of Ireland. Absolute maxima are considerably higher.

High humidity occurs when relatively warm air is cooled by the sea. This leads to reduced visibility or fog. Fog is more common in winter than in summer, with the North Sea experiencing more fog than most other areas.

Details of the meteorology of all sea areas are found in navigational publications such as *Pilots*. Such documents are published in many countries.

B.8.5 Sea Water Temperature and Salinity

In winter, sea surface temperature ranges from about 0°C in the Barents Sea to 12°C south of Ireland. In summer, the corresponding range is from about 8°C to 18°C . Both lower temperatures in winter and higher temperatures in summer are regularly attained locally.

Mean salinity is fairly constant at 35 PSU, but lower salinity occurs around the coasts of Norway and in particular in the Baltic Sea where the surface water is much less saline.

B.9 Estimates of Metocean Parameters

B.9.1 Extreme Metocean Parameters

In the northwest European region, there is a high (but not perfect) correlation between severe wind and wave events. Storm surge events are also associated with strong winds as well as with low atmospheric pressure. Tides are forced by astronomical influences, and as such are independent of meteorology.

Actions on a structure are due to the combined action of wind, waves, and current. However, all structures react differently, and without detailed knowledge of a structure it is not possible to define how wind, waves, and current should be characterized and combined to generate actions.

Metocean parameters for several locations in the region are provided in Tables B.5 to B.12. The wind, wave, and current values are independently derived marginal parameters; no account has been taken of conditional probability. This information should not replace the detailed, site-specific parameters that should be obtained for the design or assessment of a particular structure that is to be constructed for, or operated at, a particular site.

Table B.5—Indicative Values of Metocean Parameters—Sites in Celtic Sea

Metocean Parameter	Return Period (years)				
	1	5	10	50	100
10 min mean wind speed (m/s)	27	31	32	35	37
Significant wave height (m)	9.4	11.8	12.8	15.4	16.8
Spectral peak period ^a (s)	13.9	15.6	16.3	17.9	18.7
Surface current speed (m/s)	0.89	0.92	0.94	0.98	1.00

^a Assume the spectral peak period can vary by ± 10 % around these central estimates.

Table B.6—Indicative Values of Metocean Parameters—Sites in Southern North Sea

Metocean Parameter	Return Period (years)				
	1	5	10	50	100
10 min mean wind speed (m/s)	27	31	32	35	36
Significant wave height (m)	6.0	7.1	7.5	8.6	9.0
Spectral peak period ^a (s)	11.3	12.3	12.6	13.6	13.9
Surface current speed (m/s)	1.17	1.23	1.25	1.31	1.33

^a Assume the spectral peak period can vary by ± 10 % around these central estimates.

Table B.7—Indicative Values of Metocean Parameters—Sites in Central North Sea

Metocean Parameter	Return Period (years)				
	1	5	10	50	100
10 min mean wind speed (m/s)	31	33	34	36	39
Significant wave height (m)	9.8	11.2	11.8	13.1	13.6
Spectral peak period ^a (s)	13.6	14.6	15.0	15.7	16.0
Surface current speed (m/s)	0.88	0.90	1.00	1.00	1.00

^a Assume the spectral peak period can vary by ± 10 % around these central estimates.

Table B.8—Indicative Values of Metocean Parameters—Sites in Northern North Sea

Metocean Parameter	Return Period (years)				
	1	5	10	50	100
10 min mean wind speed (m/s)	35	39	40	43	45
Significant wave height (m)	12.0	13.6	14.3	15.7	16.4
Spectral peak period ^a (s)	14.6	15.5	15.9	16.7	17.0
Surface current speed (m/s)	0.60	0.65	0.70	0.85	0.90

^a Assume the spectral peak period can vary by ± 10 % around these central estimates.

Table B.9—Indicative Values of Metocean Parameters—Sites West of Shetland

Metocean Parameter	Return Period (years)				
	1	5	10	50	100
10 min mean wind speed (m/s)	35	39	40	43	45
Significant wave height (m)	13.2	15.0	15.7	17.3	18.0
Spectral peak period ^a (s)	16.2	17.1	17.4	17.9	18.2
Surface current speed (m/s)	1.64	1.78	1.80	1.95	2.00

^a Assume the spectral peak period can vary by ± 10 % around these central estimates.

Table B.10—Indicative Values of Metocean Parameters—Sites at the Haltenbank

Metocean Parameter	Return Period (years)				
	1	5	10	50	100
10 min mean wind speed (m/s)	32	35	34	36	37
Significant wave height (m)	11.6	13.3	13.9	15.7	16.4
Spectral peak period ^a (s)	15.9	16.8	17.2	17.9	18.2
Surface current speed (m/s)	0.80	0.85	0.95	1.00	1.05

^a Assume the spectral peak period can vary by ± 10 % around these central estimates.

Table B.11—Indicative Values of Metocean Parameters—Sites in Barents Sea

Metocean Parameter	Return Period (years)				
	1	5	10	50	100
10 min mean wind speed (m/s)	33	35	36	39	40
Significant wave height (m)	10.0	11.9	12.2	14.0	14.5
Spectral peak period ^a (s)	14.7	15.9	16.0	17.1	17.4
Surface current speed (m/s)	0.90	0.95	0.97	1.00	1.05

^a Assume the spectral peak period can vary by ± 10 % around these central estimates.

Table B.12—Temperature Ranges—Sites in North Sea, Eastern North Atlantic, and Norwegian Sea

Area	Air Temperature	Sea Surface Temperature	Sea Floor Temperature
	°C		
Celtic Sea	-4 to +27	-4 to +22	—
Southern North Sea	-6 to +26	0 to +22	+4 to +15
Central North Sea	-6 to +24	+1 to +21	+4 to +11
Northern North Sea	-7 to +22	+2 to +19	+3 to +13
West of Shetland	-5 to +22	+3 to +19	-2 to +12
Haltenbank	-9 to +18	+5 to +17	+5 to +9
Barents Sea	-18 to +18	+2 to +14	-1 to +7

B.9.2 Long-term Distributions of Metocean Parameters

Scatter diagrams of significant wave height versus zero-crossing period for sites in the North Sea, eastern North Atlantic, and Norwegian Sea are available for UK operating areas from Reference [51].

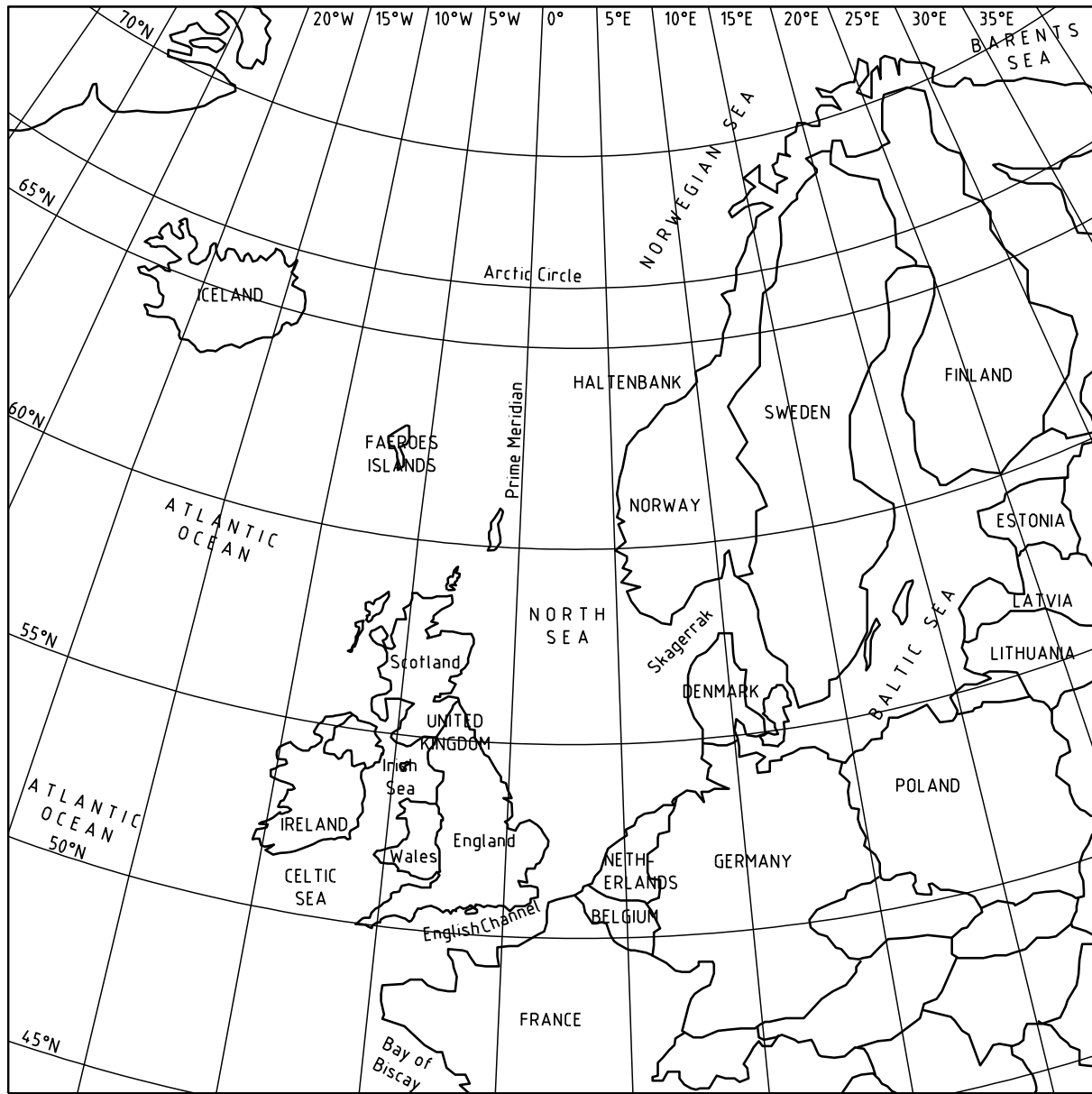


Figure B.1—Map of Northwest Europe Region

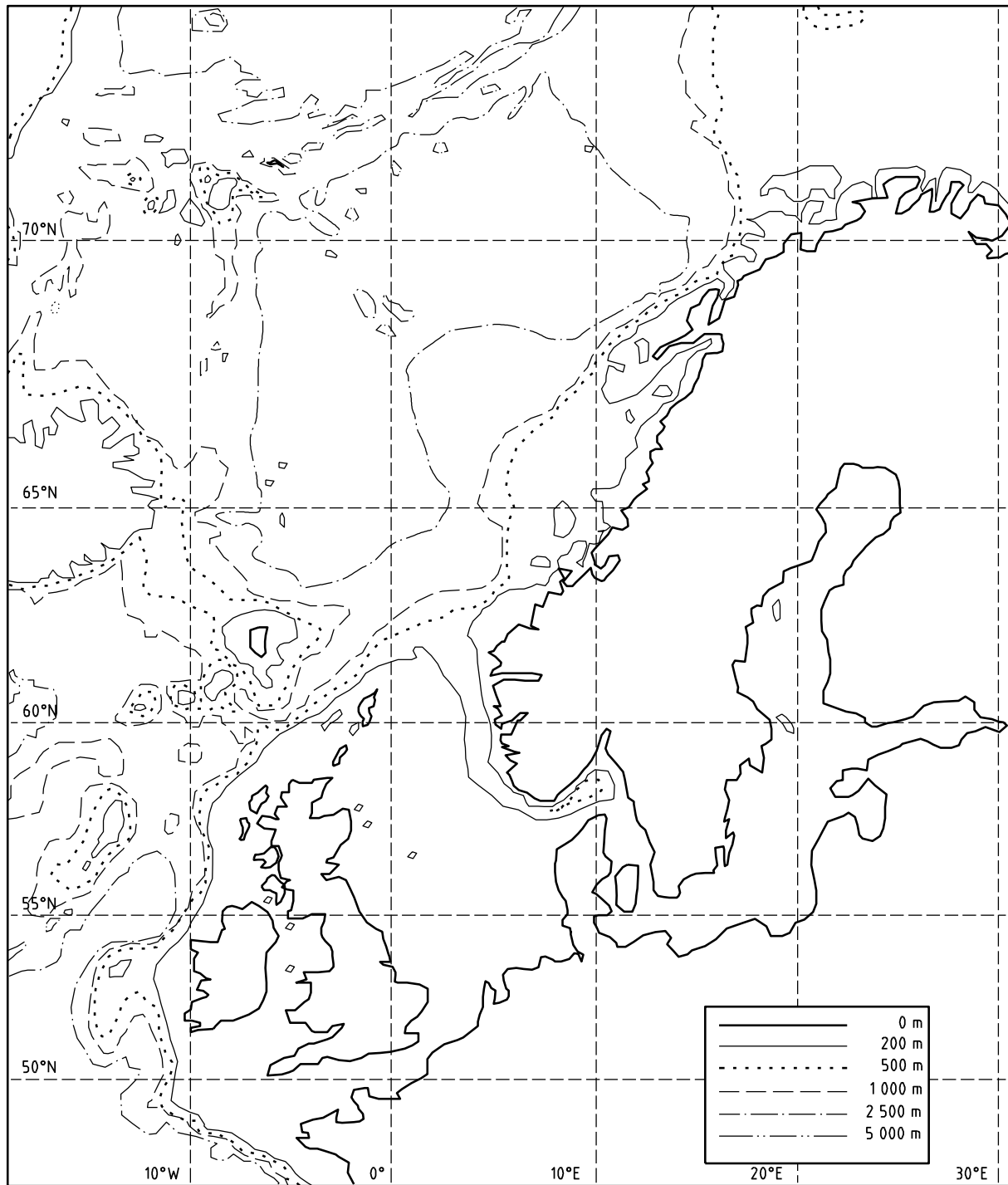


Figure B.2—Water Depths—Northwest Europe Region

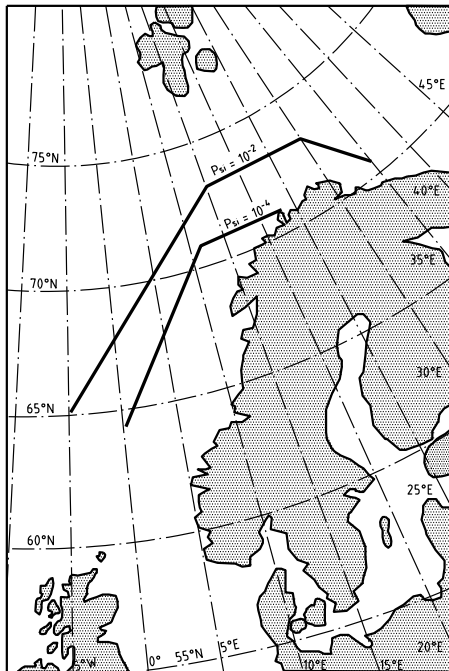


Figure B.3—Limit of Sea Ice—Northwest Europe Region—Annual Probabilities of Exceedance of 10^{-2} and 10^{-4}

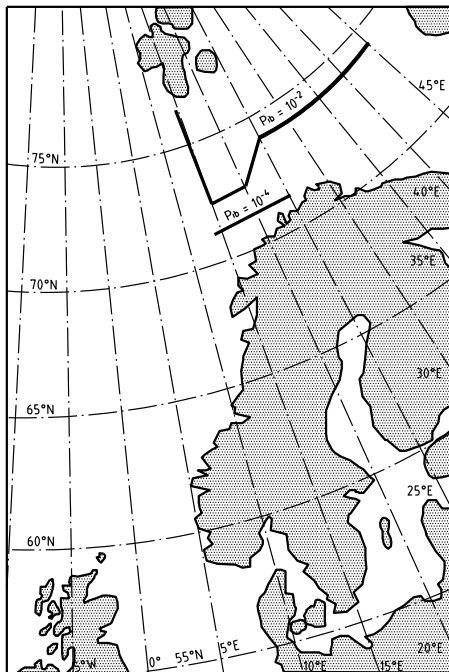


Figure B.4—Limit for Collision with Icebergs—Northwest Europe Region—Probabilities of Exceedance of 10^{-2} and 10^{-4}

Annex C (informative)

West Coast of Africa

C.1 Description of Region

The geographical extent of this region is the waters off West Africa from the Ivory Coast to Namibia (see Figure C.1). Insufficient data are available to provide guidance for other waters off West Africa.

The continental shelf is relatively narrow throughout most of the region, with a distance from the coast to the 200 m depth contour generally less than 100 km. The continental shelf is generally narrower near the equator (e.g. offshore the Ivory Coast to Nigeria) and wider in the south (e.g. offshore Namibia), although there are fluctuations along the entire coast.

A large number of rivers discharge into the area, the most significant being the Congo and the Niger.

C.2 Data Sources

Publicly available measured and modelled data are generally scarce across the region. The principal metocean hindcast data set for the region is WANE (West Africa Normals and Extremes)^[56]. The WANE hindcast model does not represent squalls, which dominate the extreme wind conditions. Detailed squall criteria have so far been derived from a small number of proprietary measured data sets. Strategic measurement programs that provide improved measurement of squalls are likely to be a focus of future joint industry projects.

A description of the environmental conditions offshore West Africa is available in Reference [57]. Much of the information in this clause has been derived from this source and from *Africa Pilot*^[58].

C.3 Overview of Regional Climatology

The northern-hemisphere summer is defined as July through to September, whereas the southern-hemisphere summer is defined as November to February.

Compared to regions such as the Gulf of Mexico and West of Shetlands, the climate offshore West Africa is often considered benign. The persistent southeasterly trade winds dominate the normal wind regime, whereas extreme winds are caused by squall events. Normal and extreme wave conditions are dominated by two sources of swell: those coming from the southeast and those from the southwest sectors. The long periods associated with some of the swell have specific consequences for design. A distinct sea wave component is usually also present.

The long-term current conditions are dominated by large-scale circulation patterns. On shorter time scales a wide range of oceanographic processes, including mesoscale activity, river outflow, inertial currents, and internal waves, complicate the current regime.

Hot and humid conditions prevail across the region, particularly near the equator. The region encounters a wide geographical variation in rainfall, with the most intense rainfall being caused by thunderstorms and squalls near the equator. Visibility is reduced by a variety of factors across the region.

C.4 Water Depth, Tides, and Storm Surges

There are three major deep ocean basins in the region, all over 5000 m deep: the Guinea basin, the Angola basin, and the Cape basin. The Guinea and Angola basins are separated by a gently sloping ridge along which exist numerous seamounts and, further inshore, an island chain. The much steeper Walvis Ridge separates the Angola and Cape basins. Between these ridges the continental slope (from the 200 m to 5000 m depth contours) varies in width from approximately 100 km offshore Ghana to over 600 km offshore Angola.

Equatorial and southwest Africa experience a semi-diurnal tidal regime. Tidal ranges are relatively small at the coast, with spring tidal ranges around 2 m and neap tidal ranges less than 1 m. The tidal range decreases rapidly further away from the shore, with a spring tidal range usually less than 1 m in deep water. Storm surges are small throughout the region.

C.5 Winds

The normal wind regime is dominated by persistent southerly trade winds, driven by large-scale atmospheric pressure systems. The trade winds are strongest in southern parts of the region where they typically range from 5.5 m/s to 7.5 m/s, and weakest in the north where they vary between 2.5 m/s to 5.0 m/s. The strongest winds generally occur during the northern-hemisphere summer and the weakest winds generally occur in the northern-hemisphere winter. These seasonal variations follow fluctuations in the latitude of the northernmost boundary of the "south-easterly trade wind regime," from about 15° N in the northern-hemisphere summer to about 7° N in the northern-hemisphere winter.

In the southern part of the region, the trade winds blow predominately from the southeast, but the direction slowly shifts until it reaches southwesterly off Nigeria.

Apart from the seasonal changes, the strength of the trade winds is fairly constant. However, there can be a significant diurnal variation in wind speed in near-shore locations influenced by sea breezes. This diurnal variation is reduced further from the shore.

Fully developed tropical or extra-tropical revolving storms (e.g. tropical cyclones) are very rare or nonexistent in the region, and extreme winds are caused by squall events. Squalls are associated with the leading edge of multi-cell thunderstorms. Thunderstorms and squalls are most frequent in equatorial West Africa, and typically stronger offshore Nigeria than offshore Angola, with around 15 to 30 significant events per year. Depending on location, there are clearly defined squall seasons that can be explained by the seasonal migration of the intertropical convergence zone (ITCZ). Squall activity is observed when the ITCZ and associated cumulonimbus formations are in the region. There is one clearly defined squall season in Angola during the northern-hemisphere winter. There are two peak squall seasons offshore Nigeria due to two passages of the ITCZ: on the way north in northern-hemisphere spring, then again on the way south in the northern-hemisphere autumn. Squalls occur for a much larger part of the year in Nigeria than in the other regions, with only a brief minimum around August.

The rapidly varying wind speed and direction associated with squalls, and large variations between the characteristics of different squalls, can lead to considerable variations in vessel or offshore structure response. Further measurements are required to better define squall characteristics, including spatial variations in the wind field, rates of increase and decay, variations in wind direction, and improved extreme value estimates. These are likely to be considered as part of a future joint industry project.

Thunderstorms and squalls are responsible for the strongest winds, but are thought to generate only weak currents and low wave heights due to the limited fetch and duration.

C.6 Waves

The wave climate offshore West Africa is dominated by swell from two distinct sources:

- high-latitude extra-tropical storms in the South Atlantic generate swell from the southwest;
- episodic increases in the trade winds offshore South Africa generate swell from the southeast.

Wind seas are driven by the local winds.

The swell is greatest in southern parts of the region, where extreme significant wave heights can be about 9 m^[59]. Wave heights decrease further north due to dissipation, where extreme values of about 3 m to 4 m are more typical. It is in these more northern regions that locally generated wind seas can become just as important as the swell component, at least for structural designs that are governed by drag.

Swell waves from distant storms can be associated with long peak periods, sometimes in excess of 20 s. Such long-period waves can be critical for the operability of some vessels. Longer period swells are generally encountered in northern parts of the region, due to the longer propagation distance from the source.

The wave spectrum is often characterized by at least two peaks, a swell component and a locally generated wind seas component, the latter having significant wave heights of about 1 m^[60]. Owing to the presence of both sea and swell, it is not appropriate to represent the sea state offshore West Africa using a spectral model with just one peak. Use of a bimodal Ochi-Hubble spectra is recommended; however, the latest results from research into appropriate spectral models of the wave climate offshore West Africa under the joint-industry West Africa Squall Project (WASP) should be considered.

As swell approaches the coast in some parts of the region, particularly along the coast of South-West Africa, it can be transformed into a phenomenon called rollers. These are large steep waves that are likely to affect both floating structures in near-shore regions and coastal infrastructure.

C.7 Currents

The long-term current conditions offshore West Africa are controlled by the large-scale anti-clockwise surface circulations of the South Atlantic Ocean. These currents undergo seasonal variations in intensity and extent, but are generally less than 0.5 m/s. Although they usually only impact the deep ocean, the key characteristics are described here, mostly derived from an excellent review conducted as part of the WAX project^[61].

The Benguela Current flows northwards along the coast of Namibia and separates from the coast to form part of the South Equatorial Current that turns westwards near the equator to flow across the Atlantic Ocean. The Benguela Current only affects the southern-most deep water parts off Namibia.

The other energetic (peaks of the order of 0.50 m/s) current system in the region, the Guinea Current, flows eastward along the Ivory Coast to Nigeria in the upper part of the water column, below which the Guinea Undercurrent flows towards the west.

Other current systems in the region are weak (0.1 m/s) but can be persistent. The Equatorial Undercurrent flows eastwards along the equator underneath the South Equatorial Current and splits into two branches when it reaches the West African coast. The northern branch enters the Gulf of Guinea and the southern branch feeds the southward-flowing Gabon-Congo Undercurrent, and then surfaces to form part of the southward-flowing Angola Current. Throughout most of the region, the current direction often reverses, through a vertical section, leading to complex current profiles with strong shear.

The large-scale circulation patterns described above are characterized by significant meanders, and numerous eddies are formed either side of the main flow. This mesoscale activity is found throughout the region and can be associated with stronger-than-average currents flowing in directions different to that of the larger scale flow.

Strong currents have been encountered near the Congo River, and these can extend perhaps 50 km north of the mouth of the river. These strong currents are confined to the uppermost few meters of the water column, but can be responsible for extreme current conditions.

Perhaps of wider impact is the effect of the major rivers on the near-surface salinity. Significantly fresher water can be observed several hundred kilometers from the mouths of the Congo and Niger. The stratification means that strong (1 m/s) inertial currents can be generated in the upper water column (approximately the top 30 m) by local winds.

Tidal currents are generally less than 0.1 m/s throughout the region, although local intensification exists in some areas due to seabed features. In such regions the tidal currents are likely to generate internal waves at the tidal period, called internal tides. These manifest themselves as currents that vary in time at the semi-diurnal tidal period, but flow in opposite directions in different depths of the water column. Shorter-period internal waves (solitons) have been reported in some parts of West Africa. Although the currents associated with these internal waves are unlikely to be much higher than 0.5 m/s in the region, they cause rapid changes in current speed and direction over periods as short as half an hour, so can be significant for design and operation of marine equipment.

Strong inertial currents have been observed in some deep-water areas offshore West Africa. The direction of these currents rotates through 360° once every inertial period (the natural period of large-scale oscillations in the ocean). The inertial period is infinite at the equator and decreases with latitude. Inertial currents are particularly notable offshore southern Namibia where the inertial period is close to 24 h, allowing a near-resonant response to diurnal variations in wind forcing. The vertical structure of inertial currents can be complex, with one or more peaks in the current speed that move vertically through the water column with time.

The description given in this subclause only provides a very general overview of current conditions likely to be experienced offshore West Africa. The processes that drive ocean currents are considerably more numerous and complex than those that drive wind and waves, and site-specific measurements can be required to derive criteria for engineering design, particularly in deeper waters.

C.8 Other Environmental Factors

C.8.1 Marine Growth

Warm water conditions coupled with an abundance of nutrients are likely to lead to extensive marine growth. The rate of growth and the particular marine species are likely to vary considerably over the region, but a typical thickness of about 0.1 m can be expected in the upper 50 m of the water column, and up to about 0.3 m above MSL in the splash zone.

C.8.2 Tsunamis

West Africa is not considered one of the high-risk areas for tsunami activity, although future events can never be completely discounted. An online tsunami database^[63] contains details of only two distinct tsunami events anywhere in the region, both of which affected the coastal regions of Ghana. The first event in 1911 was associated with a wave of height 1.5 m, and the second event in 1939 with a height of 0.6 m.

C.8.3 Sea Ice and Icebergs

Sea ice does not develop within the region, and iceberg drift is not a design consideration. Icebergs have been sighted as far north as 35° S, and are possible around the Cape of Good Hope^[58].

C.8.4 Snow and Ice Accretion

As with sea ice, snowfall and ice accumulation on structures are not design considerations.

C.8.5 Air Temperature, Humidity, Pressure, and Visibility

High air temperatures are encountered throughout the region, particularly close to the equator. In equatorial West Africa, daily temperatures range between 23 °C and 33 °C in the northern-hemisphere summer, and 20 °C to 25 °C in the northern-hemisphere winter. In southwest Africa, daily temperatures range between 26 °C and 31 °C in the southern-hemisphere summer and 20 °C to 27 °C in the southern-hemisphere winter. These figures were derived from a climate summary^[62] containing data from onshore meteorological stations and some offshore measurements.

The amount of rainfall varies considerably over the region, with very high values near the equator (annual total up to about 4000 mm) and low rates in the south (annual total as low as 40 mm). The most intense rainfall is usually associated with thunderstorms and squalls.

The relative humidity is highest in equatorial regions, where values often exceed 90 %, and generally decreases toward the south. Warm air temperatures combined with high humidity represent a potential hazard to personnel. The humidity varies throughout the day, with a maximum generally occurring in the morning and a minimum during the afternoon. Seasonal variations also exist in many parts of the region, with a maximum in the southern-hemisphere summer and a minimum in the southern-hemisphere winter. Large fluctuations in humidity can be caused locally by changes in the wind direction, with much lower values associated with dry winds blowing from the interior.

A high pressure system is usually located in the southeast Atlantic close to 30 °S 10 °W, driving the southeasterly trade winds that prevail over the region. The position of this high leads to generally higher atmospheric pressures in the south and lower pressures in equatorial regions. Seasonal variations in mean atmospheric pressure are typically between 101.0 kPa (1010 mbar) and 101.4 kPa (1014 mbar) near the equator and between 101.4 kPa (1014 mbar) and 102.2 kPa (1022 mbar) in the south. The atmospheric pressure is higher over the entire region during the southern-hemisphere summer than during the southern-hemisphere winter. Atmospheric pressure undergoes significant diurnal variations in many parts of the region.

Air temperatures, humidity, and pressure all undergo rapid changes during the passage of thunderstorms and squalls.

Visibility is reduced by fog along many parts of the coast, particularly in areas to the south influenced by the cold water of the Benguela Current. Low visibility is also caused by dust (windborne sand) or heavy rain, particularly near the equator, offshore Namibia and most notably in the Bight of Biafra.

C.8.6 Sea Water Temperature and Salinity

Sea-surface temperatures are warmest near the equator, where they typically range between 24 °C and 28 °C over the year, and cooler in the south where seasonal variations between about 13 °C and 16 °C occur. Temperatures across the region are warmer during the southern-hemisphere summer and cooler during the southern-hemisphere winter.

Cold water transported into the region by the Benguela Current is a major influence on sea-surface temperature in southern regions. Localized decreases in surface temperatures occur along several areas of the continental slope throughout West Africa, due to upwelling of cooler deep waters. The water column is generally stratified throughout the year, with temperatures less than 15 °C at 200 m depth.

Sea-surface salinities in the open ocean are generally between 35 PSU and 3 PSU, but there are very significant reductions in salinity in areas influenced by river discharge, where salinity can be as low as 28 PSU. The Congo River provides one of the largest inputs of fresh water into an ocean anywhere in the world.

C.9 Estimates of Metocean Parameters

C.9.1 Extreme Metocean Parameters

Indicative extreme values of wind, wave, and current parameters are provided in Tables C.1 to C.4 for various return periods and for four locations offshore West Africa. The wind, wave, and current values are independently derived marginal parameters; no account has been taken of conditional probability. Table C.5 gives extreme values for other metocean parameters. As for all indicative values provided within this annex, these figures are provided to assist preliminary engineering concept selection; they are not suitable for design of offshore structures.

Extreme wave conditions offshore Nigeria are caused by swell from distant storms, and Nigerian wave spectra tend to be more narrow-banded compared to most extreme conditions in other parts of the world. The Rayleigh distribution assumes narrow-band conditions, whereas the Forristall distribution is a modified Rayleigh distribution that takes account of the wider band conditions within storms. The Rayleigh distribution leads to a higher ratio of H_{\max}/H_s , typically by about 10 %^[41]. Calculations of the short-term statistics from offshore Nigeria hindcast spectra^[41] show that their distribution is close to halfway between Rayleigh and Forristall, which results in individual wave height around 5 % lower than would be predicted by the Rayleigh distribution. In addition, account is made of short-term variability, i.e. the possibility that the maximum individual wave could occur in a sea state other than the maximum sea state. The net result of the computations is that the ratio H_{\max}/H_s tends to a value of 2.0 rather than 1.9.

Structures can be sensitive to different combinations of sea and swell heights, as well as spectral peak periods and spectral widths. A representative combination of wave/swell parameters should be defined for the location of interest, and the largest action effects for the component being designed should be determined. A combination of 100 % wind waves with no swell and, separately, 100 % swell with no wind waves is a useful combination to test on structures. For swell, the longer T_p range should be used, and for wind waves the shorter T_p range.

Table C.1—Indicative Wind, Wave, and Current Parameters—Shallow Water Sites off Nigeria

Metocean Parameter	Return Period (years)				
	1	5	10	50	100
Nominal water depth	30 m				
Wind speed at 10 m above MSL (m/s)					
10 min mean	19	23	25	29	31
3 s gust	24	29	32	37	39
Wave height (m)					
Maximum	4.8	5.5	5.8	6.5	6.8
Significant	2.3	2.7	2.8	3.2	3.3
Wave direction (from)	SSW				
Spectral peak period (s)					
For swell	15 to 17	15 to 17	15 to 17	15 to 17	15 to 17
For wind seas	7 to 8	7 to 8	7 to 8	7 to 8	7 to 8
Current speed (m/s)					
Surface ^a	0.9	1.0	1.0	1.1	1.1
Mid-depth	0.8	0.9	0.9	1.0	1.0
1 m above sea floor	0.5	0.6	0.6	0.7	0.7

^a These extreme values exclude any effect from river plumes.

Table C.2—Indicative Wind, Wave, and Current Parameters—Deep Water Sites off Nigeria

Metcean Parameter	Return Period (years)				
	1	5	10	50	100
Nominal water depth	1000 m				
Wind speed at 10 m above MSL (m/s)					
10 min mean	19	23	25	29	31
3 s gust	24	29	32	37	39
Wave height (m)					
Maximum	5.7	6.4	6.8	7.5	7.7
Significant	2.7	3.2	3.4	3.7	3.8
Wave direction (from)	SSW				
Spectral peak period (s)					
For swell	14 to 16	15 to 17	16 to 18	17 to 19	17 to 19
For wind seas	7 to 8	7 to 8	7 to 8	7 to 8	7 to 8
Current speed (m/s)					
Surface ^a	1.1	1.2	1.2	1.3	1.4
Mid-depth	0.3	0.3	0.3	0.3	0.4
1 m above sea floor	0.2	0.2	0.2	0.2	0.2

^a These extreme values exclude any effect from river plumes.

Table C.3—Indicative Wind, Wave, and Current Parameters—Sites off Northern Angola

Metcean Parameter	Return Period (years)				
	1	5	10	50	100
Nominal water depth	1400 m				
Wind speed at 10 m above MSL (m/s)					
10 min mean	16	20	21	25	26
3 s gust	19	23	25	29	31
Wave height (m)					
Maximum	7.9	8.6	8.8	9.5	9.9
Significant	4.0	4.3	4.4	4.7	4.9
Wave direction (from)	SSW				
Spectral peak period (s)					
For swell	13 to 17	13 to 17	13 to 17	13 to 17	13 to 17
For wind-seas	7 to 8	7 to 8	7 to 8	7 to 8	7 to 8
Current speed (m/s)					
Surface ^a	0.9	1.0	1.0	1.2	1.2
Mid-depth	0.2	0.3	0.3	0.3	0.3
1 m above sea floor	0.2	0.3	0.3	0.3	0.3

^a These extreme values exclude any effect from river plumes.

Table C.4—Indicative Wind, Wave, and Current Parameters—Sites off Southern Namibia

Metocen Parameter	Return Period (years)				
	1	5	10	50	100
Nominal water depth	200 m				
Wind speed at 10 m above MSL (m/s)					
10 min mean	20	20	26	29	31
3 s gust	25	27	32	36	39
Wave height (m)					
Maximum	12.7	13.7	16.0	19.0	20.0
Significant	6.8	7.4	8.7	10.0	10.6
Wave direction (from)	SSE/SW				
Spectral peak period (s)					
For swell	11 to 14	12 to 15	13 to 16	14 to 17	14 to 17
For wind-seas	7 to 8	7 to 8	7 to 8	7 to 8	7 to 8
Current speed (m/s)					
Surface ^a	1.1	1.2	1.2	1.3	1.4
Mid-depth ^b	0.3	0.3	0.3	0.3	0.5
1 m above sea floor	0.3	0.3	0.3	0.4	0.5

^a These extreme values exclude any effect from river plumes.

^b Mid-depth currents off southern Namibia are below the seasonal thermocline where currents can be stronger.

Table C.5—Indicative Extreme Values for Other Metocen Parameters

Metocen Parameter	Nigeria		Northern Angola	Southern Namibia
	Shallow Water	Deep Water		
Mean spring tidal range (m)	1.9	1.5	1.4	2.0
Sea water temperature (°C)				
Minimum near surface	22	25	17	9
Maximum near surface	32	31	28	28
Minimum near bottom	20	4	4	4
Maximum near bottom	30	4	4	—
Air temperature (°C)				
Minimum	18	20	17	8
Maximum	33	33	35	26

C.9.2 Long-term Distributions of Metocen Parameters

Recorded wave spectra offshore West Africa are complex and present simultaneous long-period swell components, with various peak periods and directions, generated by storms in different parts of the Atlantic Ocean. In situ wave measurements also indicate that mixed swell and wind sea conditions are quasi-permanent. As a minimum for design purposes, one swell component should be superimposed on a wind-sea component. A refinement considers two swell partitions superimposed on a wind sea.

Wave-scatter diagrams for two areas offshore West Africa are provided in Tables C.6 and C.7, showing combinations of total significant wave height and associated spectral peak wave periods of combined wind seas and swell conditions. The information in these tables was generated from the WANE hindcast model [56,59]. It should be noted that a significant proportion of the wave energy in any given sea state offshore West Africa consists of long-period swell. These tables are not always conservative for certain applications to dynamically responding structures; therefore, designers should also test against the appropriate dual-peaked cases such as those given in Table C.8.

Table C.6—Percentage Occurrence of Total Significant Wave Height vs. Spectral Peak Period—Offshore Nigeria Location

Significant Wave Height (m)	Peak Period (s)													> 24	Total
	0 to 1.99	2 to 3.99	4 to 5.99	6 to 7.99	8 to 9.99	10 to 11.99	12 to 13.99	14 to 15.99	16 to 17.99	18 to 19.99	20 to 21.99	22 to 23.99	> 24		
0.00 to 0.49	—	—	—	0.02	—	0.03	0.02	0.03	—	—	—	—	—	0.10	
0.50 to 0.99	—	—	0.50	5.37	2.55	3.48	3.14	2.46	0.64	0.13	0.05	0.02	—	18.34	
1.00 to 1.49	—	—	0.34	11.01	16.65	9.40	11.01	8.76	2.74	0.88	0.24	0.04	—	61.07	
1.50 to 1.99	—	—	—	0.08	5.85	4.67	2.76	2.95	1.19	0.33	0.09	0.03	—	17.95	
2.00 to 2.49	—	—	—	—	0.17	0.79	0.58	0.41	0.19	0.07	0.03	—	—	2.24	
2.50 to 2.99	—	—	—	—	—	0.06	0.08	0.04	0.05	0.02	—	—	—	0.25	
> 3.00	—	—	—	—	—	—	0.02	0.03	—	—	—	—	—	0.05	
Total	0.00	0.00	0.84	16.48	25.22	18.43	17.61	14.68	4.81	1.43	0.41	0.09	0.00	100.00	

Table C.7—Percentage Occurrence of Total Significant Wave Height vs. Spectral Peak Period—Offshore Angola Location

Significant Wave Height (m)	Peak Period (s)													> 24	Total
	0 to 1.99	2 to 3.99	4 to 5.99	6 to 7.99	8 to 9.99	10 to 11.99	12 to 13.99	14 to 15.99	16 to 17.99	18 to 19.99	20 to 21.99	22 to 23.99	> 24		
0.00 to 0.49	—	—	—	0.01	0.03	0.04	0.06	0.06	—	—	—	—	—	0.20	
0.50 to 0.99	—	0.01	1.00	3.98	1.82	5.17	5.52	3.70	1.17	0.34	0.13	0.01	0.00	22.85	
1.00 to 1.49	—	—	0.60	6.28	10.48	11.49	11.38	9.19	2.87	0.83	0.19	0.06	0.00	53.37	
1.50 to 1.99	—	—	0.01	0.06	2.86	5.78	4.76	3.52	1.51	0.54	0.12	0.01	—	19.17	
2.00 to 2.49	—	—	—	—	0.07	0.94	1.33	1.05	0.34	0.10	0.01	—	—	3.84	
2.50 to 2.99	—	—	—	—	0.00	0.04	0.14	0.23	0.10	0.03	—	—	—	0.54	
3.00 to 3.49	—	—	—	—	—	—	—	0.02	0.01	—	—	—	—	0.03	
> 3.50	—	—	—	—	—	—	—	0.00	—	—	—	—	—	0.00	
Total	0.00	0.01	1.61	10.33	15.26	23.46	23.19	17.77	6.00	1.84	0.45	0.08	0.00	100.00	

Wind seas and swell conditions are considered as independent phenomena. In principle, any combination of wind seas and swell H_s-T_p classes is possible, and all permutations, with their joint frequency of occurrence, should be considered for engineering purposes.

Sea states offshore West Africa can be represented by the dual-peaked Ochi-Hubble spectra. Table C.8 provides an example of a scatter diagram for offshore Angola.

For the purposes of defining bimodal spectra representing combined swell and wind sea conditions, the total significant wave height H_s and the associated spectral peak period T_p should be divided into a swell part and a wind sea part. This can be achieved by inspection of a frequency table of the joint occurrences of H_s and T_p . The low wave heights associated with the wind sea component permit selection of relatively few significant wave height classes for wind seas. The frequency of occurrence of swell H_s with associated T_p should be calculated, conditional on the value of the wind sea H_s with its associated T_p , to determine the frequency of occurrence of each combined wind sea/swell bimodal sea state. The resolution of the swell H_s class will determine the number of combinations of wind sea and swell H_s and T_p available for engineering purposes.

The example in Table C.8 provides information on the joint frequency of occurrence of swell and wind sea conditions, giving the significant wave height, the peak period, the associated parameter γ , and the direction of swell (θ_1) and wind sea (θ_2) for a site offshore Angola.

For the example data in Table C.8, the values from any row can be used to construct a bimodal Ochi-Hubble spectrum. Sea states should be assumed to be representative of a duration of 3 h. The values of percentage occurrence in Table C.8 can be used to define the fatigue wave climate.

Table C.8—Example of Wind Sea States Used for Combined Wind Sea/Swell Bimodal Sea States—Offshore Angola

No.	% Occurrence	H_{s1} m	T_{p1} s	H_{s2} m	T_{p2} s	γ_1	γ_2	θ_1 (toward)	θ_2 (toward)
291	15.3	0.91	12	0.76	7.7	7.0	2.1	27	21
231	12.1	0.61	11	0.70	7.2	7.3	1.6	25	23
208	10.9	0.61	12	0.70	7.7	7.3	1.8	29	19
154	8.1	0.91	11	0.76	7.2	7.1	1.8	22	23
117	6.1	1.22	12	0.82	8.1	7.4	2.9	27	22
103	5.4	0.61	10	0.73	6.3	5.4	1.4	21	27
94	4.9	0.91	13	0.76	8.4	7.5	2.3	30	18
90	4.7	1.22	13	0.85	8.2	7.2	2.2	32	21
72	3.8	0.61	13	0.79	7.9	7.1	2.2	33	19
65	3.4	0.91	14	0.88	8.7	7.5	2.4	33	17
63	3.3	0.61	14	0.79	8.9	7.7	2.3	35	18
52	2.7	1.52	13	0.91	8.7	8.1	2.4	29	22
47	2.5	1.22	14	0.98	9.4	8.3	2.7	31	21
37	1.9	1.52	14	0.98	9.4	7.3	3.1	32	19
36	1.9	1.22	11	0.88	7.7	7.5	2.0	21	22
35	1.8	0.91	10	0.76	5.9	4.0	1.4	21	31
32	1.7	0.61	15	0.91	9.6	8.4	2.4	32	22
29	1.5	0.91	15	0.88	9.4	8.7	2.9	34	17
28	1.5	0.30	12	0.61	8.6	8.7	3.3	32	15
27	1.4	1.52	12	0.82	8.6	7.5	5.0	27	21
26	1.4	0.30	11	0.76	7.0	8.1	1.9	28	18
24	1.3	1.52	15	1.01	9.8	8.1	2.5	31	20
23	1.2	1.83	14	0.88	8.7	7.0	1.7	32	18
20	1.1	0.61	17	1.04	10.2	9.0	2.8	31	23

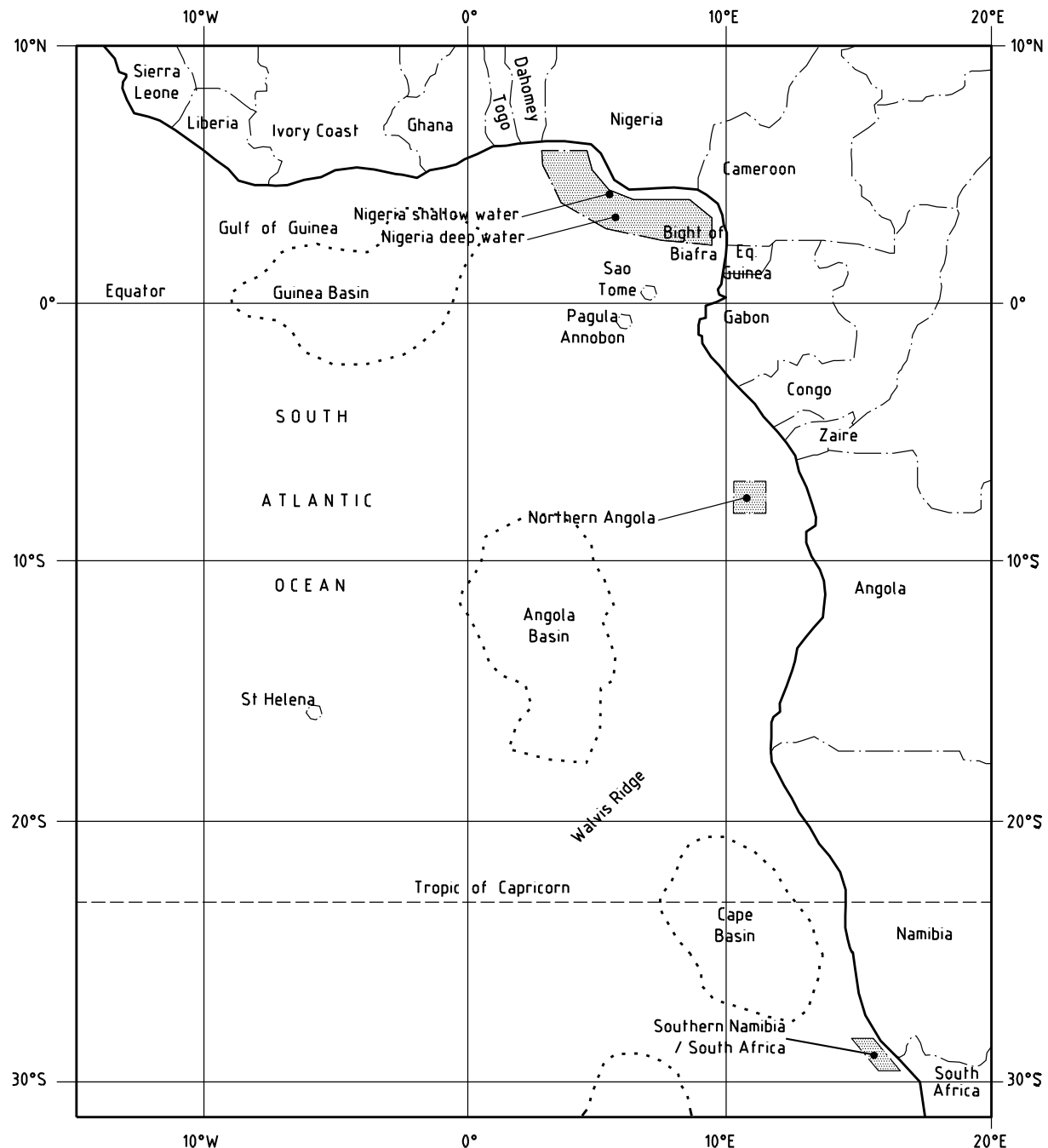


Figure C.1—Map of West Coast of Africa Region: Locations of Example Metocean Parameters

Annex D (informative)

Offshore Canada

D.1 Description of Region

D.1.1 General

The geographical scope of this annex includes current hydrocarbon-producing regions of offshore Canada: the Sable Island region offshore Nova Scotia and the Grand Banks of Newfoundland. Some areas with potential for future hydrocarbon development have also been included, such as East Coast Deepwater, the Beaufort Sea, and the Gulf of St. Lawrence.

Future updates to this annex will include other areas of interest in the Canadian offshore such as:

- offshore Labrador;
- the Sverdrup Basin (Queen Elizabeth Islands);
- west coast of Canada (offshore British Columbia).

This annex provides an overview of metocean design and operating conditions for areas offshore Canada where hydrocarbon production exists, as well as for certain areas where significant industry interest exists. A range of values based on existing data sets is provided to give an indication of the degree of variability that can be expected for a particular region. The numbers provided are indicative only and should be used in conjunction with site-specific or project-specific studies to develop environmental criteria to be used for design.

The current hydrocarbon production operations on the east coast of Canada are located offshore Newfoundland and Labrador on the Grand Banks, and offshore Nova Scotia on the Scotian Shelf near Sable Island, as shown in Figures D.1 and D.2.



Figure D.1—Map of Canada

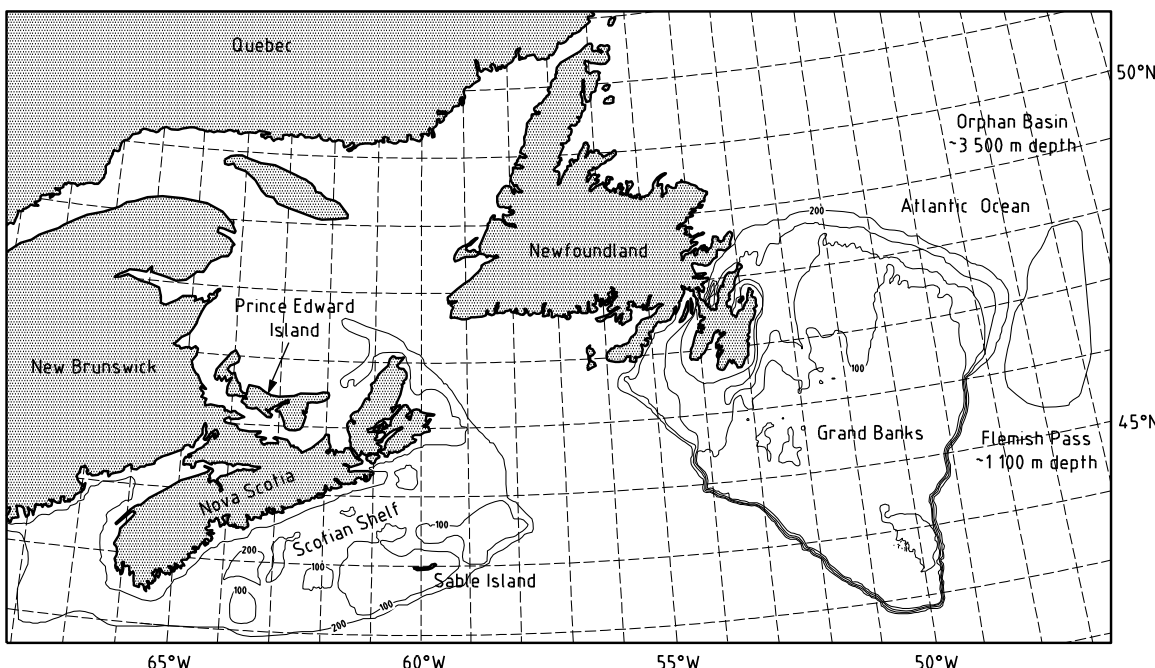


Figure D.2—East Coast of Canada Current Regions of Oil and Gas Production Operations—Near Sable Island Offshore Nova Scotia and on the Grand Banks Offshore Newfoundland and Labrador

D.1.2 Grand Banks

The Grand Banks are one of the world's largest and richest resource areas, renowned for both its valuable fish stocks and petroleum reserves. Situated off the southeast coast of the island of Newfoundland, the Grand Banks are a series of raised submarine plateaus with a water depth ranging between approximately 40 m and 200 m. Grand Bank is the largest of several banks comprising the Grand Banks of Newfoundland, and lies to the east and southeast of the Avalon Peninsula. Grand Bank has a relatively flat surface that is generally less than 120 m deep. It is separated from the island of Newfoundland by the Avalon Channel which has water depths ranging up to 200 m deep.

D.1.3 Scotian Shelf

The Scotian Shelf comprises an area of approximately 120,000 km², is over 700 km long, and ranges in width from 100 km to 250 km. The Scotian shelf physiography consists of three physiographic zones:

a) Inner Shelf

The Inner Shelf borders mainland Nova Scotia, extending roughly 25 km offshore, with water depths less than 100 m. It is characterized by rough topography.

b) Central Zone

This zone is about 80 km to 100 km in width and lies between the Inner Shelf and Outer Shelf. It is characterized by an inner trough running parallel to the coast, and isolated banks with intervening basins and valleys. Water depth varies from less than 100 m over the banks to about 180 m in the inner trough, with some basins up to 300 m in depth.

c) Outer Shelf

This zone is bounded by the eastern shelf break and is about 50 km to 70 km wide. This shelf is characterized by broad flat banks with little relief. Sable Island Bank is the largest and most extensive bank on the Scotian Shelf, with water depths less than 100 m. Sable Island is an arc-shaped sandbar more than 40 km long and about 1.3 km wide.

D.1.4 Deepwater

The Flemish Pass and Orphan Basin are two hydrocarbon fields located in deepwater. These fields are located beyond the Grand Banks, approximately 450 km offshore Newfoundland, as shown in Figure D.2. Water depth varies from 1100 m to 3500 m in the Flemish Pass and Orphan Basin, respectively.

D.1.5 Gulf of St. Lawrence

The Gulf of St. Lawrence is located at the mouth of the St. Lawrence River; it is the body of water enveloped by Quebec and the Atlantic Provinces, shown in Figure D.2. The Gulf contains channels with water depths up to 300 m.

D.1.6 Beaufort Sea

The Beaufort Sea is located along the Arctic Circle in northwestern Canada, as shown in Figure D.1. There are three main bathymetric features in the southeastern Beaufort Sea:

- a) the continental shelf, which slopes gently from the coastline to water depths of approximately 100 m;
- b) the continental slope, angling steeply from the edge of this shelf to depths of 1000 m; and
- c) the trench-like Mackenzie (or Herschel) Canyon, which transects a portion of the shelf Number-1^[173].

D.2 Data Sources

Data regarding metocean conditions in the region are available from a variety of sources. These include regulatory bodies, such as the Canada-Newfoundland Offshore Petroleum Board and the Canada-Nova Scotia Offshore Petroleum Board, Operators, federal government agencies, and published papers.

Another source of metocean related information is the MSC50 North Atlantic Wind and Wave hindcast model^[187]. This model was developed for the Meteorological Service of Canada and is a 60-year (1954 to 2013) wind and wave hindcast model of the North Atlantic. The model is currently being updated to include the years 1998 to 2003. It allows the estimation of extreme wind and wave parameters for the Scotian shelf and the Grand Banks of Newfoundland as well as other locations in the North Atlantic. A separate hindcast has been carried out for the Canadian Beaufort Sea covering the period 1970–2013^[231].

For the offshore Newfoundland and Labrador region, environmental impact statements as well as project-specific design environmental criteria were available from the Operators as well as other related information. With respect to the offshore Nova Scotia region, environmental impact statements and development plan applications were utilized such as Sable Offshore Energy Project (SOEP) (1996)^[185], Deep Panuke (2002)^[171], and Cohasset/Panuke (1990)^[170].

A description of observed variability in ice patterns over a 30-year period (1981 to 2010) has been published in map format by the Canadian Ice Service and used here to describe normal conditions^[166]. A second report of the Canadian Ice Service provides the thickness of un-deformed ice observed at landfast ice stations around the Gulf^[167]. The thicknesses are listed in Table D.1 along with observed ice drift statistics from satellite-tracked ice beacons deployed by Fisheries and Oceans Canada in the southern Gulf. Lastly, data for ice thickness of deformed mobile pack ice are listed that were collected with a helicopter-borne electromagnetic sensor over the southern Gulf. The southern Gulf is referred to as the shallow region southwest of the main shipping lane from Cabot Strait into the upper St. Lawrence Estuary. The deeper area of the Gulf, north of the shipping lane, is referred to as the northern Gulf.

Sea-ice data for the Flemish Pass has been extracted from the Provincial Airlines (PAL) (2001) report^[183]. This report was conducted on behalf of Petro-Canada to evaluate sea ice and iceberg conditions surrounding the Bay du Nord exploration site (47,55° N, 46,20° W). PAL utilized the Canadian Ice Service and the US National Ice Center (NIC) database for this purpose.

A comprehensive listing of additional related environmental and meteorological information sources is presented in D.13.

D.3 Overview of Regional Climatology

D.3.1 Atlantic Canada

D.3.1.1 General

Offshore Atlantic Canada has very complex and unpredictable weather. The variable climate of the Canadian east coast is influenced by the warm Gulf Stream and the cold water of the Labrador Current. It is also influenced by seasonal changes in air masses, exchanges in energy between the atmosphere and the ocean, seasonal variations in sun radiation, the rugged coastal topography as well as the variability of the Icelandic Low and the Bermuda High, which locally control the Jet Stream and thus storm tracks. They are described further below.

D.3.1.2 Icelandic Low

The Icelandic Low is a large low-pressure system normally located near Iceland and southern Greenland. In mid-summer, when it is at its weakest, it can lie as far west as the Hudson Strait. It exerts a major influence on the tracks of lows passing through Atlantic Canada and fosters the strong cold northwesterly Arctic air flow across the region in winter and early spring.

D.3.1.3 Bermuda High

The Bermuda High is a semi-permanent high-pressure zone with its mean centre lying east of Bermuda and southwest of the Azores. It can play a major role in the climate of eastern Canada in spring and summer, when it is most persistent. It causes air of tropical origin to penetrate the southern United States and move northward to become entrained in westerly winds. In general, this air can bring in periods of warm humid air and heavy precipitation to Atlantic Canada.

D.3.1.4 Eastern Canada Weather

High winds and storms are more common in eastern Canada during the winter months. Spring and summer months have fewer, less intense storms and moderate winds, and precipitation is usually in the form of fog, drizzle, or rain showers. Hurricanes and tropical storms from the south can threaten the region in the autumn. Air quality in the region is generally good, both onshore and offshore.

Eastern Canada can experience very cold winters, which result in the seasonal occurrence of ice. Under predominantly northwesterly winds and southward-moving Labrador Current branches, ice and icebergs travel southwards along the Labrador coast. Ice (pack ice and icebergs) is encountered seasonally offshore Newfoundland and Labrador in a variety of forms and concentrations. Icebergs of sufficient draft can make contact with the seafloor of the Grand Banks and create scours on the seabed. The maximum water depth at which scours would be expected to occur is approximately 200 m. Icebergs are rare offshore Nova Scotia, but pack ice can be encountered and should be considered in the design of offshore facilities.

The Grand Banks region offshore Newfoundland is considered to be a harsh environment due to the possibility of intense storms and the potential for ice (sea ice and icebergs). Superstructure icing can also occur between December and March because of the temperature and wind and wave conditions. Restricted visibility due to fog is also common, especially in the spring and summer months, when warm air masses overlie the cold ocean surface. The worst visibility conditions are experienced in July. During the winter months, restricted visibility can also be caused by snow in addition to fog and mist.

Major seasonal mean current patterns that influence the regional climatology, and the relative location of Greenland to the Canadian east coast, are shown in Figure D.3.

.....,.....,.....,.....,.....,.....,.....,.....,.....,.....,.....,.....

D.3.2 Beaufort Sea

Temperatures in the Beaufort Sea typically range up to +20 °C in the summer and typically down to below -35 °C in the winter. There are, on average, approximately 4500 freezing degree-days in this region each year. Winds in the Beaufort Sea are influenced by the sharp thermal contrast between the land and water, and the high coastal lands [232]. The dominant wind direction ranges from northeast to southeast during any month of the year. Southerly winds are rare during the summer months. From July to September, westerly to northwesterly winds in excess of 36 km/h become persistent. Fifty percent of all strong winds with speeds exceeding 50 km/h are from the west or northwest. These winds are responsible for the multi-year ice-pack ice intrusions into the coastal waters. The average rainfall is about 150 mm per year, and the average snowfall is 750 mm each year. Poor visibility of less than 8 km occurs about 20 % of the time due to snow, fog, etc.

NOTE: Due to the complexity of the heat exchange between ice, water, and air and their measurement, readily available air temperature measurements are often used to quantify the effect of freezing and melting conditions. More specifically, when the mean air temperature for a day is below the freezing point temperature of water, the numerical value can be expressed as the number of freezing degree-days (FDD) and, when above the freezing point temperature, expressed as the number of melting degree-days (MDD). The freezing point temperature of typical marine waters is -1.8 °C.

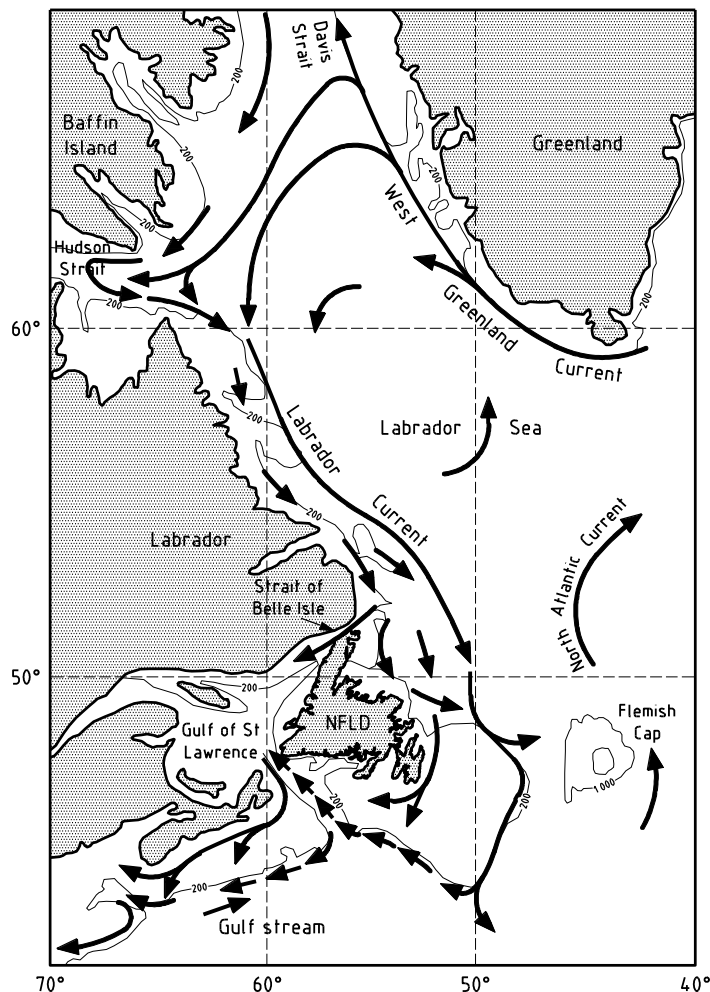


Figure D.3—Canadian East Coast Ocean Current Regime

D.4 Water Depths

The water depths on the Grand Banks are generally less than 200 m, as shown in Figure D.2.

The water depths in the offshore Nova Scotia area addressed in this annex range from 20 m to 80 m, whereas the waters of the Grand Banks current installations are on the order of 80 m to 130 m.

There are also deepwater locations offshore eastern Canada, such as the Flemish Pass and the Orphan Basin, which have depths of 1100 m and 3500 m, respectively. There are other potential deepwater hydrocarbon-producing areas offshore Newfoundland and off the Scotian Shelf.

The main characteristic of the water depths in the Gulf of St. Lawrence is the presence of channels of 300 m depth that run into the Gulf from Cabot Strait, as shown in Figure D.4. One branch runs toward the west up to the Saguenay River entrance, and others run east and north toward the Strait of Belle Isle and around Anticosti Island. The next largest feature is the southern Gulf, surrounding Prince Edward Island and the Magdalen islands, with water depths less than 100 m.

Water depth is highly variable in the Beaufort Sea. The continental shelf here has a depth of approximately 100 m. This shelf slopes down from its edge to depths of 1000 m. The trench-like Mackenzie (or Herschel) Canyon transects a portion of the shelf.

D.5 Winds

Extreme surface winds are mainly associated with the passage of extra-tropical cyclones and their associated frontal structures. Given the large gradients in sea-surface temperature in the region and the closeness of cold and warm continental air mass source zones, the boundary layer wind shear, and hence the strength of surface winds relative to the pressure-gradient-driven free atmosphere flow, tends to be strongly modulated by the stability of the boundary layer, as evidenced by the air-sea temperature difference. The strongest surface winds tend to occur in unstable sectors of storms (air colder than the sea). Extreme winds, on the order of 25 m/s (1 h average at 10 m elevation), tend to be associated with smaller (than cyclone) scale features, such as the “surface wind jet streaks” that propagate rapidly within the broader air flows about each cyclone, within narrow frontal zones, and near the cores of nascent explosively developing cyclones. At even smaller scales, convectively produced squalls can occur during seasons and in regions where cold air overlays relatively warm waters. Extreme winds in tropical cyclones are comparable to those in extra-tropical cyclones because larger-scale considerations limit the maximum intensity of tropical cyclones to a Saffir-Simpson scale intensity 2 at most (on a scale of 1 to 5). The winds vary considerably in the different regions as indicated in Table D.5.

D.6 Waves

The wind fields associated with extra-tropical and tropical cyclones excite a wide range of sea states depending on storm size, radius of curvature of the wind field, peak wind speeds, storm propagation speeds, intensity and speed of propagation of surface wind jet streaks, and proximity of land that will limit fetch for appropriate wind directions. Of course, water depth is important in the shallower development areas of the Scotian Shelf for basically all return periods of interest. Indeed, on the Grand Banks, marginally shallow water can affect sea states in the most intense systems. Even relatively small-scale features, such as the small area of high winds in the right quadrant of a propagating tropical cyclone or cyclone undergoing transformation to extra-tropical stage, or a jet-stream propagating through a larger air stream, can generate enormous sea states if the propagation speed of the wind feature and its peak wind speed allow optimum resonance coupling between the wind field and the surface waves. Extreme wave heights, with maximum individual waves up to 30 m, have been recorded in the region during previous severe storms (e.g. Hurricane Luis in 1995).

D.7 Currents

The Labrador Current is perhaps the most dominant in the Atlantic Canada region. It plays a major role in the transport of colder water to the region, and the resultant regional current pattern is a function not only of this large current, but also of tides, encounters with ocean currents (such as the warmer eddies and meanders of the Gulf Stream) and storm winds.

The Labrador Current is also responsible for the transport of icebergs from northern areas to offshore Newfoundland. Figure D.3 shows how the Labrador Current divides into an inshore branch and an offshore branch. The offshore branch of the Labrador Current is mainly responsible for the transport of icebergs to the hydrocarbon-producing region of the Grand Banks.

The main feature in the Gulf of St. Lawrence is the Gaspé current that flows out of the St. Lawrence Estuary along the Gaspé Peninsula toward the Gulf, loosely following the 50 m isobath as shown in Figure D.4. It is driven by the freshwater outflow of the St. Lawrence River and is intensified by winds. In addition, strong tidal currents are present in the Jacques Cartier Passage, north of Anticosti Island, and at the mouth of the Saguenay River.

The mean circulation pattern in the Beaufort Sea is shown in Figure D.5^[173]. Offshore in the Beaufort, the surface flow is dominated by the clockwise circulation of the Beaufort Gyre. Estimates by Newton (1973)^[180] indicate that flow speeds reach 5 cm/s to 10 cm/s at the southern rim of the Gyre over the western Beaufort Sea. Figure D.6 shows the pattern of the currents in the nearshore region for both northwest winds and east winds. During the summer season, measurements of currents made at the Kopanoar location indicate values of 0.3 m/s to 0.4 m/s at 5 m depth, and decreasing to 0.1 m/s to 0.2 m/s at 12 m depth^[174].

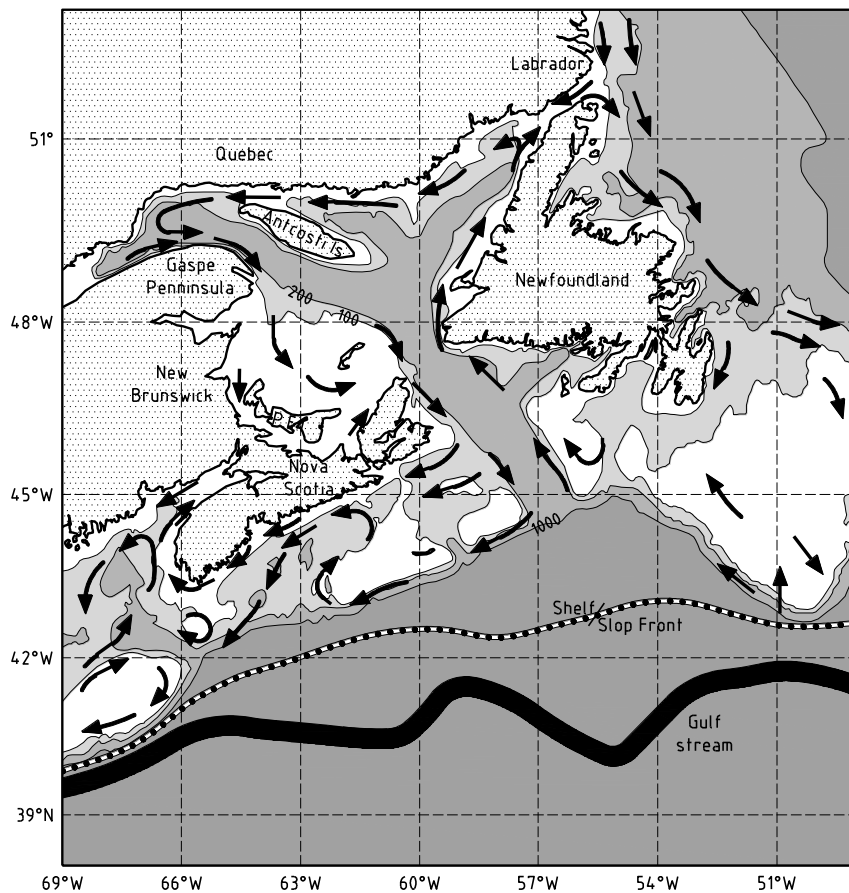
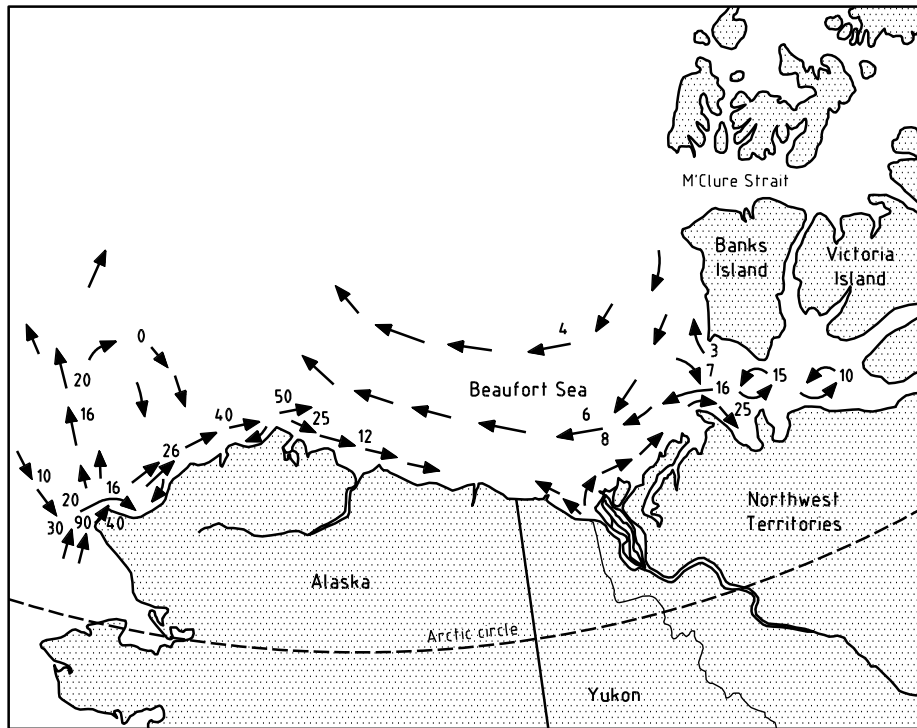
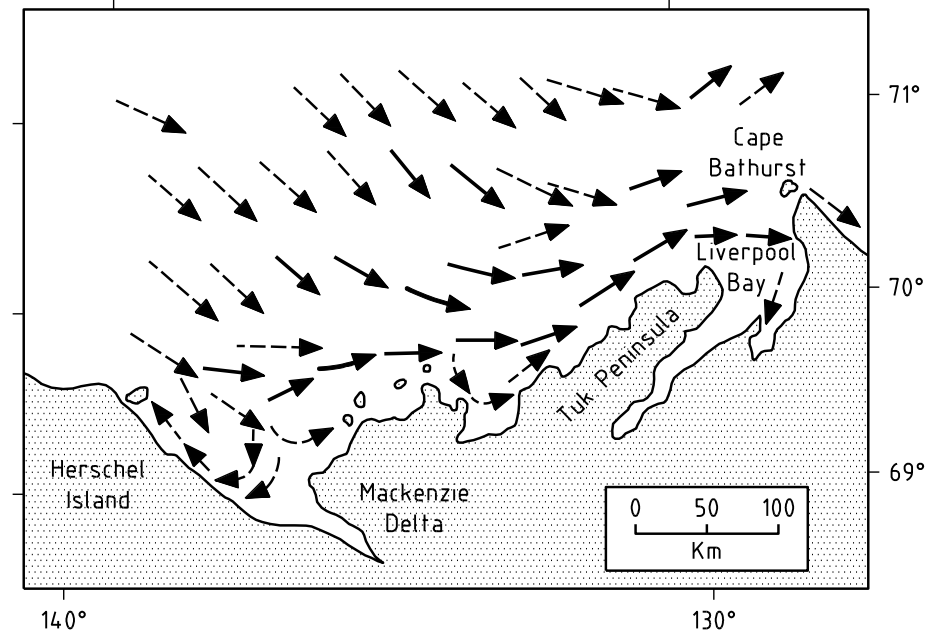


Figure D.4—Map of the Gulf of St. Lawrence Showing the General Circulation Pattern

**Key**

Flow speed (cm/s)

Figure D.5—Mean General Summer Circulation of the Surface Water in the Beaufort and Chukchi Seas [173]



a) Northwest winds

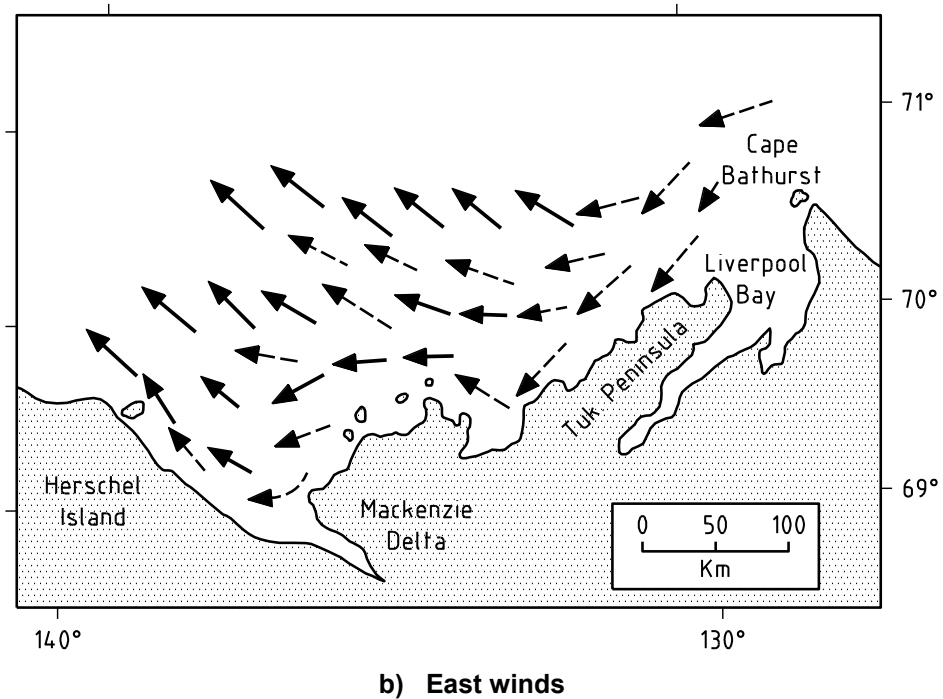


Figure D.6—Surface Circulation in the Southeastern Beaufort Sea for Northwest and East Winds from Surface Drift Studies [179]

D.8 Sea Ice

NOTE The World Meteorological Organization (WMO) Sea Ice Terminology provides an accepted description for sea ice and iceberg characterization, and these definitions will be used throughout this clause.

D.8.1 Canadian East Coast

The regional sea ice regime along the Canadian east coast starts in September with the growth of new ice in northwest Baffin Bay. Beginning in October, a combination of growth and predominantly southward drift, due to the prevailing northerly winds and the strong cold Baffin Current, advances the ice southward. By December, the leading edge of the advancing ice pack lies off northern Labrador. In typical years, the ice edge reaches the northern tip of Newfoundland in early January and the northern Grand Banks in mid-February. The pack ice off Newfoundland generally reaches annual peak coverage in March, but can remain at high levels through May. Loose (60 %) coverage of first-year ice is the dominant ice form in areas off Newfoundland.

Most sea ice on the Nova Scotia shelf originates in the Gulf of St. Lawrence. It moves under the action of winds and southerly currents generally in a south to southeast direction. It is joined by locally grown sea ice that begins to form along Nova Scotia's coast typically in January, reaching maximum concentrations in February and March. The locally formed ice is mainly confined to inlets and bays, seldom reaching a thickness greater than 30 cm. The ice usually melts if carried out to sea by winds and currents. Depending on sea-ice growth and wind conditions, it is possible that sea ice will extend further offshore Nova Scotia and impact the region of hydrocarbon production operations.

The 30-year frequency of sea ice offshore the Canadian east coast for the last week of March is presented in Figure D.7, based on information from the Canadian Ice Service *Sea Ice Climatic Atlas*^[169]. This is indicative information only and should be used in conjunction with site-specific or project-specific studies to develop pack ice criteria to be used for design.

The design of facilities for hydrocarbon operations offshore Nova Scotia and Newfoundland and Labrador should consider the possibility of sea ice occurrence. Site-specific or project-specific studies to develop appropriate sea-ice-related criteria will be required. As these criteria change according to region and facility type (i.e. jacket-type fixed platform, gravity-based structure, floating vessel, etc.), no specific guidance is provided in this standard. At a minimum, the criteria desired will provide information on sea ice occurrence, concentration, floe dimensions and thickness, ice strength and temperature, and the speed, direction, and ice type of the floe.

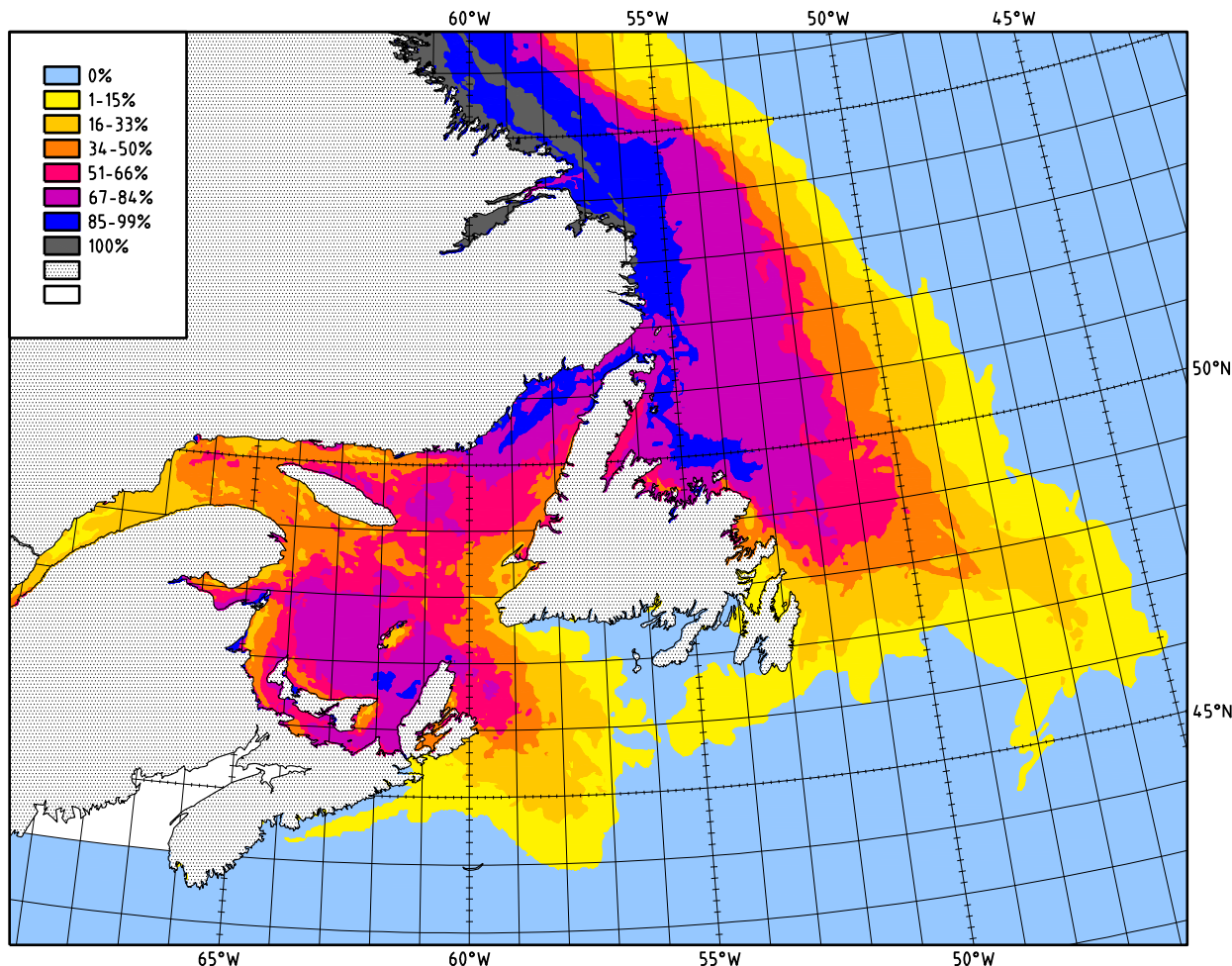


Figure D.7—30-Year Frequency of Sea Ice Offshore the Canadian East Coast for the Last Week of March (1981–2010)^[169]

D.8.2 Gulf of St. Lawrence

The ice in the Gulf of St. Lawrence is mainly locally grown, with some ice entering from the upper St. Lawrence Estuary and through the Strait of Belle Isle. The prevailing winter winds from west to north are normally cold and dry, whereas those from west through south to northeast are mild and moist. These atmospheric factors have a decided effect on ice growth and decay, the redistribution of ice within the

Gulf and the dispersal of ice from the Gulf through the Cabot Strait. Table D.1 shows ice tendencies in the Gulf of St. Lawrence.

Normally, ice starts to form in the coastal, shallow areas of New Brunswick in mid-December and then later in the coastal area in Northumberland Strait. During the last week of December, new ice forms in the deeper coastal waters of the Strait of Belle Isle and along the north shore of the Gulf of St. Lawrence. By the end of the month, the highest concentration of ice in the form of new and grey ice (less than 15 cm) can be found along the New Brunswick coast, Northumberland Strait, and along the north shore of the Gulf. During early January, the ice cover increases in concentration rather than extent. By the middle of the month, most of the southwestern corner of the Gulf is covered with grey and grey-white ice (less than 30 cm). Along the north shore, pack ice extends southwards offshore but only to 40 km to 60 km.

By the end of January, the pack ice covers most of the southern Gulf and the ice edge stretches northwards from the north end of Cape Breton Island to Anticosti Island, and then northeastwards in a 100 km band along the north shore. The ice concentration within 50 km of the ice edge is less than farther inside the pack ice. The thickness of un-deformed ice (mostly grey-white ice) is less than 30 cm, with thinner ice due to ice dispersion under the prevailing northwesterly winds occurring near the lee side of shores.

During February, the un-deformed ice within the pack ice continues to thicken to create thin first-year ice (30 cm to 70 cm) and continues to move south and east under prevailing northwest winds and ocean circulation. Storms move the pack ice back and forth within the Gulf, and cause severe rafting and ridging when the pack ice motion is impeded by coastal boundaries. Pressure events can form rubble fields and ridges up to 15 m thick, even though the original un-deformed ice was less than 70 cm thick. The most severe ridging occurs along the windward coasts of Prince Edward Island and Cape Breton Island during winds from the northerly sector. Because of the southward drift of the pack ice and the inflowing warmer Atlantic water, the ice remains thinner (grey-white stage) over the northeastern portion of the Gulf.

Old ice (second-year or multi-year ice) is defined as ice that has survived at least one melt season^[166]. It is harder than first-year ice and, because of this, is of additional concern to navigation and offshore structures. According to the Canadian Ice Service ice atlas^[166], the frequency of old ice present in the Gulf is due to importing of “old ice” from the Labrador Shelf. It occurs only in the northern Gulf in the spring (April–May) and follows the westward-flowing ocean currents along the north shore. Frequency of presence for the 30-year period was below 15 % between latitudes 49° N and 50° N, increasing to above 15 % in some areas north of latitude 50° N.

D.8.3 Flemish Pass—Bay du Nord and Mizzen

All sea ice observations fall within the period February 8 to May 3, with the peak influx centred on the month of March. The maximum probability of sea ice cover at the Bay du Nord location (south of Mizzen) during March is about 21 %. Sea ice concentrations ranged widely, from a low of 20 % to a high of 90 %. Mean concentrations are about 50 %, which is consistent with the general sea ice concentrations experienced across the Grand Banks. The Bay du Nord data can be assumed to be characteristic of Mizzen.

With respect to sea ice composition, these data were not available from the databases consulted. However, according to other industry and government reports, pack ice composition across the marginal ice zone is consistent at 40 % to 60 % coverage of thin first-year ice (70 cm to 120 cm) in small floes.

Detailed drift data were not available from the databases consulted. However, the PAL (2001) report^[183] indicates that pack ice advances toward the Bay du Nord location from the West.



Table D.1—Ice Tendencies in the Gulf of St. Lawrence

Phenomenon	Parameter	Annual Maximum Value	Range of Annual Maximum Values
Southern Gulf			
Ice drift (63 beacons)	Speed (m/s)	1.38	0.85 to 1.38
Ice thickness			
Level ice: Southeast	Landfast ice (m)	0.73	0.40 to 0.73
Level ice: Southwest	Landfast ice (m)	0.92	0.53 to 0.92
Level deformed ice	EM ^a ice thickness (m)	2.2	1.5 to 2.2
Rubble fields and ridges	Laser sail height (m)	3.5	2.0 to 3.5
	EM ^a rubble depth (m)	15.0	8.0 to 15.0
Multi-year ice	Presence	Rarely	—
Icebergs	Presence	Rarely	—
Northern Gulf			
Ice drift (no beacons)	—	—	—
Ice thickness			
Level ice: Northeast	Landfast ice (m)	0.62	0.27 to 0.62
Level ice: Northwest	Landfast ice (m)	1.12	0.50 to 1.12
EM thickness (none)	—	—	—
Multi-year ice	30-year presence	Intermittent	15 % to 20 %
Icebergs	Presence	Intermittent	—

^a Footprint of the electromagnetic (EM) sensor is 20 m.

D.8.4 Beaufort Sea

The ice in the Beaufort Sea can be subdivided into three regions (see Figure D.8):

- the arctic polar pack zone,
- the seasonal or transitional (shear) zone, and
- the landfast ice zone.

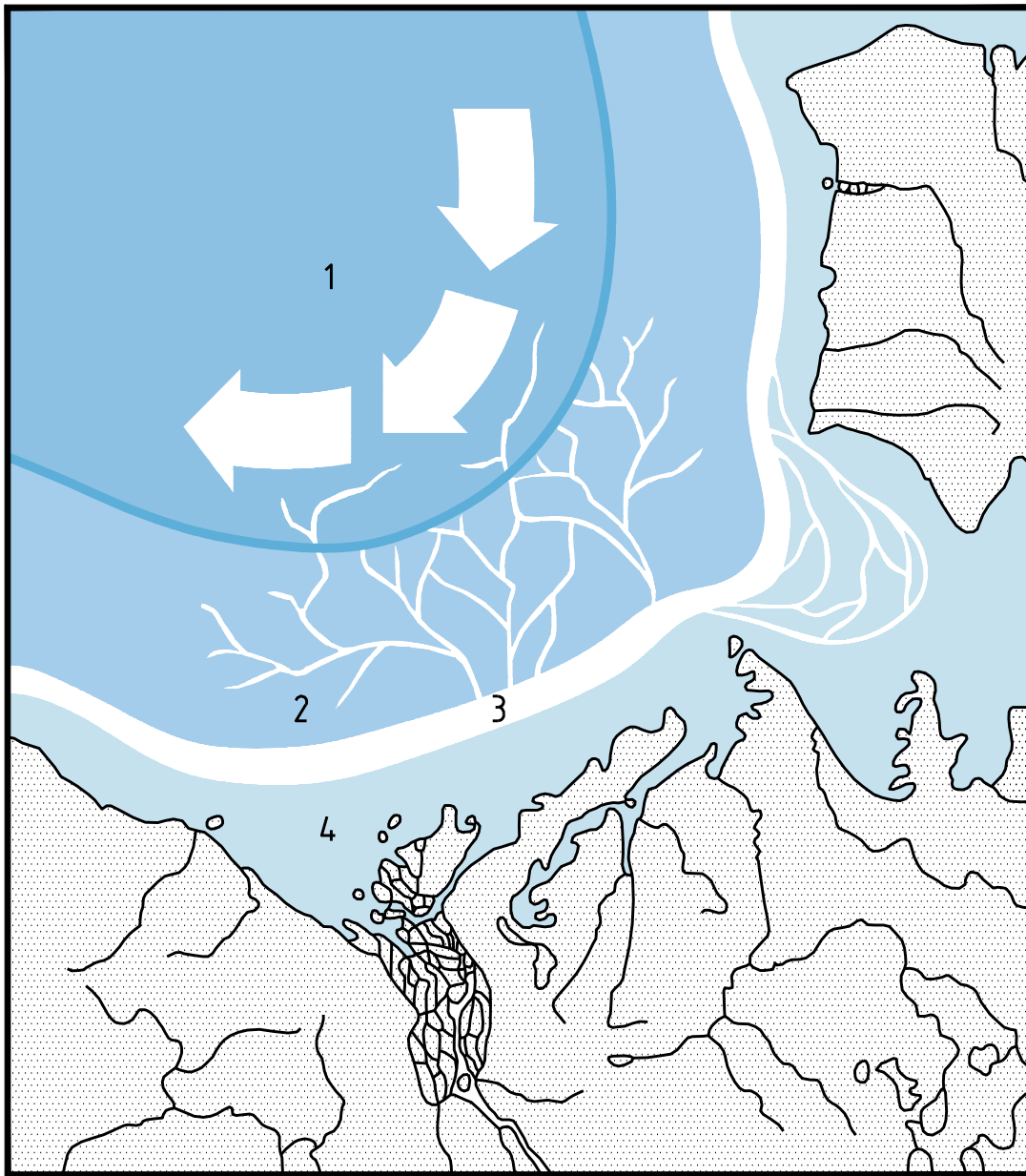
The arctic polar pack comprises old or multi-year ice with a level ice thickness up to 4.5 m, and ridges that can reach 25 m thick (see Figure D.9). The arctic polar pack continuously circulates with currents and winds in the Arctic Ocean, and is present year round. Its degree of penetration into the Beaufort Sea at any given time is dependent on the wind regime of the year. On average, the boundary of the Arctic pack lies from near Cape Prince Alfred southwestward to some 200 km north of Herschel Island and then westward some 200 km off the Alaska north coast.

The seasonal transitional zone extends from the edge of the (stationary) landfast ice to the edge of the moving polar pack ice. The width of this zone can vary from a few kilometers to over 300 km, both within a season and from year to year ^[186]. Although this region is primarily comprised of first-year ice, there can be a large number of multi-year and second-year ice floes. This ice is highly dynamic, and movement can take place throughout the winter. Movements of 3 km/day to 13 km/day are likely. The moving ice results in deformations in the ice sheet and the creation of both ridges and leads. The number of ridges increases rapidly in the first part of the winter and remains relatively constant after February. Ridge heights (sails) can range up to 6 m. The majority of the ice is below the water (the keel) and typical sail-to-keel ratios are 4.4 ^[189]. If the ridge survives the summer season, it largely desalinates and consolidates to form a multi-year ice ridge. These ridges are considerably stronger than first-year ridges, and their shape is smoother, with a sail-to-keel ratio of about 3.3 ^[189].

The landfast ice is extensive and forms out to a water depth of approximately 20 m. The edge of the landfast ice varies slightly from year to year (see Figure D.10). This region is comprised primarily of first-year ice. Multi-year ice, if present during the freeze-up period, will be frozen into the sheet. The ice begins to grow in late September and reaches a maximum thickness of approximately 1.9 m in late April (see Figure D.11). In spring, northwest winds die off, and east and southeast winds become predominant, so that a polynya develops along the edge of the landfast ice. In June, melt begins in the Mackenzie Delta and an open-water area also develops quickly there. Typically, Amundsen Gulf fractures in late June and the ice drifts out and decays. The fast ice along the Tuktoyaktuk Peninsula fractures in early July. During a cold summer, the landfast ice along the Tuktoyaktuk Peninsula may not completely break until mid-July. These cold summers occur because northwesterly winds keep the arctic pack close to shore.

Open drift ice conditions do not develop along the coast until the first week of August, and an open-water route does not develop until the first week of September. Freeze-up in the Beaufort depends to a very great extent upon the location of the southern limit of the arctic pack. New ice formation starts among the multi-year floes in late September and spreads southward, while it also spreads seaward from the coast. By late October much of the ice is at the first-year stage right out to the arctic pack.

Reduction in sea ice areal extent and concentration for the deep offshore waters are occurring at similar rates to those of the full Arctic Ocean. The largest reduction in sea ice concentration is due to the loss of old ice (second year and multi-year ice). In the late summer and autumn months, old ice concentrations over the continental slope of the Canadian Beaufort Sea are decreasing between 8 and 11 % per decade as computed from Canadian Ice Service digital ice charts over the past 45 years ^[230].

**Key**

- | | | | |
|---|-----------------|---|-------------------|
| 1 | Polar pack zone | 3 | Active shear zone |
| 2 | Transition zone | 4 | Landfast ice |

Figure D.8—Map Showing the Three Beaufort Sea Ice Zones in the Arctic ^[191]

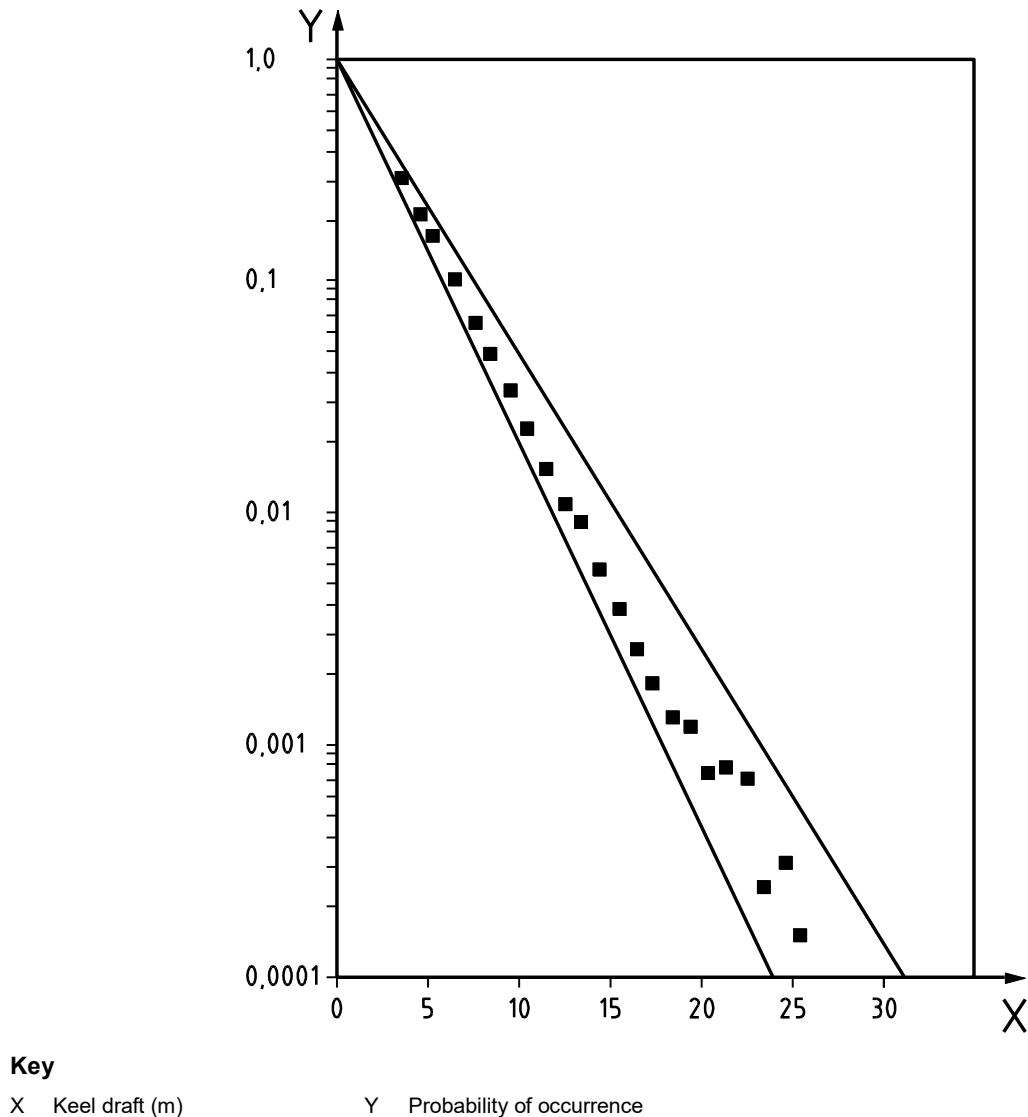


Figure D.9—Probability of Finding Pressure Ridge Keels in the Polar Ice Pack ^[192]

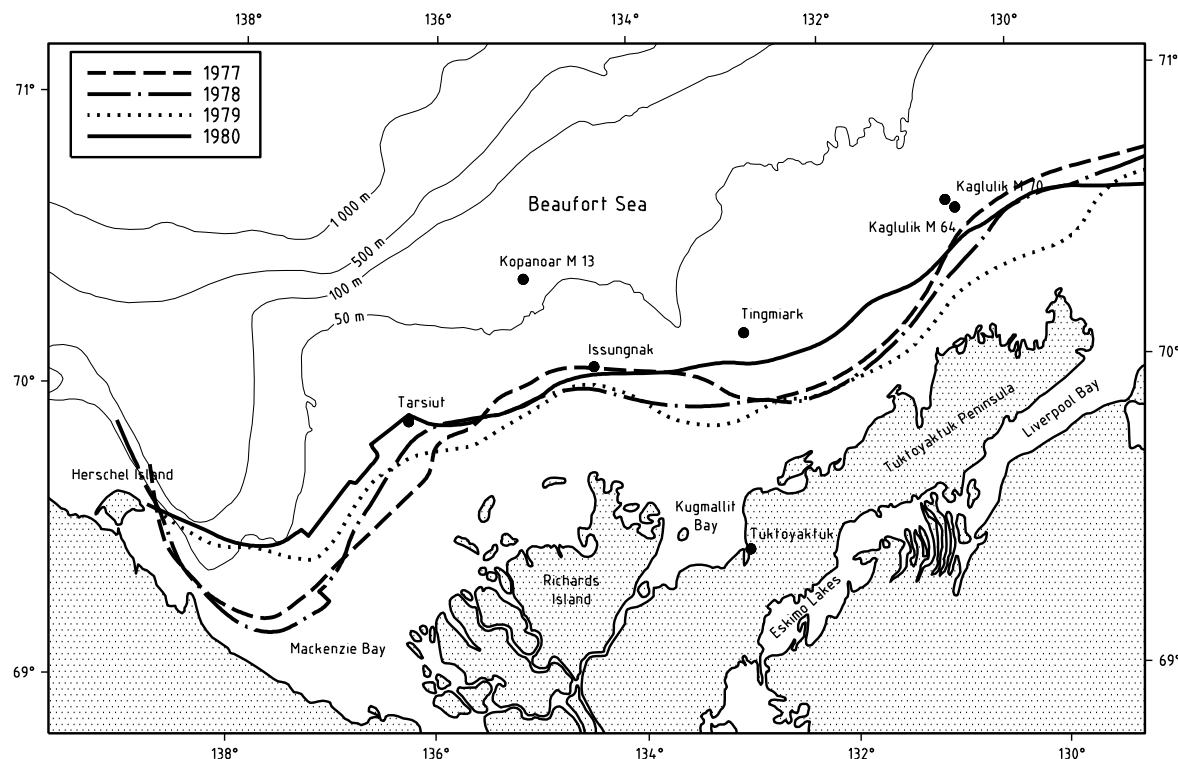


Figure D.10—Extent of the Landfast Ice from 1977 to 1980 [186]

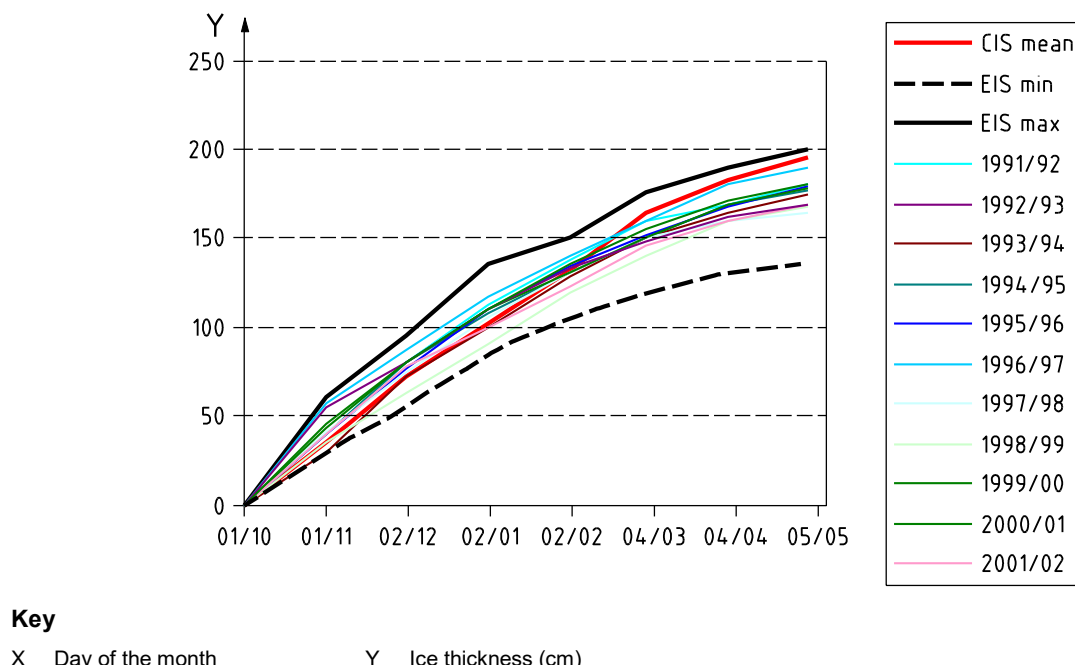


Figure D.11—Ice Thickness in the Beaufort Sea from 1991 to 2002, Including the Canadian Ice Service Mean Curve and the EIS min. and max. Curves [172]

D.9 Icebergs

The principal origin of the icebergs that travel past the east coast of Canada are the 100 tidewater glaciers of West Greenland. Between 10,000 and 15,000 icebergs are calved each year, primarily from 20 major glaciers between the Jacobshaven and Humboldt Glaciers. These glaciers account for 85 % of the icebergs that reach the Grand Banks. Ten percent of the icebergs reaching the Grand Banks are from glaciers located on the east coast of Greenland, while the remaining 5 % come from the ice shelves of Ellesmere Island. After calving, the icebergs move north with the West Greenland Current, then south with the Baffin and Labrador Currents until finally melting in the warmer waters of the southern Grand Banks and the Gulf Stream.

Icebergs typically do not travel far enough south to reach the coast of Nova Scotia, but there have been extreme situations where icebergs have been observed in this area. Iceberg sighting data for the Scotian Shelf are provided in Reference [178]. The number of infrequent sightings is insufficient to calculate reliable statistics on occurrence and impact probabilities.

According to the International Ice Patrol, the number of icebergs reaching the Grand Banks each year has varied from a low of 0 in 1966 to a high of 2202 in 1984, with the average over the past 10 years of around 800 icebergs. Of these, only a small proportion might drift in the vicinity of the various existing oil operations and require active iceberg management to reduce the probability of encounter. The average historical iceberg distribution offshore Newfoundland is shown in Figure D.12. This is indicative information only and should be used in conjunction with site-specific or project-specific studies to develop an iceberg site frequency/distribution and ice design criteria.

Local winds and currents largely determine the movements of free-floating icebergs (i.e. ungrounded icebergs in open water or in low concentrations of sea ice). Iceberg speeds and drift directions on the Grand Banks as measured over 1 h to 3 h time intervals are less than 35 km/day, and 47 % are directed toward the southwest.

Icebergs are characterized according to their height, length, and mass estimates. Iceberg strength criteria are required for the design of hydrocarbon facilities on the Grand Banks. Site-specific or project-specific studies to develop appropriate iceberg-related criteria are required, as these criteria change according to region and facility type (e.g. jacket-type fixed platform, gravity-based structure, floating vessel, etc.). Typical data include iceberg occurrence/frequency, speed and direction of travel, and physical properties such as draft, width, length, and shape that are used to estimate mass.

NOTE Additional information on the ice environment on the Grand Banks is provided in Reference [188].

Icebergs originating from glaciers in Greenland and Ellesmere Island drift south through the Grand Banks area with the Labrador Current. Bergs classified as "large" (up to 4,500,000 t) have been observed in the area.

Icebergs also enter the northern Gulf through the Strait of Belle Isle and some with the eastward current in Cabot Strait. The International Ice Patrol and Canadian Ice Service iceberg databases show iceberg sightings throughout the northern Gulf, with higher concentration near the Strait of Belle Isle. They follow the same circulation pattern along the north shore as the old ice.

The iceberg drift pattern for the Bay du Nord area is based on information in Reference [183]. In general terms, this distribution is very similar to other areas studied and is consistent with the general distributions of iceberg size south of 48.00° N.

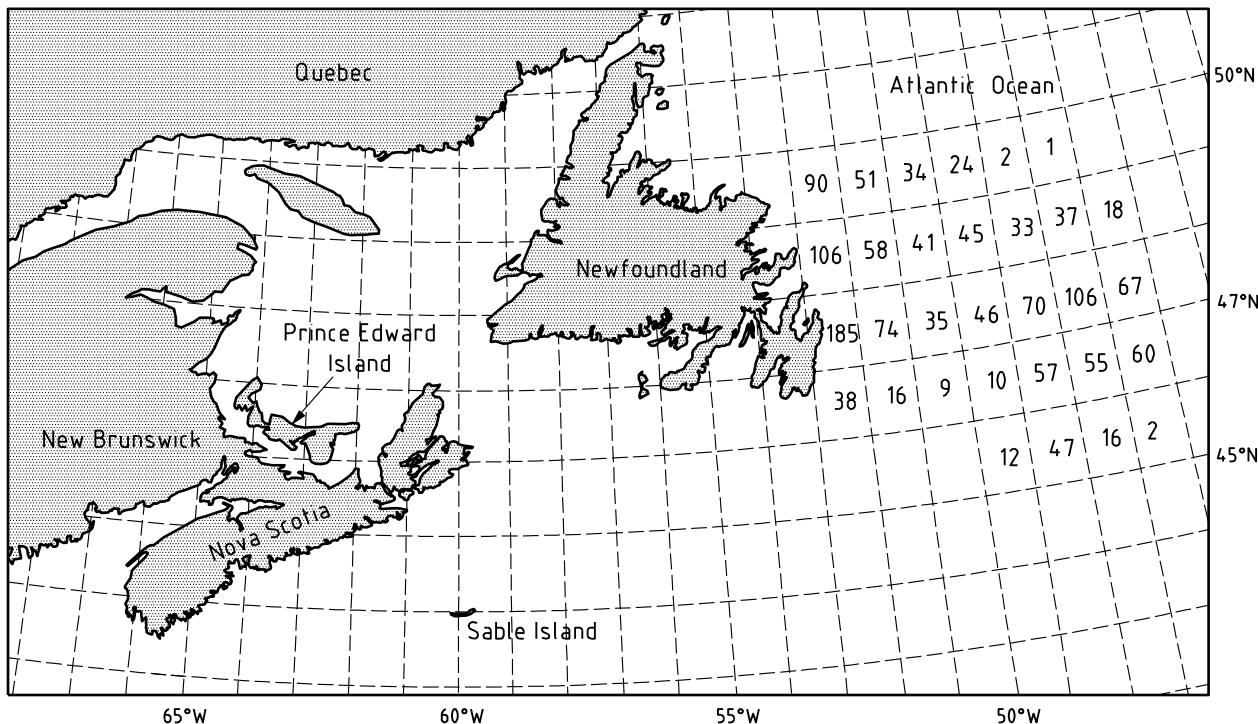


Figure D.12—Historical Yearly Mean Iceberg Distribution Offshore Newfoundland, Based on Data from 1981 to 2003^[176]

D.10 Ice Management

Offshore operations should be executed in a safe, efficient, and environmentally responsible manner. In order to ensure that wells and facilities are protected from potential hazardous ice situations, appropriate precautionary actions should be taken. These actions include, as a minimum, early detection and reporting of ice, ice tracking, and ice deflection.

The primary ice detection method is marine radar that shall include a small target detection enhancement ice radar specifically designed to minimize background clutter and enhance target detection. Other detection sources include aircraft surveillance and onboard radar, satellite radar, vessel reconnaissance, and helicopter reconnaissance.

Iceberg deflection techniques that have previously been used successfully on the Grand Banks include iceberg towing (using tow ropes or tow nets) and the use of water cannons or “propeller washing” to alter the course of a threatening iceberg.

A critical component of an ice management plan is accurate collection of ice and environmental data, forecasting of environmental conditions and ice movement, threat assessment, and an effective communications and information-sharing network. This facilitates the exchange of information on vessels (location, status), icebergs (location, speed, trajectory), weather forecasts, and other information allowing prompt decisions to be made.

Only general comments are made in this section. Clauses 17 and A.17 of CAN/CSA-ISO 19906-11 Arctic offshore structures provide more specific guidance on ice management.

D.11 Other Environmental Factors

D.11.1 Iceberg Scour

D.11.1.1 Grand Banks

A large iceberg can drift into a region where its draft exceeds the water depth, resulting in contact with the seabed and subsequent sediment displacement in the form of scours and/or pit features. Iceberg scours have occurred in various locations on the Grand Banks and have been mapped with side-scan sonar. The Grand Banks Scour Catalogue, described in Reference [168], is a compilation of data from previous seabed surveys.

For a typical location on the Grand Banks, the following typical average scour parameters have been estimated:

- average scouring frequency: $\sim 1 \times 10^{-4}$ to 1×10^{-3} scours/km²/year, depending on the region;
- average scour length: ~650 m;
- average scour width: ~25 m.

The average depth of scour depends on the type of soil conditions present at the scour location. Stiff or compacted sediments can limit the scour depth. For a typical location on the Grand Banks, the average scour depth is about 0.3 m.

Iceberg scours up to 1.5 m deep have been measured on the seafloor in the Terra Nova area. However, due to the significant water depth in the deepwater area (approximately 1100 m and greater), iceberg scour in this region is not deemed relevant.

It is noted that considerable variation exists across the region and site specific studies are necessary when designing for seabed facility protection.

D.11.1.2 Beaufort Sea

The seabed of the Beaufort Sea is heavily scoured by large ice features, both first-year and multi-year ice ridges. Table D.2 provides information on several scour parameters.

Scour depths up to 7 m have been measured in 45 m water depth [177]. The spatial frequency of ice scours varies significantly across the Beaufort shelf. Sonar records indicate that the maximum spatial frequency of the scours, expressed as a linear density, is 16.6 scours/km in water depths of 20 m to 30 m [177]. The impact rates for scouring and the time interval to re-scour 90 % of the seafloor are given in Table D.3. New technology using multi-beam sonar is continually improving the knowledge of scouring of the Beaufort Sea. The Geological Survey of Canada at the Bedford Institute of Oceanography in Dartmouth, NS, maintains an up-to-date database on information related to scouring in the Beaufort Sea.

Table D.2—Statistics for Ice Scours in the Beaufort Sea [177]

Parameter	Dimension	Population
Mean scour depth	0.5 m	10,385 events
Mean scour width	26 m	66,549 events
Scour orientation mode	115° to 295°	66,459 events
Scour length	5 km to 10 km	Estimated
Mean berm width	15.3 m	100 events
Mean berm height	0.7 m	100 events

Table D.3—Seabed Scour Statistics for the Beaufort Sea [177]

Water depth (m)	5 to 8	14 to 18	22 to 26	30 to 35	34 to 50
Location		Pullen Block	Tarsuit - Newktoralik	Corridor	
Maximum scour impact rate (events/km)	0.8	2.0	8.2		0.0
90 % re-scouring interval (years)		36	22	109	

D.11.2 Snow and Ice Accretion

Installations located offshore eastern Canada can be subject to snow accumulation and superstructure icing.

The extent to which snow can accumulate and its possible effect on the structure should be considered in the design process. In the absence of specific information, new snow may be assumed to have a density of 100 kg/m³.

Superstructure icing on fixed or floating offshore structures is a potential concern for operations in cold climates. Ice accretion can lead to several types of problems, such as safety hazards (slippery ladders, inoperable winches, ice on radar antennas, etc.). Superstructure icing is the result of both freezing sea spray and atmospheric precipitation. Ice accretion generated by wave-structure, collision-generated sea spray is the dominant source of ice accretion, due to the intensity and frequency of the spraying events. The phenomenon is seasonal, and its severity depends on the combination of wind speed, air temperature, and height above sea level. The design of offshore structures should consider the possibility of superstructure icing and its overall effect on mass, structural integrity, and stability. In the absence of other specific information, the ice that can form on the structure may be assumed to have a density of 900 kg/m³.

D.11.3 Reduced Flying Visibility

Reduced flying visibility due to fog, snow, and rain is common offshore the Canadian east coast. At a typical location on the Grand Banks, the amount of time that flying visibility is typically less than 1 km is as follows:

- from April to August: 40 %;
- from September to March: 11 %.

Based on Reference [185], the frequency of reduced visibility is somewhat less in the Nova Scotia offshore area:

- from April to August: 23 %;
- from September to March: 6 %.

D.11.4 Marine Growth

Installations in the Canadian offshore region should consider the potential effect of marine growth in terms of additional mass and hydrodynamic loading. If applicable, allowance should be made in the design for marine growth on vessel hulls, mooring lines, risers, and other subsea equipment. The profile of marine growth thickness that can occur during the operational phase of the structure should be characterized relative to the depth of the structure below the sea surface.

D.11.5 Daylight Hours

Due to the northern location of the Beaufort Sea, daylight hours for this region should be taken into account. Figure D.13 shows an illustration of the duration of sunlight at latitudes from 30° to 90°^[165]. Figure D.13 also shows the duration of sunlight at Inuvik. As can be seen, the sun does not rise above the horizon for up to 3 months during the winter at latitudes north of the Arctic Circle. Conversely, in the summer months, the sun does not set and provides 24 h of daylight.

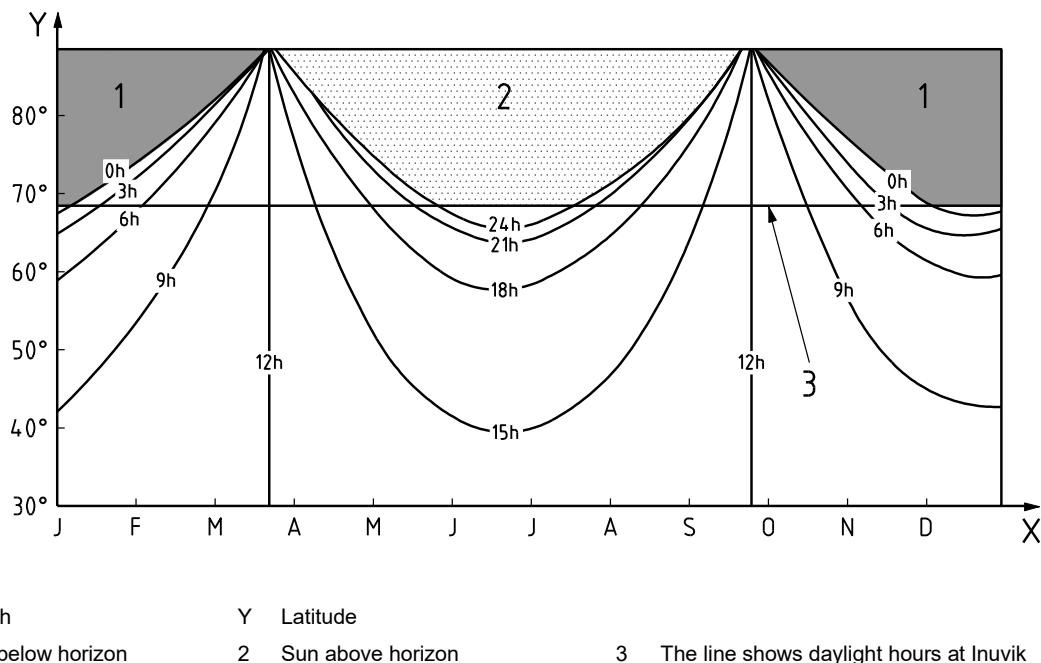


Figure D.13—Amount of Daylight Hours as a Function of Latitude ^[165]

D.11.6 Earthquakes

The Grand Banks is classified as an area of relatively low seismic activity, but seismic events of significant magnitude have occurred in the recent past. The consequences of earthquake damage to seabed equipment and anchor piling should be considered. The Flemish Pass prospects are located approximately 750 km northeast of the Grand Banks 1929 earthquake epicenter.

D.12 Estimates of Metocean Parameters

Metocean parameters for offshore Canada are provided in Tables D.4 and D.5. These values are indicative and are shown for illustration purposes only. This information should not replace detailed site-specific metocean parameters that should be obtained for the design or assessment of a particular structure that is to be constructed or operated at a particular site.

With respect to the offshore Nova Scotia area, site-specific conditions are highly variable depending on location and the effect of blockage from Sable Island, especially on waves and currents. Site-specific studies are particularly necessary in shallow areas to resolve local wave refraction and current intensification.

The return period for storm surges in the Gulf of St. Lawrence is calculated using the hourly observation of the water level at the station of Pointe-au-Père, QC, for the period 1900 to 2000^[190]. The values quoted are in meters above MSL. Storm-surge analysis at that station is valid for the Gulf of St. Lawrence, from Rimouski to Cabot and Belle-Isle Straits. West of Rimouski toward Quebec City, the funnelling effect of the coastline and bottom topography increase the storm-surge amplitude as it progresses upstream.

Table D.4—Extreme Air and Water Temperatures for Canadian Offshore Areas

Offshore Area	Newfoundland Offshore		Gulf of St. Lawrence	Beaufort Sea	Nova Scotia Offshore (Sable Island Bank)
	Grand Banks	Deepwater			
Sea Water Temperatures (°C)					
Minimum extreme near surface	-1.7	-1.7	-1.8	-1.8	-1.6
Maximum near surface	15 to 19	15 to 19	15 to 20	5 to 10	15 to 20
Minimum near bottom ^a	-1.7	3	-1.8	-1.8	-1.3
Maximum near bottom	3 to 6	3	2 to 6	-1 to 5	18
Air Temperatures (°C)					
Minimum	-17 to -19	-17 to -19		-40	-14 to -19
Maximum	22 to 25	22 to 25		15	30 to 35

^a For Gulf of St. Lawrence: minimum temperature mid-depth (°C).

No similar long series of observation is available for ocean currents as is the case with water-level observation. Time series at one station are short, 1 year at the most, and a station is rarely surveyed twice. Maximum speeds of currents and their variability are reported in Reference [175] for a number of stations in the Gulf of St. Lawrence. These observations were used to generate the values of the currents for the return period of one year in Table D.5. The amplitudes of currents given in Table D.5 for the return periods of 5, 10, 50, and 100 years are estimated using the cited ratio for Nova Scotia and Newfoundland areas between the return period of 1 year and the other return periods. Currents reported in Table D.5 of extreme metocean parameters are valid for the Jacques Cartier Passage, which is located north of Anticosti Island, and for the region north of the Gaspé Peninsula where the Gaspé Current flows. These two regions experience the highest values for the currents. Outside of these regions, current amplitude is weaker and more variable, being mainly wind-driven. On the other hand, as the shore is approached, the tidal currents increase as the bathymetry shallows. This increase in current amplitude is also observable with progress upstream. The region between Tadoussac and Quebec City experiences higher currents than stated in Table D.5. A Tidal Atlas^[164,184] is available for that region.

Table D.5—Extreme Metocean Parameters for Canadian Offshore Areas

Newfoundland Offshore (Grand Banks)					
Metocean Parameter	Return Period (years)				
	100	50	10	5 ^b	1
Wind speed^a					
10 min wind speed (m/s)	37 to 41	36 to 39	33 to 34	29 to 33	25 to 31
3 s gust wind speed (m/s)	50 to 55	48 to 52	42 to 45	38 to 42	34 to 39
Waves					
Maximum wave height (m)	28 to 31	26 to 29	24 to 26	22 to 23	19 to 21
Significant wave height (m)	14.5 to 16	14 to 15	12 to 13	11 to 12	10 to 11
Associated peak period (s)	15 to 20	15 to 20	14 to 18	13 to 18	12 to 17
Current speed					
Surface (m/s)	1.3 to 1.7	1.2 to 1.6	1.1 to 1.3	1.0 to 1.2	0.9 to 1.0
Mid-depth (m/s)	0.9 to 1.1	0.8 to 1.1	0.7 to 1.0	0.6 to 1.0	0.5 to 0.9
Near-bottom (m/s)	0.9 to 1.0	0.8 to 1.0	0.7 to 0.8	0.6 to 0.8	0.5 to 0.7
Storm surge					
Surge above MSL (m)	0.70	—	0.61	0.46	0.50
Nova Scotia Offshore (Sable Island Bank)					
Metocean Parameter	Return Period (years)				
	100	50	10	5 ^b	1
Wind speed^a					
10 min (m/s)	41 to 45	40 to 43	35 to 38	30 to 34	25 to 30
3 s gust (m/s)	50 to 58	50 to 55	45 to 48	39 to 43	34 to 37
Waves					
Maximum height (m)	19 to 27	18 to 27	16 to 26	15 to 26	15 to 26
Significant height (m)	11 to 15	11 to 14	9 to 11	8 to 10	7 to 9
Associated peak period (s)	15 to 18	15 to 17	14 to 15	13 to 15	13 to 14
Current speed					
Surface (m/s)	1.5 to 2.3	1.4 to 2.3	1.3 to 2.1	1.2 to 1.8	1.0 to 1.4
Mid-depth (m/s)	1.1 to 1.3	1.0 to 1.2	1.0 to 1.1	0.9 to 1.1	0.9 to 1.0
Near-bottom (m/s)	0.8 to 1.1	0.7 to 1.1	0.7 to 1.0	0.8 to 1.0	0.9 to 1.0
Storm surge					
Surge above MSL (m)	0.6 to 0.7	0.5 to 0.6	0.49	—	—

Table D.5—Extreme Metocean Parameters for Canadian Offshore Areas (continued)

Canadian East Coast Deepwater					
Metocean Parameter	Return Period (years)				
	100	50 ^c	10	5 ^b	1
Wind speed^a					
10 min (m/s)	31.8	30.45	29.1	27.40	25.7
3 s gust (m/s)	42.8	41.05	39.3	37.05	34.8
Waves					
Maximum height (m)	27.3	25.80	24.3	22.35	20.4
Significant height (m)	14.6	13.75	12.9	11.85	10.8
Associated peak period (s)	16.1	15.60	15.1	14.40	13.7
Current speed					
Surface (m/s)	1.3	1.23	1.15	1.08	1
Mid-depth (m/s)	1.09	1.03	0.97	0.92	0.86
Near-bottom (m/s)	0.96	0.90	0.83	0.77	0.7
Storm surge					
Surge above MSL (m)	—	—	—	—	—
Gulf of St. Lawrence (East of Rimouski to Cabot Strait)					
Metocean Parameter	Return Period (years)				
	100	50	10	5	1
Wind speed^a					
10 min (m/s)	—	—	—	—	—
3 s gust (m/s)	—	—	—	—	—
Waves					
Maximum height (m)	18.972	17.856	15.438	14.136	11.16
Significant height (m)	10.2	9.6	8.3	7.6	6
Associated peak period (s)	12.4	12.2	11.7	11.4	10.4
Current speed					
Surface (m/s)	1.4 to 2.1	1.4 to 2.0	1.2 to 1.8	1.1 to 1.6	0.9 to 1.3
Mid-depth (m/s)	0.6 to 0.7	0.5 to 0.7	0.5 to 0.6	0.5 to 0.6	0.4 to 0.5
Near-bottom (m/s)	0.5 to 0.6	0.5 to 0.6	0.4 to 0.5	0.4 to 0.5	0.3 to 0.4
Storm surge					
Surge above MSL (m)	1.4 to 1.8	1.3 to 1.6	1.2 to 1.3	1.1	0.6

Table D.5—Extreme Metocean Parameters for Canadian Offshore Areas (continued)

Beaufort Sea					
Metocean Parameter	Return Period (years)				
	100	50	10	5	1
Wind speed^a					
Hourly average (m/s)	31.67	29.17	26.94	23.89	16.67
1 min average (m/s)	41.67	38.89	35.83	32.22	29.72
Waves					
Maximum height (m) - shelf (< 60 m) - deep (> 60 m)	5 to 8 9 to 15	5 to 8 9 to 14	4 to 8 9 to 12	3 to 7 7 to 10	2 to 4 4 to 5
Significant height (m) - shelf (< 60 m) - deep (> 60 m)	3 to 5 5 to 8	3 to 5 5 to 8	2 to 4 4 to 6	2 to 4 3 to 5	1 to 2 2 to 3
Associated peak period (s) - shelf (< 60 m) - deep (> 60 m)	8 to 10 10 to 11	7 to 10 10 to 11	7 to 9 9 to 11	7 to 8 8 to 10	5 to 7 7 to 8
Current speed					
Surface (m/s)					
Mid-depth (m/s)					
Near-bottom (m/s)					
Storm surge					
Surge above MSL (m)	1.4 to 1.8	1.3 to 1.6	1.2 to 1.3	1.1	0.6

^a Based on a reference height of 10 m above sea level.
^b Based on average of 1-year and 10-year data. To be updated in future revisions of this annex.
^c Based on average of 10-year and 100-year data. To be updated in future revisions of this annex.

D.13 Sources of Additional Information

D.13.1 Information on Meteorological Parameters, Prediction of Severe Weather, Sea State, and Icing Conditions

Information Services Division
 National Archives and Data Management Branch
 Meteorological Service of Canada
 Environment Canada
 4905 Dufferin Street
 Toronto, Ontario M3H 5T4
 Canada

D.13.2 Oceanographic Information

- a) Department of Fisheries and Oceans Canada
Marine Environmental Data Service
12W082-200 Kent Street
Ottawa, Ontario K1A 0E6
Canada
- b) Department of Fisheries and Oceans Canada
Bedford Institute of Oceanography
Ocean Sciences Division
P.O. Box 1006
Dartmouth, Nova Scotia B2Y 4A2
Canada
- c) Department of Fisheries and Oceans
Institute of Ocean Sciences
Ocean Sciences and Productivity Division
P.O. Box 6000
9860 West Saanich Road
Sidney, British Columbia V8L 4B2
Canada
- d) Pêches et Océans Canada/Fisheries and Oceans Canada Institut Maurice-Lamontagne/Maurice Lamontagne Institute
850 Route de la Mer, C.P. 1000
Mont-Joli, Québec
Canada G5H 3Z4

In collaboration with Environmental Canada, the Canadian Ice Service and the Canadian Hydrographic Service, 48 h forecasts of surface currents, sea ice, surface water temperature, and water levels are available in real time for the Gulf of St. Lawrence. Development is ongoing to expand this service to all coastlines of Canada.

D.13.3 Water Depths and Tides

Department of Fisheries and Oceans
Canadian Hydrographic Service
615 Booth Street
Ottawa, Ontario K1A 0E6
Canada

D.13.4 Ice-related Information

- a) Environment Canada
Meteorological Service of Canada
Canadian Ice Service
Operations Division
Client Service Section
373 Sussex Drive, Block E-3
Ottawa, Ontario K1A 0H3
Canada

- b) National Research Council Canada
Canadian Hydraulics Centre
Building M-32, Montreal Road
Ottawa, Ontario K1A 0R6
Canada

D.13.5 Canadian East Coast Seabed Conditions

Natural Resources Canada
Geological Survey of Canada (Atlantic)
P.O. Box 1006
Dartmouth, Nova Scotia B2Y 4A2
Canada

Annex E (informative)

Sakhalin/Sea of Okhotsk

E.1 Description of the Region

Sakhalin Island is located at the eastern side of the Siberian mainland. It is surrounded by the Sea of Okhotsk on the northern and eastern sides and the Tartar Strait, which separates Sakhalin from the mainland (see Figure E.1). The population density on Sakhalin is small and mostly lower than 1.5 people per square kilometer. The only town with significant population is Yuzhno-Sakhalinsk, having about 200,000 inhabitants.

The Sea of Okhotsk is separated from the Pacific Ocean by the Kuril Islands and the Kamchatka Peninsula. The Sea of Okhotsk is connected to the Sea of Japan and the Tartar Strait by La Perouse Strait. By far the largest river in the area is the Amur, covering a catchment area of about 2 million square kilometers. The average discharge of the river Amur is $11,700 \text{ m}^3/\text{s}$ ($369 \text{ km}^3/\text{year}$). Almost 75 % of the annual discharge occurs during spring and summer (May to September), whereas only 25 % of the annual discharge occurs during autumn and winter.

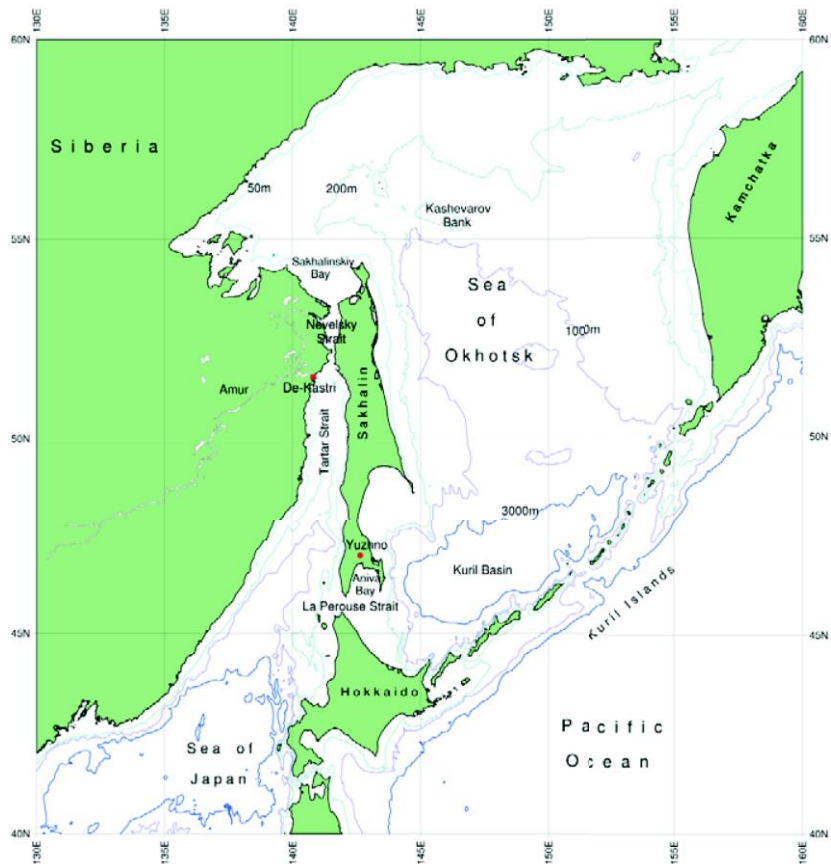


Figure E.1—Map of Sakhalin Showing Locations of Example Metocean Parameters

E.2 Data Sources

Meteorological data for the Sakhalin area comes mainly from the Sakhalin Territorial Administration for Hydrometeorology and Environmental Monitoring (Sakhydromet) in Yuzhno-Sakhalinsk. Sakhydromet runs a comprehensive network of 35 observation stations, of which 21 are coastal stations. Observations of the most important meteorological parameters are made every 3 h. Depending on the station, continuous data sets over periods ranging from 10 years to more than 50 years are available.

Oceanographic data are available at Sakhydromet (mainly coastal observations of sea level, salinity, and sea temperature) and at the Ecological Company of Sakhalin (ECS). Apart from the coastal observations, most of these data cover only small periods of time. Large amounts of current (profile) and water-level data were collected at several locations during periods of 6 months to 7 months in 1996–2003 along the Sakhalin northeast coast, in Aniva Bay (for 1 year) and near the De Kastri Terminal.

The most comprehensive hindcast database of winds, waves, (total) currents, and water levels is the SIMOS-3 database, which was produced by Oceanweather Inc. as a joint industry project. This database can provide continuous hourly time series at hundreds of grid points all around Sakhalin Island over the period 1980 to 2005^[193].

Sea-ice data collected in the area consists of airborne observations, satellite imagery, local ice observations from coastal locations, and field data collected with an ice-profiling sonar. Ice maps were produced during several decades until the early 1990s, based on visual observations and aerial photographs from aircraft and helicopters. Weekly ice coverage maps have been generated since 1972 by the National Ice Centre, based on satellite imagery. Since the early 1930s, ice observations have been made at several coastal stations on Sakhalin Island. On the Sakhalin east coast, several marine radars were installed that are able to monitor the ice drift along the Sakhalin east coast^[194]. More recently, large amounts of ice draft (and keel depth) data were collected at several locations during periods of 6 to 7 months in 1996–2003 along the Sakhalin northeast coast. Finally, ice and ice/structure interaction observations have been made from the Molikpaq platform since its deployment in the Sea of Okhotsk in 1998.

E.3 Overview of Regional Climatology

Considering its longitude, latitude, and marine location, the climate on Sakhalin is very severe, a result of its proximity to the Siberian continental land mass. The winter in Sakhalin is long and cold, and the summer is short. In winter, strong winds from the continent can cause a drop in air temperature to –40 °C. In the southern part of the island winter temperatures are milder, but nevertheless there are frequent snowstorms, strong winds, and generally heavy overcast cloud conditions.

Sea ice engulfs the coast from November to June in the north, from December to May along most of the east coast, and from January to March in Aniva Bay. The southwestern coastline of the island is always ice-free. Because of the presence of sea ice, the island is in fact an extension of the mainland during winter. Although the west coast climate is generally more severe than that of the east coast, ice extends further southward on the east coast of the island as a result of the cold southward-flowing East Sakhalin current. West of the island, the relatively warm Tsushima current flows northward on the western coast up to 51° N. Ice generally does not break up along the northern coast until the end of June.

The climate varies widely throughout Sakhalin, due to the mountain ranges that include peaks up to 1400 m high, as well as the proximity of the sea. As a consequence, there is a large difference between the immediate coastal areas and the interior of the island. During winter, the sea provides additional warmth to the eastern coast, whereas during summer the sea significantly cools the northern and eastern portions of the island. This is attributed to the effect of the cold East Sakhalin current, as well as to the effect of the remaining drift ice. This effect contributes to the extreme fogginess along the eastern coastal areas in late spring and summer. Sunshine is rare in summer and the humid, cool weather is conducive to thick fog and drizzle.

E.4 Water Depth, Tides, Storm Surges, and Tsunamis

The Sea of Okhotsk consists of a moderately broad shelf to the north, which gradually steepens to depths > 3000 m to the south. Depths shallower than 200 m extend approximately 100 km off the coast of Kamchatka Peninsula and Sakhalin Island. Beyond the 200 m contour, the water depth increases to a broad area between 1000 m and 2000 m in the central part of the sea. Shallow banks are found in the northwestern basin, e.g. at the Kashevarov Bank.

The Sea of Japan is a deep basin with maximum depths of 3700 m and has many of the circulation features found in deep ocean basins. The bottom topography slopes gently upward toward the northeast until reaching the Tartar Strait. Tartar Strait has a characteristic width of about 130 km. Water depths range from a maximum of 1500 m in the south and a minimum water depth of about 4 m in the Nevel'sky Strait.

Tidal amplitudes vary widely over the area. Large tidal amplitudes have been observed along the shallow bays in the northwestern Sea of Okhotsk, in the Nevel'sky Strait, and near the northern edge of the Kuril Islands. Tides in the Sea of Okhotsk are dominated by diurnal constituents K1 and O1, whereas in most of the Tartar Strait, the semi-diurnal constituents M2 and S2 dominate^[195].

Storm surges along the coastlines are mostly smaller than 1.5 m to 2.0 m. Only at specific locations, such as along the north side of Aniva Bay, can higher surges sometimes be observed during periods with strong onshore winds. Tsunami waves can affect the area all around Sakhalin. Three sources can generally be distinguished:

- a) trans-Pacific tsunamis caused by large earthquakes in the Pacific Ocean (typical period: 40–45 min);
- b) tsunami sources in the Sea of Japan (typical period: 15 min); and
- c) tsunamis caused along the Kuril Island chains (typical period: 12 min).

Extreme 100-year tsunami crest heights range from about 1.5 m along the Sakhalin east coast to about 2 m to 2.5 m in Aniva Bay.

E.5 Winds

The location of Sakhalin in the area between continental Asia and the Pacific Ocean is the major factor for its monsoonal climate.

During winter, a strong pressure gradient forms over Sakhalin, between the Siberian high-pressure system and the Aleutian low-pressure system, driven by the strong contrast in temperatures between the relatively warmer air over the Arctic Ocean and Bering and Okhotsk Seas and the much cooler air over the Siberian mainland. These strong pressure gradients produce consistently strong winds blowing from northerly directions (generally north and northwest) with prevailing speeds between 5 m/s and 10 m/s. The frequency and intensity of storms is highest during November and December. Extreme wind speeds during storms can reach 30 m/s to 35 m/s. Winter storms originate from the Chinese mainland or from waters near Japan, and they all tend to move northeastward into the Bering Sea or Gulf of Alaska. Most of the storm tracks lie in the southern part of the island during winter.

The Siberian high-pressure system begins to break up in March, and the most rapid weather changes occur in April and May. Spring brings storms with strong winds and snowfalls, the storms continuing to move off the Asian mainland toward the western Aleutians. However the major storm tracks have, by this time of the year, moved northward and often cross Sakhalin Island. In spring, a high-pressure system starts to form over the Sea of Okhotsk, the high pressure being caused by the contrast between the cold frozen sea surface and the warming effect of the lands to the north.

With the onset of summer, the Siberian mainland becomes warmer than the surrounding seas, and a low-pressure system forms over the continent. Pressure gradients are weaker than in the winter, so the summer air circulation is less consistent over the region than during the winter. A large, semi-permanent, quasi-stationary high-pressure system dominates the entire North Pacific, including the Sea of Okhotsk. This pressure distribution generates predominantly light easterly or southeasterly winds (2 m/s to 5 m/s) that predominate across the island during the summer monsoon months. Extra-tropical storms, common

during other months, decrease in number and intensity. The mean tracks run from the Chinese mainland northeastward to the Aleutians. Typhoons can affect the Sakhalin area during late summer. Such storms generally do not approach closely to the island, although the widespread clouds and precipitation can affect it. On occasion, typhoons leaving the East Asian Sea have caused cyclonic storms, associated with the polar front, to regenerate. In these cases, the storms stall and cause prolonged rainfall. Dying typhoons very occasionally enter the Sea of Okhotsk.

Autumn is a transitional season. The effects of the Pacific monsoon continue to enhance rainfall. Extratropical storms become more intense and frequent, causing the Aleutian low-pressure system to intensify and the North Pacific high-pressure system to weaken. Extra-tropical storms continue to form over the Asian continent and the waters around Japan. One of the principal storm tracks continues to cross Sakhalin Island. The other lies south of Japan. With the increase in storms, gales become more frequent.

E.6 Waves

The annual variation in wave climate is closely related to the atmospheric circulation over the Sea of Okhotsk. During the summer monsoon period (June to August), waves from the southeast or southerly sectors with heights between 0.5 m and 1.5 m occur mostly along the east coast. On the west coast, wave heights are often lower than 0.5 m during summer. In September, the wave height and direction become more variable in time because of the changing atmospheric processes, with prevailing waves of 1 m to 2 m along the east coast and 0.5 m to 1.5 m along the west coast. With the onset of the winter monsoons, the frequency of waves from the north and northeastern sectors grows in the Sea of Okhotsk. Prevailing wave heights are between 1.5 m and 2.5 m. In storms, wave heights are often between 5 m to 7 m high and they can even exceed 8 m during extremely severe storms. In the Tartar Strait, however, wave heights rarely exceed 4 m and are mainly from directions between southwest and northwest.

E.7 Currents

Both in the Sea of Okhotsk and Tartar Strait, a significant anti-clockwise residual current pattern is observed along its edges. In the centre of the Sea of Okhotsk, currents are usually small or negligible, whereas at the western boundary, along the Sakhalin east coast, there is a clear southward flow of water called the East Sakhalin Current^[196]. Residual currents are highest at the northeastern tip of Sakhalin Island, where the eastward outflow from the Amur River and the anti-clockwise current in the Sea Of Okhotsk come together. Further south along the east coast, the residual current gradually decreases. Typical residual currents flow at between 0.2 m/s and 0.4 m/s. This cold southward flow occurs most of the year except for the months of May and June, when the flow sometimes reverses direction due to the prevailing south-southeasterly winds. Along the west coast of Sakhalin Island, a relatively warm northward flow occurs that can reach as far as 51° N.

Tidal currents are significant all around the island, except for the inner parts of Aniva Bay and some of the deeper parts of the Sea of Okhotsk and Tartar Strait where currents are mainly driven by the wind. Along the west coast of Sakhalin, semi-diurnal tidal constituents mainly control the current pattern. The highest tidal currents are found along the northeast coast of Sakhalin. This is due to the wide, shallow shelf in the northern part of the Sea of Okhotsk and the near-resonant trapping nature, because the natural frequency of the free oscillation is close to the diurnal tidal frequencies. This all results in a strong amplification of diurnal tidal currents, which are of the order of 1 m/s over the Kashevarov Bank^[197] and even higher along the northeast coast of Sakhalin Island.

E.8 Sea Ice

The ice cover that is found off Sakhalin Island is completely seasonal in nature, as the region is entirely ice-free during the summer and fall months. Only first-year ice is found in the area. It does not contain any multi-year ice floes, or glacial ice features such as icebergs. The waters off the eastern coastline of Sakhalin Island and in the northern half of the Tartar Strait are typically covered by sea ice for about half of the year^[198]. The duration of the ice season gradually reduces southwards, to only 2 months in Aniva Bay. The southwestern coastline of Sakhalin Island is always ice-free, due to the northward flow of relatively warm water along the west coast.

Some indicative values for a number of ice parameters are given in Table E.1.

Table E.1—Summary of Ice Conditions

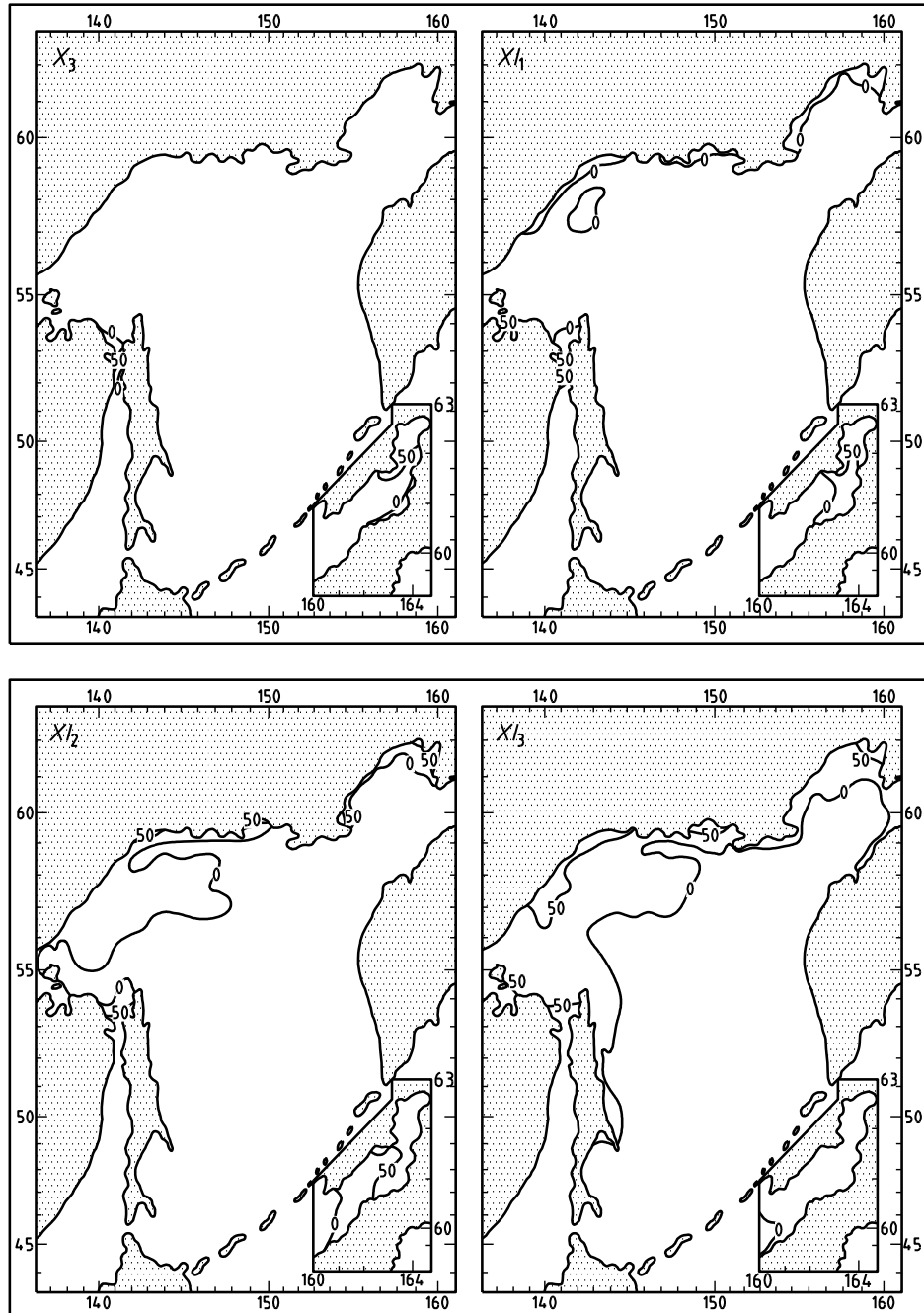
Sea Ice Parameter	Indicative Values of Ice Parameter					
	Sakhalin East Coast (51° N to 55° N)		Aniva Bay (Northern Part)		Tartar Strait (51° N to 52° N)	
	Typical	Extreme	Typical	Extreme	Typical	Extreme
Start of ice season (date), ice concentration > 1/10	10 December	25 November	15 January	15 December	6 November	21 October
End of ice season (date), ice concentration < 1/10	1 June	15 June	1 April	20 April	12 May	6 June
Level ice thickness (m)	0.3 to 1.35	1.5	0.1 to 0.4	0.85	0.2 to 0.8	0.8
Rafted ice thickness (m)	1 to 2	3	0.2 to 0.8	1.25	0.5 to 0.8	1.0
Sail height (m)	1 to 2	5 to 6	0.5 to 1.0	3	0.5 to 1.0	2 to 3
Keel depth (m)	10 to 15	25	2.0 to 4.0	12	2 to 6	10
Ice movement (m/s)	0.5 to 1	1.5 to 2	0.1 to 0.2	0.7	0.3 to 0.5	1

Figure E.2 a) to g) shows the probability lines of any ice in the Sea of Okhotsk in an average year^[199]. At the start of the ice season mid-November, the first ice forms in the northerly and northwesterly reaches of the Sea of Okhotsk. Simultaneously, thin ice also forms locally in the shallow water parts along the Sakhalin northeast coast and in Sakhalinskiy Bay as air temperatures fall and the sea surface begins to cool.

During December, the ice formed in the northerly reaches of Sea of Okhotsk quickly spreads southward under the influence of winds and currents, typically reaching locally formed ice cover off the northeast Sakhalin shelf in the early January period. In fact, most of the heavier ice that is found off the northeast coast of Sakhalin Island originates in the northwesterly part of the Sea of Okhotsk, which is often referred to as the “ice kitchen.” By mid-January, the regional sea-ice has usually progressed towards the southern end of Sakhalin Island and the northern coast of Hokkaido, where ablation counterbalances its southward advance. Over the course of the winter, the ice cover continues to grow in general thickness and offshore extent, progressively becoming more heavily deformed with time, due to substantial relative motions within the pack. The winter pack-ice cover off Sakhalin Island typically reaches its maximum extent and severity sometime in March. Gradual loosening and deterioration of the ice begins to occur thereafter, as air temperature rises and spring approaches. Break-up usually commences in early to mid-May, with complete ice clearance normally seen by early June.

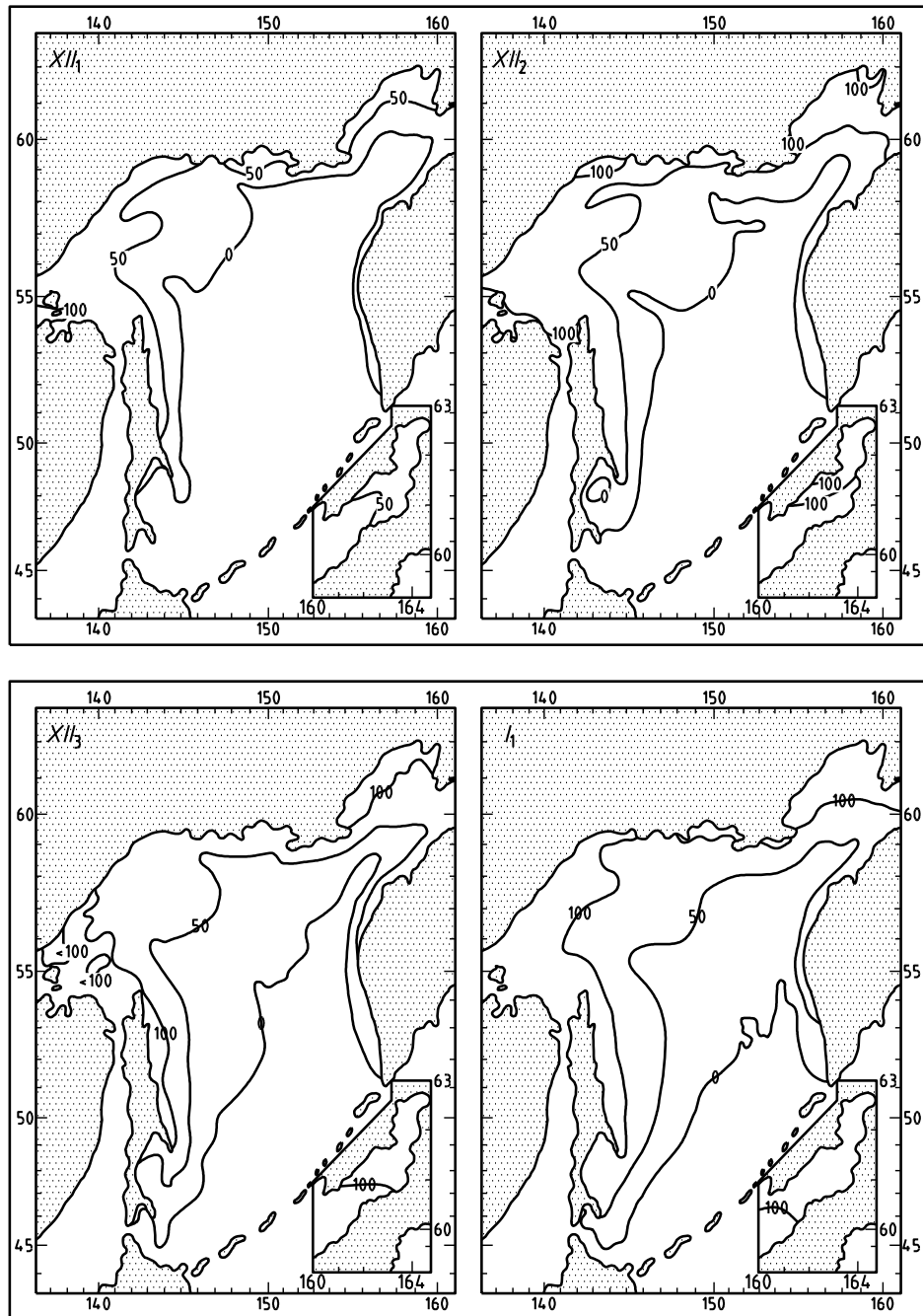
An important feature of the ice conditions that are found on the northeast Sakhalin shelf is the periodic presence of a band of open water or very thin ice, running parallel to the coast between the narrow landfast ice zone and the heavier pack-ice areas toward the east. This feature, termed a “flaw lead” or “polynya,” is transient but can persist for periods of a few days to several weeks during winter. Flaw lead conditions occur in particular during the period early January to early March, when predominant winds and ice motions are from the northerly quadrants. From mid-March onward, flaw lead conditions occur less frequently, because wind and ice drift directions become more mixed, and are often from south to north or from east to west.

Figure E.3 a) to g) shows the probability lines of any ice in the Tartar Strait in an average year^[200]. In contrast to the ice found in the Sea of Okhotsk, the ice in the Tartar Strait is much less deformed, due to slower current speeds and also the milder wave climate. Ice formation in the Tartar Strait starts end of November. During January and February, the ice extent and ice thickness steadily grow. In March, the area north of 49° N. is mostly covered with sea ice. Depending on prevailing wind direction, the heaviest ice is found along the Sakhalin west coast or against the Siberian mainland. Depending on the wind direction, leads are often formed along one of these coastlines, which can be used by vessels moving through the ice northward or southward. During early April melting starts, and in early May most of the Tartar Strait is free of ice, whereas there is usually still some ice around along the Sakhalin east coast around that time.



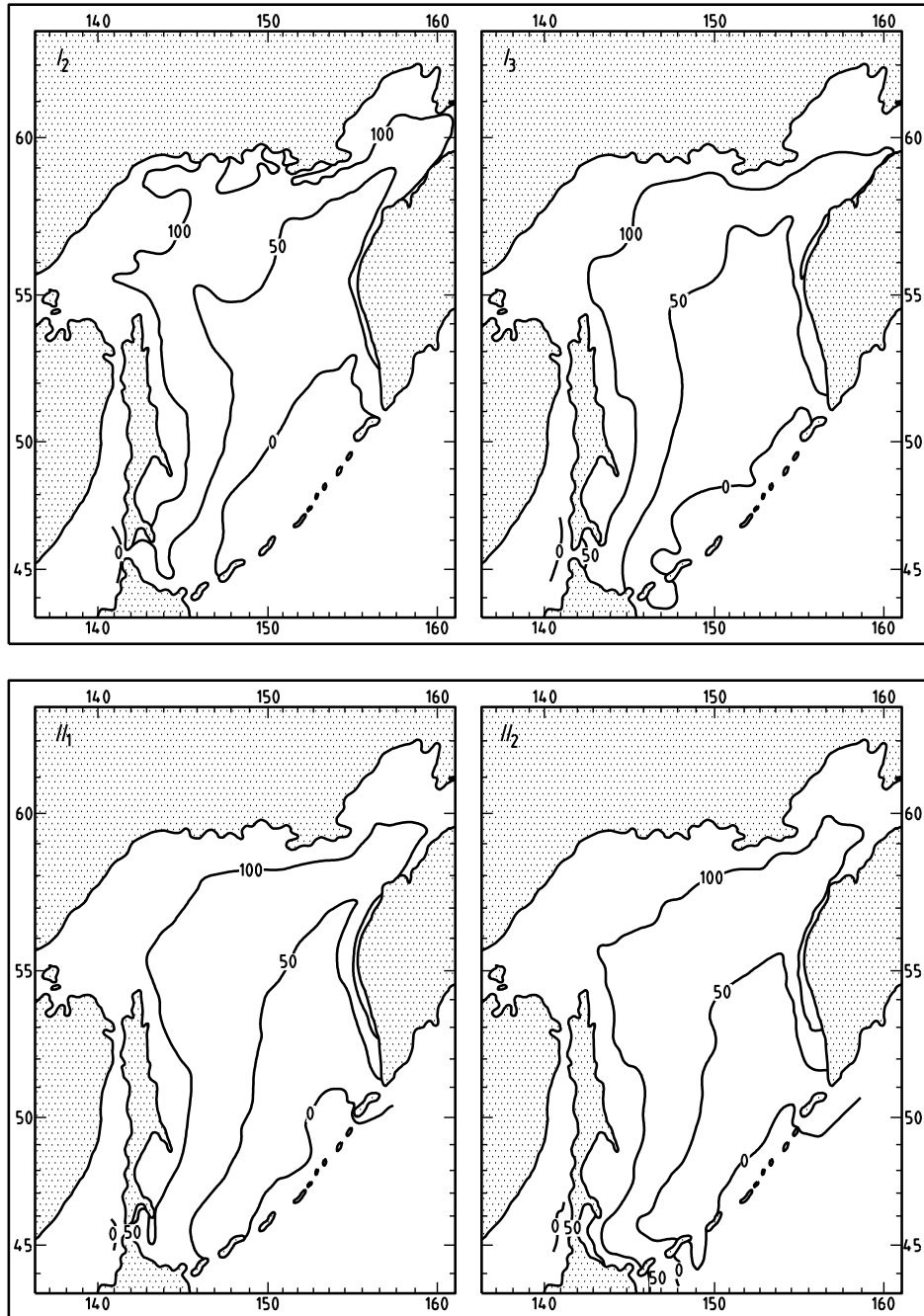
a) Probability lines of any ice in the Sea of Okhotsk—October (3rd period) to November (3rd period)

Figure E.2—Probability of Any Ice in an Average Year^[199] per Given 10-day Period



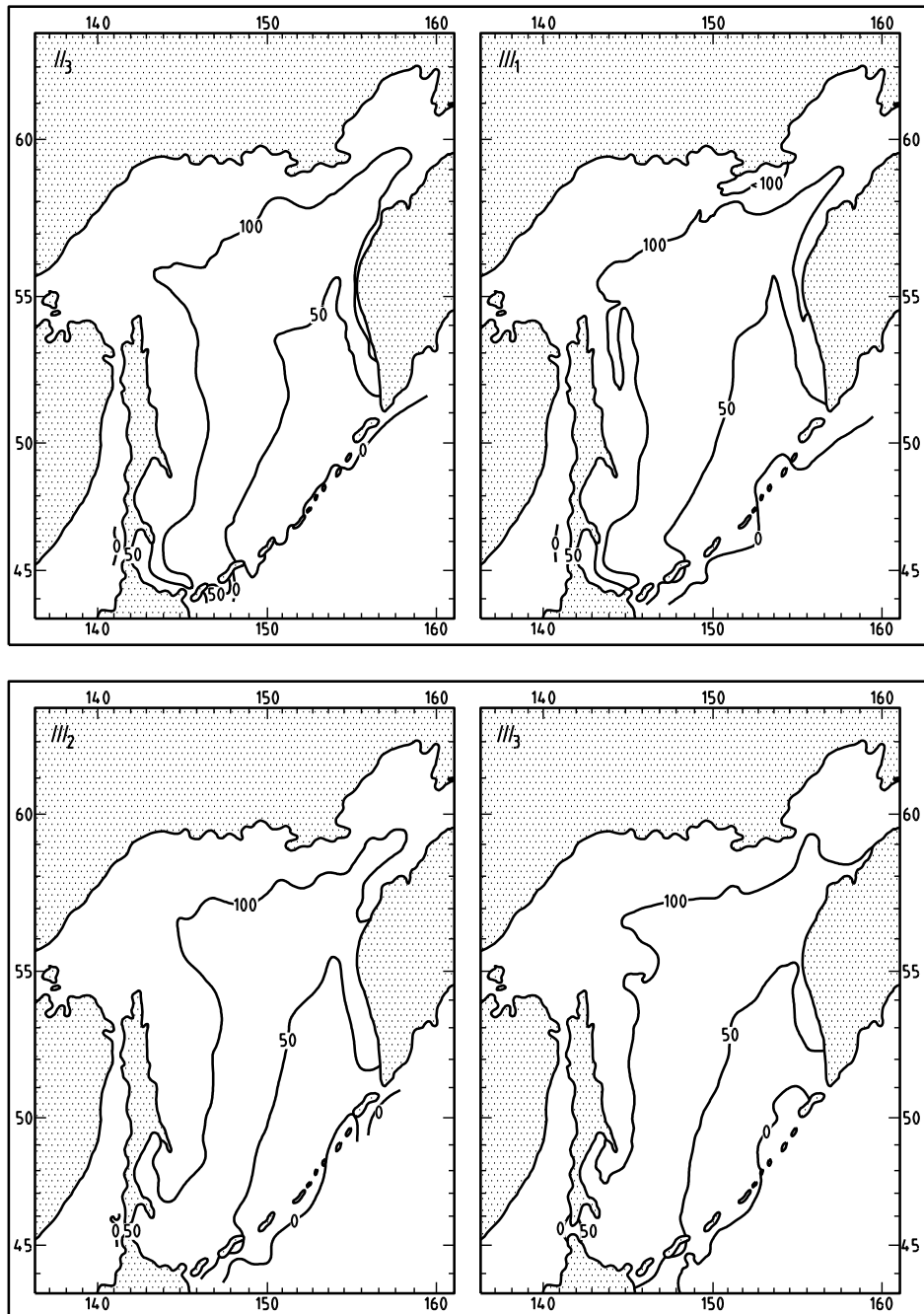
b) Probability lines of any ice in the Sea of Okhotsk—December (1st period) to January (1st period)

Figure E.2—Probability of Any Ice in an Average Year^[199] per Given 10-day Period (continued)



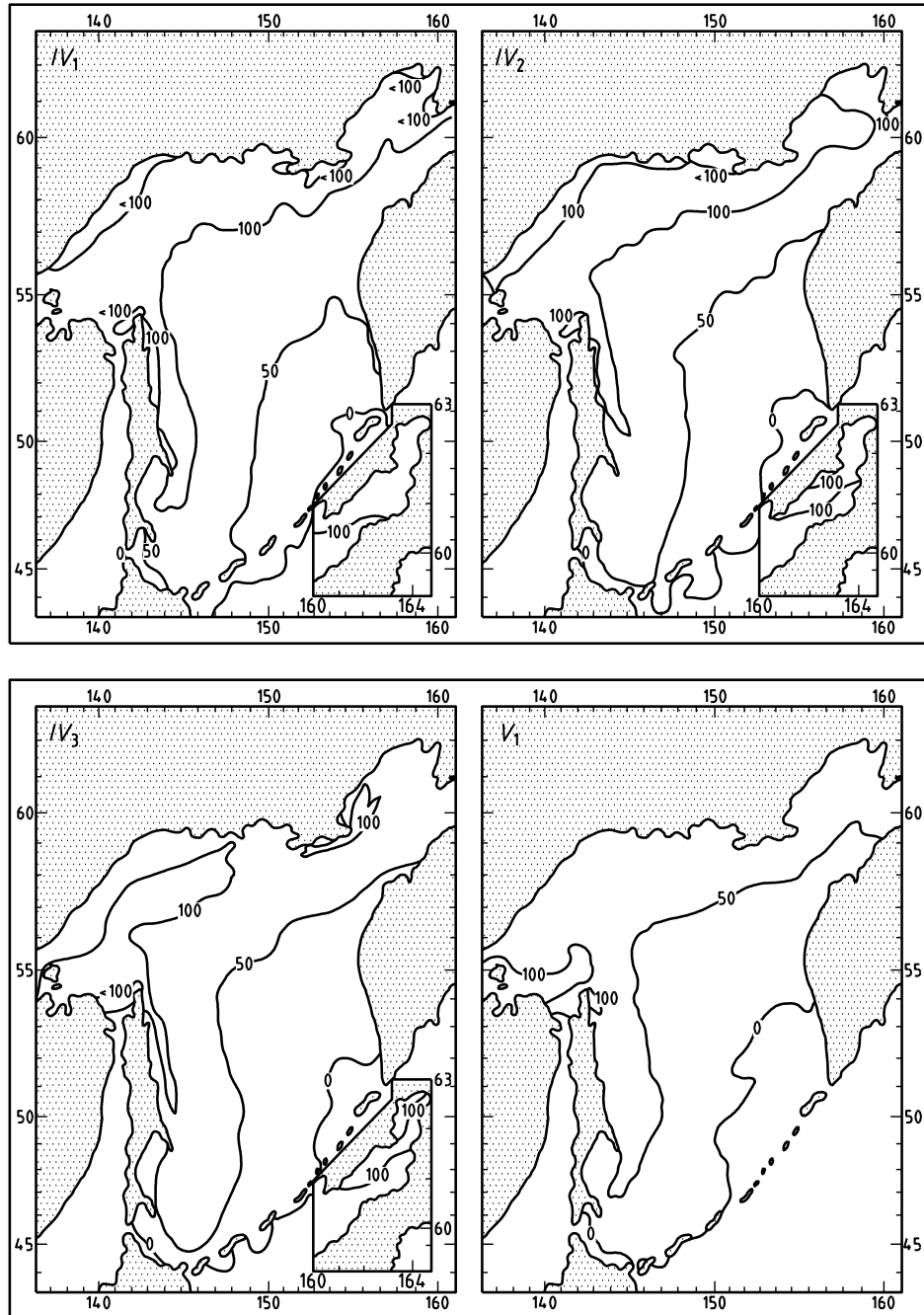
c) Probability lines of any ice in the Sea of Okhotsk—January (2nd period) to February (2nd period)

Figure E.2—Probability of Any Ice in an Average Year^[199] per Given 10-day Period (continued)



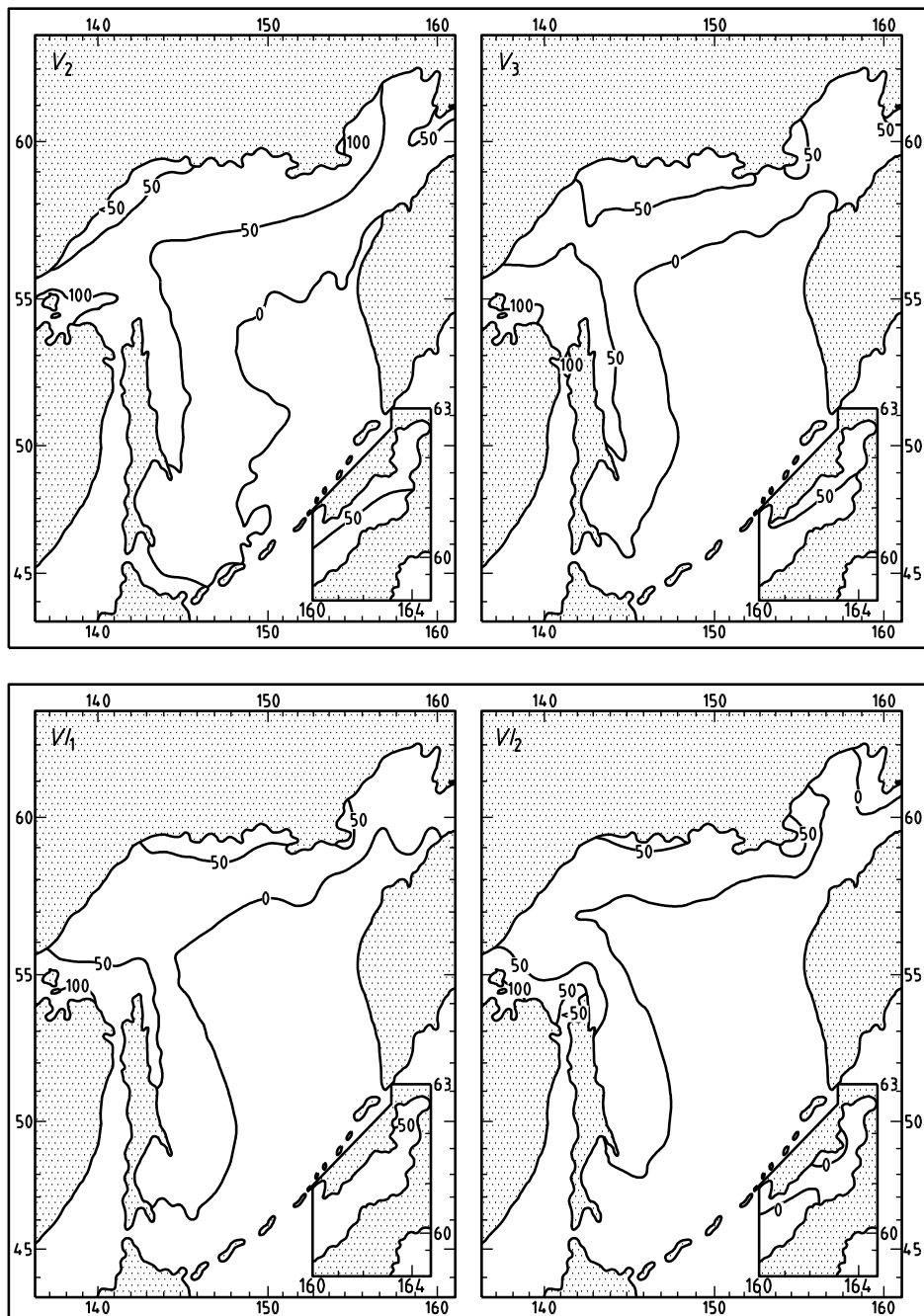
d) Probability lines of any ice in the Sea of Okhotsk—February (3rd period) to March (3rd period)

Figure E.2—Probability of Any Ice in an Average Year^[199] per Given 10-day Period (continued)



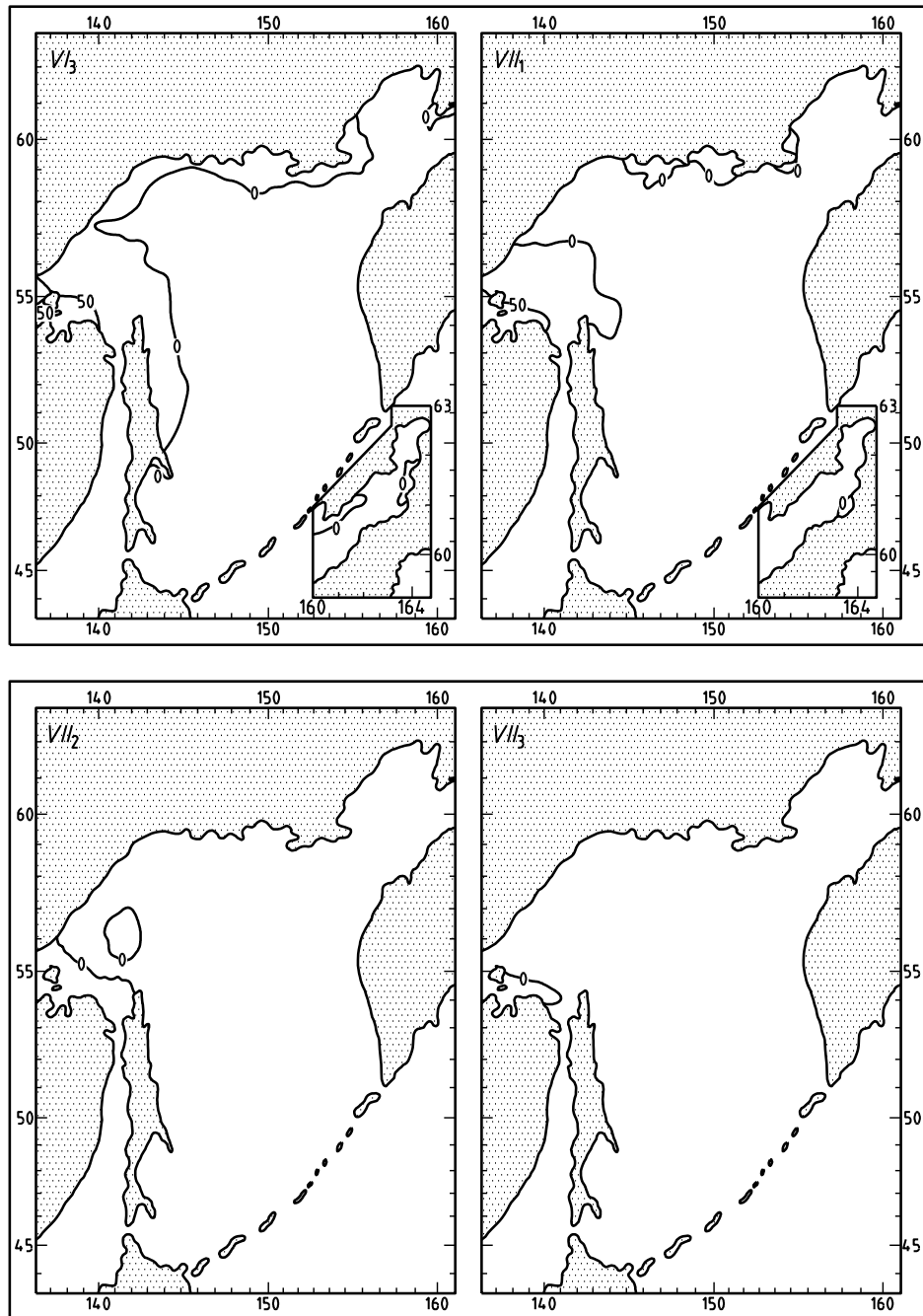
e) Probability lines of any ice in the Sea of Okhotsk—April (1st period) to May (1st period)

Figure E.2—Probability of Any Ice in an Average Year^[199] per Given 10-day Period (continued)



f) Probability lines of any ice in the Sea of Okhotsk—May (2nd period) to June (2nd period)

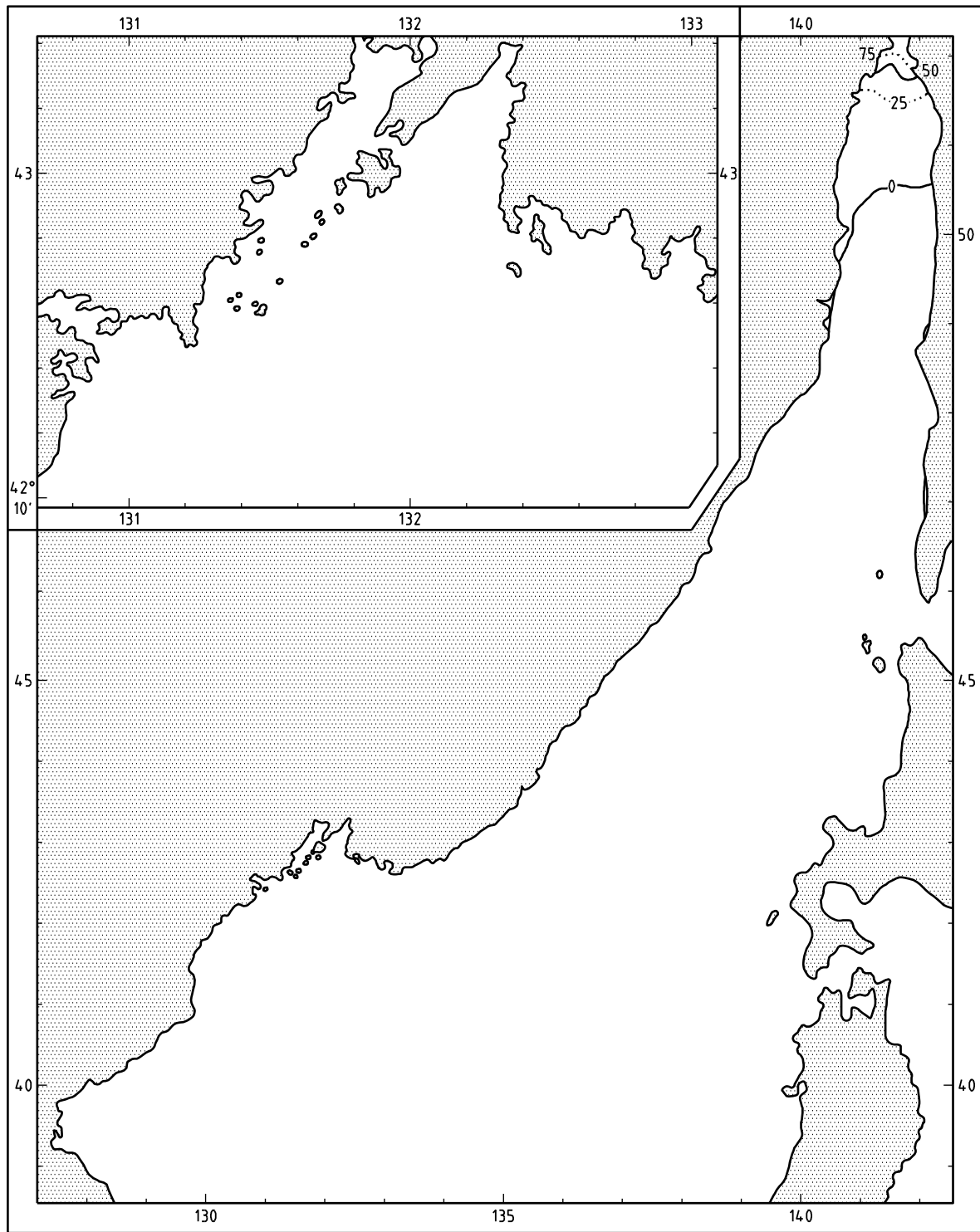
Figure E.2—Probability of Any Ice in an Average Year ^[199] per Given 10-day Period (continued)



g) Probability lines of any ice in the Sea of Okhotsk—June (3rd period) to July (3rd period)

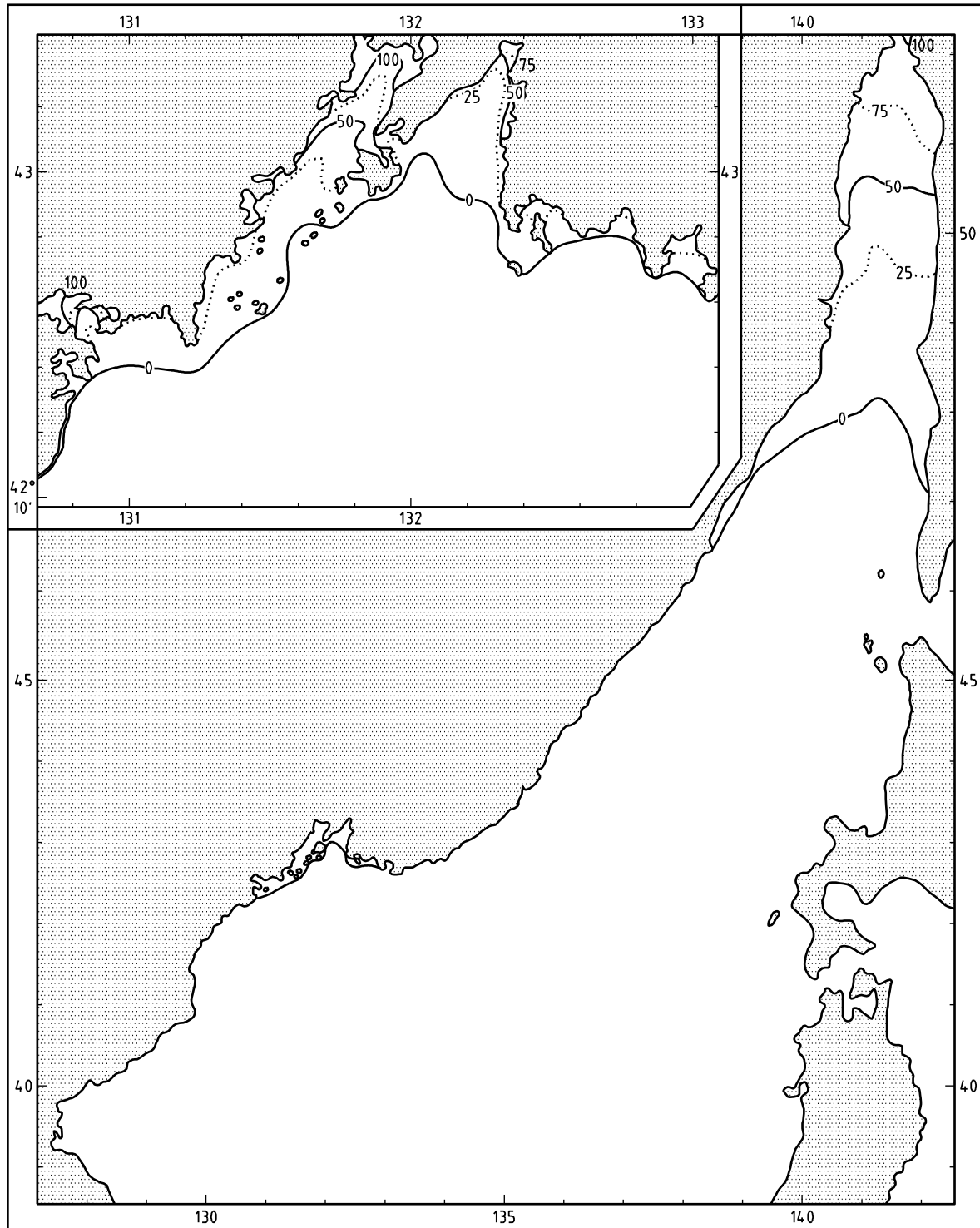
NOTE Index in the upper left corner indicates month (roman numeral) and 10-day period in the month.

Figure E.2—Probability of Any Ice in an Average Year^[199] per Given 10-day Period (continued)



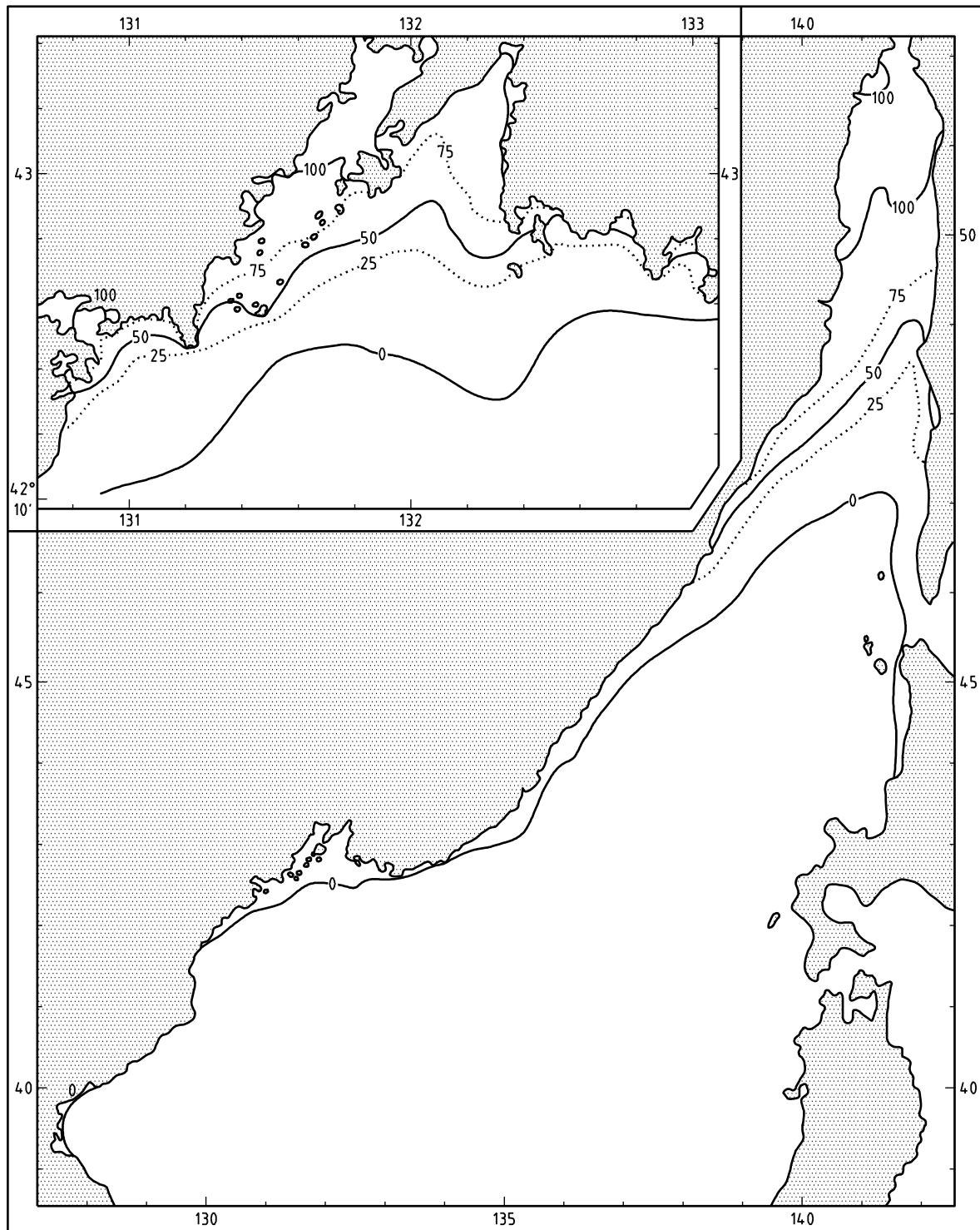
a) Probability of any ice in the Tartar Strait—Mid-November

Figure E.3—Probability of Any Ice in the Tartar Strait in an Average Year^[200]



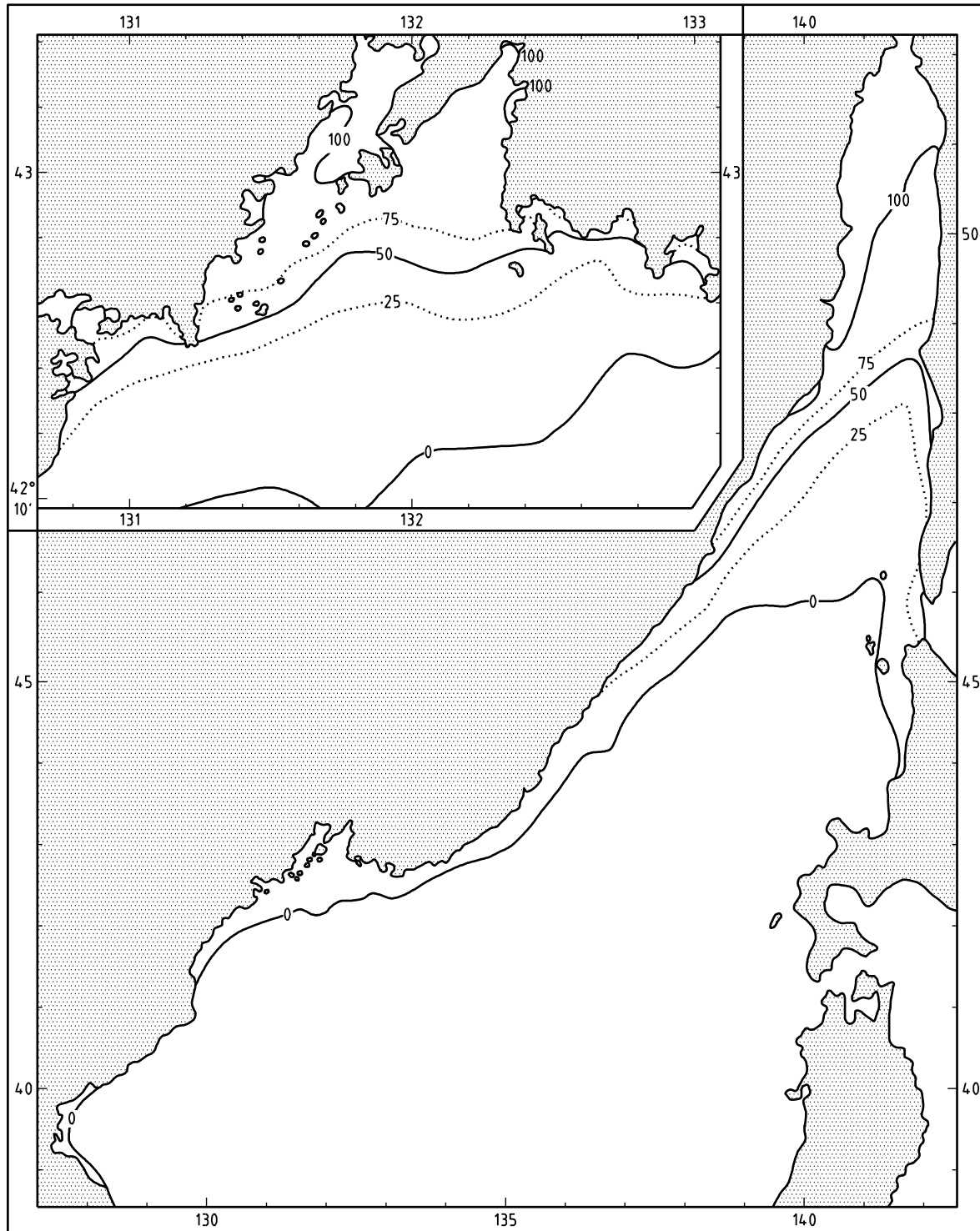
b) Probability of any ice in the Tartar Strait—Mid-December

Figure E.3—Probability of Any Ice in the Tartar Strait in an Average Year ^[200] (continued)



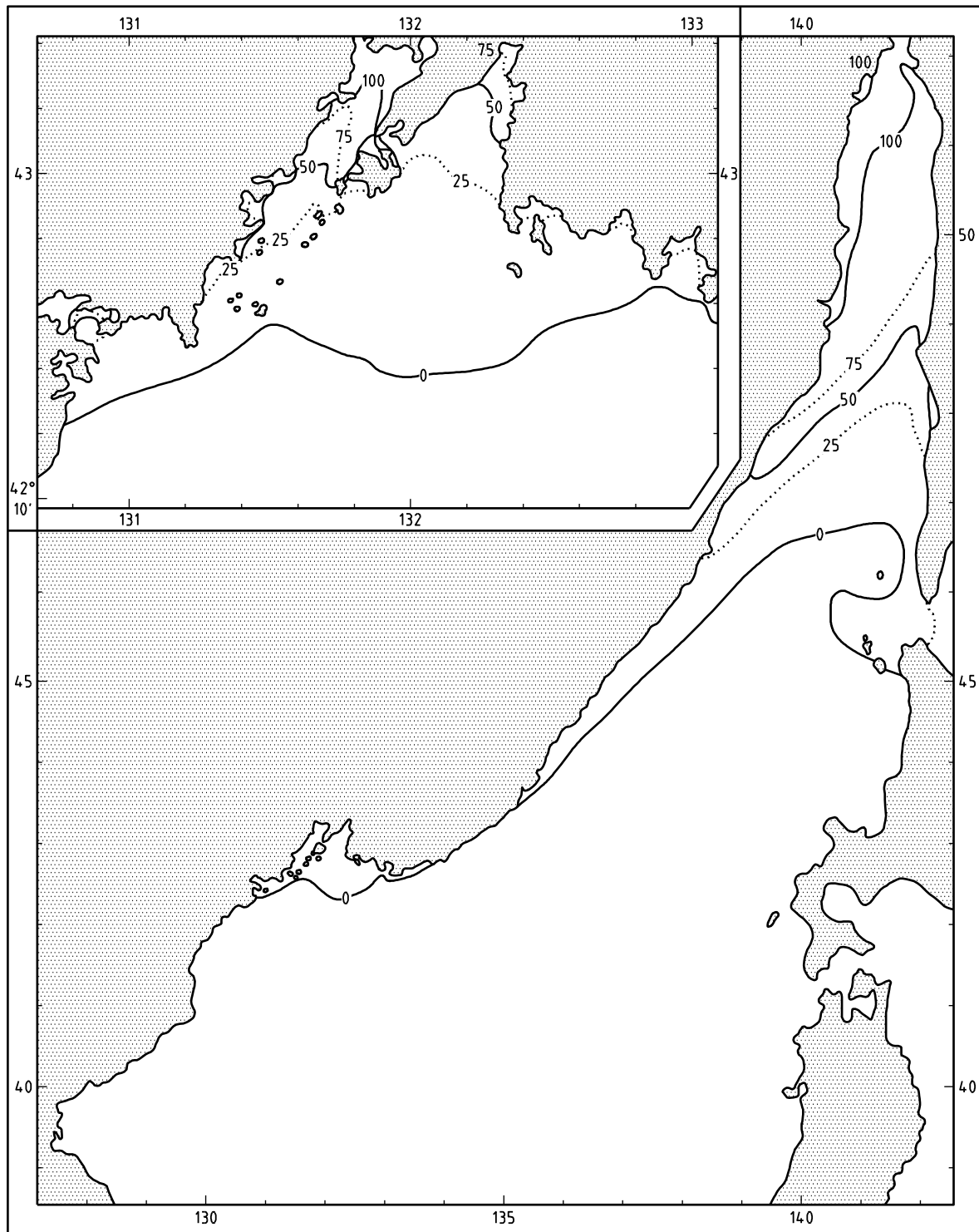
c) Probability of any ice in the Tartar Strait—Mid-January

Figure E.3—Probability of Any Ice in the Tartar Strait in an Average Year [200] (continued)



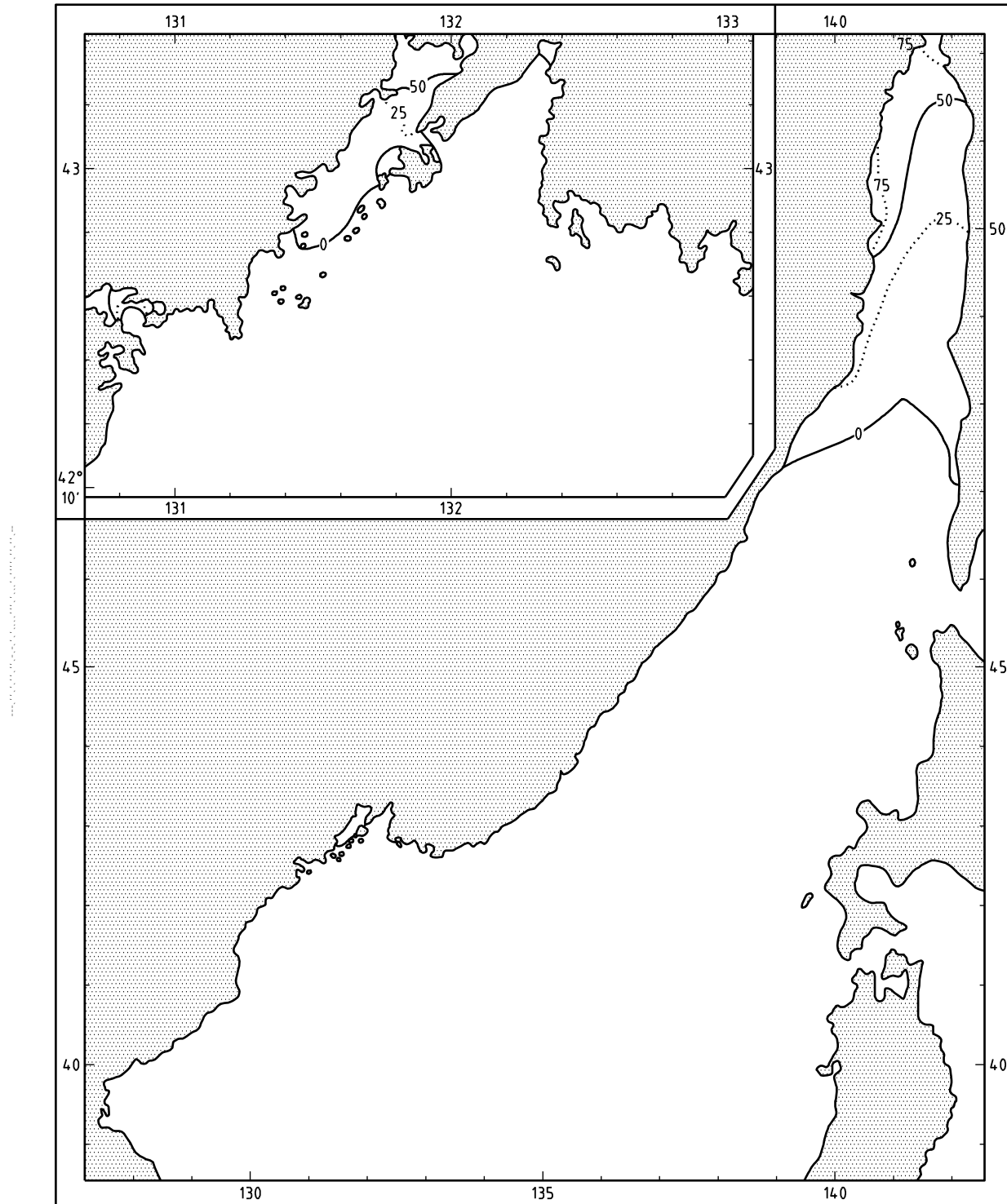
d) Probability of any ice in the Tartar Strait—Mid-February

Figure E.3—Probability of Any Ice in the Tartar Strait in an Average Year^[200] (continued)



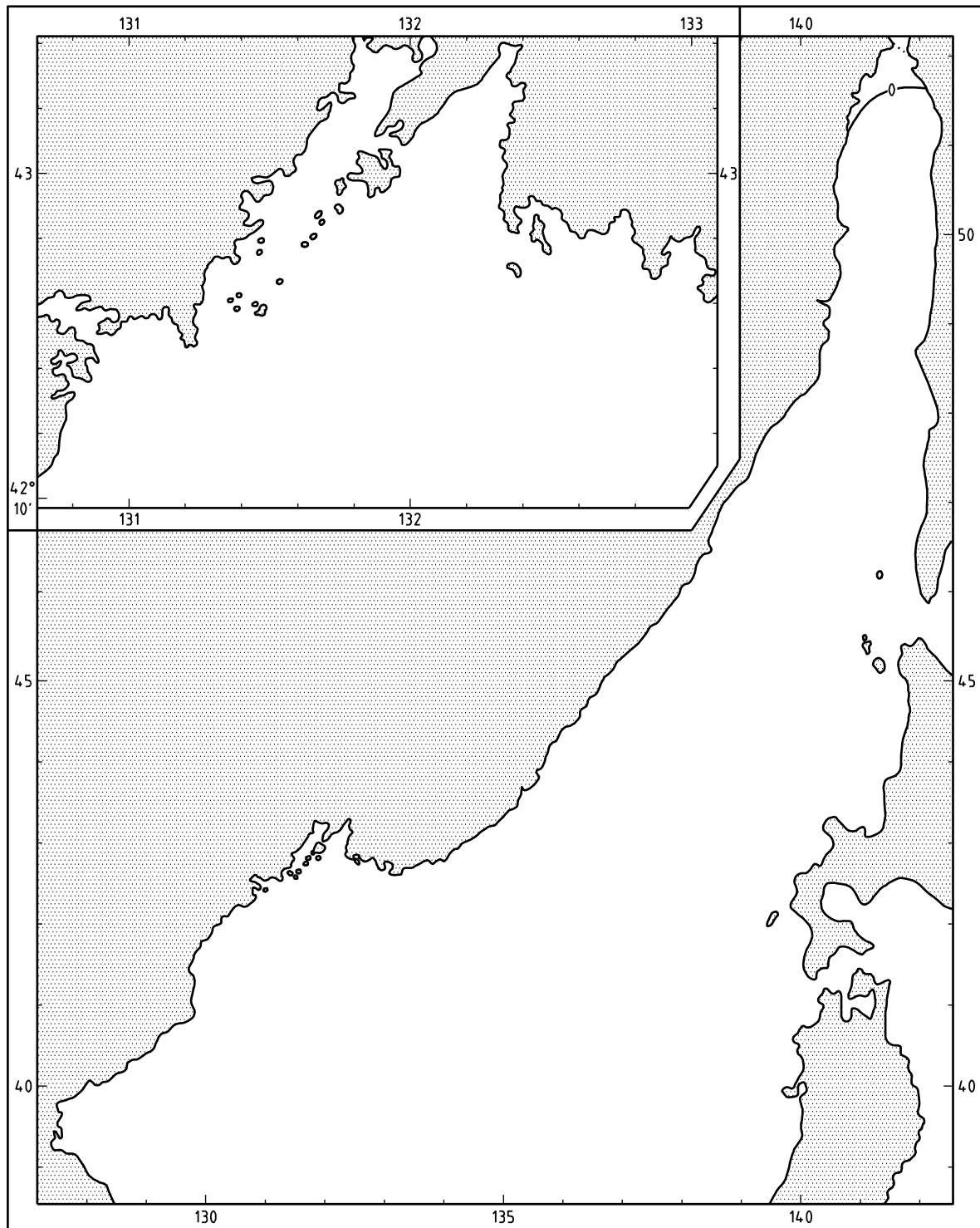
e) Probability of any ice in the Tartar Strait—Mid-March

Figure E.3—Probability of Any Ice in the Tartar Strait in an Average Year [200] (*continued*)



f) Probability of any ice in the Tartar Strait—Mid-April

Figure E.3—Probability of Any Ice in the Tartar Strait in an Average Year [200] (*continued*)



g) Probability of any ice in the Tartar Strait—Mid-May

Figure E.3—Probability of Any Ice in the Tartar Strait in an Average Year [200] (*continued*)

E.9 Other Environmental Factors

E.9.1 Air Temperature, Precipitation, Humidity, and Visibility

In winter, typical air temperatures range from -25°C in the northwestern parts of the Sea of Okhotsk to -10°C just south of Sakhalin Island. Absolute minima are considerably less than this and can reach as low as -40°C in the north and -30°C in the south. In summer, typical air temperatures range from 10°C in the north to almost 20°C just south of Sakhalin Island. Absolute maxima range between 30°C and 35°C .

Low visibility and fog occur when the cooler sea meets relatively warm air. Fog occurs in particular along the Sakhalin east coast during summer, when the relatively warm and moist air is cooled by the cold seawater. Along the Sakhalin west coast, fog occurs less frequently due to the northward flow of relatively warm water.

Precipitation (which can be rain, sleet, or snow) varies greatly across the island, largely due to its topography. The Pacific slopes of Sakhalin Island are particularly wet. Precipitation on the island is highest during the April to October warm season, with smaller amounts falling during the November to March cold season. Except for the northernmost tip of the island, the maximum precipitation falls in September for most locations. The mean annual precipitation ranges from < 600 mm/year in the northern parts of Sakhalin Island to > 1100 mm/year locally in the south.

E.9.2 Sea Temperature and Salinity

In general, the sea surface temperature increases from north to south. Significant annual variations in sea temperature occur throughout the area, which attenuate with depth. Between May and November sea temperatures are positive, with the warmest water found near La Perouse Strait and near Hokkaido Island. During October and November, sea temperatures drop significantly to -1°C to -1.8°C , resulting in a large part of the Sea of Okhotsk and the Tartar Strait becoming covered with ice.

The salinities in the Sea of Okhotsk and Tartar Strait are largely determined by a balance between precipitation and evaporation, the effect of sea-ice formation and the discharge of fresh water, in particular by the Amur River. During summer and autumn, the salinity is generally less than during winter, when it increases due to sea-ice formation and a significant reduction of the continental freshwater discharge. During summer, there is a marked salinity minimum around the northern tip of Sakhalin Island, associated with the freshwater discharge of the Amur.

E.9.3 Snow, Atmospheric Icing, and Sea-spray Icing

On Sakhalin Island, snow cover generally persists for up to 200 days per year. Snow is expected in September in the north and by October along the entire coast. The snow season extends until May in the south and June in the north. About 70 to 90 days of snow occur yearly along Sakhalin Island shores. Blizzards occur frequently in winter, especially along coasts exposed to the north and west winds. Along the coasts, the snow melts in April or May, melting a few weeks later in the interior. Mean winter snowfall totals between 100 mm and 150 mm. In the northern half of the island in the mountains, the mean maximum depth of snowfall may reach 100 cm, but at most places it is usually not higher than 40 cm to 60 cm.

Ice accumulation on the hulls of floating vessels and on superstructures has the potential to become a serious hazard in the Sakhalin area. Atmospheric icing can occur when saturated air moves against a surface with temperatures below freezing (rime ice), during periods of fog that are accompanied by freezing conditions, and during freezing rain or drizzle (glaze ice). Sea-spray icing can occur if the air temperature is near the freezing point of seawater. Immediately near the sea surface, the main role is played by sea-spray icing. Its intensity decreases with height. From heights exceeding 40 m, atmospheric icing is predominant. Sea-spray icing can be considered negligible at elevations above 50 m to 60 m. In the Sakhalin area, sea-spray icing mainly occurs from October to December when the seawater is not yet frozen. In Aniva Bay, it can occur throughout the entire winter period.

E.9.4 Waves in Ice

Waves in ice regularly occur during winter along the Sakhalin east coast, in particular when the pack ice/open sea boundary is in the vicinity of the monitoring site. Waves can easily penetrate into the outer pack ice with a thickness of 1.5 m to 2.5 m. Low-frequency waves have been observed in ice up to hundreds of kilometers from wave source regions^[200].

E.10 Estimates of Metocean Parameters

E.10.1 Extreme Metocean Parameters

Indicative extreme values of metocean parameters are provided in Tables E.2 to E.8 for four areas around Sakhalin. The wind, wave, and current values are independently derived marginal parameters; no account has been taken of conditional probability. As for all indicative values provided within the regional annexes of this standard, these data are provided to assist preliminary engineering concept selection; they are not suitable for design of offshore structures.

**Table E.2—Indicative Values of Metocean Parameters—Sakhalin East Coast
(52.5° N to 55° N and Water Depths from 30 m to 100 m)**

Metocean Parameter	Return Period (years)				
	1	5	10	50	100
10 min mean wind speed (m/s)	26	28	29	31	32
Significant wave height (m)	8	9	9.5	10.7	11.5
Spectral peak period (s) ^a	12.9	13.7	14.1	14.9	15.5
Surface current speed (m/s) ^b	2.3	2.6	2.7	2.9	3.0

^a Assume the peak spectral period can vary by ± 10 % around these central estimates.
^b Assume the extreme current can vary by ± 30 % around these central estimates.

**Table E.3—Indicative Values of Metocean Parameters—Sakhalin East Coast
(51° N to 52.5° N and Water Depths from 30 m to 100 m)**

Metocean Parameter	Return Period (years)				
	1	5	10	50	100
10 min mean wind speed (m/s)	27	29	30	32	34
Significant wave height (m)	8.5	9.5	10	10.7	11.5
Spectral peak period (s) ^a	13.3	14.1	14.4	14.9	15.5
Surface current speed (m/s) ^b	1.5	1.7	1.8	1.9	2.0

^a Assume the peak spectral period can vary by ± 10 % around these central estimates.
^b Assume the extreme current can vary by ± 30 % around these central estimates.

Table E.4—Indicative Values of Metocean Parameters—Aniva Bay (Central, Northern Half)

Metocean Parameter	Return Period (years)				
	1	5	10	50	100
10 min mean wind speed (m/s)	25	27	28	30	31
Significant wave height (m)	4.8	5.5	6	6.7	7.0
Spectral peak period (s) ^a	10	10.7	11.2	11.8	12.1
Surface current speed (m/s)	0.5	0.6	0.65	0.67	0.7

^a Assume the peak spectral period can vary by ± 10 % around these central estimates.

Table E.5—Indicative Values of Metocean Parameters—Tartar Strait (51° N to 52° N and Water Depth of About 30 m)

Metocean Parameter	Return Period (years)				
	1	5	10	50	100
10 min mean wind speed (m/s)	27	30	33	35	36
Significant wave height (m)	5.5	6	6.5	7	7.5
Spectral peak period (s) ^a	10.7	11.2	11.6	12.1	12.5
Surface current speed (m/s)	0.3	0.4	0.6	0.7	0.8

^a Assume the peak spectral period can vary by ± 10 % around these central estimates.

Table E.6—Monthly Air Temperature in Korsakov (46° 37' N, 142° 47' E) from 1966 to 2000

	Monthly Air Temperature (° C)												
	Jan	Feb	Mar	Apr	May	Jun	Jul	Aug	Sep	Oct	Nov	Dec	Year
Mean	-10.5	-9.9	-4.8	1.5	6.1	10.4	14.8	16.7	13.7	7.7	-0.1	-6.3	3.3
Highest	3.0	4.6	8.8	16.5	23.7	27.7	28.6	30.4	27.3	21.8	15.5	7.9	30.4
Lowest	-32.7	-29.1	-25.2	-17.5	-9.0	-2.2	1.7	4.6	-2.2	-8.0	-19.1	-26.2	-32.7

Table E.7—Monthly Air Temperature in Odoptu (53° 22' N, 143° 10' E) from 1975 to 2000

	Monthly Air Temperature (° C)												
	Jan	Feb	Mar	Apr	May	Jun	Jul	Aug	Sep	Oct	Nov	Dec	Year
Mean	-18.5	-16.8	-12.0	-3.7	1.1	6.0	10.5	13.0	9.9	3.1	-7.3	-14.4	-2.4
Highest	-0.1	-0.8	8.0	11.8	25.6	31.3	32.1	32.4	25.0	17.8	9.0	1.0	32.4
Lowest	-38.6	-35.0	-33.2	-26.1	-11.0	-2.8	0.6	3.5	-0.4	-15.4	-25.2	-33.6	-38.6

Table E.8—Sea Temperature Ranges—Indicative Monthly-mean Values

Area	Sea Surface Temperature (° C)	Sea Floor Temperature (° C)
Sakhalin east coast (49° N to 54° N)	-1.8 to +11	-1.8 to +2
Aniva Bay	-1.8 to +18	-1.8 to +14
Tartar Strait	-1.8 to +16	-1.8 to +xx

E.10.2 Long-term Distributions of Metocean Parameters

Long-term joint frequency distributions of the significant wave height H_s vs. the spectral peak period are given in Tables E.9 to E.11 for three locations around Sakhalin Island based on the 25-year continuous hindcast data produced by Oceanweather Inc.^[193] The presence of sea ice is indicated by $H_s < 0.01$.

**Table E.9—Percentage Occurrence of Total Significant Wave Height vs. Spectral Peak Period
Offshore Sakhalin NE Coast (52.50° N, 143.66° E)**

Significant Wave Height (m)	Spectral Peak Period (s)										TOTAL
	0 to 1.99	2 to 3.99	4 to 5.99	6 to 7.99	8 to 9.99	10 to 11.99	12 to 13.99	14 to 15.99	16 to 17.99	> 18	
< 0.01											33.38
0.01 to 0.99	0.51	3.74	13.74	9.36	3.19	0.49	0.08	0.00	0.00	0.00	31.11
1.00 to 1.99	—	0.13	9.01	7.96	5.59	1.67	0.40	0.05	0.00	0.00	24.80
2.00 to 2.99	—	—	1.07	3.04	1.97	1.04	0.27	0.06	—	—	7.44
3.00 to 3.99	—	—	0.00	0.50	0.94	0.59	0.15	0.02	—	—	2.20
4.00 to 4.99	—	—	—	0.03	0.27	0.31	0.09	—	—	—	0.71
5.00 to 5.99	—	—	—	0.00	0.03	0.15	0.07	0.00	—	—	0.25
6.00 to 6.99	—	—	—	—	0.00	0.04	0.04	0.00	—	—	0.08
7.00 to 7.99	—	—	—	—	—	0.00	0.01	—	—	—	0.01
8.00 to 8.99	—	—	—	—	—	—	0.01	—	—	—	0.01
TOTAL	0.51	3.86	23.82	20.89	11.98	4.30	1.10	0.14	0.00	0.00	100.0

**Table E.10—Percentage Occurrence of Total Significant Wave Height vs. Spectral Peak Period in
Aniva Bay (46.45° N, 142.75° E)**

Significant Wave Height (m)	Spectral Peak Period (s)										TOTAL
	0 to 1.99	2 to 3.99	4 to 5.99	6 to 7.99	8 to 9.99	10 to 11.99	12 to 13.99	14 to 15.99	16 to 17.99	> 18	
< 0.01											6.34
0.01 to 0.99	3.55	40.09	20.13	3.03	0.98	0.46	0.34	0.11	0.00	0.00	68.70
1.00 to 1.99	—	0.30	19.24	1.68	0.12	0.01	0.01	0.01	—	—	21.36
2.00 to 2.99	—	—	1.24	1.83	0.10	0.00	0.00	—	—	—	3.18
3.00 to 3.99	—	—	0.00	0.26	0.10	0.00	0.00	—	—	—	0.37
4.00 to 4.99	—	—	—	0.00	0.03	0.00	—	—	—	—	0.04
5.00 to 5.99	—	—	—	—	0.01	0.00	—	—	—	—	0.01
6.00 to 6.99	—	—	—	—	0.00	—	—	—	—	—	0.00
TOTAL	3.55	40.39	40.61	6.80	1.35	0.48	0.35	0.12	0.00	0.00	100.0

**Table E.11—Percentage Occurrence of Total Significant Wave Height vs. Spectral Peak Period in
Northern Tartar Strait (51.48° N, 141.44° E)**

Significant Wave Height (m)	Spectral Peak Period (s)										TOTAL
	0 to 1.99	2 to 3.99	4 to 5.99	6 to 7.99	8 to 9.99	10 to 11.99	12 to 13.99	14 to 15.99	16 to 17.99	> 18	
< 0.01											21.81
0.01 to 0.99	3.64	25.96	18.59	3.14	0.50	0.05	—	—	—	—	51.89
1.00 to 1.99	—	0.19	17.82	2.48	0.17	0.02	—	—	—	—	20.68
2.00 to 2.99	—	—	1.69	2.86	0.13	0.00	—	—	—	—	4.68
3.00 to 3.99	—	—	0.00	0.43	0.38	0.00	—	—	—	—	0.80
4.00 to 4.99	—	—	—	0.01	0.10	0.00	—	—	—	—	0.12
5.00 to 5.99	—	—	—	—	0.00	0.01	—	—	—	—	0.01
6.00 to 6.99	—	—	—	—	—	0.00	—	—	—	—	0.00
TOTAL	3.64	26.15	38.10	8.92	1.28	0.09	0.00	0.00	0.00	0.00	100.0

Annex F (informative)

Caspian Sea

F.1 Description of the Region

This annex covers the Caspian Sea region. The Caspian Sea is situated east of the Black Sea, roughly within the coordinates 36° N to 47° N and 47° E to 54° E. It is a land-locked sea and extends approximately 1200 km from north to south, with an average width of 325 km east to west, covering a total area of some 400,000 km²^[208]. As of 2005, the MSL of the Caspian Sea was -27.0 m below Baltic Datum (equivalent to global mean sea level) and 1.0 m above Caspian Datum.

The Caspian Sea offers unique challenges to the oil and gas industry. The northern area is characterized by shallow water, is subject to winter icing and negative surges that can limit marine operations. The northern area also receives a large volume of freshwater discharge from rivers such as the Volga and Ural. The meteorology of the Caspian is complex, with the presence of nearby mountain ranges also causing significant area variations^[208].

The Caspian can be considered to have four parts: northern, central, Apsheron, and southern (Figure F.1). The north and central areas can be considered to be separated by a line from Chechen Island to Bautino, while the central and southern areas can be considered to be separated by the Apsheron Ridge, which stretches across the Caspian from Baku to Turkmenbashy. Most of the northern Caspian Sea is very shallow, with water depths of 10 m or less. In the northeast Caspian Sea, depths are around 4 m. The central Caspian Sea in the Derbent Depression has a depth of 788 m at its deepest point, whereas the southern Caspian has a maximum depth of 1025 m in the South Caspian Depression. The Apsheron Ridge, stretching from between the Apsheron Peninsula and the Cheleken Peninsula, separates the central and southern Caspian Seas, has water depths of less than 200 m.

The nations bordering the Caspian Sea region, and their corresponding lengths of coastline^[208], are:

- Azerbaijan: 850 km;
- Iran: 900 km;
- Kazakhstan: 2320 km;
- Russia: 695 km;
- Turkmenistan: 1200 km.

In the middle Caspian Sea, the continental shelf is limited to depths of about 100 m. The shelf is narrow (about 40 km) along the western coast, but much wider (about 130 km) along the eastern coast. The continental slope extends between the shelf edge with depths of 500 m to 600 m^[216].

In the southern Caspian Sea, the continental slope is very steep and extends to depths of 700 m to 800 m. The width of the continental shelf is broadly similar to that of the middle Caspian Sea, except on the southern coast where it is much narrower, with depths of 400 m only 5 km to 6 km from the coast^[208].

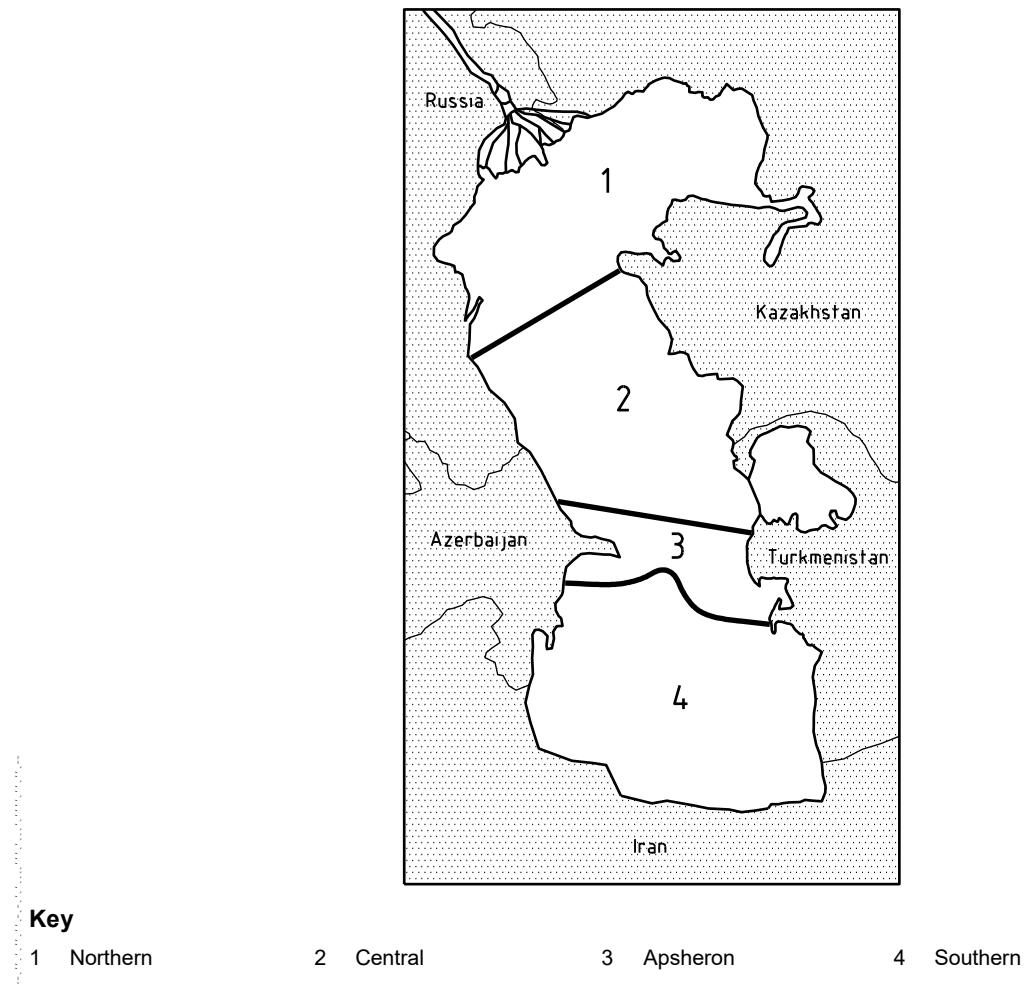


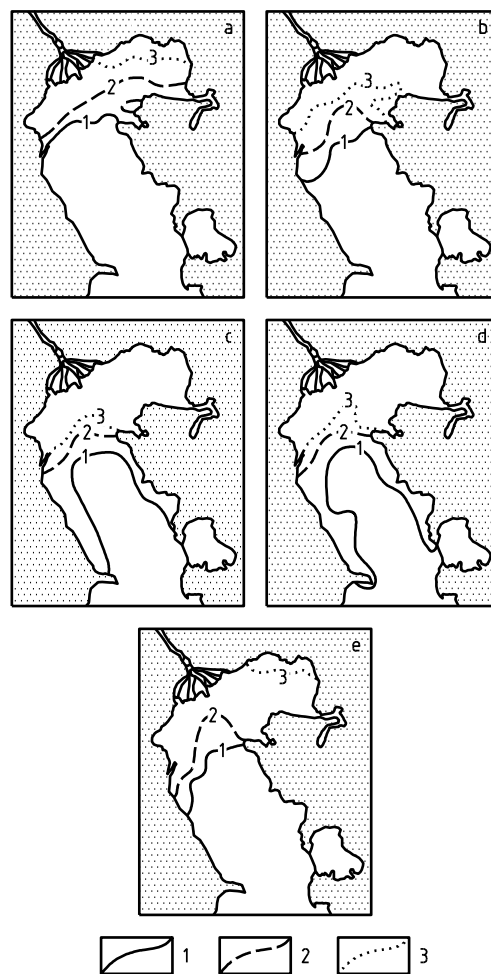
Figure F.1—Map of the Caspian Sea^[202], Showing Four Designated Regions: Northern, Central, Apsheron, and Southern Caspian

F.2 Data Sources

The Caspian Environment Programme website, <http://www.caspianenvironment.org/caspian.htm>, gives a general overview of the Caspian Sea region. The book *The Caspian Sea*^[208] describes the metocean conditions encountered in the Caspian Sea and specifically refers to the ice conditions that can be expected in the northern Caspian Sea during the winter months.

Publicly available measured and modelled data are limited for the offshore areas of the Caspian Sea; most measured data are confined to land and coastal stations. With the growth in offshore oil industry activity from the late 1990s onward, more extensive offshore metocean and ice data have now been collected. A number of national institutions have carried out hindcast modelling of the Caspian Sea. In 2002, a dedicated oil industry joint industry project (CASMOS: Caspian Sea Meteorological and Oceanographic Study^[210]) hindcast the wind, wave, water-level, and current conditions for the Caspian Sea. In 2006 to 2007, this work was updated to produce a 50-year continuous hindcast of metocean conditions on a grid of 10 km × 10 km at hourly intervals^[229].

Following the Second World War, the Astrakhan Hydrometeorological Observatory routinely collected ice data. However, in 1984/85 data collection ceased, and ice reports have not been available from this source since then^[7] (see Figure F.2). From 1992 onward, earth-observing satellites have collected data on ice coverage.

**Key**

- | | |
|-------------------|------------|
| a November | b December |
| c January | d February |
| e March | |
| 1 Severe winter | |
| 2 Moderate winter | |
| 3 Mild winter | |

Figure F.2—Positions of the Ice Edge in the Caspian Sea by Month and by Winter Severity [208]

F.3 Overview of Regional Climatology

The Caspian Sea is approximately 1200 km from north to south, spanning more than one climatic zone, so the meteorology differs significantly across the region. In general terms, weather conditions in the Caspian Sea can be categorised, in oil industry terms, as ranging from mild to rough.

The Caspian Sea is influenced by a continental climate regime, which results in large ranges of temperature and widely varying seasonal wind regimes. In the south, summers are hot and dry, while the winters are warm. In the north, summers are similar to the south but the winters by contrast are cold with relatively low snowfall. During the winter, weather is dominated by the Siberian anti-cyclone that creates east to southeasterly winds of cold, clear air over the northern Caspian Sea. During the summer, the weather is influenced by the Azores high-pressure zone, with the strongest and most persistent winds flowing from between west and north.

The region is subject to extra-tropical cyclones at the rate of about 10 strong events per year^[212]. These approach from the west, southwest, or south, although a significant number are also generated locally. Cyclones most often appear in January, March, and October. In the south, in the region of the Apsheron Peninsula, the number of days with wind speeds higher than 15 m/s is between 60 days and 80 days. In the northern Caspian Sea, the number is reduced to about half this value.

In the northern Caspian Sea, the strongest winds occur between November and April, with typical annual maxima of around 25 m/s, rising to near 30 m/s for a 25-year return period storm. The summer months are more benign, with wind speeds only rarely exceeding 15 m/s. The strongest winds in the northern Caspian tend to be from between southwest and west, although a more northwesterly component is apparent during the latter part of the year. The weather conditions can be locally quite variable due to topographic effects, notably due to the Caucasus mountains to the west and the localized topography to the north of Aktau. In the south, the topographic influence of the Apsheron Peninsula and Caucasus is notable, with frequent winter storms that can last from 3 h to 120 h, with typical durations of 15 h to 18 h. These local storms are difficult to forecast accurately.

In the northern Caspian Sea, daily mean air temperatures vary significantly seasonally and from year to year, specifically during the winter period, when temperatures can fall to below -25 °C in some years, but only to around -10 °C in others. In the summer, air temperatures rise to between 30 °C and 35 °C.

In the southern Caspian Sea winter temperatures are warmer, at 3 °C to 12 °C, with infrequent snow and frosts. There are, however, occasional short-lived cold spells with temperatures as low as -19 °C. Temperatures rapidly increase in the spring and summer, reaching up to 30 °C offshore but as high as 36 °C in coastal regions to the west and 42 °C in the east.

F.4 Overview of Regional Hydrology

More than 130 rivers flow into the Caspian Sea, with a catchment of about $3.5 \times 10^6 \text{ km}^2$. The Volga is the single largest river and accounts for nearly 80 % of the total river discharge into the Caspian Sea. Other significant rivers include the Kura (second largest), Ural, Terek, and Sulak. These, with the Volga, account for 90 % of the total annual discharge into the Caspian Sea.

The greater part of the Volga River inflow enters the Caspian Sea through the western arms of the Volga Delta and becomes entrained in the flow down the western coast of the central Caspian Sea. Flow in the Volga reaches a maximum in May/June due to melt water, and slows to a minimum in July/August.

In the winter, the seawater temperature at the ice edge of the northern Caspian varies from 0 °C to 0.5 °C; in the central Caspian temperature ranges from 10 °C to 11 °C; and in the southern Caspian it is around 10 °C. In the summer months, the central and northern Caspian seawater temperatures are 24 °C to 25 °C; in the southern Caspian they are around 25 °C to 26 °C. Temperatures near the east coast are 1 °C to 2 °C lower than those near the west coast.

With the climatic differences between the northern and southern Caspian, the non-summer distribution of water temperatures is several degrees Centigrade between the major basins in the upper water column^[208]. As summer approaches, temperatures become more uniform across the entire sea. Vertical thermal differences are small during most of the year; however, a strong thermocline develops in the upper 20 m to 40 m of the deeper portions of the central and southern Caspian in mid-summer, and persists into early autumn.

The salinity of the Caspian Sea is roughly one-third that of oceanic seas, being usually in the range 12.8 PSU to 12.9 PSU. Salinity may be as low as 2 PSU in regions subject to freshening by river inflow from the Volga and Ural Rivers, and may be as high as 14 PSU to 15 PSU in "evaporation patches" in high summer.

F.5 Water Depth, Tides, Long-term Water Levels, and Storm Surges

F.5.1 Water Depth

The Caspian Sea can be categorized into four distinct regions based on their physico-geographical characteristics:

- a) the southern Caspian Sea, which is 1025 m at its deepest point and is bounded to the north by the Apsheron Ridge;
- b) the Apsheron Ridge, which lies between Zhiloi Island and Cape Kuuli and has water depths ranging from a few meters to 200 m;
- c) the central Caspian, commonly termed the Derbent Depression, which is 788 m at its deepest point;
- d) the northern Caspian, which is typically less than 20 m deep, and is the shallow water region to the north of the Mangyshlak threshold.

In the southern Caspian Sea, the continental slope is very steep and extends to depths between 700 m and 800 m. The shelf is narrow (about 40 km) along the western coast, but much wider (about 130 km) along the eastern coast. The width of the shelf along the southern coast is much narrower; depths of 400 m occur only 5 km to 6 km from the coast.

Water depths in the Caspian Sea are generally referred to the Caspian Datum. This Datum is defined as 28 m below the Baltic Datum.

F.5.2 Long-term Water Levels

F.5.2.1 General

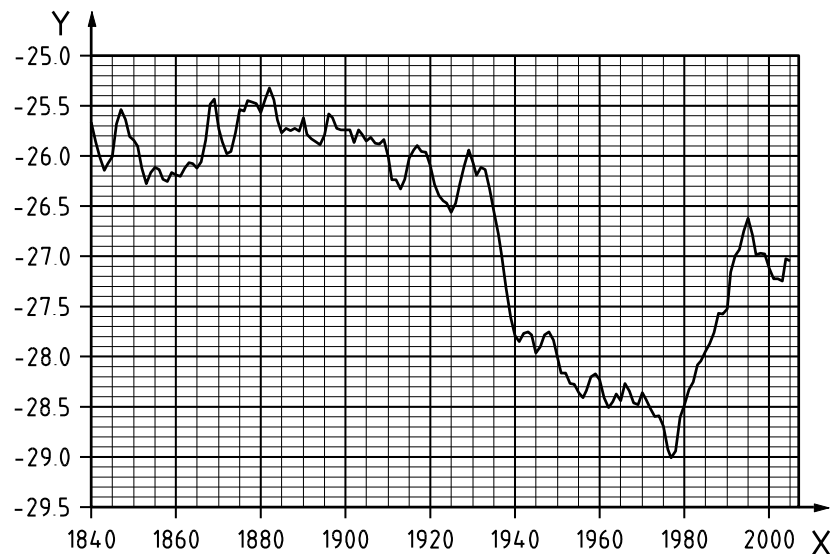
The water level in the Caspian Sea in 2005 was 27 m below the level of the world's oceans and 1 m above the Caspian Datum. However, the level is subject to considerable variation over various timescales. Long-term water level fluctuations of up to 10 m have been recorded for the Caspian Sea^[202]. Figure F.3 shows variations in MSL from 1840 to 2005. The main sources of these fluctuations are natural long-term changes in climate, the effects of global warming on the local climate, as well as anthropogenic effects such as changes in consumption of water from the Volga River and the effects of dikes on the Caspian surface area.

Recent work^[225] has illustrated a strong correlation between the North Atlantic Oscillation (NAO) and the Caspian Sea level, probably as a result of depression activity associated with a strong NAO. At the present time, approximately 79 % of the inflow into the Caspian Sea is from rivers, with the Volga and Ural accounting for 94 % of this value^[212]. About 20 % of the total inflow comes from rain, and the remaining 1 % comes from groundwater. Evaporation is the major source of outflow, accounting for some 97 %. The remaining 3 % of the outflow is through the Kara Bogaz Gol, which acts as an evaporation basin. In the late 1970s, the USSR constructed a dam across the Gol, separating it from the Caspian Sea, in an attempt to arrest the declining sea level in the Caspian. This dam was removed in June 1992, allowing water to once again flow from the Caspian to the Gol^[202].

In December 1998, when the sea level was 27.0 m below Baltic Datum, this implied^[202] a seabed area of 392,600 km², and a water volume of 78,648 km³.

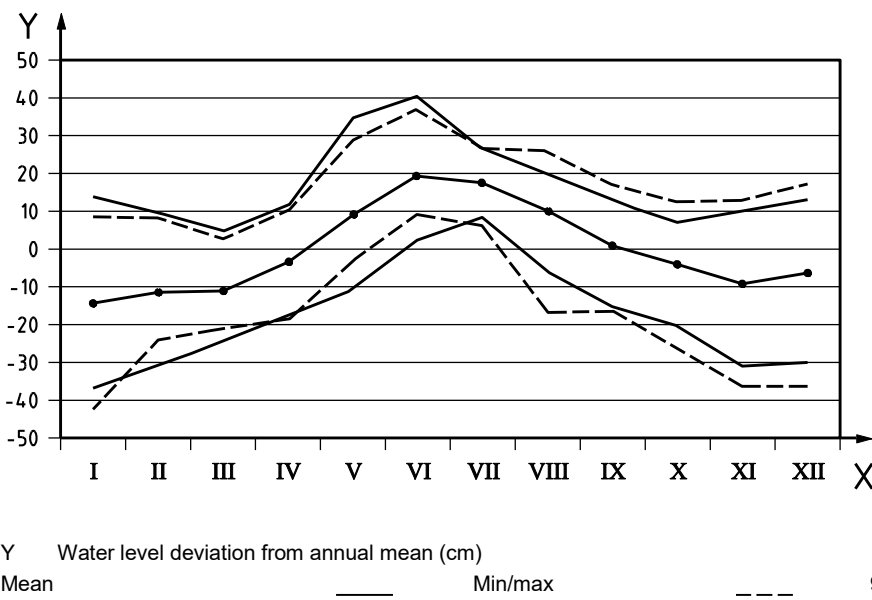
F.5.2.2 Seasonal Water Level

In addition to long-term trends, the level of the Caspian Sea is also subject to seasonal fluctuations. Levels are highest in July and lowest in December, with a mean annual level variation in the range 0.30 m to 0.40 m. This is shown in Figure F.4, which includes a 95 % confidence interval around the mean, based on the period 1978 to 1998. The seasonal peak has shifted from the month of July to June over the past century (see Figure 1.4 in Reference [208]).

**Key**

X Time

Y CSL (Meter Baltic datum)

Figure F.3—Long-term Variation in Caspian Sea MSL**Key**

X Month

Y Water level deviation from annual mean (cm)

Mean

——

Min/max

———

95 %

Figure F.4—Seasonal Fluctuations in Caspian Sea MSL

F.5.3 Tides, Storm Surges, and Seiches

The tidal range in the Caspian Sea is very small, on the order of only 0.1 m. However, significant water level fluctuations do occur as a result of wind forcing and seiching. Prolonged northerly winds can cause a drop in sea level that prevents the safe operation of vessels in shallow waters. A sudden reduction in the wind can cause the water to flow back rapidly and oscillate at a period consistent with a longitudinal seiche over the whole of the Caspian Sea, excluding the extremely shallow northern section. The dominant periods are 8.5 min to 8.7 min for a single seiche, and 4.4 h to 4.4 h for a double-node seiche. Detailed reports on the magnitude of the seiches are not available, although seiching has been observed in data in the vicinity of Bautino with an amplitude of less than 5 cm.

An example of negative and positive surges in the northern Caspian Sea is shown in Figure F.5. In the southern Caspian Sea, storm surges are generally small, varying from -0.1 m to $+0.2\text{ m}$.

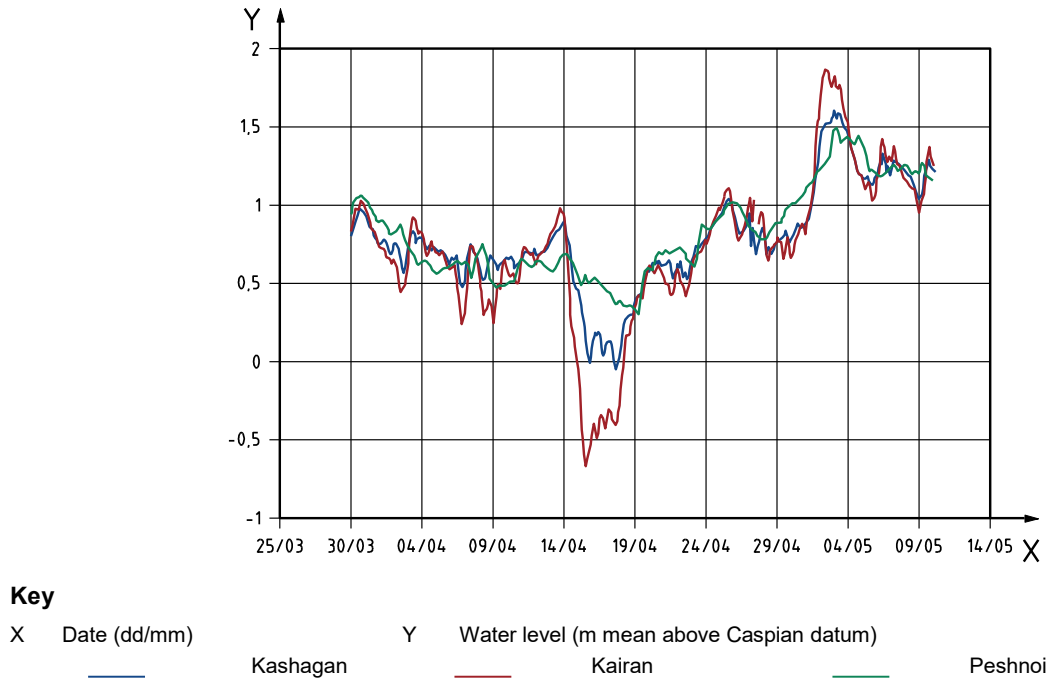


Figure F.5—Storm Surges in the Northern Caspian Sea

F.6 Winds

In very general terms, the most frequent wind directions over the Caspian Sea are:

- summer—northerly;
- winter—southeasterly.

The prevailing wind direction does vary in different regions. For example, in the western part of the central Caspian Sea, near the spurs of the Caucasian Mountains, the prevailing winds throughout the year are northwest and southeast, while “monsoon” traits are clearly evident in the wind regime on the southern Caspian’s east coast. A similar regime is noted in the northern Caspian Sea, although dominant directions are closer to east and west.

Median wind speeds are in the range 5 m/s to 7 m/s , and a little higher (up to 9 m/s) in particularly windy regions such as the Apsheron Peninsula. Ten percent of wind speeds exceed 10 m/s to 12 m/s . Storms associated with wind speeds in excess of 25 m/s are usually from the northwest, north, northeast, or southeast.

F.7 Waves

The most severe sea states occur when strong winds blow over the longest fetches, namely during periods of sustained north/northwest or south/southeast winds.

The greatest storm activity develops over the open waters of the middle Caspian between Bautino and the Apsheron Peninsula (see Table F.1).

Table F.1—Number of Events per Year with Winds > 15 m/s

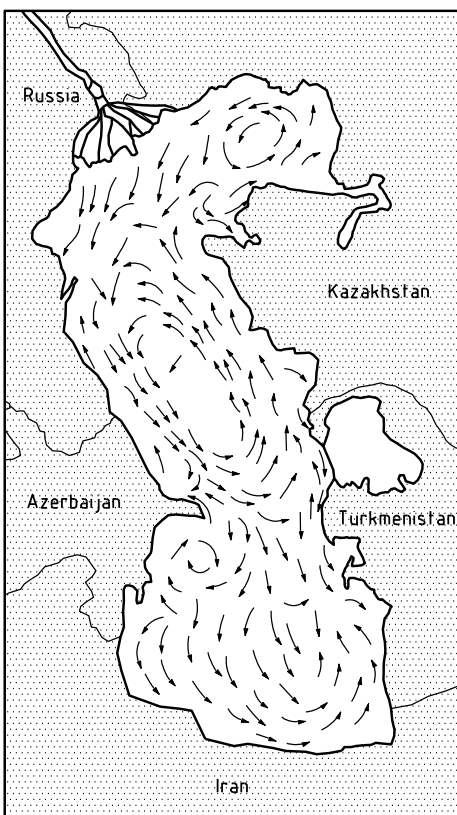
Location	Average Number of Events per Year with Wind Speed > 15 m/s	Maximum Number of Events per Year with Wind Speed > 15 m/s
Bautino	13	27
Apsheron Peninsula	20 to 30	45

F.8 Currents

The circulation of the Caspian Sea is unusual in that tides are very small, and currents are driven largely by regional weather systems [216,227]. The relationship between the forcing mechanisms and the actual observed currents is complex. The currents can be large, with speeds dependent on the location (water depth, position in the basin, shape of the seabed topography) and the wind system acting on the sea surface (magnitude, direction, and degree of wind curl). Regional descriptions of the currents in the Caspian Sea describe several anti-clockwise gyres, but these give only a broad indication of the flow. To understand the currents at a particular location, it is necessary to make site-specific measurements over a suitable period. Such measurements are strongly recommended for detailed engineering design.

Although currents are largely storm-driven, depending on the location and the wind direction, the peak currents can occur at the same time as the peak wind and waves or be delayed by several hours. For example, in the southern Caspian Sea the storm-generated currents from north or northwesterly winds peak approximately one day after the wind and waves, and come from the southwest. In this area, strong near-bed currents can occur during periods of benign wind and wave activity at the surface.

Generalized current flows in the Caspian Sea are shown in Figure F.6.

**Figure F.6—Generalized Current Flows in the Caspian Sea** [222]

F.9 Other Environmental Factors

F.9.1 Marine Growth

The density of fouling organisms in the Caspian Sea is expected to be from $\sim 13 \text{ kg/m}^2$ to a maximum of 30 kg/m^2 to 40 kg/m^2 (barnacles being a major contributor). Fouling densities of 10 kg/m^2 to 12 kg/m^2 have occurred on ships, leading to 20 % to 30 % reduction in ship speed.

The hydroid Bougainvillia megas can develop dense accretions inside intakes and pipelines open to the sea, hindering the flow of water. (Bougainvillia is a gelatinous organism that spreads itself in the form of a jellyfish or medusa.)^[208]

The extent of marine growth needs to be reviewed on an annual basis. If necessary, any growth will need to be removed by mechanical means.

F.9.2 Air Temperature, Precipitation, Humidity, Pressure, Clouds, and Visibility

F.9.2.1 Air Temperature

Air temperature varies greatly over the Caspian Sea due to the lengthy meridional dimension of its main axis. The average annual air temperature is 8°C to 10°C , 11°C to 14°C , and 15°C to 17°C for the northern, central, and southern regions, respectively. A large variation in extreme temperatures also occurs. In the north the temperature can drop to -30°C with the arrival of arctic air, whereas in the southern Caspian Sea the minimum temperature is -10°C . The variation in air temperature is less in summer. High temperatures up to 42°C to 44°C are observed on the east coast.

Annual freezing degree-days: Freezing degree-days in the northern Caspian can vary significantly from year to year, with values as high as 1500 in some years, and as low as 300. The number of freezing degree-days has been related to ice thickness^[223].

F.9.2.2 Precipitation—Rainfall

The amount of precipitation over the Caspian coastline is a function of the interaction of different air masses with the relief of the coastal areas and mountains. It can vary between 200 mm/year and 1200 mm/year, depending on the location. The distribution of precipitation above the sea area is relatively uneven but averages $\sim 200 \text{ mm/year}$ ^[228].

Rainfall in Atyrau (northern Caspian) has been measured since the end of the 19th century. Average annual rainfall at this site is $\sim 160 \text{ mm}$, although this is highly variable with annual values falling as low as 50 mm and as high as 280 mm. Weekly rainfall is typically between 2 mm and 3 mm for most of the year, although double this amount can be expected between April and June. Heavy rainfall can occur at any time of the year, and weekly totals in excess of 15 mm have been recorded throughout the year. The highest weekly total was 95 mm, measured in July. See Figure F.7.

NOTE Snowfall is discussed in F.9.4.

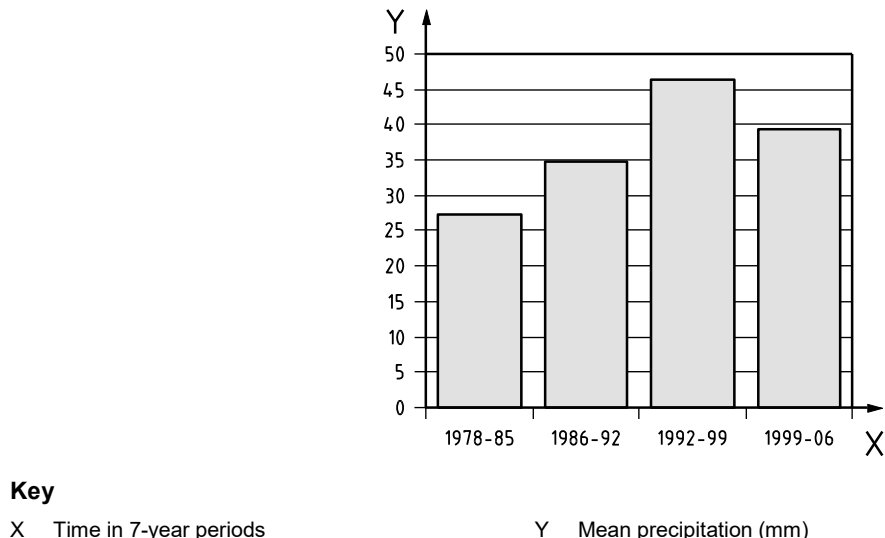


Figure F.7—Precipitation (mm) Over Winter Season in Atyrau, Northern Caspian Sea

F.9.2.3 Humidity

The humidity of the air above the Caspian Sea broadly increases from south to north and from east to west^[228]. It does not change significantly during the cold months, measuring on average 80 % to 87 % on the western coast and 75 % to 80 % on the eastern coast. Over the sea, it decreases from 90 % in the central parts of the Caspian Sea to 85 % in the southern Caspian. In the summer, at the coast humidity ranges on average between 55 % and 70 %, whereas over the sea it reaches an average of 80 %.

Along the northern shore, the mean daily humidity values vary from 90 % during December to February, to around 50 % during the summer (July and August). Fully saturated air can occur at anytime between October and March, with daily mean values of 100 % routinely recorded. During the summer months the air is drier, with daily maxima rarely exceeding 90 % between April and October. Minimum daily mean values rarely drop below 20 % in the summer and below 60 % in the winter. The humidity levels offshore tend to be higher than those recorded at the coastal stations during the winter months, but offshore humidity tends to be greater between April and September.

F.9.2.4 Visibility—Fog and Dust Storms

For the majority of the Caspian Sea, fog is mostly observed during the spring. Its frequency decreases from the shore toward the open sea areas. In summer, fogs are mainly observed at daybreak and dissipate within 1 h to 3 h after sunrise, with heating of the atmosphere. In winter, advective fog at sea occurs at the outflow of warm air masses from the land. Its average duration is about 7 h to 8 h, and it can be observed at any time of the day. The greatest number of days with fog based on mean multi-year data (32 days to 38 days) is typical of the central Caspian Sea. More than half of fogs are observed during the cold period of the year.

In the northern Caspian Sea, fog is most common during both autumn and late winter; this is associated with the high humidity values during this period. The number of days with fog is highly variable from year to year, but poor visibility can persist for several days at a time.

The average number of days per month of dust storms at Fort Shevchenko is given in Table F.2.

Table F.2—Average Number of Days per Month with Dust Storms at Fort Shevchenko

Days per Month with Dust Storms at Fort Shevchenko												
Jan	Feb	Mar	Apr	May	Jun	Jul	Aug	Sep	Oct	Nov	Dec	Per Year
0.2	0.5	0.7	1	0.5	—	0.2	0.07	0.2	0.3	—	—	3.6

F.9.2.5 Daylight Hours

Hours of daylight are a function of latitude. Over the Caspian Sea region, they range from 8 h to 9 h in December and from 15 h to 16 h in June.

F.9.2.6 Tornadoes/Waterspouts

Waterspouts and tornadic waterspouts are considered to be rare occurrences in the Caspian Sea, although there have been sightings in the northeast Caspian, at Baku, and between Fort Shevchenko and Aktau in recent years. Waterspouts form when there is moist unstable air, a warm water surface and a convergent boundary (i.e. a land- or sea-breeze front or other mesoscale wind feature). Tornadic waterspouts form in the same manner, but in addition the vertical wind shear causes rotation of the convective cloud (almost always a full-grown cumulonimbus). The strong winds associated with these features can cause considerable damage. The most recent documented sighting indicated that the tornadic waterspouts were Force 2 on the Fujita scale (wind speeds between 50 m/s and 70 m/s).

F.9.3 Sea Ice and Icebergs

Ice forms in the northern portions of the Caspian Sea in winter, but there is considerable variability in both the onset and the duration of the ice cover. During severe winters, ice formation can begin as early as October, but has been as late as the end of December or early January. The ice formation starts along the northern and eastern coastlines and works southward, typically reaching its maximum southward extension by January or February, as indicated in Figure F.2^[208].

Thermal ice growth is modest compared to arctic regions; however, the lack of snow cover and wind-induced ice movements during the freeze-up mean that the ice can layer easily, resulting in thicker ice. Level ice thicknesses can reach 90 cm in severe winters, but are typically nearer to 60 cm during an average year. Locally, thicknesses can be considerably greater due to rafting or other factors. The low salinities also result in relatively strong ice.

The ice around the northern and eastern boundaries of the sea is typically landfast; in the central region of the northeast Caspian Sea the stability of the ice is dependent on the severity of the winter, but pack ice will often be present for parts of the winter season. There are usually several significant movements in the course of a typical year, with recorded speeds of more than 0.5 m/s. The formation of ice piles (stamukha) and ridges is common over much of the northern Caspian Sea; stamukha can reach heights of more than 10 m, but are typically less than 8 m. These features are grounded and result in indentation of the seabed and the formation of scours in the event that they move. The ice typically tends to start receding in March, commencing in the Ural Furrow in the centre of the basin. The entire region is generally ice-free by mid to end April. No multi-year ice is present in the Caspian Sea.

Four winters (1949/50, 1953/54, 1968/69, and 1971/72) were observed with severe ice conditions over the period 1950 to 1975^[217].

As there are no glaciers discharging into the Caspian, there are no icebergs.

Ice thickness and characteristics vary significantly across the area; data given in Table F.3 are for the central part of the northern Caspian. Ice formation further to the northeast tends to begin earlier and last longer; ice thickness also increases.

F.9.4 Snow, Ice Accretion, and Sea Spray Icing

As with sea ice, snowfall and ice accumulation on oil industry structures are design considerations only in the northern Caspian Sea.

Snowfall in the northern Caspian Sea is highly variable from year to year, with typical precipitation amounts between 25 mm and 50 mm per season (Atyrau) (see Figure F.7). This is equivalent to between 25 cm and 50 cm of snowfall, given average ratio of 1:10; typical values for the ratio vary between 1:5 and 1:15 for fresh snow. Snow accretion is relatively rare offshore, but snowdrifts of more than 25 cm can develop during exceptional years. In exceptional years, precipitation over the winter season can exceed 100 mm.

Sea spray icing will occur on exposed structures during the winter period when air temperatures are low and wave action is significant. Light icing will also be encountered during foggy conditions when air temperatures are below freezing.

Table F.3—Summary of Ice Conditions in the Northern Caspian Sea

Sea Ice	Parameter	Average Annual Maximum Value	Uncertainty in Annual Maximum Values
Occurrence	First ice	Mid-December	Mid-November to early January
	Last ice	End March	End February to mid-April
Level ice (first year)	Landfast ice thickness (m)	0.6	± 0.3
	Floe thickness (m)	0.3	Variable due to rafting
Rafted ice	Rafted ice thickness (m)	Rafted ice thickness can vary considerably in local areas; values of > 1 m are not uncommon	Variable
Rubble fields	Sail height (m)	2 to 5	± 3
	Length (m)	≤ 1 000	Variable
Ridges (first year)	Sail height (m)	1 to 2	Variable
	Keel depth (m)	Water depth limited	n/a
Stamukhas	Water depth range (m)	0 to 8	
	Sail height (m)	≤ 20	Variable
Ice movement	Speed in near-shore (m/s)	0.5	± 0.3
	Speed in offshore (m/s)	0.5	± 0.3
Ice-induced scour	Scour depth (m)	0.2 to 0.5	≤ 1.5

F.9.5 Tsunamis

Information on past tsunamis in the Caspian Sea is limited; only qualitative data are available. Table F.4 lists observations of past tsunami events ^[226]. In the Caspian Sea, earthquakes, mud volcanoes, or submarine landslides can create tsunamis.



Table F.4—Historical Tsunamis and Tsunami-like Events Observed in the Caspian Sea [226]

Date	Location	Description
743	Derbent	The area of the coast with fortifications was submerged in the sea.
918	Derbent	The part of the coast with fortifications was submerged in the sea.
957	Derbent	The fall of sea level caused horizontal displacement of the shoreline by 150 m from the equilibrium position.
1668	Terka	Part of the beach was submerged in the sea. The rise of water level was observed in the delta of the Terek River.
26.04.1868	Baku	Short-term rise and fall of sea level with amplitude about 0.45 m were observed.
09.03.1876	Oblivnoy Island	Unusual sea level oscillations occurred after strong underwater boom in conditions of dead calm. Event was observed from a ship.
27.06.1895	Krasnovodsk Bay	Flooding of north and west areas of Uzun-Ada as result of a large increase in water level in the bay. Large waves caused flooding of buildings and dock. A few wooden houses were taken away to the sea. Pipeline was destroyed.
31.12.1902	Baku	Unusual waves resulted in dangerous motion of ships in the port. Event was observed after destructive earthquake near Shimaha.
09.05.1933	Kuuli-Mayak	Sudden rise of sea level up to 1.35 m for 10 min. Fishing boats and equipment were taken away to sea.
12.04.1939	Livanov Shoal	The passing of a solitary wave of a large height was observed from two ships that were 15 miles from each other.
26.04.1960	Baku	Oscillations of sea level up to 1 m were observed for 2–3 h.
06.03.1986	Livanov Shoal	Unusual high-frequency sea level oscillations of 2 cm to 3 cm amplitude were observed over epicenter of earthquake during 1 min to 1.5 min. The event was fixed from a seiner and 45 fishing boats.

Seven offshore seismic areas have been identified as tsunamigenic (see Figure F.8). As tsunami sources are located on the continental shelf, tsunami waves are trapped along the coast. Thus tsunamis are anticipated to have a local character. Preliminary estimates of tsunami heights range from 0.5 m to 3 m.

As tsunami hazards are site-specific, it is recommended to carry out a site-specific assessment to estimate the risk. Such studies should be carried out in parallel with a seismic hazard assessment.

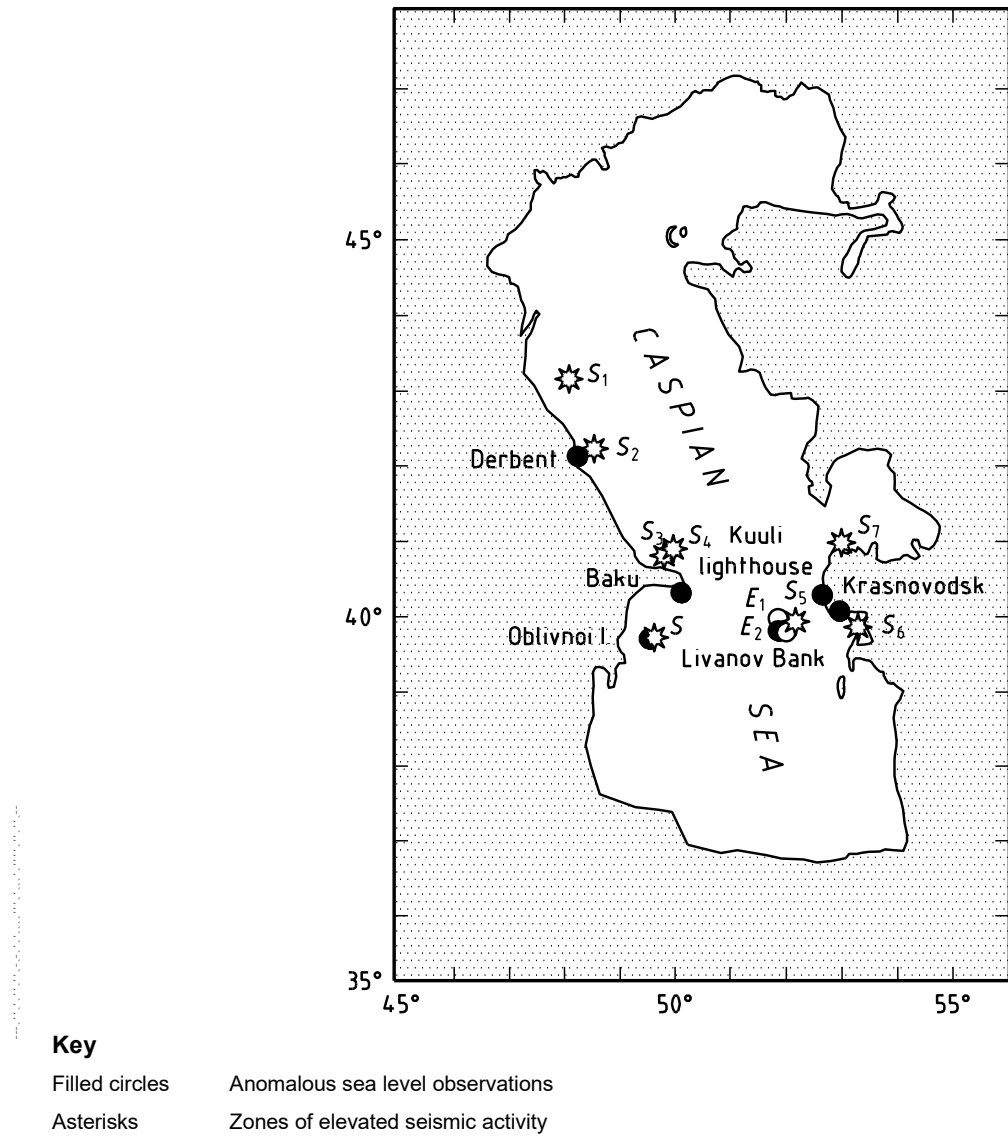


Figure F.8—Region of the Caspian Sea Where Historical Tsunamis or Anomalous Sea Levels Were Observed [226]

F.10 Estimates of Metocean Parameters

F.10.1 Extreme Metocean Parameters

Indicative extreme values of metocean parameters are provided in Tables F.5 to F.9 for four locations in the Caspian Sea. The wind, wave, and current values are independently derived marginal parameters; no account has been taken of conditional probability. As for all indicative values provided within the regional annexes, these tables are provided to assist preliminary engineering concept selection; they are not suitable for design of offshore structures.

Table F.5—Indicative Values of Metocean Parameters for the Northern Caspian Sea Region

Metocean Parameter	Return Period (years)			
	1	10	50	100
Nominal water depth (m)	4.2	4.2	4.2	4.2
Wind speed at 10 m above MSL				
10 min mean (m/s)	30.7	36.0	39.7	41.3
3 s gust (m/s)	36.0	45.5	50.7	53.0
Waves				
Maximum height (m)	2.2	2.5	2.8	2.9
Significant height (m)	1.3	1.5	1.7	1.8
Direction (from)	W	W	W	W
Spectral peak period (s)	4.8	5.0	5.1	5.2
Surge				
Positive surge (m)	0.8	1.4	1.8	2.0
Negative surge (m)	0.7	1.4	1.9	2.1
Current speed				
Surface (m/s)				
Mid-depth (m/s)	0.59	0.78	0.92	0.97
1 m above sea floor (m/s)				

Table F.6—Indicative Values of Metocean Parameters for the Central Caspian Sea Region

Metocean Parameter	Return Period (years)			
	1	10	50	100
Nominal water depth (m)	450	450	450	450
Wind speed at 10 m above MSL				
10 min mean (m/s)	25.8	32.0	37.1	39.4
3 s gust (m/s)	31.6	39.9	46.3	50.4
Waves				
Maximum height (m)	11.2	17.5	20.8	21.6
Significant height (m)	5.8	9.0	10.7	11.6
Direction (from)	NW/SE	NW/SE	NW/SE	NW/SE
Spectral peak period (s)	9.7	11.9	13.0	13.4
Surge				
Positive surge (m)	0.2	0.4	0.55	0.6
Negative surge (m)	0.3	0.4	0.55	0.6
Current speed				
Surface (m/s)	0.95	1.2	1.30	1.40
Mid-depth (m/s)	0.60	0.8	0.80	0.95
1 m above sea floor (m/s)	0.60	0.8	0.80	0.95

Table F.7—Indicative Values of Metocean Parameters for the Apsheron Ridge Area of the Caspian Sea

Metocean Parameter	Return Period (years)			
	1	10	50	100
Nominal water depth (m)	160	160	160	160
Wind speed at 10 m above MSL				
10 min mean (m/s)	28.8	34.6	38.9	41.1
3 s gust (m/s)	35.2	43.0	49.0	51.6
Waves				
Maximum height (m)	10.4	14.5	17.4	18.6
Significant height (m)	5.7	7.8	9.3	10.0
Direction (from)	N	N	N	N
Spectral peak period (s)	10.4	12.1	13.2	13.6
Surge				
Positive surge (m)	0.17	0.29	0.37	0.41
Negative surge (m)	0.08	0.22	0.31	0.35
Current speed				
Surface (m/s)	0.40	0.70	0.91	1.00
Mid-depth (m/s)	0.40	0.70	0.91	0.90
1 m above sea floor (m/s)	0.50	0.50	0.80	1.00

Table F.8—Indicative Values of Metocean Parameters for the Southern Caspian

Metocean Parameter	Return Period (years)			
	1	10	50	100
Nominal water depth (m)	500	500	500	500
Wind speed at 10 m above MSL				
10 min mean (m/s)	29.0	34.7	39.1	41.2
3 s gust (m/s)	35.4	43.1	49.3	52.0
Waves				
Maximum height (m)	5.9	10.9	13.8	15.6
Significant height (m)	3.1	5.7	7.3	8.2
Direction (from)	NE	NE	NE	NE
Spectral peak period (s)	7.2	9.2	11.4	12.0
Surge				
Positive surge (m)	0.22	0.30	0.40	0.44
Negative surge (m)	0.10	0.23	0.34	0.39
Current speed				
Surface (m/s)	0.20	0.36	0.53	0.60
Mid-depth (m/s)	0.20	0.36	0.53	0.60
1 m above sea floor (m/s)	0.16	0.30	0.43	0.49

.....

Table F.9—Indicative Temperatures Ranges for the Caspian Sea

Area	Air Temperature (°C)	Sea Surface Temperature (°C)	Sea Floor Temperature (°C)
Northern Caspian	-30 to +38	-0.5 to +30	-0.5 to +30
Central Caspian	-6 to +39	1 to 28	5 to 5
Apsheron Ridge	-7 to +40	0 to 27	5.5 to 6.0
Southern Caspian	-7 to +40	0 to 27	4.5 to 6.0

F.10.2 Long-term Distributions of Wave Parameters

Wave-scatter diagrams for two areas in the Caspian Sea are provided in Tables F.10 and F.11, comprising significant wave height and associated spectral peak wave period for combined wind sea and swell conditions based on data for a 50-year hindcast.

The shallow waters of the Mangyshlak threshold, defining the boundary between the central and northern Caspian Sea, largely prevent swell from the south entering the northern Caspian area. For the northern Caspian Sea, the wave climate is significantly influenced by water depth. In the deeper parts (where waves are larger) a JONSWAP spectrum with a gamma of between 1.2 and 3 has been recorded; however, in the shallower areas where wave heights are restricted, higher values between 2.6 and 6 are more appropriate. For the rest of the Caspian Sea, a gamma value in the range 1.0 to 2.5 has been found.

The information in Tables F.10 and F.11 was generated from the CASMOS-2 hindcast model [210,215,229]. CASMOS-2 was validated against a limited number of in situ wave data sets. Sea states should be assumed to represent a duration of 3 h.

Table F.10—Percentage Occurrence of Total Significant Wave Height vs. Spectral Peak Period for a Location in the Northern Caspian Sea [229]

Significant Wave Height (m)	Peak Period (s)								Total
	0 to 0.99	1 to 1.99	2 to 2.99	3 to 3.99	4 to 4.99	5 to 5.99	6 to 6.99		
0.00 to 0.49	20.1	17.2	19.8	20.1	—	—	—	—	77.2
0.50 to 0.99	—	—	—	22.3	0.1	—	—	—	22.4
1.00 to 1.49	—	—	—	0.05	0.3	0.05	—	—	0.4
> 1.50	—	—	—	—	—	—	—	—	—
TOTAL	20.1	17.2	19.8	42.45	0.4	0.05	0.01	100.00	

Table F.11—Percentage Occurrence of Total Significant Wave Height vs. Spectral Peak Period for a Location on the Apsheron Ridge Area of the Caspian Sea

Significant Wave Height (m)	Peak Period (s)													
	0 to 0.99	1 to 1.99	2 to 2.99	3 to 3.99	4 to 4.99	5 to 5.99	6 to 6.99	7 to 7.99	8 to 8.99	9 to 9.99	10 to 10.99	11 to 11.99	> 12	TOTAL
0.00 to 0.49	0.84	2.64	5.40	10.97	4.49	0.83	0.04	0.01	0.00	0.00	0.00	0.00	0.00	25.22
0.50 to 0.99	—	—	—	6.88	16.13	6.76	1.65	0.22	0.00	0.00	0.00	0.00	0.00	31.64
1.00 to 1.49	—	—	—	0.20	5.25	10.94	2.17	1.25	0.24	0.01	0.00	0.00	0.00	20.06
1.50 to 1.99	—	—	—	0.01	0.14	5.01	4.18	1.01	0.63	0.13	0.00	0.00	0.00	11.11
2.00 to 2.49	—	—	—	—	0.01	0.18	3.78	1.07	0.46	0.26	0.02	0.00	0.00	5.79
2.50 to 2.99	—	—	—	—	—	0.01	0.73	1.60	0.43	0.20	0.07	0.00	0.00	3.04
3.00 to 3.49	—	—	—	—	—	—	0.02	0.76	0.44	0.15	0.07	0.01	0.00	1.45
3.50 to 3.99	—	—	—	—	—	—	—	0.11	0.43	0.16	0.06	0.02	0.00	0.78
4.00 to 4.49	—	—	—	—	—	—	—	—	0.17	0.19	0.06	0.01	0.00	0.43
4.50 to 4.99	—	—	—	—	—	—	—	—	0.04	0.12	0.05	0.01	0.00	0.22
5.00 to 5.49	—	—	—	—	—	—	—	—	—	0.05	0.05	0.01	0.00	0.11
5.50 to 5.99	—	—	—	—	—	—	—	—	—	0.02	0.03	0.01	0.00	0.06
6.00 to 6.49	—	—	—	—	—	—	—	—	—	—	0.02	0.01	0.00	0.03
6.50 to 6.99	—	—	—	—	—	—	—	—	—	—	0.01	0.01	0.00	0.02
7.00 to 7.49	—	—	—	—	—	—	—	—	—	—	—	0.01	0.00	0.01
7.50 to 7.99	—	—	—	—	—	—	—	—	—	—	—	0.01	0.00	0.01
TOTAL	0.84	2.64	5.40	18.06	26.02	23.74	12.57	6.02	2.84	1.31	0.44	0.11	0.01	100.00

Annex G

(informative)

Southern East Asian Sea

G.1 Description of Region

The geographical extent of the region of the southern East Asian Sea is bounded by the land masses of Vietnam, Cambodia, Thailand, and Malaysia to the north and west, the Borneo land mass to the south, and the Philippines to the east, and is limited at 15° N to the north and the equator to the south, as shown in Figure G.1. The region includes the following areas, moving anti-clockwise around the southern East Asian Sea:

- the waters offshore Vietnam;
- the Gulf of Thailand;
- the waters offshore Peninsular Malaysia;
- the waters offshore Natuna Island;
- the waters offshore Borneo;
- the waters offshore Philippines.

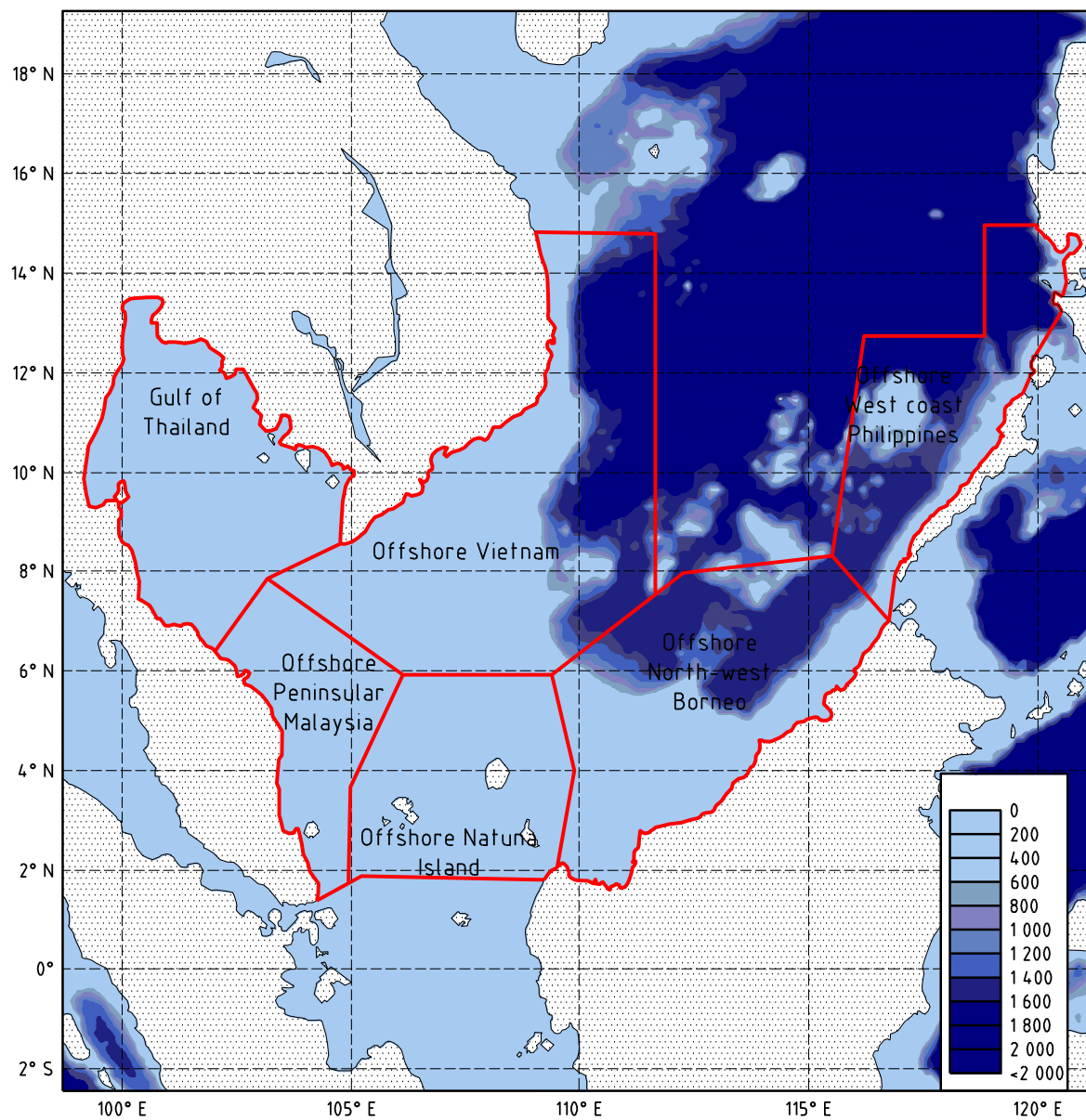


Figure G.1—Geography of the Southern East Asian Sea

G.2 Data Sources

Measured data have been collected at many stations throughout the region, however much of the national data collected by government bodies is restricted to land stations or the coastal strip aimed at flood prevention and port operation. Data collected further offshore are often proprietary. Data can also be obtained from commercial organizations.

Satellite data are a major source of information for this region for wind and wave, as well as typhoon track data, a major consideration for many locations.

In addition to measured data, some joint industry-sponsored hindcast studies have been performed leading to extensive (but usually proprietary) data sets of winds, waves, and, to a limited extent, currents. The main metocean hindcast data set for the whole East Asian Sea is SEAMOS (South East Asia Meteorological and Oceanographic Study).

The SEAMOS wind and wave typhoon and monsoon hindcast data set is not a continuous data set, but models the 246 most severe monsoon and typhoon events in the whole of the East Asian Sea between 1946 and 1996 on a 1 h data interval and a 25 km grid. These data are not seasonally balanced and have some additional limitations for more southerly locations. For example, many of the storms were not severe events in the southern East Asian Sea, and storms that were more significant in the southern East Asian Sea have not been included. As a result, if this data set is used in isolation to derive criteria in the southern East Asian Sea, the assigned probabilities of these events are unlikely to be correct and can impact both the 100-year extreme value and the slope of the distribution.

SEAMOS Operational Update (SOUP) wind and wave hindcast data set is a continuous data set for the East Asian Sea between 1980 and 1999 on a 3 h data interval and a 25 km grid. This data set avoids the problems associated with missing storms prevalent in the SEAMOS storm hindcast. However, most of the small-scale temporal and spatial events particularly associated with the southwest monsoon are not modelled, the wind speeds are lower than expected and in some areas the impact of the typhoon events in the southern East Asian Sea appear to be under-predicted for waves.

To rectify some of these problems, a new joint industry project is in progress to produce SEAFINE (South East Asia Fine Grid Study). This aims to produce a 50-year continuous wind and wave hindcast on a 1 h data interval and a 7 km grid. However, even with SEAFINE some criteria, such as current and squall criteria, will still need to be derived from measured data sets.

G.3 Overview of Regional Climatology

Compared to regions such as the Gulf of Mexico and the waters west of Shetland, the climate of the southern East Asian Sea is considered benign. The region is within the equatorial tropics and under the influence of the general wind systems of Southeast Asia produced by the wider regional atmospheric pressure distribution. There is typically a four-season pattern to the climate, with the following characteristics and approximate timings (both of which have considerable inter-annual variability):

- a) northeast monsoon (November to March), characterized by predominantly northeast winds, increased cloudiness and the heavy rainfall and thunderstorms often associated with the low pressure “trough” termed the “intertropical convergence zone” (ITCZ); regular “surges” in the monsoon winds increase wind speeds and raise wave heights; the risk of typhoons affecting the area continues through November and December only;
- b) transition (April and May), when the winds are light (except during occasional squalls) and variable in direction, wave heights are low;
- c) southwest monsoon (June to September), which is dominated by southwest winds, that occasionally increase in speed due to typhoons approaching east of the Philippines, raising waves heights; typically the duration, wind, speed, and wave heights are lower than those experienced during the northeast monsoon except on the eastern boundary; squall frequency and severity increase during this period;
- d) transition (October/November), showing changeable wind directions with an increase in wind speed and frequency of squalls; at this time of year the risk of typhoons affecting the region is greatest.

G.4 Water Depths, Tides, and Storm Surges

Water depths in the areas are shown in Figure G.2. Much of the area within the East Asian Sea covering the Gulf of Thailand, waters offshore Peninsular Malaysia, waters offshore Natuna Island and the western part of the area denoted offshore Borneo, is contained within the continental shelf and is less than 200 m in depth. However, in water offshore Philippines, water offshore Vietnam and the eastern part of the area denoted waters offshore Borneo, water depths extend to 2000 m. The southern East Asian Sea reaches a depth of approximately 5000 m in the area near 120° E and 15° N.

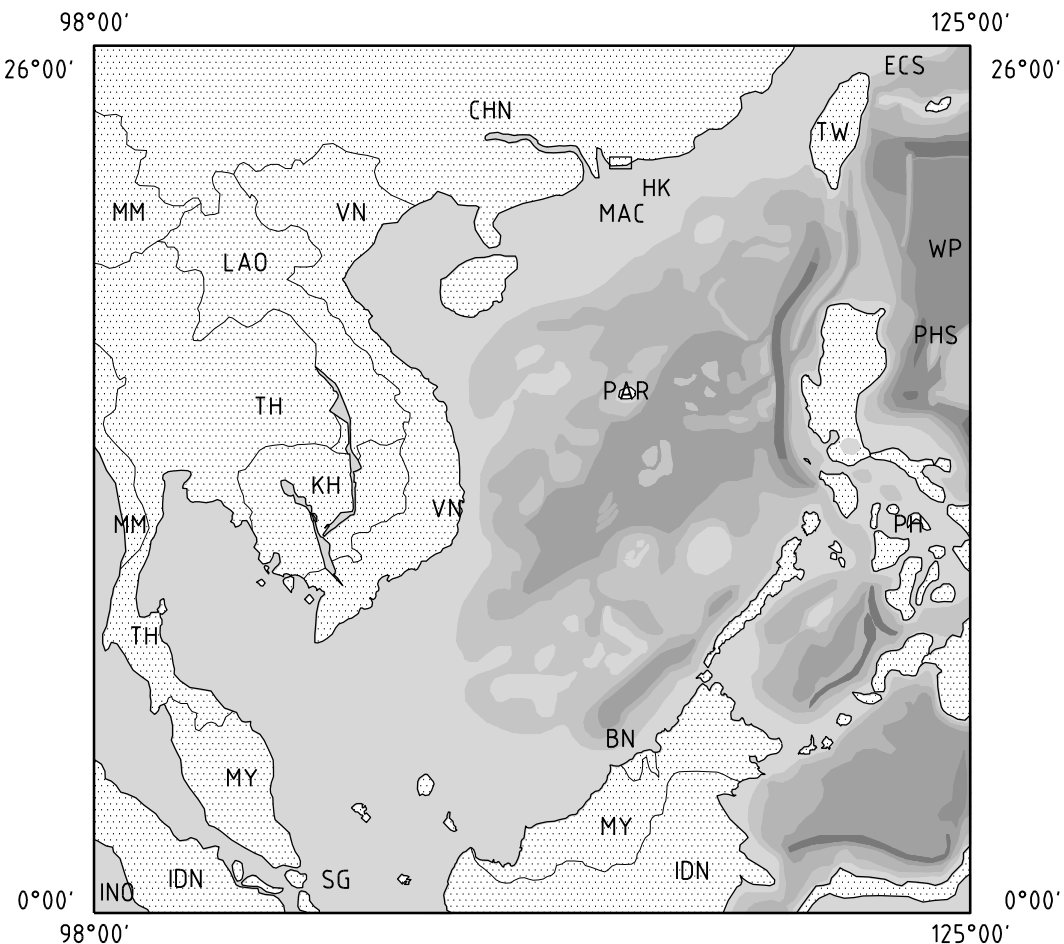


Figure G.2—Bathymetry of the East Asia Sea

The tides in the bulk of the East Asian Sea are diurnal, with only one high tide and low tide per day and tidal ranges not exceeding 2 m. However, there are exceptions, particularly around in the Gulf of Thailand and the waters offshore south Peninsular Malaysia toward the Strait of Karimata, where the tidal wave is reflected back, leading to semi-diurnal tides (two high and low tides per day). The largest tidal ranges are found in these areas; for example, near the Sarawak River the tidal range is 3.6 m.

Storm surges can result from two mechanisms: monsoon surges and typhoons; the susceptibility of each area is dependent on its location relative to these forcing mechanisms. Vietnam and the Gulf of Thailand are particularly susceptible to storm surges associated with the passage of typhoons, whereas offshore Borneo and Peninsular Malaysia are more susceptible to storms surges associated with the northeast monsoon. Monsoon storm surges in conjunction with high tides are a common cause of flooding in these areas.

G.5 Winds

There are four main sources of winds in the southern East Asian Sea:

- monsoon winds,
- squalls,
- winds associated with the passage of a typhoon, and
- land-sea breezes, which can be enhanced by local topography.

The significance of each is dependent on its relative location within the southern East Asian Sea.

In a typical northeast monsoon (November to March), there is low pressure over northern Australia and high pressure over China, causing the monsoon winds to blow over the whole of the East Asian Sea, with typically the strongest winds over the northern part of the East Asian Sea. Occasionally, pressure will rise rapidly over southern China resulting in a “surge” of increased wind and swell, during which the winds can reach gale force, even offshore Borneo. Between surges, the coastal land breeze can sometimes be fresh to strong in the late afternoon and early evening.

By April, the overall surface pressure gradient in Southeast Asia is weak, causing the winds to become southwesterly in the southern East Asian Sea. The coastal sea breeze develops during this time. Squalls develop, often inland and drift out to sea overnight, but later in the period they form offshore overnight and then drift inshore in the morning.

In the southwest monsoon (June to September), the pressure is high over Australia and low over southwest China. The southeasterlies from Australia “re-curve” as they cross the Equator to become southwesterly, blowing toward China. The onset of the southwest monsoon is often abrupt and vigorous, starting about mid-June with sustained winds of 15 m/s to 20 m/s for 2 to 3 days and high seas offshore. Surges in the southwest monsoon, from a variety of causes, usually last about 2 days and often result in a series of “stream squalls” moving from the southwest but also occasionally off the coast. The land breeze can become reasonably strong.

By October a weak area of low pressure develops over northwest Australia, and pressure over China starts to increase. At this time, northeasterly flow to the north of the ITCZ can trigger late surges in the southwesterly winds south of the ITCZ. The passage of typhoons across the Philippines into the East Asian Sea also increases at this time of the year. Although typhoons are rare south of 10° N, they enter the East Asian Sea more frequently in La Niña years. Typhoons can often produce heavy swell that, combined with rough seas from a simultaneous surge in the southwesterly monsoon, can produce severe cross-seas offshore. The winds usually increase during this time of the year and change direction. Squalls from the land also increase in frequency.

G.6 Waves

The East Asian Sea is effectively a semi-enclosed sea and hence, while strong winds can occur over the whole area, the wave characteristics vary according to the water depth and the fetch over which they have been generated. Where the fetch is restricted, the storm waves are shorter, steeper, and lower. The two main mechanisms for the generation of storm waves are:

- waves associated with the monsoon surges;
- waves associated with the passage of a typhoon.

However, the fetch and water depth restriction typically means that conditions during southwest monsoon are most severe in the eastern part of the East Asian Sea and conditions during the northeast monsoon are most severe in the southern and western parts.

In a typical northeast monsoon (November to March), the strong north-northeast winds over the northern part of the East Asian Sea generate waves that propagate down the East Asian Sea, and high swells can reach waters offshore Borneo even if the local winds are fairly light. Oceanic swells are restricted in their ability to enter the East Asian Sea, and hence the longest swells in the southern East Asian Sea have a maximum period of 16 s to 18 s.

Figures G.3 to G.5 depict spatial representations of maximum significant wave heights in the East Asian Sea over the period of a year.

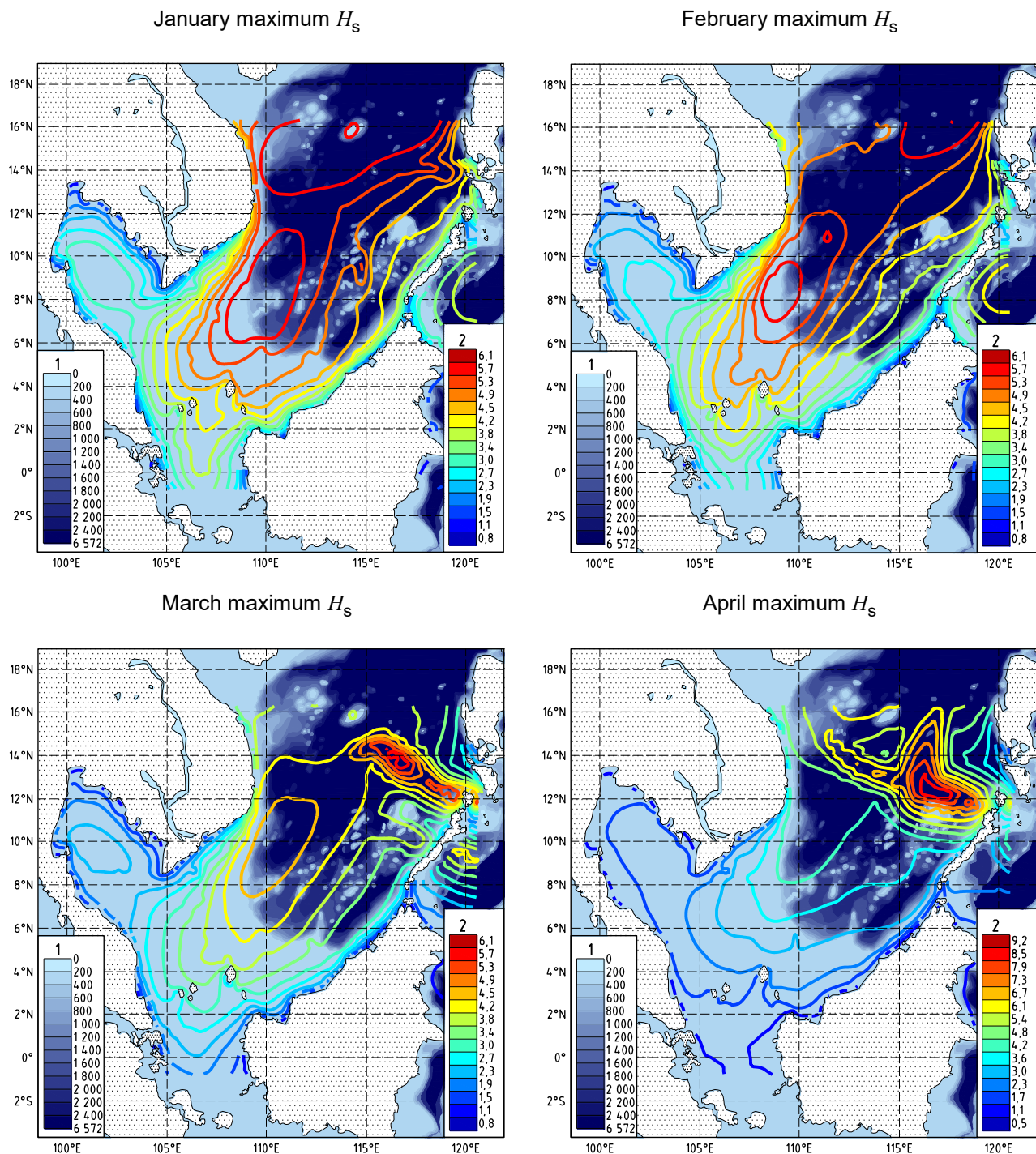


Figure G.3—Spatial Representation of Maximum Significant Wave Height for January, February, March, and April

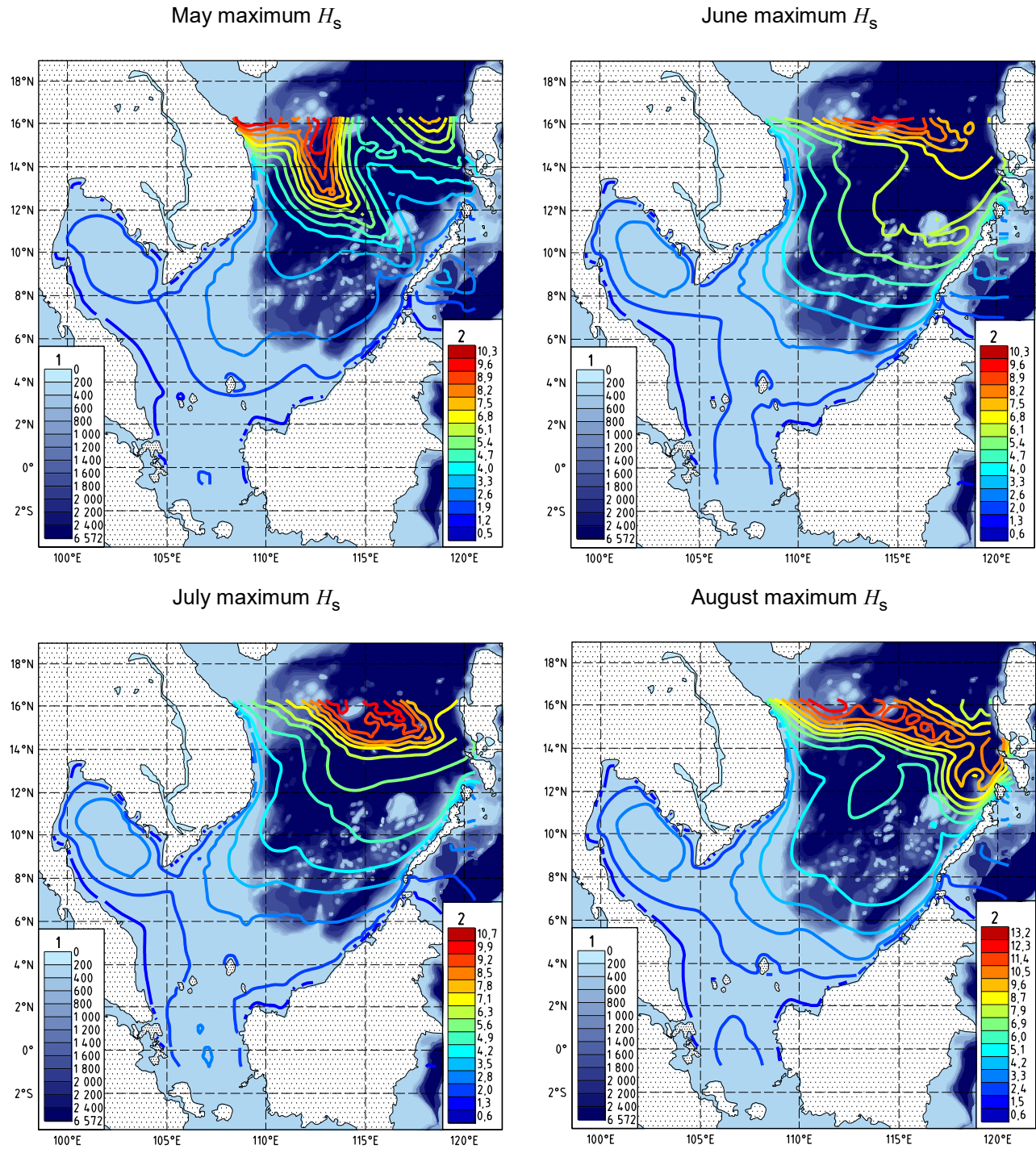


Figure G.4—Spatial Representation of Maximum Significant Wave Height for May, June, July, and August

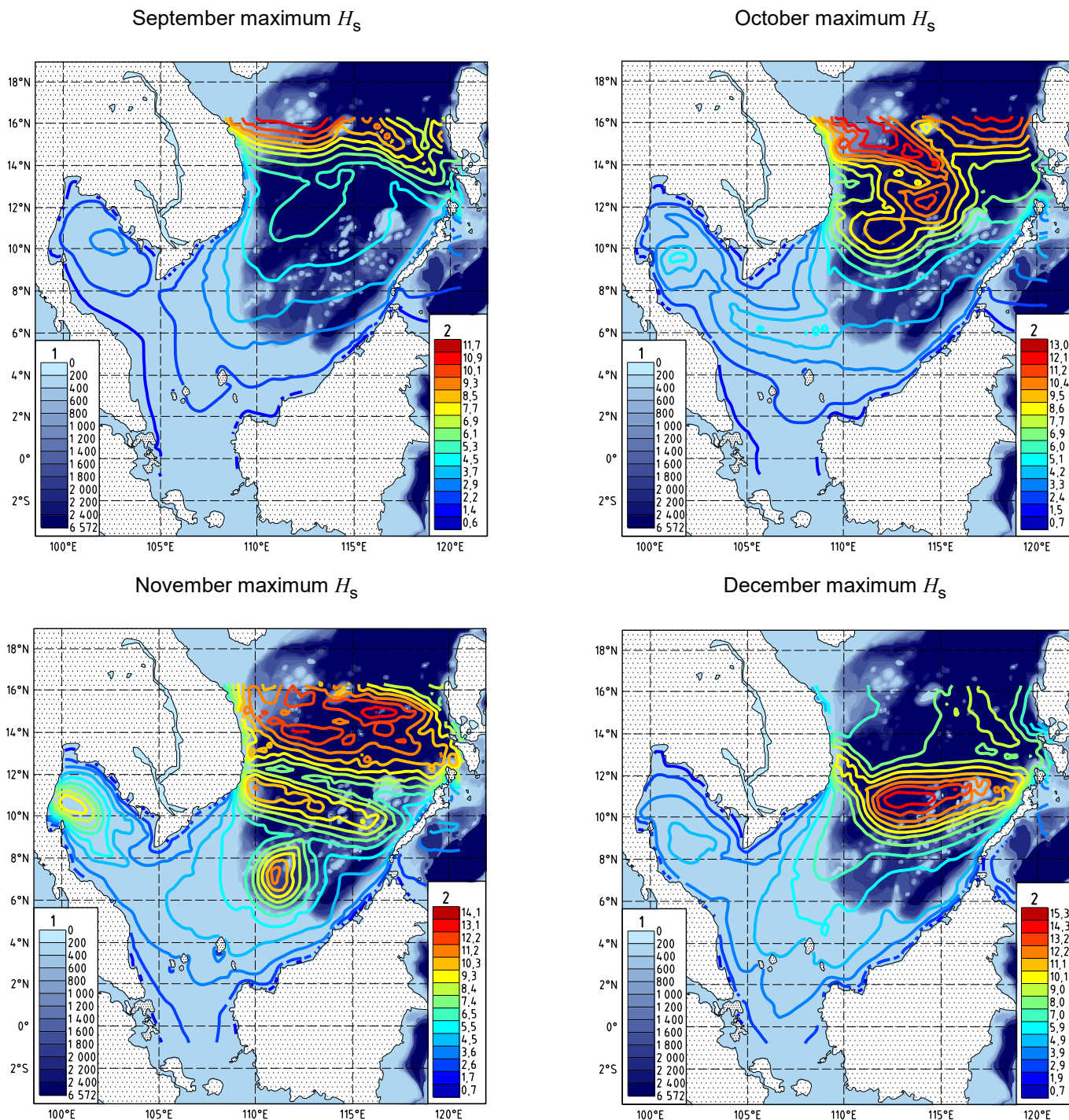


Figure G.5—Spatial Representation of Maximum Significant Wave Height for September, October, November, and December

G.7 Currents

G.7.1 General

Currents in the East Asian Sea are complex, vary substantially with location, and are driven by a number of mechanisms, which include:

- tidal currents;
- surface-wind–driven currents;
- basin-response currents derived from tropical storms or strong monsoon surges;
- density-driven currents (particularly near the outflow of large rivers);
- internal waves.

G.7.2 Tidal Currents

In many areas, particularly where the diurnal regime predominates, tidal currents are low in comparison to residual currents. However, areas near the coast, around shoals and islands, and in channels can experience stronger tidal currents.

In addition, several measurements have shown examples of high currents where fluctuations of the residual currents occur at the principal tidal period. This suggests that at some locations and with some forcing mechanisms, including typhoons, there can be coupling between tidal and residual currents.

G.7.3 Surface-Wind–Driven Currents

The East Asian Sea is an enclosed sea forced by monsoonal winds. In the northeast monsoon, winds cause a flow to the south and southwest in most areas of the southern East Asian Sea. Offshore Vietnam and offshore Peninsular Malaysia, tide and wind-driven currents can combine to provide strong southwesterly and southerly currents, respectively. Additionally, the reduced depth between Peninsular Malaysia and Borneo in the Strait of Karimata restricts the amount of water moving this way and causes the set-up of a circulation that results in an almost constant flow towards the northeast offshore Borneo. In the southwest monsoon, currents primarily move to the north or northwest in most locations.

G.7.4 Density-driven Currents (Particularly Near the Outflow of Large Rivers)

The presence of less-saline water masses due to the outflow of major rivers including the Mekong River, the Chao Phraya River flowing into the Gulf of Thailand, and the Kuching, Rajang, and Baram rivers flowing into the South China Sea from Sarawak, causes some density-driven flow. However, it should be noted that most Southeast Asian rivers hold considerable sediments, and the waters might be denser than expected from their salinity and temperature. Under some circumstances turbidity currents can be expected, especially during high flow periods.

G.7.5 Basin-response Currents Derived from Tropical Storms or Strong Monsoon Surges

Strong currents have been observed offshore Vietnam and offshore Borneo along the edge of the continental shelf. At several locations, these strong currents coincided with a low-pressure system in the southern half of the East Asian Sea and tended to lag monsoon surges. Typically, the strong currents could also be observed in Vietnam several days preceding those in Borneo and appeared to progress as a Kelvin wave around the East Asian Sea, tracking the edge of the continental shelf and turning northeast along the Sabah coast.

G.7.6 Internal Waves

Internal waves occur in the East Asian Sea in three regions:

- a) between the Luzon Strait and Hainan,
- b) along the Vietnamese coast, and
- c) between Vietnam and Borneo.

They are observed most frequently during the summer (June and July) but have been observed in all months except November and December. It is thought that the waves are generated as follows.

- Between the Luzon Strait and Hainan (outside the scope of this annex) waves are:
 - 1) trans-basin waves generated by the shallow topography under the influences of the tide and the Kurshio current, and
 - 2) internal waves generated near the continental shelf break by incident trans-basin waves or by tidal forcing.
- Along the Vietnamese coast waves are:
 - 1) trans-basin waves coming from the Luzon strait,
 - 2) disorganized internal waves of unknown origin,
 - 3) organized internal waves probably generated near the continental shelf break by incident tides.
- Between Vietnam and Borneo, internal waves are influenced by:
 - 1) the outflow of the Mekong river where internal waveforms are associated with the river plume, and
 - 2) the broad continental shelf and appear to be tidally generated.

The areas covered by this annex where internal wave activity is known to occur (although this list may not be exclusive) include:

- offshore Vietnam;
- offshore Peninsular Malaysia;
- offshore Natuna Island.

G.8 Other Environmental Factors

G.8.1 Marine Growth

Offshore in the southern East Asian Sea, the tropical marine environment means that marine growth of the order of 500 mm is common, with maximum marine growth occurring near the surface but below the surf zone. However, site-specific studies are required to determine the variation with depth.

G.8.2 Snow and Ice Accretion

Snowfall and ice accumulation on structures are not design or operational considerations for the southern East Asian Sea.

G.8.3 Tsunamis

Tsunamis have been measured in the East Asian Sea, with seismic events along the tectonic plate boundaries as the most likely sources. The East Asian Sea is protected by low seismic activity

landmasses to the north, west, and south; consequently, it can be affected only by a tsunami that originates in or is able to enter the East Asian Sea. It is unlikely that seismic events along the Sumatra-Java plate boundary would seriously affect the East Asian Sea (the 2004 Indian Ocean tsunami had little measurable effect in the East Asian Sea) and there is only a low probability that any tsunami generated in the Pacific would have the correct directional and energy characteristics to enter the southern part of the East Asian Sea. The East Asian Sea is exposed to tsunami risk from the east due to the high level of seismic activities in the Taiwan and Philippines areas, associated with the Philippines plate boundary. The most active part of the Philippines plate boundary is around the island of Taiwan, which has experienced several earthquakes resulting in the generation of tsunamis, although recorded levels were only 0.2 m above sea level. There have been about 100 recorded tsunami events in and around the Philippines, although many of these have been small or confined to the east coast. There have been some significant events on the edge of the East Asian Sea and within the Sulu and Celebes Seas.

G.8.4 Air Temperature, Humidity, Pressure, and Visibility and Rainfall

High air temperatures are encountered throughout the region, with daily temperatures ranging between 22 °C and 36 °C. Maximum air temperatures generally occur between May and July, and minimum air temperatures can occur at any time of the year. Although minimum temperatures are often associated with night, they are also caused by squall (downdraft) events and can occur at any time of the day. January and February exhibit the smallest variation in daily temperature.

The relative humidity in this region is high and its value often exceeds 90 %, varying between 45 % and 100 %. Humidity varies both through the day and seasonally. Minimum humidity generally occurs between May and July, although maximum humidity can occur at any time of the year. Maximum humidity often occurs before dawn and in association with rainfall events.

Atmospheric pressure shows a significant diurnal (twice-daily) cycle caused by global atmospheric tides with a variation in the order of 0.5 kPa (5 mbar). Typically the pressure varies between 100 kPa (1000 mbar) and 102 kPa (1020 mbar), excluding typhoon events when pressure can drop below this range depending on the severity of the typhoon and its track. There are some seasonal variations of pressure, with minimum pressure typically occurring in the April to May monsoon transition, or associated with the passage of a typhoon (typically July to December), and maximum pressures typically occurring with northeast monsoon surges. The range of typical atmospheric pressures increases with latitude.

Visibility is not typically affected by fog in this region, although onshore locations can experience fog or mist most often at dawn. In an El Niño year with the associated dry conditions, haze from dust and smoke due to forest fires can affect visibility over large areas of the East Asian Sea, particularly during the southwest monsoon since the typical sources of smoke particles are Sumatra, Peninsular Malaysia, and Borneo. Smoke and the associated atmospheric condensation can have a significant detrimental effect on visibility. Heavy rain associated with squalls and thunderstorms can also significantly reduce local visibility for short periods.

G.8.5 Seawater Temperature and Salinity

Sea surface temperatures in the East Asian Sea south of 15° N range between 24 °C and 31 °C, and are typically warmer the nearer the equator. Surface water temperatures start to decrease with the onset of the northeast monsoon as the cold water pushes south, with a significant drop in temperature starting in November for offshore Vietnam but typically in December for the other locations, and the minimum monthly mean sea surface temperatures are usually experienced in January. In April, the temperature increases, with the maximum typically occurring in May or June prior to the onset of the southwest monsoon.

The water column is generally stratified for water depths greater than 80 m, except during the northeast monsoon when the wave energy in the monsoon surges acts to break up the thermocline and cause mixing through the water column. For depths of 80 m to 140 m, maximum sea-bottom temperatures are often coincident with the first monsoon surge. Where the water is too shallow for a permanent thermocline, sea-bottom temperatures typically track the surface temperatures.

Sea surface salinities are generally between 32 PSU and 34 PSU. However, there is a significant reduction in salinity near the inflow of major rivers. The most significant of these is the Mekong River, the 12th-largest river in the world, by volume, discharging 475 km³ of water annually. The inflow of this river also acts to significantly reduce water temperatures at times of high flow. Other significant rivers include the Chao Phraya River flowing into the Gulf of Thailand, and the Kuching, Rajang, and Baram rivers flowing into the East Asian Sea from Sarawak.

G.9 Estimates of Metocean Parameters

G.9.1 Extreme Metocean Parameters

G.9.1.1 General

Indicative extreme values for wind, wave, and current parameters are provided in Tables G.1 to G.13 for various return periods and for 13 locations across the waters of offshore Vietnam, the Gulf of Thailand, the waters offshore Peninsular Malaysia, the waters offshore Natuna Island, the waters offshore Borneo, and the waters offshore Philippines. The wind, wave, and current values are independently derived marginal parameters, and no account has been taken of conditional probability. Table G.14 gives indicative values for other metocean parameters for offshore Borneo. As with all values in the regional annexes of this standard, these figures are provided to assist with engineering concept selections and are not suitable for the design of offshore structures.

Extreme-value conditions in most areas of the East Asian Sea are dominated by typhoons, either because of the direct passage of typhoons or due to the swell generated by typhoons. In the areas further south, conditions can be dominated by the northeast monsoon.

G.9.1.2 Waters Offshore Vietnam

Offshore Vietnam, as the location farthest to the north, which is covered in this annex, is subject to the frequent passage of typhoons; the typhoon track is significantly affected by the ENSO, with October, November, and December the months most frequently affected. The area is also significantly influenced by the northeast monsoon.

Table G.1—Offshore Vietnam—Shallow Water

Metocean Parameter	Return Period (years)				
	1	5	10	50	100
Nominal water depth	20 m (10° N, 108° E)				
Wind speed at 10 m above MSL					
1 h mean (m/s)	23.1	25.8	26.7	29.1	30.0
10 min mean (m/s)	26.8	29.9	31.0	33.8	34.8
1 min mean (m/s)	31.9	35.6	36.8	40.2	41.4
3 s gust (m/s)	38.6	43.1	44.6	48.6	50.1
Waves					
Significant height (m)	3.7	4.7	5.4	5.7	6.2
Maximum height (m)	7.1	9.0	10.2	10.7	11.8
Mean period (s)	6.7	7.6	8.1	8.3	8.7
Spectral peak period (s)	9.5	10.7	11.4	11.7	12.3
Wave direction (from)					
Extreme	NE	NE	NE	NE	NE
Prevailing	NE	NE	NE	NE	NE
Current speed					
Surface (m/s)	1.14	1.22	1.31	1.41	1.50

Table G.2—Offshore Vietnam—Deep Water

Metocean Parameter	Return Period (years)				
	1	5	10	50	100
Nominal water depth	1800 m (12° N, 110° E)				
Wind speed at 10 m above MSL					
1 h mean (m/s)	38.5	43.0	44.5	48.5	50.0
10 min mean (m/s)	44.7	49.9	51.6	56.3	58.0
1 min mean (m/s)	53.1	59.3	61.4	66.9	69.0
3 s gust (m/s)	64.3	71.8	74.3	81.0	83.5
Waves					
Significant height (m)	7.3	8.3	8.7	9.6	10.0
Maximum height (m)	13.7	15.5	16.2	17.8	18.6
Mean period (s)	9.4	10.0	10.3	10.8	11.0
Spectral peak period (s)	13.3	14.2	14.5	15.2	15.6
Wave direction (from)					
Extreme	NE	NE	NE	NE	NE
Prevailing	NE	NE	NE	NE	NE
Current speed					
Surface (m/s)	1.75	1.86	2.00	2.16	2.30

G.9.1.3 Gulf of Thailand

The Gulf of Thailand is to some extent protected from both northeast and southwest monsoons; however, typhoons do occasionally track into the Gulf of Thailand, causing extreme wave heights and wind speeds, and make extreme conditions in this area difficult to predict and requiring long data sets. The highest risk months for typhoon activity are October, November, and December.

Table G.3—Gulf of Thailand—North

Metocean Parameter	Return Period (years)				
	1	5	10	50	100
Nominal water depth	75 m (10° N, 101° E)				
Wind speed at 10 m above MSL					
1 h mean (m/s)	35.4	39.6	40.9	44.6	46.0
10 min mean (m/s)	41.1	45.9	47.5	51.8	53.4
1 min mean (m/s)	48.9	54.6	56.5	61.6	63.5
3 s gust (m/s)	59.2	66.1	68.4	74.5	76.8
Waves					
Significant height (m)	7.3	8.3	8.7	9.6	10.0
Maximum height (m)	13.7	15.5	16.2	17.8	18.6
Mean period (s)	9.4	10.0	10.3	10.8	11.0
Spectral peak period (s)	13.3	14.2	14.5	15.2	15.6
Wave direction (from)					
Extreme	E	E	E	E	E
Prevailing	WSW	WSW	WSW	WSW	WSW
Current speed (m/s)					
Surface					

Table G.4—Gulf of Thailand—South

Metocean Parameter	Return Period (years)				
	1	5	10	50	100
Nominal water depth	85 m (8° N, 103° E)				
Wind speed at 10 m above MSL					
1 h mean (m/s)	27.0	30.1	31.2	34.0	35.0
10 min mean (m/s)	31.3	34.9	36.1	39.4	40.6
1 min mean (m/s)	37.2	41.5	43.0	46.9	48.3
3 s gust (m/s)	45.0	50.3	52.0	56.7	58.5
Waves					
Significant height (m)	5.1	5.8	6.1	6.7	7.0
Maximum height (m)	9.7	11.0	11.5	12.6	13.2
Mean period (s)	7.9	8.4	8.6	9.0	9.2
Spectral peak period (s)	11.1	11.9	12.1	12.7	13.0
Wave direction (from)					
Extreme	NE	NE	NE	NE	NE
Prevailing	E	E	E	E	E
Current speed					
Surface (m/s)					

G.9.1.4 Offshore Peninsular Malaysia

Offshore Peninsular Malaysia is protected from the southwest monsoon but exposed to the northeast monsoon. The direct impact of typhoons is less likely due to the low latitude, but their influence should be considered.

Table G.5—Offshore Peninsular Malaysia

Metocean Parameter	Return Period (years)				
	1	5	10	50	100
Nominal water depth	70 m (6° N, 106° E)				
Wind speed at 10 m above MSL					
1 h mean (m/s)	22.3	24.9	25.8	28.1	29.0
10 min mean (m/s)	25.9	28.9	29.9	32.6	33.6
1 min mean (m/s)	30.8	34.4	35.6	38.8	40.0
3 s gust (m/s)	37.3	41.6	43.1	47.0	48.4
Waves					
Significant height (m)	5.8	6.6	7.0	7.7	8.0
Maximum height (m)	11.0	12.5	13.1	14.4	15.0
Mean period (s)	8.4	9.0	9.2	9.7	9.9
Spectral peak period (s)	11.9	12.7	13.0	13.6	13.9
Wave direction (from)					
Extreme	NE	NE	NE	NE	NE
Prevailing	NE	NE	NE	NE	NE
Current speed					
Surface (m/s)					

G.9.1.5 Offshore Natuna Island

Offshore Natuna Island is protected from the southwest monsoon but exposed to the northeast monsoon. The direct impact of typhoons is less likely due to the low latitude, but their influence should be considered.

Table G.6—Offshore Natuna Island (South Natuna Sea)

Metocean Parameter	Return Period (years)				
	1	5	10	50	100
Nominal water depth	60 m (3.5° N, 106° E)				
Wind speed at 10 m above MSL					
1 h mean (m/s)	20.0	22.4	23.1	25.2	26.0
10 min mean (m/s)	23.2	25.9	26.8	29.3	30.2
1 min mean (m/s)	27.6	30.9	31.9	34.8	35.9
3 s gust (m/s)	33.4	37.3	38.6	42.1	43.4
Waves					
Significant height (m)	5.1	5.8	6.1	6.7	7.0
Maximum height (m)	9.7	11.0	11.5	12.6	13.2
Mean period (s)	7.9	8.4	8.6	9.0	9.2
Spectral peak period (s)	11.1	11.9	12.1	12.7	13.0
Wave direction (from)					
Extreme	NE	NE	NE	NE	NE
Prevailing	NE	NE	NE	NE	NE
Current speed					
Surface (m/s)					

Table G.7—Offshore Natuna Island (North Natuna Sea)

Metocean Parameter	Return Period (years)				
	1	5	10	50	100
Nominal water depth	140 m (5° N, 110° E)				
Wind speed at 10 m above MSL					
1 h mean (m/s)	22.3	24.9	25.8	28.1	29.0
10 min mean (m/s)	25.9	28.9	29.9	32.6	33.6
1 min mean (m/s)	30.8	34.4	35.6	38.8	40.0
3 s gust (m/s)	37.3	41.6	43.1	47.0	48.4
Waves					
Significant height (m)	5.8	6.6	7.0	7.7	8.0
Maximum height (m)	11.0	12.5	13.1	14.4	15.0
Mean period (s)	8.4	9.0	9.2	9.7	9.9
Spectral peak period	11.9	12.7	13.0	13.6	13.9
Wave direction (from)					
Extreme	NNE	NNE	NNE	NNE	NNE
Prevailing	NE	NE	NE	NE	NE
Current speed					
Surface (m/s)	114	122	131	141	150

G.9.1.6 Waters Offshore Borneo

The relative influence of the northeast and southwest monsoons varies across the waters offshore Borneo, with the northeast monsoon dominating in the western part, but reducing in the eastern part due to sheltering provide by the Philippines. Conversely, the longer fetch length means that the southwest monsoon becomes more significant in the eastern part. The direct impact of typhoons is less likely due to the low latitude, but their influence should be considered and can still dominate design considerations.

Table G.8—Offshore Borneo—Sarawak Shallows

Metocean Parameter	Return Period (years)				
	1	5	10	50	100
Nominal water depth	70 m				
Wind speed at 10 m above MSL					
1 h mean (m/s)	18.5	20.6	21.4	23.3	24.0
10 min mean (m/s)	21.4	23.9	24.8	27.0	27.8
1 min mean (m/s)	25.5	28.5	29.5	32.1	33.1
3 s gust (m/s)	30.9	34.5	35.7	38.9	40.1
Waves					
Significant height (m)	4.0	4.6	4.8	5.3	5.5
Maximum height (m)	7.7	8.7	9.1	10.0	10.4
Mean period (s)	7.0	7.5	7.6	8.0	8.2
Spectral peak period (s)	9.9	10.5	10.8	11.3	11.5
Wave direction (from)					
Extreme	N	N	N	N	N
Prevailing	NNE	NNE	NNE	NNE	NNE
Current speed					
Surface (m/s)	1.06	1.13	1.22	1.32	1.40

Table G.9—Offshore Borneo—Sarawak Shelf Edge

Metocean Parameter	Return Period (years)				
	1	5	10	50	100
Nominal water depth	140 m				
Wind speed at 10 m above MSL					
1 h mean (m/s)	21.6	24.1	24.9	27.2	28.0
10 min mean (m/s)	25.0	27.9	28.9	31.5	32.5
1 min mean (m/s)	29.8	33.2	34.4	37.5	38.6
3 s gust (m/s)	36.0	40.2	41.6	45.4	46.8
Waves					
Significant height (m)	5.5	6.3	6.6	7.3	7.6
Maximum height (m)	10.5	11.9	12.5	13.7	14.2
Mean period (s)	8.2	8.8	9.0	9.4	9.6
Spectral peak period (s)	11.6	12.4	12.6	13.3	13.6
Wave direction (from)					
Extreme	NW	NW	NW	NW	NW
Prevailing	NNE	NNE	NNE	NNE	NNE
Current speed					
Surface (m/s)	1.56	1.66	1.78	1.93	2.05

Table G.10—Offshore Borneo—Sabah Shallows

Meteocean Parameter	Return Period (years)				
	1	5	10	50	100
Nominal water depth	50 m				
Wind speed at 10 m above MSL					
1 h mean (m/s)	20.0	22.4	23.1	25.2	26.0
10 min mean (m/s)	23.2	25.9	26.8	29.3	30.2
1 min mean (m/s)	27.6	30.9	31.9	34.8	35.9
3 s gust (m/s)	33.4	37.3	38.6	42.1	43.4
Waves					
Significant height (m)	3.7	4.2	4.4	4.8	5.0
Maximum height (m)	6.6	7.5	7.9	8.6	9.0
Mean period (s)	6.5	6.9	7.1	7.4	7.6
Spectral peak period (s)	10.1	10.7	11.0	11.5	11.8
Wave direction (from)					
Extreme	W	W	W	W	W
Pervailing	NNE/W	NNE/W	NNE/W	NNE/W	NNE/W
Current speed					
Surface (m/s)	0.99	1.05	1.13	1.22	1.30

Table G.11—Offshore Borneo—Sabah Shelf Edge

Metocean Parameter	Return Period (years)				
	1	5	10	50	100
Nominal water depth	120 m				
Wind speed at 10 m above MSL					
1 h mean (m/s)	20.8	23.2	24.0	26.2	27.0
10 min mean (m/s)	24.1	26.9	27.9	30.4	31.3
1 min mean (m/s)	28.7	32.0	33.2	36.1	37.3
3 s gust (m/s)	34.7	38.8	40.1	43.7	45.1
Waves					
Significant height (m)	4.9	5.6	5.8	6.4	6.7
Maximum height (m)	9.3	10.6	11.1	12.2	12.7
Mean period (s)	7.3	7.8	8.0	8.4	8.5
Spectral peak period (s)	10.3	11.0	11.2	11.8	12.0
Wave direction (from)					
Extreme	WNW	WNW	WNW	WNW	WNW
Prevailing	NNE/W	NNE/W	NNE/W	NNE/W	NNE/W
Current speed					
Surface (m/s)	2.13	2.27	2.44	2.63	2.80

Table G.12—Offshore Borneo—Sabah Deepwater

Metocean Parameter	Return Period (years)				
	1	5	10	50	100
Nominal water depth	1500 m				
Wind speed at 10 m above MSL					
1 h mean (m/s)	20.8	23.2	24.0	26.2	27.0
10 min mean (m/s)	24.1	26.9	27.9	30.4	31.3
1 min mean (m/s)	28.7	32.0	33.2	36.1	37.3
3 s gust (m/s)	34.7	38.8	40.1	43.7	45.1
Waves					
Significant height (m)	5.1	5.8	6.1	6.7	7.0
Maximum height (m)	9.7	11.0	11.5	12.7	13.2
Mean period (s)	7.7	8.2	8.4	8.8	9.0
Spectral peak period (s)	10.8	11.5	11.8	12.4	12.7
Wave direction (from)					
Extreme	NW	NW	NW	NW	NW
Prevailing	NNE/WSW	NNE/WSW	NNE/WSW	NNE/WSW	NNE/WSW
Current speed					
Surface (m/s)	1.40	1.56	1.64	1.80	1.86

G.9.1.7 Offshore Philippines

Offshore Philippines (Palawan Island), being in the north of the area covered in this annex, is subject to the frequent passage of typhoons, both those that cross into the East Asian Sea and those that remain east of the Philippines. Although the typhoon track is significantly affected by the ENSO, typhoons can typically influence the area from May to December.

Table G.13—Offshore Philippines—Palawan Area

Metocean Parameter	Return Period (years)				
	1	5	10	50	100
Nominal water depth	1000 m				
Wind speed at 10 m above MSL					
1 h mean (m/s)	38.5	43.0	44.5	48.5	50.0
10 min mean (m/s)	44.7	49.9	51.6	56.3	58.0
1 min mean (m/s)	53.1	59.3	61.4	66.9	69.0
3 s gust (m/s)	64.3	71.8	74.3	81.0	83.5
Waves					
Significant height (m)	11.7	13.3	13.9	15.4	16.0
Maximum height (m)	21.6	24.4	25.5	28.1	29.2
Mean period (s)	11.9	12.7	13.0	13.7	14.0
Spectral peak period (s)	16.8	17.9	18.3	19.3	19.7
Wave direction (from)					
Extreme	NNW	NNW	NNW	NNW	NNW
Prevailing	NNE/WSW	NNE/WSW	NNE/WSW	NNE/WSW	NNE/WSW
Current speed (m/s)					
Surface	1.22	1.30	1.39	1.50	1.60

Table G.14—Indicative Extreme Values for Other Metocean Parameters

Metocean Parameter	Temperature (°C)				
	1-Year	5-Year	10-Year	50-Year	100-Year
Minimum					
Air	22.4	22.0	21.8	21.2	21.0
Sea surface	23.1	22.7	22.5	22.1	22.0
Seabed at					
1000 m	4.1	4.1	4.0	4.0	4.0
800 m	4.6	4.6	4.5	4.5	4.5
600 m	6.6	6.6	6.6	6.5	6.5
400 m	8.4	8.3	8.3	8.2	8.2
200 m	11.4	11.4	11.3	11.2	11.2
140 m	14.0	13.8	13.7	13.6	13.5
80 m	18.8	18.6	18.5	18.3	18.2
20 m	24.3	24.0	23.8	23.6	23.0
Air humidity (%)	43	38	37	35	35
Maximum					
Air	36.8	37.9	38.4	39.5	39.9
Sea surface	33.7	34.4	34.6	35.1	35.4
Seabed at					
1000 m	5.8	5.9	5.9	6.0	6.0
800 m	6.4	6.5	6.5	6.6	6.6
600 m	8.7	8.8	8.9	9.0	9.0
400 m	11.7	11.8	11.9	12.0	12.0
200 m	20.4	20.6	20.7	20.9	21.0
140 m	25.5	25.7	25.8	25.9	26.0
80 m	30.4	30.6	30.7	30.9	31.0
20 m	32.8	33.1	33.2	33.4	33.5
Air humidity (%)	100	100	100	100	100

G.9.2 Long-term Distribution of Metocean Parameters—The Impact of Climate Change

In climate studies and models, the areas near the equator seem to be the least affected by climate change and so far have experienced smaller changes in temperature and precipitation than other areas. However, the East Asian Sea's extreme weather events are affected by phenomena outside the equatorial belt and are likely to be impacted by climate change, including:

- the mode and periodicity of the El-Niño–Southern Oscillation (ENSO);
- the severity of the Siberian high pressure forming in the northern hemisphere winter;
- the severity of the Australian high pressure forming in the southern hemisphere winter;
- the precipitation associated with cyclonic events in the Pacific;
- the frequency of typhoons and range of typhoon tracks in the East Asian Sea.

There is evidence that there have been some changes (possibly due to climate change) that act to weaken the monsoon circulation and reduce cyclonic activity in the East Asian Sea. However, there are also indications that the variability associated with all of the above might increase, and the timescales of any oscillation might change, making it important to use longer databases to achieve a good understanding of such variability and also the longer-term implication of the global changes. However, the low occurrence rates of tropical storms near the equator make determining the probability of such events in terms of metocean design criteria very difficult.

Annex H (informative)

US Gulf of Mexico

H.1 Description of Region

The geographical extent of the region is the waters of the Gulf of Mexico that fall within the United States exclusive economic zone, which is generally the portion of the Gulf of Mexico north of 26 °N, as shown in Figure H.1, and which includes the lease blocks shown in Figure H.2 and Figure H.3.

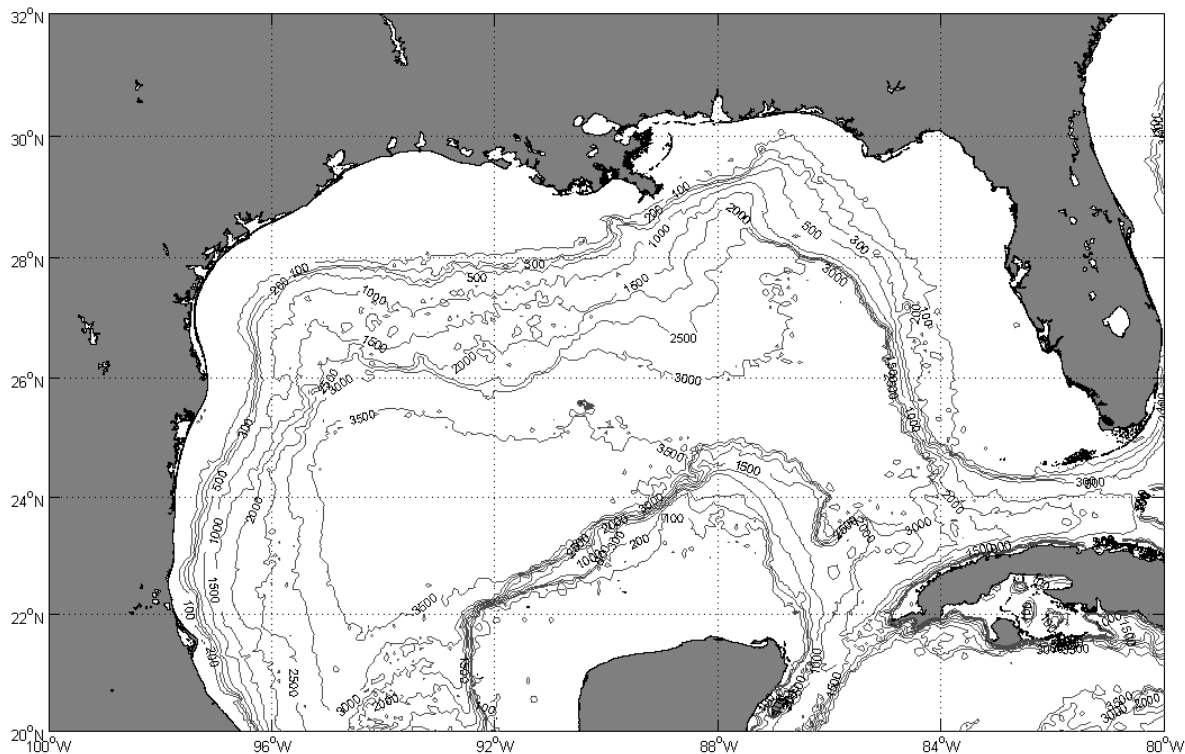


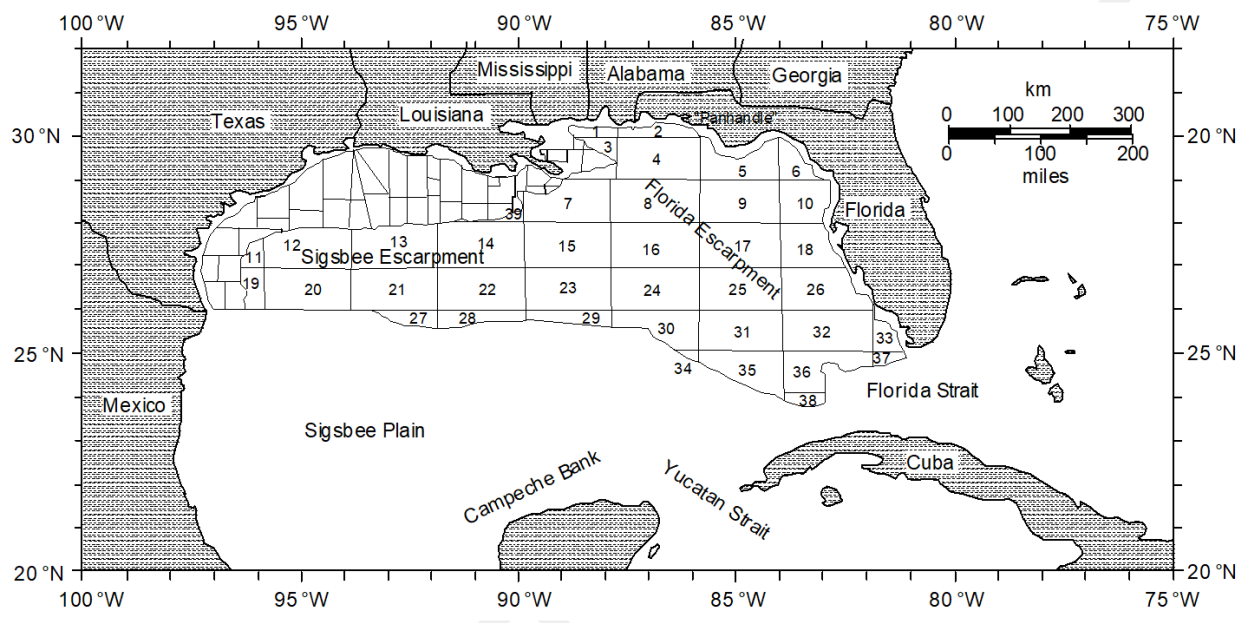
Figure H.1—Gulf of Mexico (Bathymetry in m)

The Gulf of Mexico has a total area of 1,587,000 km². The US Gulf coast is 2625 km long and comprises the coasts of the following US states (from west to east with coastline lengths):

- Texas 591 km;
- Louisiana 639 km;
- Mississippi 71 km;
- Alabama 85 km;
- Florida 1239 km (Gulf coastline only).

Offshore Florida, Alabama, and Mississippi, the width of the continental shelf varies between 25 km and 125 km wide, with water depths at the shelf break of between 60 m and 100 m. Further west, off the Mississippi River delta, the continental shelf width is less than 20 km and increases to 200 km offshore central and western Louisiana and Texas. Waters along the shelf are generally less than 100 m deep. Water depths off the shelf can exceed 3000 m.

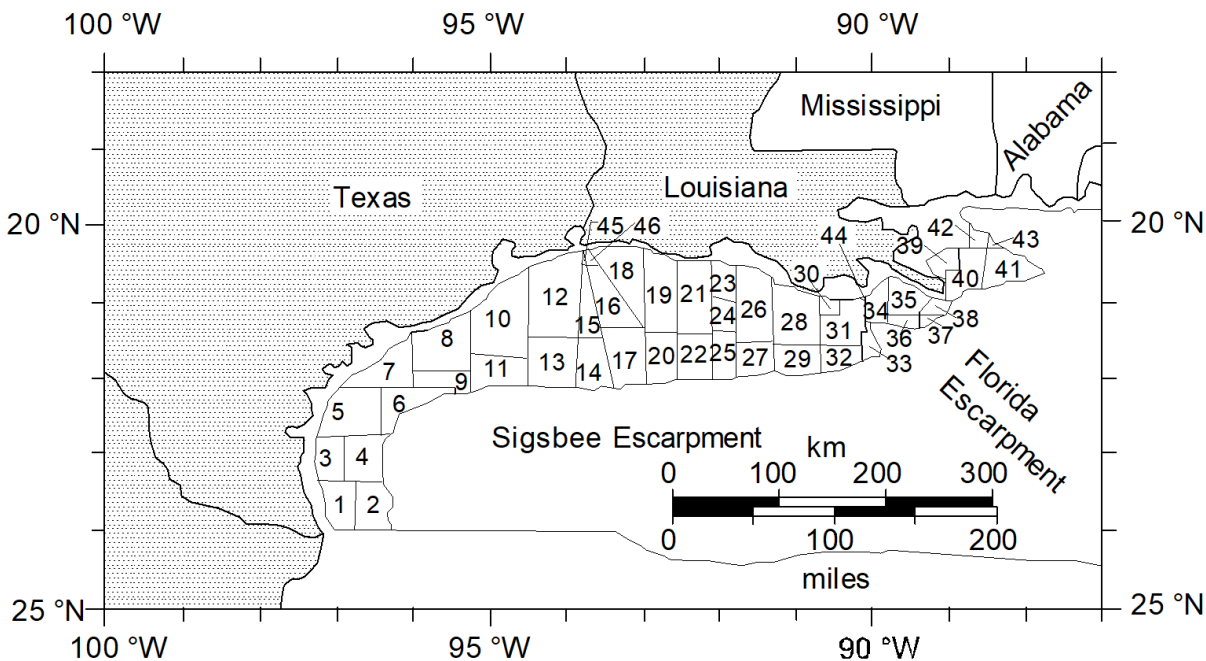
Freshwater runoff from approximately two-thirds of the continental United States empties into the northern Gulf, with most of the inflow coming via the Mississippi River.



Key to lease block names

1	Mobile	14	Green Canyon	27	Sigsbee Escarpment
2	Pensacola	15	Atwater Valley	28	Amery Terrace
3	Viosca Knoll	16	Lloyd Ridge	29	Lund South
4	Destin Dome	17	The Elbow	30	Florida Plain
5	Apalachicola	18	Saint Petersburg	31	Howell Hook
6	Gainesville	19	Port Isabel	32	Pulley Ridge
7	Mississippi Canyon	20	Alaminos Canyon	33	Miami
8	De Soto Canyon	21	Keathley Canyon	34	Campeche Escarpment
9	Florida Middle Ground	22	Walker Ridge	35	Rankin
10	Tarpon Springs	23	Lund	36	Dry Tortugas
11	Corpus Christi	24	Henderson	37	Key West
12	East Breaks	25	Vernon Basin	38	Tortugas Valley
13	Garden Banks	26	Charlotte Harbor	39	Ewing Bank

Figure H.2—US Outer Continental Shelf and Deep Water Lease Areas



Key to lease block names

1	South Padre Island	17	West Cameron South	33	Grand Isle
2	South Padre Island East	18	West Cameron	34	Grand Isle
3	North Padre Island	19	East Cameron	35	West Delta
4	North Padre Island East	20	East Cameron South	36	West Delta South
5	Mustang Island	21	Vermilion	37	South Pass South & East
6	Mustang Island East	22	Vermilion South	38	South Pass
7	Matagorda Island	23	South Marsh Island North	39	Breton Sound
8	Brazos	24	South Marsh Island	40	Main Pass
9	Brazos South	25	South Marsh Island South	41	Main Pass South & East
10	Galveston	26	Eugene Island	42	Chandeleur
11	Galveston South	27	Eugene Island South	43	Chandeleur East
12	High Island	28	Ship Shoal	44	Bay Marchand
13	High Island South	29	Ship Shoal South	45	Sabine Pass (TX)
14	High Island East South	30	South Peltot	46	Sabine Pass (LA)
15	High Island East	31	South Timbalier		
16	West Cameron West	32	South Timbalier South		

Figure H.3—US Inner Continental Shelf Lease Areas

H.2 Data Sources

The northern offshore area of the Gulf of Mexico is one of the most studied regions in terms of its meteorology and physical oceanography. Wind, wave, and meteorological measurements have been made at many stations throughout the area over the past 30 years, both on and off the continental shelf. Much of these data have been recorded under sponsorship of the US government and are available from the National Data Buoy Center [65]. Extensive data on the statistics and climatology of tropical cyclones affecting the Gulf of Mexico may be obtained from the archives of the National Hurricane Center [104]; however, there is evidence that cyclone data from the early (pre-1950) period are biased low [126, 127].

Various industry-sponsored measurement programs have also been conducted, and data are generally available for purchase or trade.

In addition to measured wind and wave data, several important industry-sponsored numerical hindcast studies of both extreme and operational winds and waves (including storm surges and storm currents) have been performed, most notably the Gulf of Mexico Storm Hindcast of Oceanographic Extremes (GUMSHOE^[66]) and Winter Extremes (WINX^[67]) studies from the early 1990s, and more recently the proprietary Gulf of Mexico Oceanographic Study (GOMOS^[68]). The US Army Corps of Engineers (USACE) MORPHOS numerical studies provide an additional source of information for storm surges and shallow water wave conditions^[105]. Select wind, wave, current, and surge hindcasts of individual major hurricanes have also been sponsored by the US Minerals Management Service (MMS); its successor organization, the Bureau of Ocean Energy Management, Regulation, and Enforcement (BOEMRE); and finally the Bureau of Safety and Environmental Enforcement (BSEE) and the Bureau of Ocean Energy Management (BOEM), which replaced BOEMRE in 2011^[106].

A number of current and water quality measurements (temperature, salinity, chemical composition) have also been made in the region over the years, both in shallow and deep water. Many of these studies have been sponsored by the MMS^[69 to 71]. In 1982, MMS began a series of data collection programs starting in the eastern Gulf^[72] and culminating in 1985 with the LATEX study of the central northern Gulf. The LATEX study results have been archived with the National Oceanographic Data Center (NODC)^[70]. MMS contracted with Texas A&M University to reanalyse and synthesize all available data (including some industry data) on the Gulf; the results of this comprehensive study were published in 2001^[73]. BOEM has supported studies of deep water Gulf currents as part of its Gulf of Mexico Region's Environmental Studies Program^[109]. Measurements made along the Sigsbee Escarpment as part of this program provide data on topographic Rossby waves (TRWs).

The industry has also taken an active role in collecting measurements^[74]. The Eddy joint industry project (EJIP), an industry collaborative effort, has sponsored measurements in the deeper waters of the region over the period from 1983 through 2004. The Climatology and Simulation of Eddies (CASE) joint industry project, another industry effort, used the EJIP data to develop numerical models for use in estimating design currents in deep water associated with the Loop Current and warm eddies, the most notable being the Gulf Eddy Model (GEM)^[107] and a corresponding historical hindcast database of eddies and Loop Current intrusions. CASE and EJIP merged in 2005 to become CASE-EJIP, and since that time have sponsored numerical models for eddy forecasting, investigations of cold core eddies, updates to the GEM hindcast database (through 2013 as of the date of this document), hurricane and Loop Current/eddy interaction (both wave fields and currents), development of a new synthetic eddy model and studies of storm wave crests. The ongoing EddyWatch^[108] program in the Gulf of Mexico is also a source of historical eddy observations. Eddy tracking with satellite data and drifting buoys is now routine in the Gulf, and forecast services are available from several vendors.

The industry DeepStar^[110] program also supports research into the Gulf of Mexico environment; recent projects have included an evaluation of Loop Current forecast models, an examination of the connection between the frequency of intense hurricanes and the presence of the Loop Current, and a numerical study of TRWs.

H.3 Overview of Regional Climatology

The climate in the Gulf of Mexico ranges from tropical to temperate. Summer wind and wave conditions are generally benign, with warm temperatures and high relative humidity. Some coastal areas are periodically affected by fog. In winter there are occasional freezes in the coastal areas. Sea ice and snow are not encountered in the Gulf.

There are occasional thunderstorms, squalls, waterspouts, and on rare occasion, tornadoes in the coastal areas. Overall the storm climate in the Gulf is dominated by tropical cyclones in the summer season and extratropical cyclones and cold air intrusions in the winter season.

Locally, tropical cyclones are referred to as a tropical depression if the maximum 10 m 1 min sustained wind is less than 17.5 m/s, a tropical storm if the wind is between 17.5 and 32.9 m/s, and a hurricane if the wind is greater than or equal to 32.9 m/s.

The North Atlantic Basin Hurricane Season, which includes the Gulf of Mexico, officially runs from June 1 through November 30; however, tropical cyclones have occurred in every calendar month. The months typically seeing the highest frequency of tropical cyclone activity are August, September, and October. On average, three tropical storms or hurricanes can be expected to form in or enter the Gulf each year, although the number is highly variable. These storms can originate in the Gulf, the Caribbean Sea, or in the North Atlantic Ocean, with the largest most intense storms generally being those that form outside the Gulf and propagate into it (see Figure H.4 for typical storm tracks). Cyclones that bring tropical storm force winds to the operating areas of the Gulf of Mexico within 24 h of storm genesis are generally referred to as "sudden storms." Tropical cyclone activity is believed related to cycles in the North Atlantic Oscillation (NAO) and "El Niño" events, and hence there may exist decadal variations in severity patterns. There is much debate about the effect of global climate change on tropical cyclone activity [133, 134]. Changes in storm occurrence rates, central pressure, and track positions are possible and could affect the long-term distribution of extreme wind, wave, and current conditions. There is also strong evidence that within the Gulf of Mexico the presence of the Loop Current and eddies from it (described below) are responsible for regional variations of the rate of encounter of large intense hurricanes [122, 124, 125, 135].

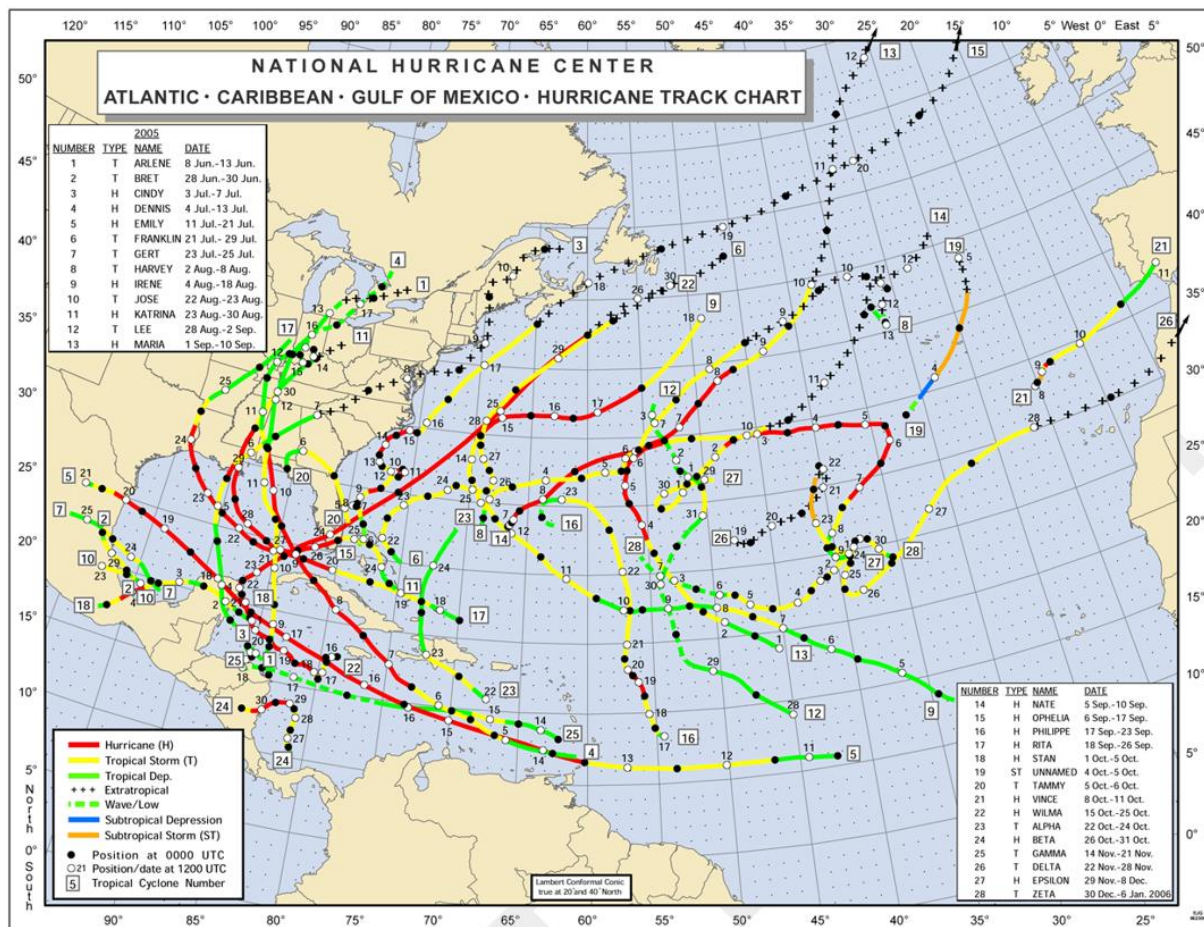


Figure H.4—Tracks of Tropical Cyclones, 2005

The most severe extratropical cyclones and cold air intrusions generally occur in the months of October through March, hence the local term “winter storms.” Fronts associated with extratropical cyclones generally move over the Gulf from the north, or sweep across the Gulf from west to east. The cyclone centers are generally located well to the north of the Gulf, but on occasion enter it or actually form within it. Depending on the geometry of passage, an extratropical storm may generate strong winds from the southeast, and will hence be referred to as a “Southeaster.” Cold air intrusions can also result in severe storm conditions in the Gulf. These events, typically referred to as “Northerns,” consist of intrusions of cold arctic air out over the Gulf behind cold fronts^[76]; the cold air overlying the relatively warmer Gulf waters results in an unstable atmosphere and consequently strong winds and rain.

An important oceanographic feature of the deep water Gulf is the Loop Current (see Figure H.5). The Loop Current is a warm-water current that enters the Gulf through the Yucatan Strait, flows generally northward in the eastern Gulf, then turns southward along the west Florida coast, and exits through the Florida Strait as the Florida Current. It is detectable to around 800 m below the surface. A characteristic of the Loop Current is its periodic northward intrusion into the eastern Gulf; these intrusions occur every 4 to 16 months. The northward penetration of the Loop usually reaches about 28–29° N and is followed by the shedding of a large eddy (a Loop Current Eddy, also known as a Warm Core Eddy) with a diameter ranging from 150 to 450 km with clockwise rotation. After an eddy is shed, the Loop Current retracts to the south, usually below 26° N, and starts the cycle again.

After separating, a Loop Current Eddy can attach and detach several times. Eventually, the eddy moves to the west or southwest at an average translation speed of about 3 km/day. The energy of the eddy slowly decays to about half its original strength by the time it gets to the western Gulf. There, the Loop Current Eddy usually slowly breaks down into a series of smaller cyclonic and anti-cyclonic eddies. The dissipation process can take more than a year.

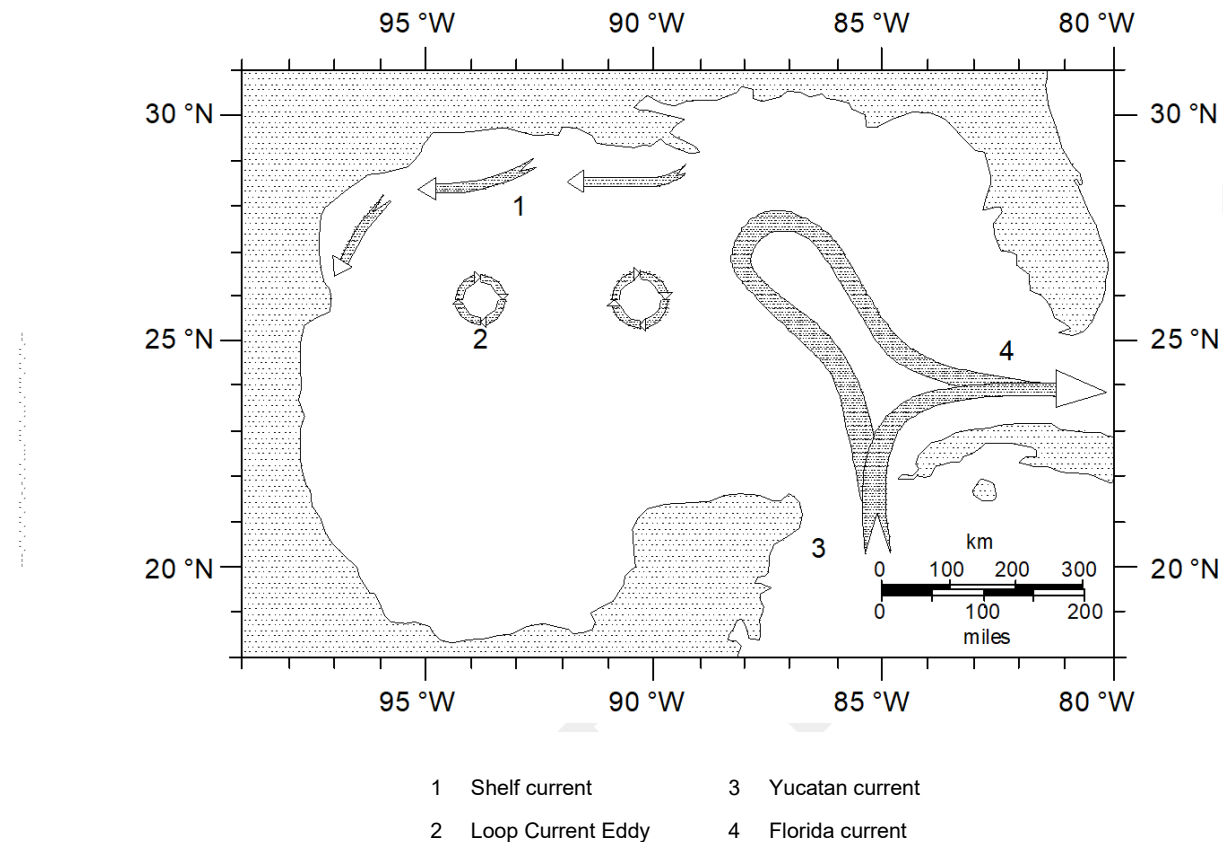


Figure H.5—Circulation in the Gulf of Mexico

H.4 Water Depth, Tides, and Storm Surge

Tides in much of the US Gulf of Mexico can be characterized as diurnal, although some areas of the Florida coast show semi-diurnal behavior, whereas others along the Texas coast are mixed semi-diurnal. Tide range is generally less than 1.0 m in near shore areas, and decreases rapidly offshore to about 0.3 m in deep water.

With the modest tide ranges within the Gulf, mean lower low water (MLLW) and mean higher high water (MHHW) are often taken as the low and high water references for Gulf of Mexico metocean criteria. MLLW is the average of the lower low water height of each tidal day. Likewise, MHHW is the average of the higher high water height of each tidal day.

The highest storm surge in the Gulf results primarily from the passage of hurricanes and can exceed 8 m along the low-lying coastal areas as in Hurricane Katrina (2005) [112]. Surge decreases offshore, but can still reach levels of 1 m in deep water [75]. Winter storms will not generally create high surge conditions along the northern Gulf coast; however, some events like the "Storm of the Century" (1993) have caused surges in excess of 3 m along the Florida coast [113].

H.5 Winds

The mean background wind flow in the northern portion of the Gulf of Mexico is governed by the mid-latitude westerlies, whereas in the southern portion, south of 26 °N, it is dominated by the easterly trade winds. The general circulation is controlled by the North Atlantic subtropical high (known as the Bermuda High when it is in the western portion of the Atlantic). Anti-cyclonic flow around the southern edge of the Bermuda High produces the Trade Winds.

Winds from hurricanes will dominate extreme design conditions. In addition to generating 1 h 10 m winds in excess of 30 m/s, the passage of a hurricane is associated with high seas, heavy rain, and strong currents in the upper layer of the ocean. The most intense hurricanes will generate 1 min 10 m winds in excess of 69 m/s. The direction of the wind at a particular site depends on the direction of hurricane travel, and its position relative to the site. Tropical storms and hurricanes are relatively localized events, even when considering large storms (see Figure H.6); the most severe winds are generally within 100 km of the storm track, and conditions are more severe on the right side of the storm track. The passage of a hurricane typically affects a site for 24 h or less. Hurricane severity is often reported with reference to the Saffir-Simpson wind speed scale; it is emphasized that this scale is solely a measure of sustained wind speeds, and may be an extremely poor indicator of how severe other environment conditions such as waves and surge may be. An example of this is Hurricane Ike (2008), which while being a Category 2 storm, generated wave heights and surge levels commonly associated with more intense storms by virtue of its large size and slow speed.

Extratropical cyclones and cold air intrusions will dominate conditions outside the summer months, generating 1 h 10 m winds in excess of 15 m/s. Gusty winds and rain associated with their passage will affect large areas of the Gulf and can last for several days. Severe occurrences of these winter storms can produce 1 h 10 m winds exceeding gale force (24.5 m/s).

For the Gulf of Mexico, wind profiles and time-averaging relations appropriate for winter storms conditions are defined in A.7.3.2, for hurricanes (tropical cyclones) are defined in A.7.3.3, and for squalls are defined in A.7.3.4. Wind spectra for appropriate for winter storm conditions are defined in A.7.4.2 and for hurricanes are defined in A.7.4.3. Squalls are highly transient events and are normally analyzed in the time domain.

Thunderstorms, squalls, waterspouts, and on rare occasion tornadoes will also be encountered in the Gulf of Mexico. The 10-year 1 min 10 m peak wind associated with squalls is nearly 30 m/s. Waterspouts may produce localized 3 s 10 m gusts in excess of 30 m/s. Tornadoes are generally not considered as a design condition in the Gulf of Mexico due to their infrequency and small area of effect (northern edge of the Gulf, and small spatial scale).

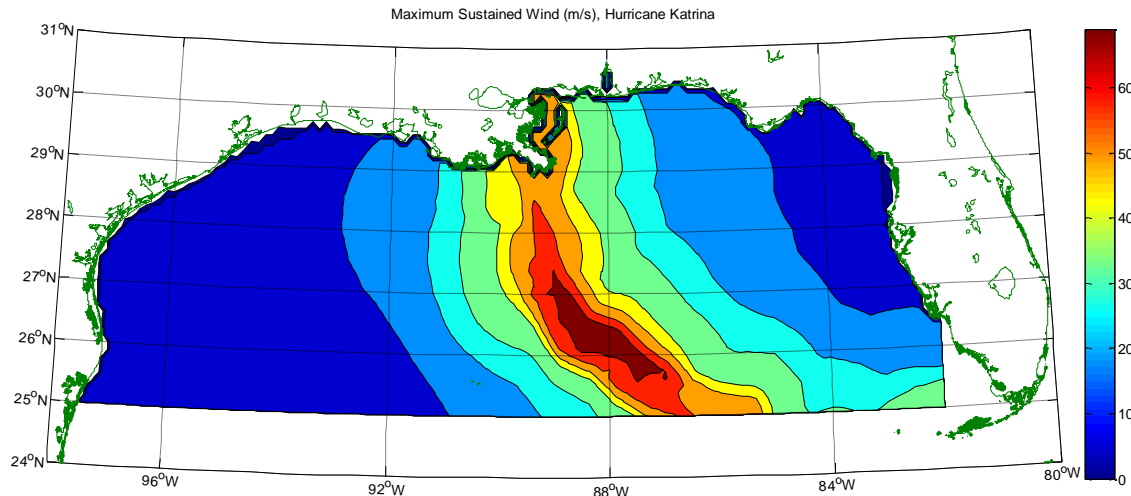


Figure H.6—Maximum Sustained Wind Speed—Hurricane Katrina (2005)

H.6 Waves

The Gulf of Mexico is effectively a semi-enclosed sea. While strong winds can occur over the whole region, the wave characteristics vary according to the water depth and fetch over which they are generated.

Most of the waves in the northern Gulf are less than 3 m in height. Summer wave heights are typically 1.5 m or less, with wave periods in the range of 4 to 8 s. There are occasional episodes of long-period swell propagating into the region via the Florida Strait or the Yucatan Channel during the summer months, but this is not considered a significant design condition.

The highest waves encountered in the Gulf are generated by intense hurricanes. In deep water, peak seas (H_s) generated by hurricanes can exceed 16 m, with individual waves in excess of 30 m. The highest seas are generally within 100 km of the storm track and typically affect a site for 24 h or less. The highest seas will be found on the right side of the storm track. To date, there have been no published high-quality measurements of rogue or freak waves in Gulf of Mexico tropical cyclones, whereas measurements made during storms such as Ivan [123] clearly show large individual waves, the largest do not appear statistically unexpected. Hurricane waves on the continental shelf are reduced somewhat by shoaling and refraction effects, and are depth-limited in the shallow areas. In shallow water close to shore, the highest waves in a hurricane will generally occur at the same time as the highest storm surge. Hurricane-generated seas tend to be fairly confused and short-crested, and exhibit more spreading than those generated by winter storms. Wave spreading can generally be represented using the form $\cos^n(\theta)$ as described in A.8.3.2.1, with n in the range of 2.0 to 2.5; a corresponding wave kinematics factor of 0.88 is typically applied. The wave spectrum is typically defined by the JONSWAP form shown in A.8.3.1.2 with a γ in the range of 1.5 to 2.6.

Severe winter storms usually produce seas in excess of 6 m; however, events-generating seas of 9 m have been observed. High seas associated with winter storms often persist for several days. Winter storm seas tend to be longer-crested, due to the large spatial nature of these storms. Wave spreading can generally be represented using the form $\cos^n(\theta)$ as described in A.8.3.2.1, with $n \geq 4.0$; a wave kinematics factor of 0.91 to 1.0 is typically applied. The wave spectrum is typically defined by the JONSWAP form shown in A.8.3.1.2 with a γ in the range of 1.0 to 3.3.

The presence of the Loop Current or a Loop Current Eddy may have significant effects on the wave fields generated by hurricanes and winter storms. Recent numerical studies [117] indicate that the surface current field of a Loop Current Eddy may result in the focusing of the storm wave field, resulting in higher effective sea states as compared to ignoring the presence of the current.

H.7 Currents

Currents in the Gulf vary substantially according to location. On the continental shelf (less than 100 m depth), currents are primarily driven by the local wind. Tidal currents in most of the Gulf are negligible (less than 0.1 m/s) compared to the other current processes and are noticeable only in areas where the flow is constrained by the topography, such as river mouths, passes between islands, and near the Florida panhandle. The Mississippi River can have a substantial influence at sites up to 100 km away.

In the deep waters (300+ m) of most of the Gulf, currents are dominated by the Loop Current and its associated eddies. The Loop Current either directly or indirectly influences the deep water circulation of the entire northern Gulf. In the eastern and central Gulf, Loop Current intrusions and Loop Current eddies can generate surface currents with speeds on the order of 2.5 m/s, and moderate (1.0 m/s) speeds over a substantial portion of the water column (300 m). Currents from Loop Current eddies are somewhat weaker in the western Gulf. The Loop Current or one of its eddies can affect a site for weeks.

Hurricanes drive the extremes in shallow water and the transition regions to 300 m. Hurricane-generated currents on the shelf can exceed 2.0 m/s. These currents will generally flow westward parallel to the smoothed local bathymetry, peaking in strength several hours after the passage of a storm and persisting for several days. Hurricanes also generate strong currents in deep waters of the Gulf because of the strong winds and shallow mixed-layer (30 m) found during hurricane season. Measurements show intense hurricanes can generate currents in excess of 2.0 m/s near the surface, and generate substantial currents at depths of 100 m or more. These currents will also generally peak several hours after the passage of a storm and will persist for 3 to 5 days. In deep water far from the continental slope, the current direction will rotate clockwise in time under the action of Coriolis force as the current speed decays following the passage of a storm. For the latitude range of the Gulf, the current heading will rotate a full 360° clockwise approximately every 25 h or so. Close to a steep slope, the current direction in deep water will appear fairly uniform, with the flow directed west parallel to the local bathymetry. Hurricane inertial currents can be traced to depths beyond 1000 m. The decay of these events shows in the water column as a series of inertial oscillations that propagate downward (and horizontally) over several days, in some cases generating currents near 1.0 m/s at depths of 700 m or more.

Recent analyses of measurements have indicated that the deepwater jet phenomenon once suspected of being generated by small intense cold eddies does not exist^[119]. However, measurements and numerical modeling efforts^[116] indicate that there can be a nonlinear coupling between inertial currents generated by a hurricane and currents generated along the front of a Loop Current Eddy, leading to very strong (1.0 m/s or more) jet-type currents at 200 m to 300 m several days after the passage of a hurricane across an eddy front.

Another important current phenomenon in the deep Gulf is currents generated by TRWs. Rossby waves are planetary waves with wave lengths of several hundred kilometers and periods on the order of 2 weeks. TRWs typically generate bottom currents less than 0.25 m/s; however, in areas of steep bathymetry such as that near Green Knoll and the Sigsbee Escarpment, they can become enhanced, i.e. their energy is trapped and amplified, resulting in bottom current speeds in excess of 1.0 m/s. TRW currents are strongest parallel to the bathymetry, and an event will typically consist of several current "pulses" each 3 to 7 days in duration. The mechanism by which TRWs are generated in the Gulf is not well understood; however, there is evidence that they are related to the movement of the Loop Current or the presence of Loop Current eddies. There are also recorded incidents of them affecting sites simultaneously with Loop Current eddies^[136].

H.8 Other Environmental Factors

H.8.1 Air Temperature and Humidity

Air temperatures over the Gulf typically range from 10 °C to 30 °C in the areas within 200 km of the coast, with winter lows close to freezing (0 °C) and summer highs above 34 °C. Lows in the southern portion of the US Gulf tend to range 5 °C to 10 °C higher than those in the north. Relative humidity averages 70 to 80% over the year, and is generally highest in the summer months.

H.8.2 Sea Temperature

Surface sea temperatures range from 20 °C to 30 °C during the year, with the water stratified into a warm upper layer approximately 30 m deep in the summer, and 70 m deep in the winter. Surface temperatures in the northern Gulf trend 3 °C to 4 °C cooler than those in the southern Gulf during winter. Bottom temperatures in the deeper (1000+ m) parts of the Gulf are generally 4 °C to 5 °C. The annual range of sea temperatures for a location in the western Gulf of Mexico is shown in Figure H.7.

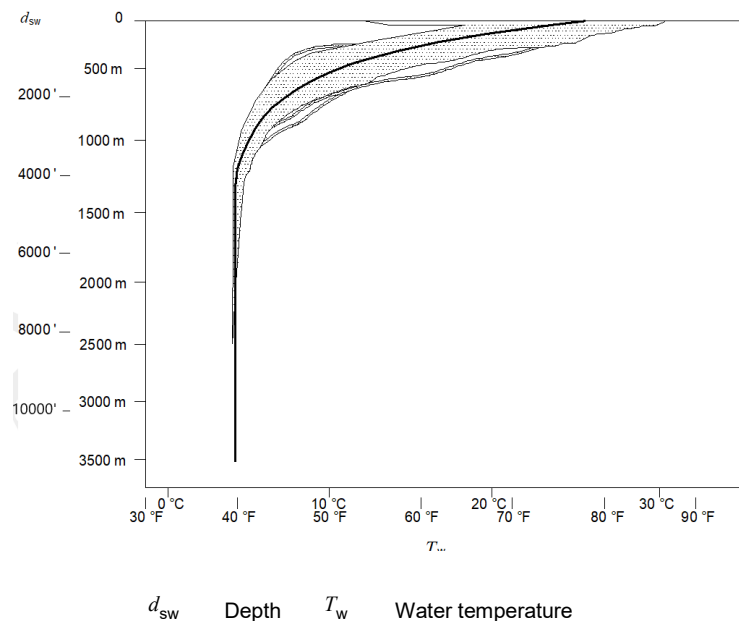


Figure H.7—Annual Sea Temperature Range—Western Gulf of Mexico

H.8.3 Marine Growth

The marine growth thickness may be taken as shown in Table H.1 (linearly interpolate between levels), unless site-specific studies are conducted to determine more appropriate values. The growth in Table H.1 is an estimate of the compressed thickness of hard and soft marine growth on platforms installed for over ten years. As such, these values may be taken as the climax growth profile. In addition to the results presented in Reference [130], this profile also considered the mean profile of hard plus one-half soft growth from over 1000 visual estimates and was further validated with thickness estimates determined by measuring leg circumferences with a pi tape at a limited number of platforms. Measuring leg circumference with a pi tape stretched around the leg and basing the effective thickness on the increase in the circumference from the as-built value is a more objective method for estimating a growth thickness relevant for hydrodynamic calculations than using visual estimates. Soft marine growth of varying thickness has been observed in depths as deep as 2000 m.

Table H.1—Compressed Marine Growth Thickness

Depth	Thickness (mm)
MHHW to MLLW	60
20 m below MLLW	30
50 m below MLLW	10
100 m below MLLW	10
140 m below MLLW	0

NOTE 1 Thickness is constant between MHHW and MLLW. Below MLLW, thickness is defined at specific depths. Linearly interpolate between the specific depths.

NOTE 2 Growth specific gravity is 1.2.

H.8.4 Visibility

Coastal areas of the Gulf of Mexico will occasionally be affected by fog.

H.8.5 Precipitation

Extreme rainfall rates may average 10 cm/h, increasing to effective rates over 20 cm/h for short (10 min) windows during extreme storms such as squalls and hurricanes.

H.9 Estimates of Metocean Parameters

H.9.1 General

The US Gulf annex provides select indicative values for metocean parameters. While intended for preliminary or concept studies, these values may be used for the design of fixed platforms in those portions of the US Gulf of Mexico west of 87.5° W in water depths between 10 m and 120 m, as referenced from API 2A-WSD, assessment of fixed platforms in the same depths in accordance with API 2SIM, and may also be used for assessment of MODU moorings in accordance with API 2SK C-1 (low consequence) situations, in lieu of obtaining values of a site-specific metocean study. However, performance of a site-specific metocean study is always recommended as the preferred method for developing design criteria for these situations, properly accounting for local variation in metocean conditions. For all other situations outside of these exceptions for API 2A-WSD, API 2SIM, and API 2SK, a comprehensive site-specific metocean study shall be performed in order to develop appropriate design criteria. Site-specific studies for Gulf of Mexico locations shall be performed within the guidelines of A.5 and H.10.

H.9.2 Extreme Metocean Parameters

H.9.2.1 General

Estimates of extreme metocean parameters are provided for the principal phenomena that dominate extremes in the Gulf of Mexico. These include:

- hurricanes;
- winter storms;
- squalls;
- Loop Current and Loop Current eddies;
- combined Loop Current and storm events;
- TRWs;
- air and sea temperatures.

H.9.2.2 Hurricanes

H.9.2.2.1 General

Hurricane-driven metocean conditions are provided for most areas of the Gulf of Mexico north of 26° N, in water depths greater than or equal to 10 m MLLW. The conditions are based primarily on industry studies [120, 121] performed using extrapolations from the 2014 update to the GOMOS hindcast [68].

Three sets of hurricane conditions are provided:

- full population or “annual” hurricane conditions;
- sudden hurricane conditions, derived from a subpopulation of the storms used to develop the annual conditions; this population represents those storms that can cause sustained winds of tropical storm force (17.5 m/s) or higher to sites north of 28° N within 24 h of becoming a named storm;
- seasonal hurricane conditions, for those months outside of those (August–October) with the most frequent occurrence of storms.

The hurricane conditions in this annex do not apply to the following.

- a) Water depths less than 10 m: Shallow areas near the coast will be subject to high surge levels that will depend on the steepness of the local terrain (both bathymetry and overland elevation) as well as the coastal profile. The storm surge very near the coast may allow for the existence of large waves that otherwise would not be possible for mean water levels.
- b) Areas marked by cross-hatching on Figure H.8: These areas will be subject to sheltering, limited fetch, and possible attenuation of waves by interaction with a soft seafloor, and may have complicated surge and current patterns, whereas areas east of the barrier islands will be subject to complicated currents.

H.9.2.2.2 Full Population Conditions

Independent extreme values of wind, wave, and current, along with associated surge, are presented in Table H.2 through Table H.4 and Figure H.9 through Figure H.17 for three approximate US Gulf areas, all north of 26° N (Figure H.8):

- Western Gulf, between 92° W and 98° W;
- Central Gulf, between 85° W and 92° W;
- Eastern Gulf, between 82° W and 85° W.

Users should be aware that the Central Gulf values envelope areas of transitions between the three regions; towards the east and west edges of the Central area (i.e. the unshaded regions between the West, Central and East regions of Figure H.8), the values shown in the annex may be much higher than those derived from a proper site-specific study.

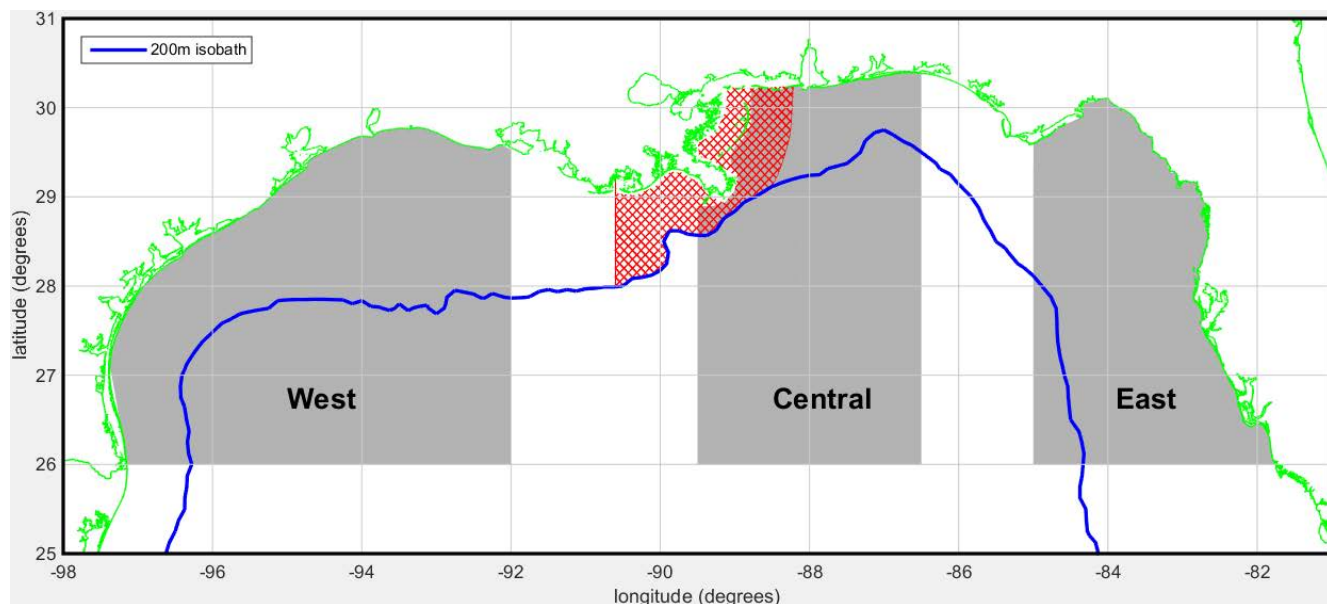


Figure H.8—Full Population Hurricane Areas of the Gulf

Each table shows the following parameters for a given region:

- N -year wind velocities for all water depths;
- N -year waves for water depths greater than or equal to 120 m;
- associated periods for N -year waves in all water depths;
- N -year current profiles for water depths greater than 50 m;
- N -year depth-averaged currents for water depths between 10 and 50 m;
- N -year surge for water depths greater than or equal to 120 m;
- astronomical tide amplitude (0.42 m) from MLLW for all water depths (constant for all return periods).

The figures show the following parameters for each region over the water depth range from 10 to 120 m:

- N -year H_{\max} ;
- N -year η_{\max} (including associated storm surge and astronomical tide);
- N -year associated storm surge including astronomical tide.

Table H.2—Hurricane Winds, Waves, Currents, and Surge in Deep Water—Western Gulf of Mexico (92° W to 98° W)

Load Case	Return Period (years)							
	10	15	25	50	100	300	500	1000
Wind speed (10 m elevation)								
1 h mean wind speed (m/s)	30.2	33.3	36.6	40.4	44.1	49.4	51.8	54.9
10 min mean wind speed (m/s)	31.4	34.7	38.0	42.1	45.8	51.4	53.9	57.1
1 min mean wind speed (m/s)	34.6	38.2	41.8	46.3	50.4	56.5	59.2	62.8
3 s gust (m/s)	42.0	46.4	50.8	56.2	61.1	68.5	71.8	76.1
Waves (depth ≥ 120 m)								
Significant wave height (m)	9.0	10.6	11.8	13.2	14.4	16.0	16.7	17.6
Maximum wave height (m)	16.0	18.6	20.9	23.3	25.4	28.3	29.5	31.1
Extreme water level (m)	10.3	12.0	13.5	15.0	16.3	18.2	18.9	19.9
Peak spectral period (s)	12.9	13.6	14.2	14.9	15.4	16.2	16.5	17.0
Period of maximum wave (s)	11.6	12.3	12.8	13.4	13.9	14.6	14.9	15.3
Currents (depth ≥ 50 m)								
Surface speed (m/s)	1.42	1.57	1.72	1.90	2.07	2.32	2.43	2.58
Bottom of profile (m)	57.3	63.3	69.4	76.8	83.7	93.9	98.4	104.4
Currents (depth 10 m to 50 m)								
Uniform speed (m/s)	1.42	1.57	1.72	1.90	2.07	2.32	2.43	2.58
Water level (depth ≥ 120 m)								
Associated storm surge (m)	0.22	0.27	0.34	0.43	0.53	0.65	0.69	0.74
Tidal amplitude (m)	0.42	0.42	0.42	0.42	0.42	0.42	0.42	0.42
NOTE 1	Wind speeds for a given return period are applicable to all water depths throughout the region.							
NOTE 2	Extreme water level is referenced to MLLW and consists of extreme crest elevation plus associated surge and tide.							
NOTE 3	See H.9.2.2.5 for guidance if air gap relative to n -year extreme water level is not positive.							
NOTE 4	See Figure H.9 and Figure H.10 for wave and extreme water level values for water depths between 10 m and 120 m.							
NOTE 5	The peak spectral period and period of maximum wave apply to waves in all water depths. When assessing systems with dynamic sensitivity, a ± 2 s variation in wave period should be considered.							
NOTE 6	For depths ≥ 50 m, the current profile is defined by a three-point shape (see H.9.2.2.6).							
NOTE 7	Reference Figure H.11 for surge and tide in water depths less than 120 m.							

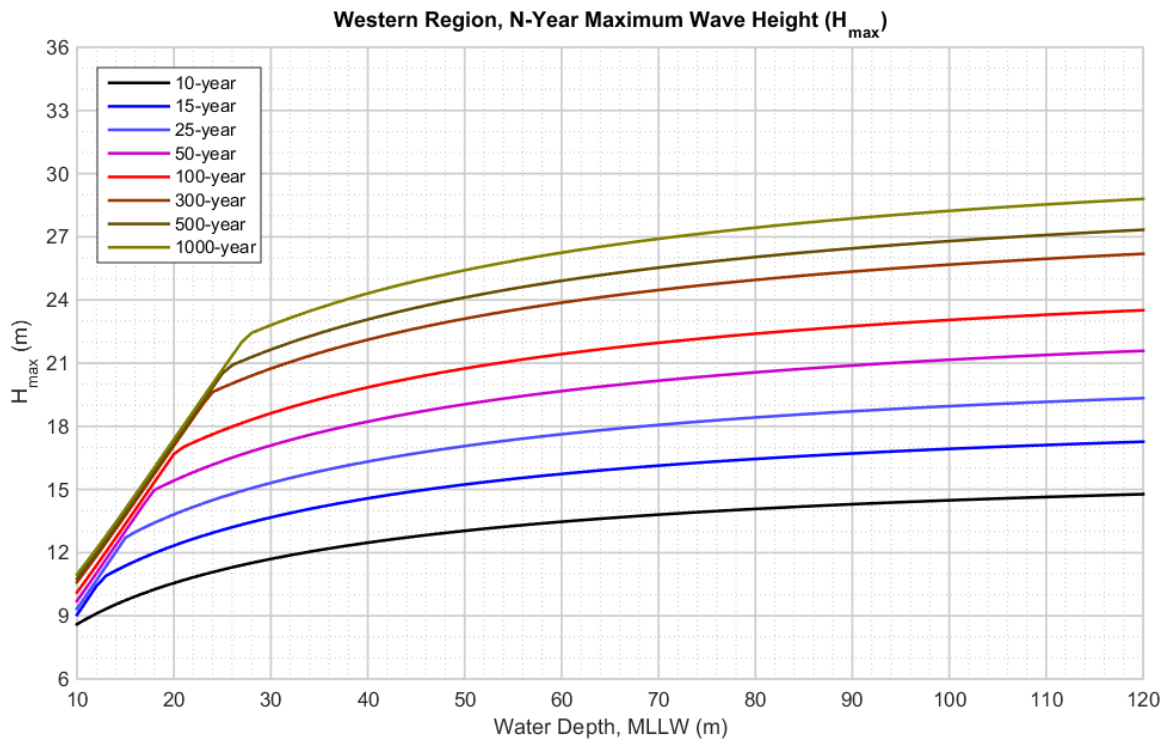


Figure H.9—N-year H_{\max} —Western Gulf of Mexico

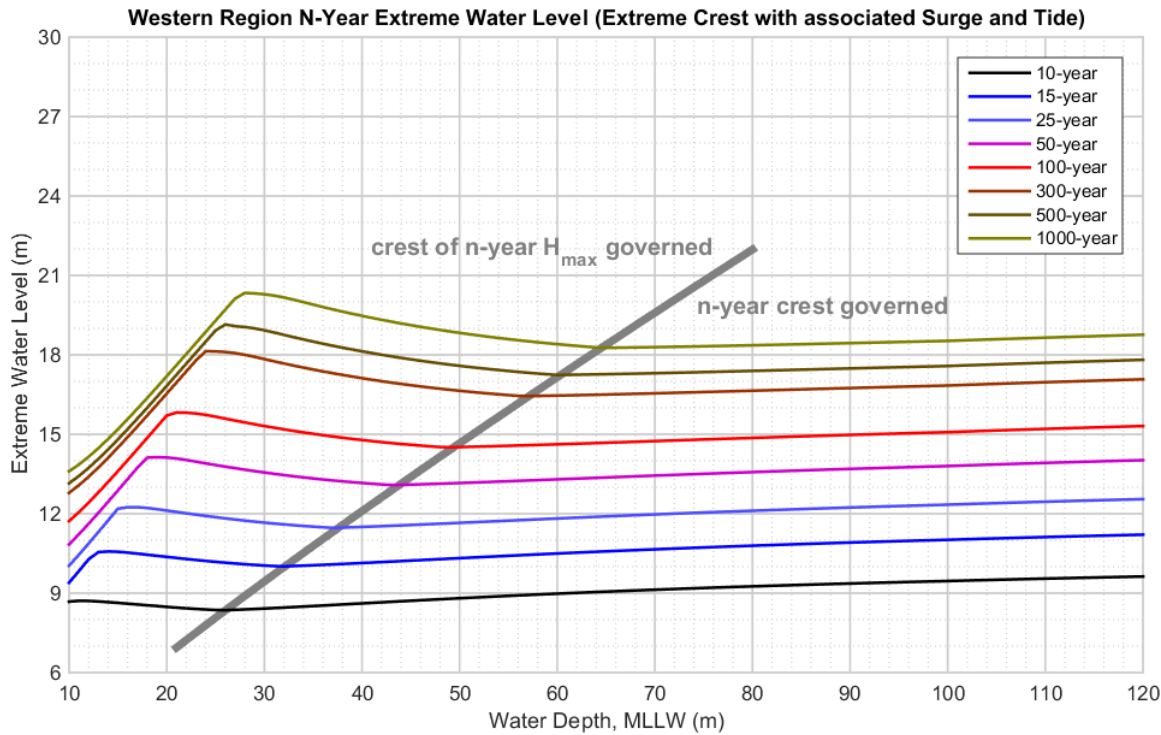
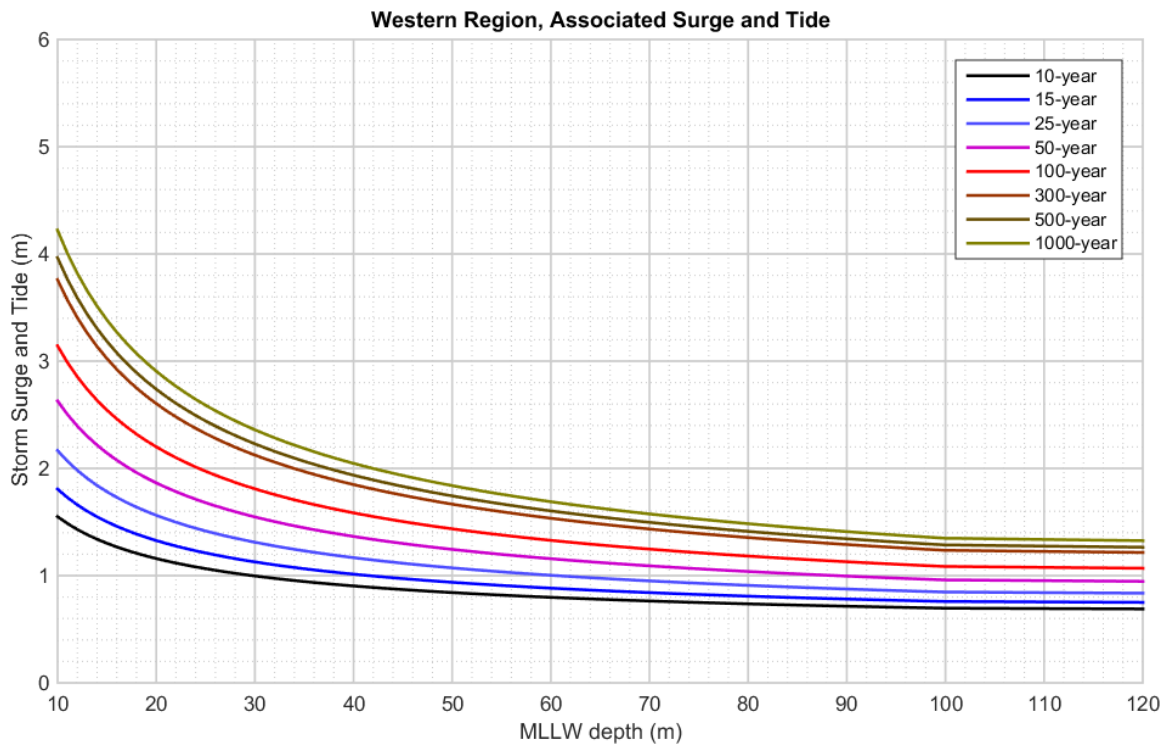
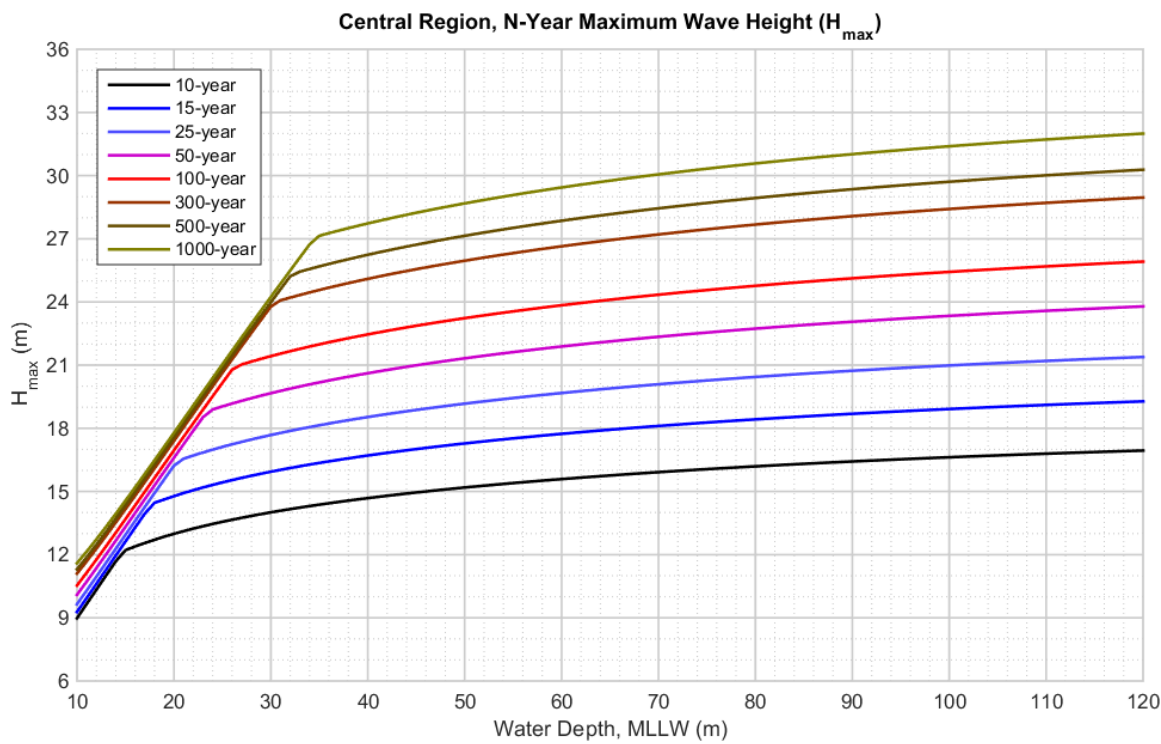


Figure H.10—N-year Extreme Water Level—Western Gulf of Mexico

**Figure H.11—Associated Surge with Tide—Western Gulf of Mexico****Figure H.12—N-year H_{\max} —Central Gulf of Mexico**

**Table H.3—Hurricane Winds, Waves, Currents, and Surge in Deep Water—Central Gulf of Mexico
(84° W to 92° W)**

Load Case	Return Period (years)							
	10	15	25	50	100	300	500	1000
Wind speed (10 m elevation)								
1 h mean wind speed (m/s)	32.8	35.9	39.6	44.2	48.5	54.7	57.4	60.9
10 min mean wind speed (m/s)	34.1	37.3	41.2	46.0	50.4	56.9	59.7	63.3
1 min mean wind speed (m/s)	37.5	41.1	45.3	50.6	55.4	62.5	65.6	69.6
3 s gust (m/s)	45.6	49.9	55.0	61.3	67.2	75.7	79.5	84.3
Waves (depth ≥ 120 m)								
Significant wave height (m)	10.4	11.8	13.1	14.5	15.8	17.7	18.5	19.6
Maximum wave height (m)	18.3	20.8	23.1	25.7	28.0	31.3	32.7	34.5
Extreme water level (m)	11.9	13.5	15.0	16.7	18.2	20.3	21.2	22.3
Peak spectral period (s)	13.1	13.7	14.3	14.9	15.5	16.3	16.6	17.1
Period of maximum wave (s)	11.8	12.4	12.9	13.4	13.9	14.6	15.0	15.4
Currents (depth ≥ 50 m)								
Surface speed (m/s)	1.64	1.79	1.98	2.21	2.42	2.73	2.87	3.05
Bottom of profile (m)	68.8	75.4	83.1	92.8	101.8	114.8	120.5	128.0
Currents (depth 10 m to 50 m)								
Uniform speed (m/s)	1.64	1.79	1.98	2.21	2.42	2.73	2.87	3.05
Water level (depth ≥ 120 m)								
Associated storm surge (m)	0.26	0.33	0.42	0.53	0.64	0.78	0.83	0.90
Tidal amplitude (m)	0.42	0.42	0.42	0.42	0.42	0.42	0.42	0.42
NOTE 1	Wind speeds for a given return period are applicable to all water depths throughout the region.							
NOTE 2	Extreme water level is referenced to MLLW and consists of extreme crest elevation plus associated surge and tide.							
NOTE 3	See H.9.2.2.5 for guidance if air gap relative to n -year extreme water level is not positive.							
NOTE 4	See Figure H.12 and Figure H.13 for wave and extreme water level values for water depths between 10 m and 120 m.							
NOTE 5	The peak spectral period and period of maximum wave apply to waves in all water depths. When assessing systems with dynamic sensitivity, a ± 2 s variation in wave period should be considered.							
NOTE 6	For depths ≥ 50 m, the current profile is defined by a three-point shape (see H.9.2.2.6).							
NOTE 7	Reference Figure H.14 for surge and tide in water depths less than 120 m.							

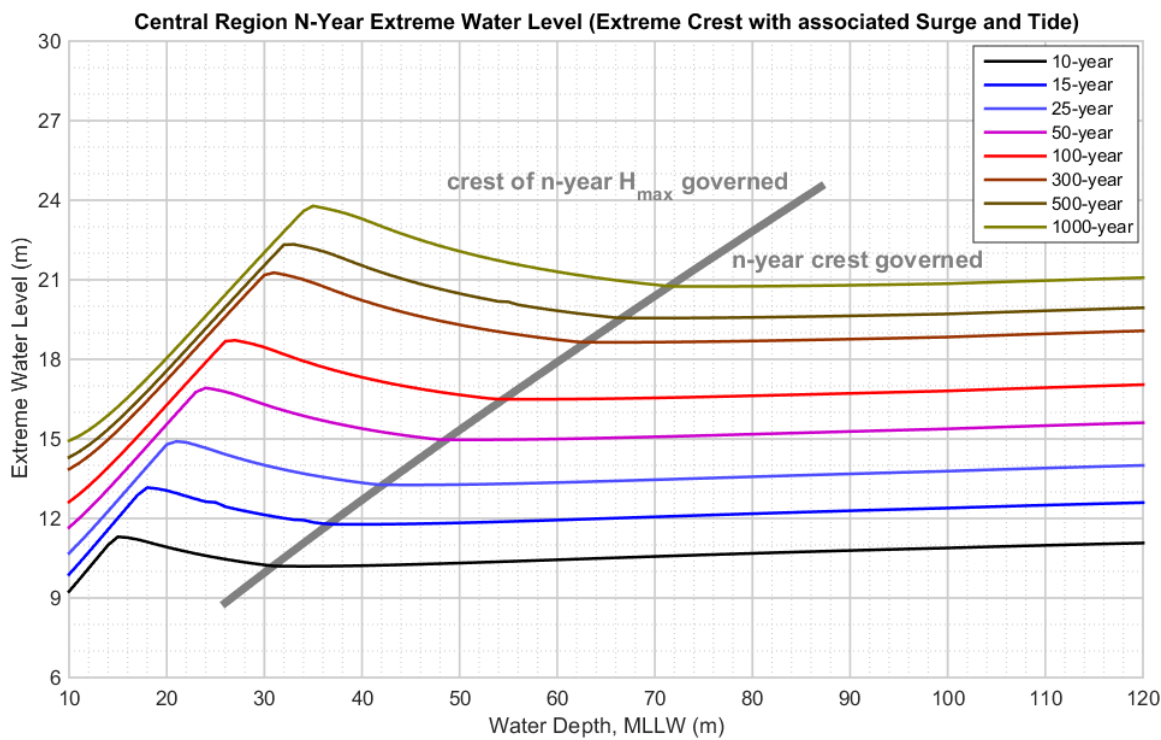


Figure H.13—N-year Extreme Water Level—Central Gulf of Mexico

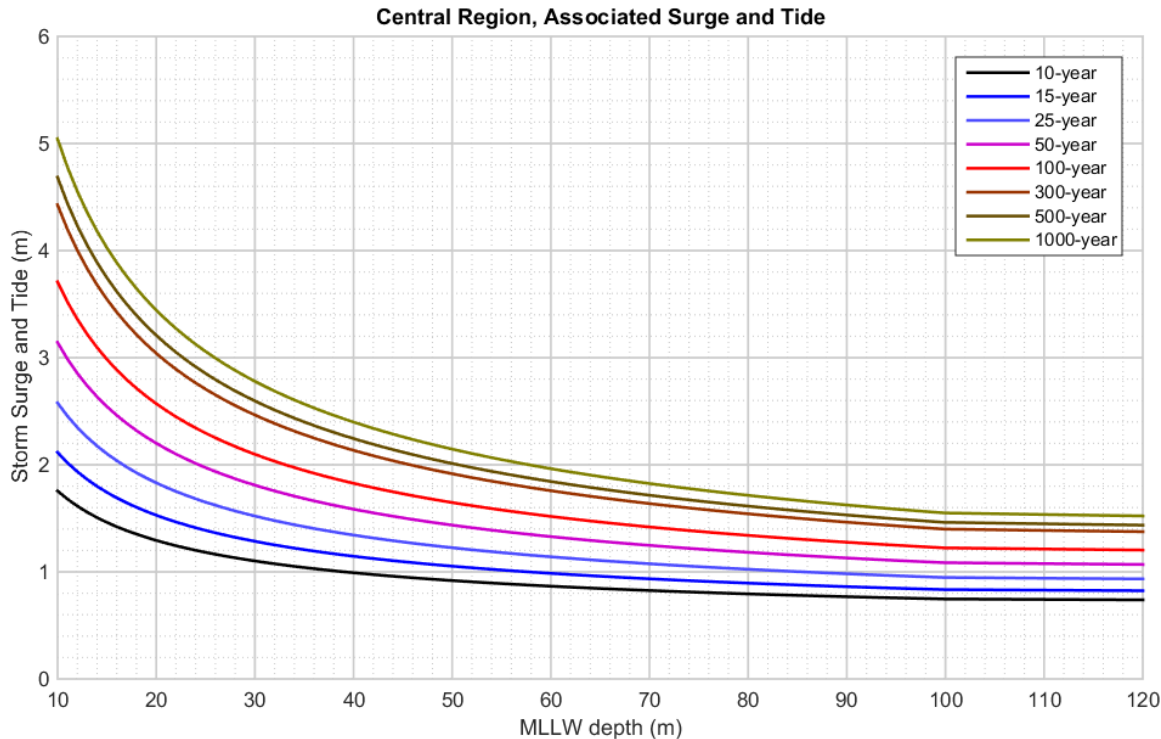
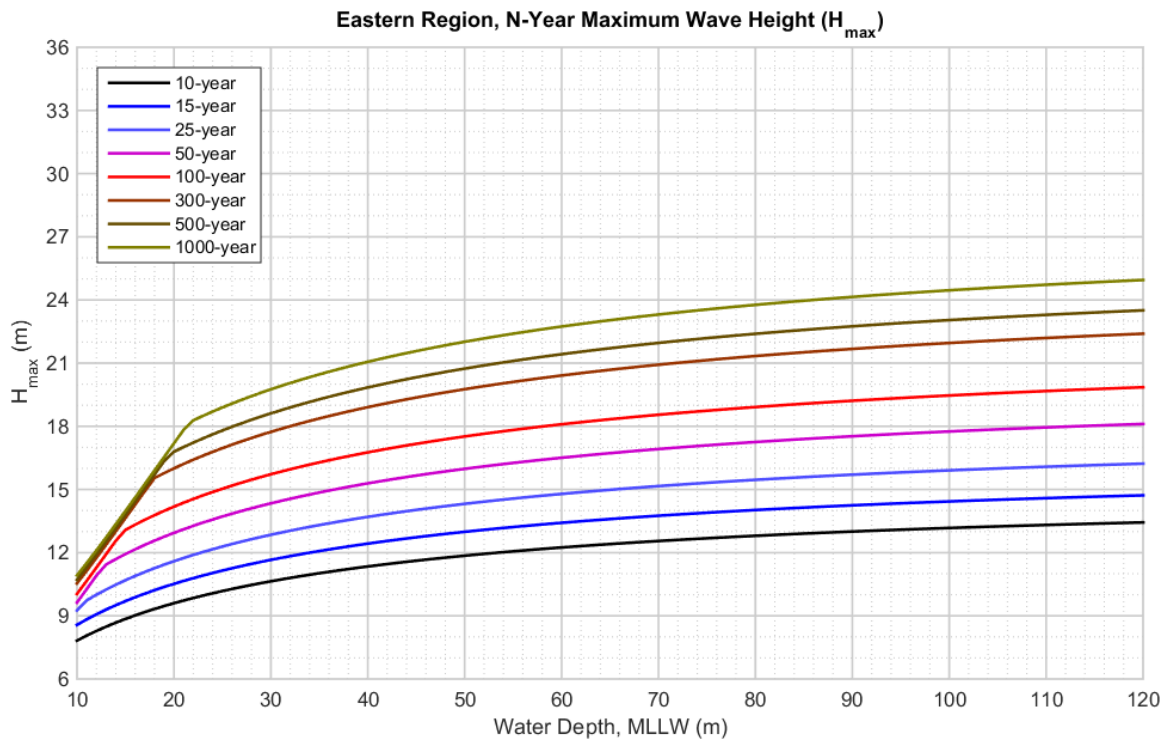
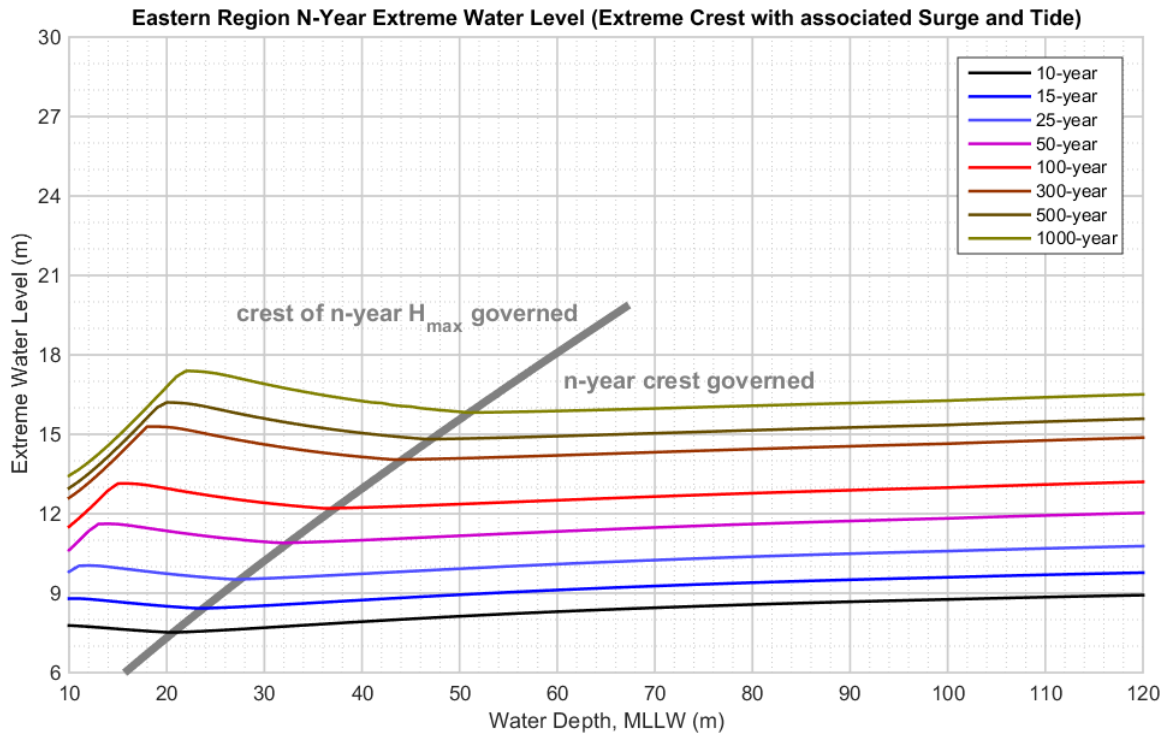


Figure H.14—Associated Surge with Tide—Central Gulf of Mexico

**Table H.4—Hurricane Winds, Waves, Currents, and Surge in Deep Water—Eastern Gulf of Mexico
(82° W to 84° W)**

Load Case	Return Period (years)							
	10	15	25	50	100	300	500	1 000
Wind speed (10 m elevation)								
1 h mean wind speed (m/s)	30.6	33.3	36.5	40.5	44.2	49.6	51.9	54.9
10 min mean wind speed (m/s)	31.8	34.7	38.0	42.2	46.0	51.5	53.9	57.1
1 min mean wind speed (m/s)	35.0	38.2	41.8	46.4	50.6	56.7	59.3	62.7
3 s gust (m/s)	42.6	46.4	50.8	56.3	61.4	68.7	71.9	76.0
Waves (depth \geq 120 m)								
Significant wave height (m)	8.2	9.0	9.9	11.1	12.1	13.7	14.4	15.3
Maximum wave height (m)	14.5	15.9	17.5	19.6	21.4	24.2	25.4	26.9
Extreme water level (m)	9.6	10.5	11.6	12.9	14.1	15.9	16.6	17.6
Peak spectral period (s)	11.8	12.2	12.7	13.3	13.9	14.7	15.0	15.5
Period of maximum wave (s)	10.6	11.0	11.4	12.0	12.5	13.2	13.5	14.0
Currents (depth \geq 50 m)								
Surface speed (m/s)	1.44	1.57	1.72	1.91	2.08	2.33	2.44	2.58
Bottom of profile (m)	58.1	63.3	69.4	77.0	84.0	94.2	98.6	104.3
Currents (depth 10 m to 50 m)								
Uniform speed (m/s)	1.44	1.57	1.72	1.91	2.08	2.33	2.44	2.58
Water level (depth \geq 120 m)								
Associated storm surge (m)	0.22	0.27	0.34	0.43	0.53	0.65	0.69	0.74
Tidal amplitude (m)	0.42	0.42	0.42	0.42	0.42	0.42	0.42	0.42
NOTE 1	Wind speeds for a given return period are applicable to all water depths throughout the region.							
NOTE 2	Extreme water level is referenced to MLLW and consists of extreme crest elevation plus associated surge and tide.							
NOTE 3	See H.9.2.2.5 for guidance if air gap relative to n -year extreme water level is not positive.							
NOTE 4	See Figure H.15 and Figure H.16 for wave and extreme water level values for water depths between 10 m and 120 m.							
NOTE 5	The peak spectral period and period of maximum wave apply to waves in all water depths. When assessing systems with dynamic sensitivity, a ± 2 s variation in wave period should be considered.							
NOTE 6	For depths \geq 50 m, the current profile is defined by a three-point shape (see H.9.2.2.6).							
NOTE 7	Reference Figure H.17 for surge and tide in water depths less than 120 m.							

**Figure H.15—N-year H_{\max} —Eastern Gulf of Mexico****Figure H.16—N-year Extreme Water Level—Eastern Gulf of Mexico**

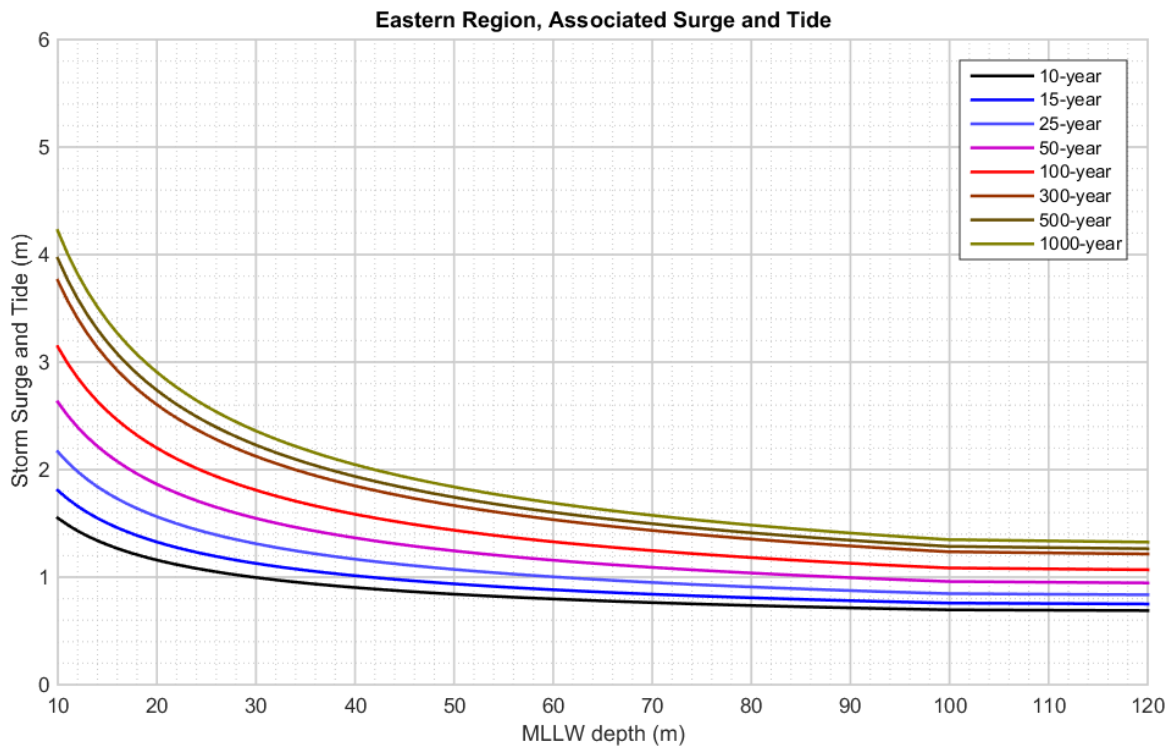


Figure H.17—Associated Surge with Tide—Eastern Gulf of Mexico

H.9.2.2.3 Winds

The 10 m elevation wind velocities provided are applicable to all water depths. The extreme winds should be treated as omni-directional. When adjusting these hurricane wind speeds to different averaging intervals and/or elevations, or when developing wind spectra, the equations in A.7.3.3 and A.7.4.3 should be used.

H.9.2.2.4 Wave Heights

Wave conditions are provided in the form of H_s , H_{max} , and extreme water level as well as associated T_p and $T_{H_{max}}$. The wave heights in the tables are applicable for water depths greater than or equal to 120 m (they may be very conservative toward 120 m), whereas the associated periods in the tables are applicable to all water depths. When assessing systems with dynamic sensitivity, a ± 2 s variation in the wave period should be considered. For wave heights in depths between 10 m and 120 m, the appropriate regional wave height depth decay curve figure should be consulted.

The extreme waves provided are omni-directional. Directional extreme waves for return periods greater than 10 years and for water depths greater than 30 m can be approximated by factoring the omni-directional value using Figure H.18. The principal wave heading varies with longitude. The factors listed apply within $\pm 22.5^\circ$ of the headings shown. In addition to factoring the wave height, the wave period should be adjusted by the square-root of the factor, i.e. assume constant steepness. When estimating directional extreme waves, the directional extreme should not be reduced below the level of the omni-directional 10-year return period wave or period. The principal directions shown in Figure H.18 do not apply to depths less than 30 m, as inside this depth refraction will begin to turn the wave crests parallel to the local bathymetry. The principal direction between 10 m and 30 m can be approximated by interpolation, assuming the direction at 10 m is perpendicular to the lines of local bathymetry, and the direction at 30 m is equal to that shown in the figure. In addition, Figure H.18 does not apply to the Eastern Gulf, where principal wave direction becomes quite variable depending on proximity to the Florida coast.

Hurricane-driven seas can be reasonably represented by the JONSWAP spectrum with a γ of 1.5–2.6. Wave spreading can be represented using the form $\cos^n(\theta)$, with n in the range of 2.0–2.5. A wave kinematics factor of 0.88 is considered representative.

H.9.2.2.5 Crest Elevations

The extreme water levels provided in Figure H.10, Figure H.13, and Figure H.16 (and Figure H.21 for sudden hurricanes) consist of the maximum crest elevation with associated surge and tide and are an important input into assessing adequacy of deck elevation for fixed platforms (note that if the crest of the n -year wave exceeded the n -year crest value it was used instead of the n -year crest as indicated by the two regions demarcated with a grey line on the figures). The extreme water levels provided do not include any artificial air gap allowance like the 1.5 m previously recommended in API 2A-WSD, nor do they include any allowance for local crest variation as described in A.8.7.

When selecting an extreme water level for an n -year condition, the higher of the following should be used: a) the n -year extreme water level provided or b) the extreme water level computed as the crest of the n -year wave as determined with an appropriate high-order wave theory plus the associated surge and tide.

Each of the extreme water level plots provided show the approximate demarcation between regions where the provided n -year value is governed by the n -year extreme crest elevation or where it is governed by crest of the n -year H_{\max} wave.

The crest elevation computed using high-order wave theory will vary slightly based on the associated value of current. The extreme water level curves provided here were developed comparing n -year crests to crests of n -year waves where the minimum associated current of 0.1 m/s. Higher associated currents will lead to slightly higher crests associated with n -year waves. If the computed extreme water level based on maximum wave height, period of maximum wave, associated current, and associated surge and tide is higher than the extreme water level provided here, the higher computed value shall be used.

On the deeper parts of the shelf where the extreme water level statistics are governed by the n -year crest, the extreme water level based on the crest of the n -year wave will not be as high as the value provided. This mismatch in n -year crest versus crest of the n -year wave is known as the “crest conundrum”^[238]. In this region:

- 1) If the platform being considered has positive air gap above the (higher) provided extreme water level, then the platform may be assessed with the provided design wave conditions (H_{\max} , $T_{H_{\max}}$, associated current, associated tide plus surge) with no modification.
- 2) If the platform being considered does not have positive air gap above the provided extreme water level, then the following assessment cases shall be carried out:
 - a) Analyze the platform precisely in accordance with the design wave conditions (H_{\max} , $T_{H_{\max}}$, associated current, associated tide plus surge) provided with no modification. In this analysis case, the inundation level will be incorrect (or there may be no inundation at all), but all members of the platform should be able to pass the original kinematics. In addition, this run will give the initial higher order wave crest elevation from which the “conundrum” may be estimated. In this water depth region the conundrum will be a negative number and will equal:

$$\text{Conundrum} = \text{Extreme water level based crest of } H_{\max} \text{ wave} - \text{Extreme water level based on } n\text{-year crest} \quad (\text{H.1})$$

If using values from this document rather than site specific criteria, then the “extreme water level based on n -year crest” is the value from one of the figures.

- b) Analyze the platform with the water depth increased and the wave period shortened ($T_{H_{max}}$) such that the velocity at the crest of the wave matches the velocity that would be achieved by matching crest elevation solely through increasing wave height alone. For return periods and water depths in the “ n -year crest” dominated zones of Figure H.10, Figure H.13, Figure H.16, and Figure H.21, this can be achieved by simultaneously:
- Increasing the surge + tide allowance by the amount specified in Table H.5.
 - Decreasing the associated period by adding $\delta T_{H_{max}}$ to associated period in accordance with Equation H.2 (which also refers to Table H.5). The wave period adjustment also enters a modification to account for the associated in-line current speed (v_{il}).

$$\delta T_{H_{max}} = \delta T_{H_{max}, \text{Table H.5}} - 0.15 v_{il} (m/s) \quad (\text{H.2})$$

Table H.5—Recommended Adjustments to “Surge + Tide” and $T_{H_{max}}$ for Gulf of Mexico Conditions

Conundrum (m)	δ Surge + Tide (m)	$\delta T_{H_{max}}$ (s)	Conundrum (m)	δ Surge + Tide (m)	$\delta T_{H_{max}}$ (s)
-1.80	1.45	-0.70	-0.80	0.69	-0.70
-1.70	1.38	-0.70	-0.70	0.62	-0.70
-1.60	1.30	-0.70	-0.60	0.54	-0.70
-1.50	1.23	-0.70	-0.50	0.46	-0.70
-1.40	1.15	-0.70	-0.40	0.39	-0.70
-1.30	1.07	-0.70	-0.35	0.35	-0.70
-1.20	1.00	-0.70	-0.30	0.30	-0.60
-1.10	0.92	-0.70	-0.20	0.20	-0.40
-1.00	0.85	-0.70	-0.10	0.10	-0.20
-0.90	0.77	-0.70	0.00	0.00	0.00

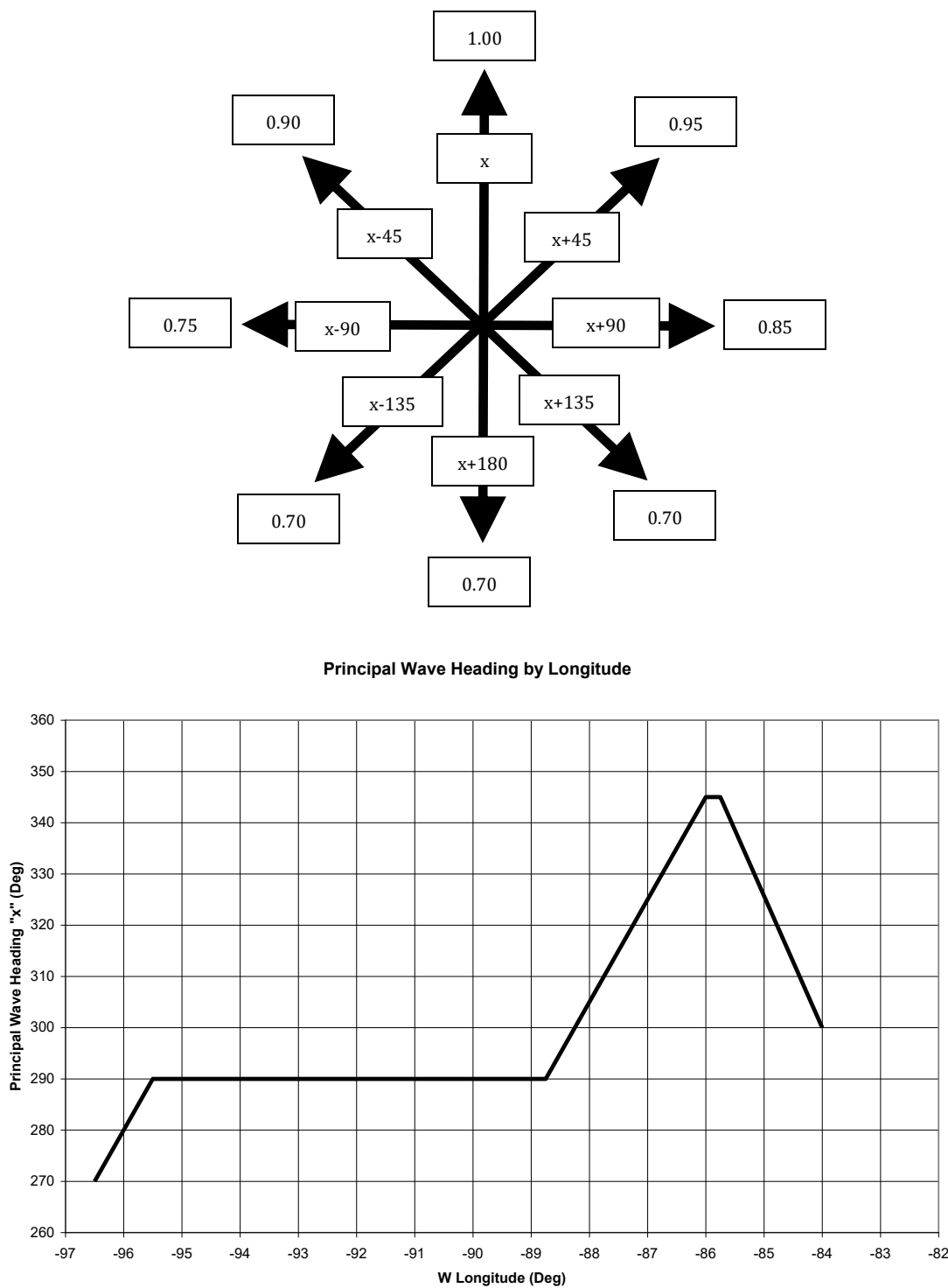


Figure H.18—Direction Factor for Wave Heights North of 26° N, West of 84° W, Depths ≥ 30 m, Return Periods > 10 Years

Source: API RP 2A

H.9.2.2.6 Currents

Currents are provided for water depths greater than 10 m.

Currents in water depths less than 50 m are essentially uniform from top to bottom, and follow the shelf contours in a westerly direction. Figure H.19 provides guidance for current headings in water depths less than 50 m. In the absence of site-specific data, a variation in heading of $\pm 22.5^\circ$ from that shown in the figure should be considered, with the direction selected to maximize overall hydrodynamic load.

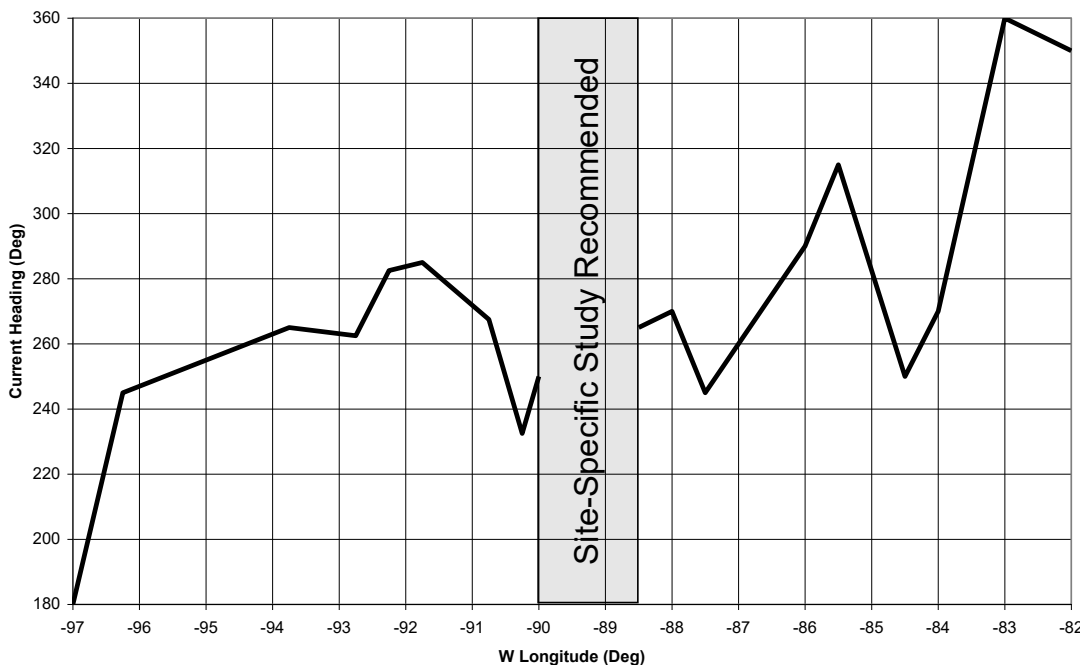


Figure H.19—Current Heading, Depth ≤ 50 m

Currents in water depths greater than or equal to 50 m are represented as a three-point profile.

- 1) Surface: The surface ($depth = 0$) of the ocean, including any surge and tide.
- 2) Mid-profile: A depth of either 50 m, or halfway between the surface ($depth = 0$) and the depth of the bottom of the profile, whichever is greater.
- 3) Bottom of profile: The depth, measured from the surface, at which the current speed decays to background values (assumed 0.1 m/s for depths at and below the bottom of the profile).

The current is constant (equal to the surface speed shown in the table) between the surface and mid-profile, and then varies linearly with depth between the mid-profile point to the bottom of the profile. The current profile should be treated as omni-directional.

The current component colinear with the wave direction should never be less than 0.1 m/s at all depths.

For indicative purposes, a 100-year deep water bottom hurricane current of 1.0 m/s should be assumed for all depths, when considering scour and pipeline loads. These bottom currents will occur hours if not days following storm passage, i.e. they will not be in phase with the peak wind, wave, and current cases described in this section.

H.9.2.2.7 Surge and Tide

The tables show storm surge for water depths greater than or equal to 120 m, and astronomical tidal amplitude applicable to all water depths. The surge conditions provided have been selected based on association with the waves, in order to maximize wave conditions. For storm surge in water depths between 10 and 120 m, the appropriate regional figure should be consulted; note that the curves in the figures include the tidal amplitude.

H.9.2.2.8 Wind, Wave, Current, and Surge/Tide Combinations

The metocean conditions provided are extreme values. To combine all extremes at the same return period together when constructing a wind, wave, current, and surge load case is very conservative, as the different variables will seldom peak at the same time during a given storm, and the n -year values of different parameters may not even occur in the same storm event. A set of combination factors is provided in Table H.6 and Table H.7 to allow for derivation of associated wind, wave, and current parameters to go with the n -year peak wave, peak wind, or peak current. It is emphasized that these factors are specific to the conditions provided in H.9.2.2; they should not be used with other data sets or the results of site-specific studies.

Where appropriate, directional offsets of wind heading from wave heading and current heading from wave heading are also provided. These are always measured as positive clockwise, i.e. if the table lists “current direction from the wave direction” as $+50^\circ$, the meaning is that the current heading (to) is rotated 50° to the right of the wave heading (to). For deepwater structures with dynamic sensitivity, variations of $\pm 22.5^\circ$ from the listed offsets should be considered. When determining the alignment of currents relative to the waves, the component of current in-line with the waves should never be less than 0.1 m/s regardless of the relative offset angle.

The surge conditions provided have already been selected based on association with the waves, in order to maximize wave conditions.

**Table H.6—Factors for Combining Independent Extremes into Load Cases in Shallow Water
(10 m ≤ Depth ≤ 50 m)**

Load Case	Return Period (years)						
	10	25	50	100	200	1000	2000
Wind dominant							
Wind speed	1.00	1.00	1.00	1.00	1.00	1.00	1.00
Wave height	1.00	0.95	0.95	0.95	0.95	0.95	0.95
Uniform current	0.80	0.80	0.80	0.80	0.80	0.80	0.80
Wind Direction from wave (deg)	-15	-15	-15	-15	-15	-15	-15
Wave dominant							
Wind speed	1.00	0.95	0.95	0.95	0.95	0.95	0.95
Wave height	1.00	1.00	1.00	1.00	1.00	1.00	1.00
Uniform current	0.80	0.80	0.80	0.80	0.80	0.80	0.80
Wind direction from wave (deg)	-15	-15	-15	-15	-15	-15	-15
Current dominant							
Wind speed	0.80	0.75	0.75	0.75	0.75	0.75	0.75
Wave height	0.80	0.75	0.75	0.75	0.75	0.75	0.75
Uniform current	1.00	1.00	1.00	1.00	1.00	1.00	1.00
Wind direction from wave (deg)	0	0	0	0	0	0	0
NOTE 1 Current headings in WD ≤ 50 m are independent of wind and wave, and are given by Figure H.19.							
NOTE 2 At a return period of 15 years, the same factors may be used as for 10 years.							

**Table H.7—Factors for Combining Independent Extremes into Load Cases in Deep Water
(Depth > 50 m)**

Load Case	Return Period (years)						
	10	25	50	100	200	1000	2000
Wind dominant							
Wind speed	1.00	1.00	1.00	1.00	1.00	1.00	1.00
Wave height	1.00	0.95	0.95	0.95	0.95	0.95	0.95
Current (both speed and depth level)	0.80	0.80	0.80	0.80	0.80	0.80	0.80
Wind direction from wave (deg)	-15	-15	-15	-15	-15	-15	-15
Current direction from wave (deg)	+15	+15	+15	+15	+15	+15	+15
Wave dominant							
Wind speed	1.00	0.95	0.95	0.95	0.95	0.95	0.95
Wave height	1.00	1.00	1.00	1.00	1.00	1.00	1.00
Current (both speed and depth level)	0.80	0.80	0.80	0.80	0.80	0.80	0.80
Wind direction from wave (deg)	-15	-15	-15	-15	-15	-15	-15
Current direction from wave (deg)	+15	+15	+15	+15	+15	+15	+15
Current dominant							
Wind speed	0.80	0.75	0.75	0.75	0.75	0.75	0.75
Wave height	0.80	0.75	0.75	0.75	0.75	0.75	0.75
Current (both speed and depth level)	1.00	1.00	1.00	1.00	1.00	1.00	1.00
Wind direction from wave (deg)	0	0	0	0	0	0	0
Current direction from wave (deg)	+45	+45	+45	+45	+45	+45	+45
NOTE	At a return period of 15 years, the same factors may be used as for 10 years.						

H.9.2.2.9 Event Duration

The passage of a hurricane will generally affect a site for 24–48 h, although a large slow-moving storm could affect a site for as long as 96 h. A hurricane event can be approximated as an increase of winds and waves from background conditions to peak conditions over 24 h, persistence of peak conditions for 3 h, and then decay back to background conditions over another 24 h. Currents will similarly increase from background conditions over 24 h and will peak in the hours following the highest winds and waves. Decay of the currents to background values is generally occurs over 3 to 5 days.

H.9.2.3 Reduced-exposure Hurricanes

H.9.2.3.1 Sudden Hurricane Conditions

A “sudden” hurricane is one that forms locally in the Gulf of Mexico, and due to speed of formation and proximity to infrastructure at time of formation may not allow sufficient time to evacuate manned facilities. The exact population of storms used to derive sudden hurricane conditions at a given site may be based on where storms form and how quickly storms move and intensify after formation, in comparison to the accuracy of storm forecasts and how quickly personnel and/or facilities may be removed from the site.

A set of sudden hurricane conditions is provided in Table H.8 and Figure H.20 through Figure H.22 developed based on those storms which generate 10 m 1 h wind speeds of 15 m/s or greater at locations inshore of 120 m depth within 24–48 h of becoming named storms. One set of conditions is provided, applicable to all regions within the limits of H.9.2.2.2 for water depths of 120 m or less.

Load cases for sudden hurricane conditions may be developed in accordance with the guidelines of H.9.2.2.8, using the following modifications.

- a) Sudden hurricane load cases with return periods of 200 years or less should be developed using the combination factors in the 10-year column. The sudden hurricane wave condition for these return periods should be considered omni-directional.
- b) 1000-, 2000-, and 2500-year sudden hurricane load cases should be developed using the combination factors in the 100-year column. The 1000-, 2000-, and 2500-year sudden hurricane directional wave conditions may be approximated using Figure H.18.

Table H.8—Sudden Hurricane Winds, Waves, Currents, and Surge (All Regions, Depth ≤ 120 m)

Load Case	Return Period (years)					
	50	100	200	1000	2000	2500
Wind speed (10 m elevation)						
1 h mean wind speed (m/s)	26.0	29.1	32.5	40.5	44.0	45.1
10 min mean wind speed (m/s)	27.0	30.3	33.9	42.2	45.7	46.9
1 min mean wind speed (m/s)	29.7	33.3	37.3	46.4	50.3	51.6
3 s gust (m/s)	36.0	40.5	45.3	56.3	61.1	62.6
Waves						
Peak spectral period (s)	11.7	12.3	12.9	14.2	14.7	14.9
Period of maximum wave (s)	10.6	11.1	11.6	12.8	13.3	13.4
Currents (depth ≥ 50 m)						
Surface speed (m/s)	1.30	1.46	1.63	2.03	2.20	2.26
Bottom of profile (m)	54.6	61.1	68.3	85.1	92.4	94.7
Currents (depth 10 m to 50 m)						
Uniform speed (m/s)	1.30	1.46	1.63	2.03	2.20	2.26
NOTE 1	Wind speeds for a given return period are applicable to all water depths throughout the region.					
NOTE 2	Extreme water level is referenced to MLLW and consists of extreme crest elevation plus associated surge and tide.					
NOTE 3	See H.9.2.2.5 for guidance if air gap relative to n -year extreme water level is not positive.					
NOTE 4	See Figure H.20 and Figure H.21 for wave and extreme water level values for water depths between 10 m and 120 m.					
NOTE 5	The peak spectral period and period of maximum wave apply to waves in all water depths. When assessing systems with dynamic sensitivity, a ± 2 s variation in wave period should be considered.					
NOTE 6	For depths ≥ 50 m, the current profile is defined by a three-point shape (see H.9.2.2.6).					
NOTE 7	Reference Figure H.22 for surge and tide in water depths less than 120 m.					

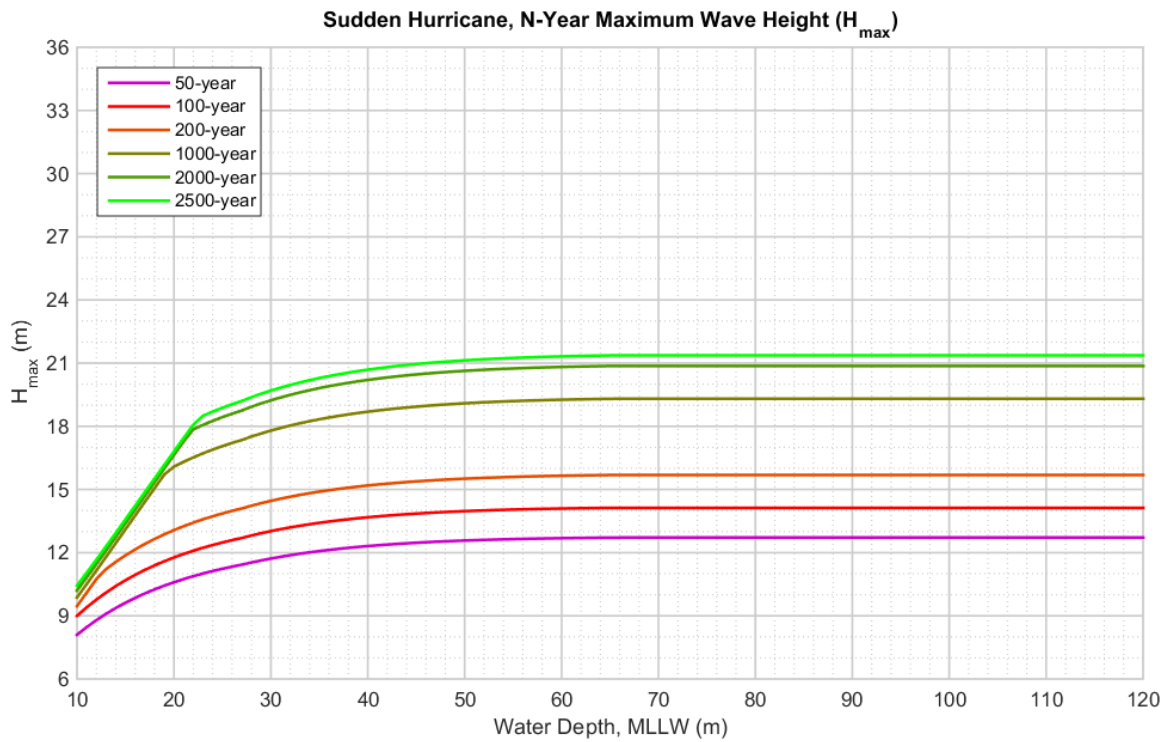


Figure H.20—N-year H_{\max} —All Regions

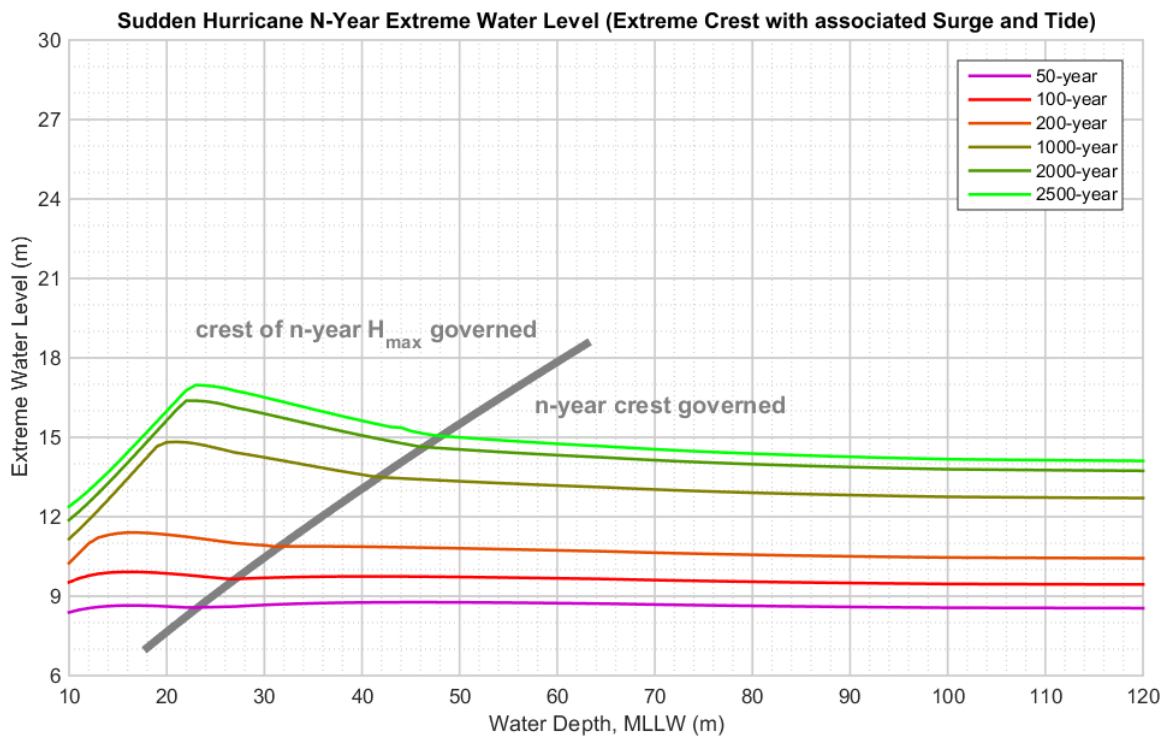


Figure H.21—N-year Extreme Water Level—All Regions

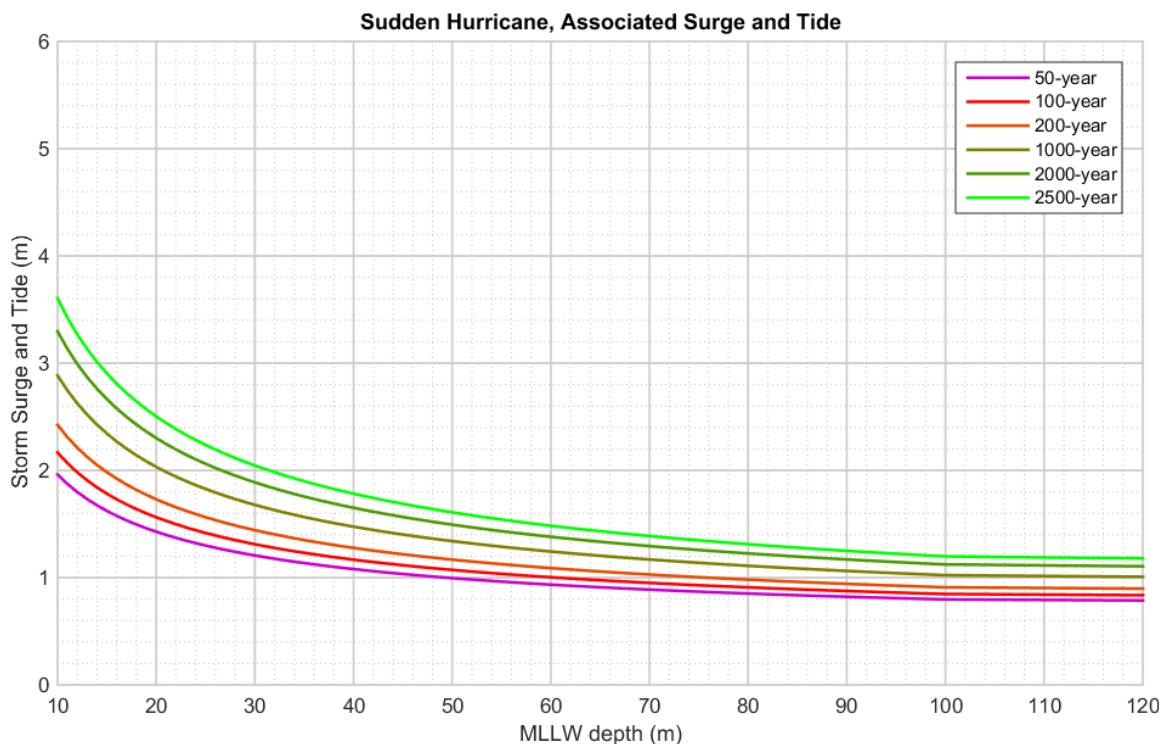


Figure H.22—Associated Surge with Tide—All Regions

H.9.2.3.2 Seasonal Conditions

The conditions provided in H.9.2.2.2 assume an exposure period to hurricane encounters over the full year. Should a facility operate in such a manner as to restrict its exposure to hurricanes in the Gulf of Mexico (or one of the regions in the Gulf of Mexico) to periods less than 1 year, i.e. a seasonal operation, it would be reasonable to consider the facility subject to hurricane conditions derived from a limited exposure period.

Hurricane season in the North Atlantic Basin officially runs from June 1 through November 30, with the most severe storm activity generally occurring in August, September, and October. The storms that occur in these 3 months effectively control the annual hurricane extremes; extremes derived just considering storms that occur in these 3 months will be essentially identical to extremes derived using the full population of storms irrespective of month. The severe months are preceded by a period of moderate cyclone activity during June and July, and then followed by a period of rapidly decreasing cyclone activity from the end of October through November. While rare, tropical storms have formed or entered in the Gulf of Mexico in both May and December, outside the official hurricane season.

A set of seasonal hurricane conditions for water depths greater than or equal to 120 m are provided for the Western and Central Gulf between 88° and 98° W and for the Eastern and Central Gulf between 82° and 88° W in Table H.9 through Table H.12. Conditions are provided for an “early season” period, covering June 1 to August 1, and a “late season” period, covering October 21 through November 30. Peak hurricane season is considered to cover the period from August 14 through October 7; during this period, the hurricane conditions in H.9.2.2.2, i.e. the annual conditions, should be used. For the periods between August 1 to August 14, and between October 7 and October 21, conditions should be derived by linearly interpolating over 2-week ramp periods between the annual conditions in H.9.2.2.2 and the early and late season conditions presented here.

When applying the seasonal conditions in this section, the following should be noted.

- a) The conditions presented in this section are for water depths of 300 m or greater. They should not be interpolated or extrapolated to shallow water.
- b) The seasonal conditions are for the full population of early and late season tropical cyclones. They do not include winter storms, which should be treated as a separate storm population with its own set of derived extremes. Some of the extremes presented in this section, particularly in the post-peak period, may not represent the highest storm-driven n -year wind or wave conditions which could be encountered in the periods described. Application of these conditions should include a comprehensive risk assessment accounting for all storm conditions which could be encountered during the period of operation considered, in order to evaluate total risk.
- c) The conditions in this section should be treated as complete load cases, and the wind, waves, and current should be treated as omni-directional. Do not use the factors in Figure H.18 to adjust the wave heights shown in the seasonal tables; however, the seasonal wave heights should not be higher in any given direction than the annual extreme waves adjusted for direction using Figure H.18.
- d) Planning for operations in the pre-peak hurricane season should consider the possibility of delayed completion due to late arrival of equipment at the beginning of the operation, contingencies during the operation itself, delays due to Loop Current intrusions, and delays due to tropical storm occurrences. Wind, waves, and current corresponding to the latest likely completion date should be used in planning.
- e) Planning for operations in the post-peak hurricane season should consider the possibility of an early start due to early availability of equipment. Wind, waves, and current corresponding to the earliest likely start date should be used in planning, or the operator should be in a position to terminate any operation and take precautionary measures in response to realistic tropical cyclone forecast conditions.

Table H.9—Early Season (June 1 to August 1) Hurricane Winds, Waves, Currents, and Surge—Central and Western Gulf of Mexico (88° W to 98° W), Depth ≥ 120 m

Load Case	Return Period (years)						
	10	25	50	100	200	1000	2000
Wind speed (10 m elevation)							
1 h mean wind speed (m/s)	20.6	24.9	27.3	29.6	31.8	36.5	38.4
10 min mean wind speed (m/s)	21.4	25.9	28.4	30.7	33.1	38.0	39.9
1 min mean wind speed (m/s)	23.3	28.5	31.3	33.9	36.4	41.8	43.9
3 s gust (m/s)	28.0	34.5	38.0	41.2	44.2	50.7	53.3
Waves							
Significant wave height (m)	5.5	6.9	7.7	8.4	9.0	10.4	10.9
Maximum wave height (m)	9.7	12.2	13.6	14.8	15.9	18.3	19.2
Extreme water level (m)	6.6	8.2	9.1	9.9	10.7	12.2	12.8
Peak spectral period (s)	9.9	11.0	11.5	12.0	12.4	13.2	13.5
Period of maximum wave (s)	8.9	9.9	10.4	10.8	11.1	11.9	12.1
Currents							
Surface speed (m/s)	1.03	1.25	1.37	1.48	1.59	1.82	1.92
Speed at mid-profile (m/s)	0.77	0.94	1.02	1.11	1.19	1.37	1.44
Bottom of profile (m)	43.2	52.4	57.4	62.1	66.8	76.6	80.6
Water level							
Associated storm surge (m)	0.16	0.26	0.33	0.40	0.47	0.56	0.60
Tidal amplitude (m)	0.42	0.42	0.42	0.42	0.42	0.42	0.42

Table H.10—Late Season (October 21 through November 30) Hurricane Winds, Waves, Currents, and Surge—Central and Western Gulf of Mexico (88° W to 98° W), Depth ≥ 120 m

Load Case	Return Period (years)						
	10	25	50	100	200	1000	2000
Wind speed (10 m elevation)							
1 h mean (m/s)	17.1	20.7	22.7	24.5	26.4	30.3	31.9
10 min mean (m/s)	17.7	21.5	23.5	25.5	27.4	31.5	33.1
1 min mean (m/s)	19.3	23.5	25.8	28.0	30.2	34.7	36.5
3 s gust (m/s)	22.9	28.2	31.1	33.9	36.6	42.2	44.3
Waves							
Significant wave height (m)	4.6	5.8	6.4	7.0	7.5	8.6	9.0
Maximum wave height (m)	8.0	10.2	11.3	12.3	13.2	15.2	16.0
Extreme water level (m)	5.6	6.9	7.7	8.4	9.0	10.2	10.7
Peak spectral period (s)	9.1	10.1	10.6	11.0	11.4	12.1	12.4
Period of maximum wave (s)	8.2	9.1	9.5	9.9	10.2	10.9	11.2
Currents							
Surface speed (m/s)	0.85	1.04	1.13	1.23	1.32	1.51	1.59
Speed at mid-profile (m/s)	0.64	0.78	0.85	0.92	0.99	1.14	1.19
Bottom of profile (m)	35.9	43.5	47.6	51.5	55.4	63.6	66.9
Water level							
Storm surge (m)	0.14	0.22	0.27	0.34	0.39	0.47	0.50
Tidal amplitude (m)	0.42	0.42	0.42	0.42	0.42	0.42	0.42

Table H.11—Early Season (June 1 to August 1) Hurricane Winds, Waves, Currents, and Surge—Eastern and Central Gulf of Mexico (82° W to 88° W), Depth ≥ 120 m

Load Case	Return Period (years)						
	10	25	50	100	200	1000	2000
Wind speed (10 m elevation)							
1 h mean (m/s)	22.3	25.9	28.5	31.0	33.5	38.9	41.1
10 min mean (m/s)	23.2	26.9	29.6	32.2	34.9	40.5	42.7
1 min mean (m/s)	25.4	29.6	32.6	35.5	38.4	44.6	47.0
3 s gust (m/s)	30.6	35.9	39.7	43.1	46.7	54.1	57.1
Waves							
Significant wave height (m)	6.0	7.2	8.0	8.8	9.5	11.1	11.7
Maximum wave height (m)	10.5	12.7	14.2	15.5	16.8	19.5	20.6
Extreme water level (m)	7.1	8.5	9.5	10.4	11.2	13.0	13.7
Peak spectral period (s)	10.3	11.2	11.7	12.2	12.7	13.6	13.9
Period of maximum wave (s)	9.2	10.1	10.6	11.0	11.4	12.2	12.5
Currents							
Surface speed (m/s)	1.12	1.30	1.42	1.55	1.68	1.95	2.05
Speed at mid-profile (m/s)	0.84	0.97	1.07	1.16	1.26	1.46	1.54
Bottom of profile (m)	46.9	54.4	59.8	65.1	70.4	81.8	86.3
Water level							
Associated storm surge (m)	0.19	0.28	0.35	0.43	0.49	0.61	0.69
Tidal amplitude (m)	0.42	0.42	0.42	0.42	0.42	0.42	0.42

Table H.12—Late Season (October 21 through November 30) Hurricane Winds, Waves, Currents, and Surge—Eastern and Central Gulf of Mexico (82° W to 88° W), Depth ≥ 120 m

Load Case	Return Period (years)						
	10	25	50	100	200	1000	2000
Wind speed (10 m elevation)							
1 h mean (m/s)	21.0	24.3	26.7	29.1	31.5	36.5	38.5
10 min mean (m/s)	21.7	25.2	27.8	30.2	32.7	38.0	40.1
1 min mean (m/s)	23.8	27.7	30.6	33.3	36.0	41.8	44.1
3 s gust (m/s)	28.6	33.5	37.1	40.5	43.8	50.8	53.6
Waves							
Significant wave height (m)	5.6	6.7	7.5	8.3	8.9	10.4	10.9
Maximum wave height (m)	9.9	11.9	13.3	14.6	15.8	18.3	19.3
Extreme water level (m)	6.7	8.0	8.9	9.8	10.6	12.2	12.9
Peak spectral period (s)	10.0	10.9	11.4	11.9	12.3	13.2	13.5
Period of maximum wave (s)	9.0	9.8	10.3	10.7	11.1	11.9	12.2
Currents							
Surface speed (m/s)	1.05	1.21	1.33	1.45	1.57	1.83	1.93
Speed at mid-profile (m/s)	0.79	0.91	1.00	1.09	1.18	1.37	1.45
Bottom of profile (m)	44.0	51.0	56.1	61.0	66.0	76.7	80.9
Water level							
Storm surge (m)	0.17	0.26	0.31	0.39	0.45	0.55	0.62
Tidal amplitude (m)	0.42	0.42	0.42	0.42	0.42	0.42	0.42

H.9.2.4 Winter Storms

Extratropical cyclones and cold air mass intrusions, collectively referred to as winter storms, dominate extremes outside of the peak of hurricane season, with the most severe events generally occurring in the period January through March.

This section provides values of wind, wave, and current, along with associated surge and tide, for a range of return periods between 1 and 100 years. The conditions are based on extrapolations from measurements made at NOAA buoys supplemented by the WINX hindcast. Independent extremes are shown in Table H.13, whereas factors for construction of wind-dominant (n -year wind with associated parameters), wave-dominant (n -year waves with associated parameters), and current-dominant (n -year currents with associated parameters) cases are provided in Table H.14. The conditions are applicable to all Gulf of Mexico locations north of 26° N. The uncertainty of the 100-year values is estimated to be at least 15%; an H_s measurement of 9.2 m was recorded at Buoy 42001 during the March 1993 storm.

The following guidance is provided governing the use of the information provided in the tables.

- a) The winds, waves, and current should be treated as omni-directional. A variation of $\pm 45^\circ$ should be considered in the relative direction offsets.
- b) When adjusting winter storm wind speeds to different averaging intervals and/or elevations, or when developing wind spectra, the formulas in A.7.3.2 and A.7.4.2 should be used.
- c) Wave conditions are provided in the form of H_s , H_{max} , and η_{max} as well as associated T_p and $T_{H_{max}}$. When assessing systems with dynamic sensitivity, a ± 2 s variation in the wave period should be considered.
- d) The crest elevations η_{max} provided include associated surge and tide. The crest elevations provided do not include any artificial air gap allowance like the 1.5 m previously recommended in API 2A-WSD or any allowance for local crest variation. When selecting a crest for an n -year condition, the higher of either the n -year crest provided or the crest of the n -year wave as determined by an appropriate high-order wave theory should be used.
- e) Winter storm-driven seas can be reasonably represented by the JONSWAP spectrum with a γ of 1.0–3.3. Wave spreading can be represented using the form $\cos^n(\theta)$, with n equal to 4.0. A wave kinematics factor of 0.91 is considered representative.
- f) The current profile shape is a uniform speed over the depth indicated (or to the bottom, whichever is less).
- g) When determining the alignment of currents relative to the waves, the component of current in-line with the waves should never be less than 0.1 m/s over all depths regardless of the relative offset angle.

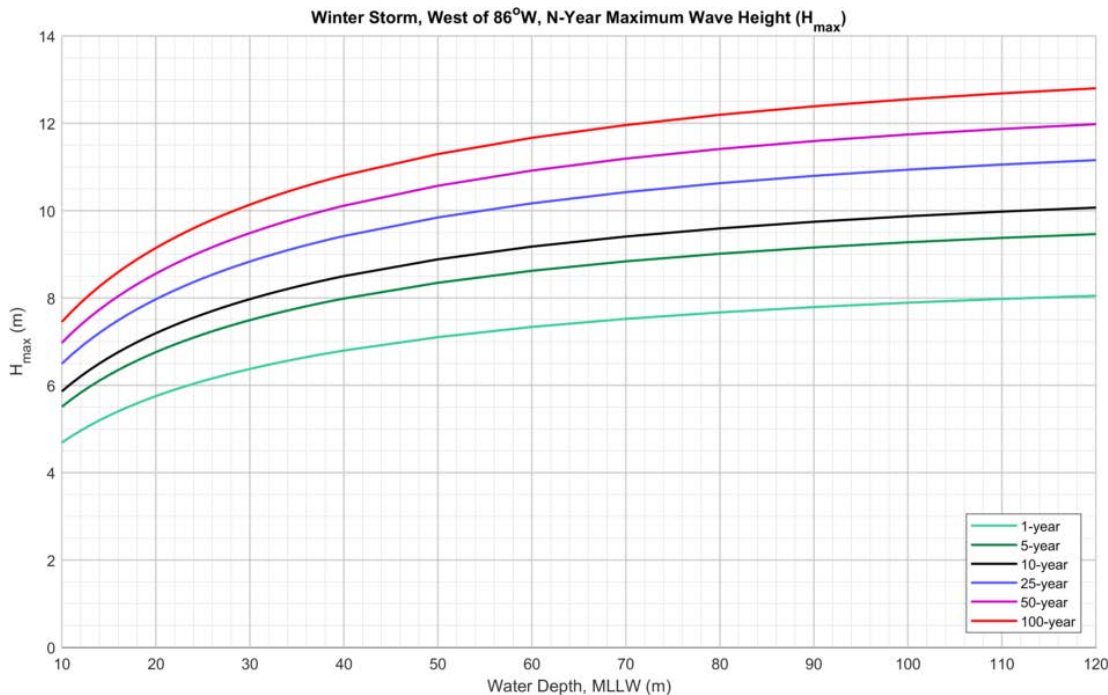
The variation of winter storm H_{max} extremes in water depths less than 120 m and west of longitude 86° W is shown in Figure H.23. In the Eastern Gulf, east of 86° W, the winter storm wave climate is more severe and H_{max} extremes should be taken as 1.2 times those presented in Figure H.23.

Table H.13—Winter Storm Winds, Waves, Currents, and Surge, Depth ≥ 120 m

Load Case	Return Period (years)					
	1	5	10	25	50	100
Wind speed (10 m elevation)						
1 h mean (m/s)	18.1	20.0	20.8	22.9	24.2	25.6
10 min mean (m/s)	19.5	21.6	22.5	24.9	26.4	28.0
1 min mean (m/s)	21.3	23.7	24.8	27.5	29.2	31.0
3 s gust (m/s)	23.7	26.5	27.7	30.8	32.8	35.0
Waves						
Significant wave height (m)	4.9	6.0	6.4	7.2	7.6	8.3
Maximum wave height (m)	8.9	10.9	11.6	13.1	13.8	15.1
Extreme water level (m)	5.3	6.5	7.0	7.8	8.3	9.0
Peak spectral period (s)	9.8	10.8	11.1	11.8	12.0	12.5
Period of maximum wave (s)	8.9	9.7	10.0	10.6	10.8	11.3
Currents						
Speed (m/s)	0.40	0.47	0.55	0.65	0.72	0.79
Depth (m)	75	75	75	75	75	75
Water level						
Surge (m)	0.06	0.13	0.16	0.21	0.24	0.27
Tidal amplitude (m)	0.42	0.42	0.42	0.42	0.42	0.42

Table H.14—Factors for Combing Independent Extremes into Load Cases

Load Case	Return Period (years)					
	1	5	10	25	50	100
Wind dominant						
Wind speed	1	1	1	1	1	1
Wave height	0.90	0.90	0.90	0.90	0.90	0.90
Current speed	0.75	0.75	0.65	0.65	0.60	0.60
Surge/tide	0	0	0	0	0	0
Wind direction from wave (deg)	0	0	0	0	0	0
Current direction from wave (deg)	0	0	0	0	0	0
Wave dominant						
Wind speed	0.93	0.93	0.93	0.93	0.93	0.93
Wave height	1	1	1	1	1	1
Current speed	0.75	0.75	0.65	0.65	0.60	0.60
Surge/tide	0	0	0	0	0	0
Wind direction from wave (deg)	0	0	0	0	0	0
Current direction from wave (deg)	0	0	0	0	0	0
Current dominant						
Wind speed	0.70	0.70	0.70	0.70	0.70	0.70
Wave height	0.75	0.75	0.75	0.75	0.75	0.75
Current speed	1	1	1	1	1	1
Surge/tide	0	0	0	0	0	0
Wind direction from wave (deg)	0	0	0	0	0	0
Current direction from wave (deg)	+90	+90	+90	+90	+90	+90

**Figure H.23—N-year Winter Storm H_{max} , West of 86° W**

H.9.2.5 Squalls

Peak squall winds do not rival hurricane wind extremes, but at the 10- and 100-year return period do exceed winter storm gusts at averaging intervals shorter than 1 min. Typical squall events are not stationary over the duration of an hour so comparison at the standard wind averaging interval is not meaningful. Because of their transient nature, squalls do not generate significant associated waves or currents. Squalls are a significant concern operationally because they are difficult to forecast and they can be associated with extremely rapid shifts in wind direction. The rapid increase in wind speed and shift in wind direction can pose a severe challenge to DP station-keeping systems, and there have been emergency disconnects during squalls.

The squall gusts in this section are based on extreme value analysis of NOAA buoys, CMAN coastal stations and offshore platform wind measurements^[237]. For consistency with criteria for other load cases in this annex the 5 s extremes in Reference [237] were converted to 3 s gusts. The 1 min gusts presented here were back-calculated using the squall gust factors in A.7.3.4. Associated sea states and pre-existing wind conditions were based on the same deepwater NOAA buoys used in Reference [237]. Guidance on the speed of extreme directional wind shifts is based on high sample rate measurements from Gulf of Mexico platform data made during the 3 April 2013 squall event at multiple sites supplemented by West Africa squall measurements during multiple events. Using West Africa squall data was needed as the Gulf of Mexico based measurements from NOAA/CMAN stations do not have the needed continuous temporal resolution to address rate of wind shift.

The following guidance is provided governing the use of the information provided in the tables.

- a) Squalls may occur any time of the year.
- b) When adjusting wind speeds to different elevations, the equations specifically developed for squall winds should be used (see A.7.3.4).
- c) When evaluating the sensitivity of a design or operation to a rapid shift in wind:
 - A pre-existing 10 m, 1 h wind speed of 10 m/s should be considered.
 - Associated wave and current may be taken as aligned with the pre-existing wind.
 - Consider that during a squall event the wind will increase rapidly and can shift through an angle greater than 90° in less than 5 min.
 - Associated wave and current should remain constant in magnitude and direction throughout the wind shift.

Table H.15—Squall Gust Extremes and Associated Sea State and Current

Load Case	Return Period (years)	
	10	100
Wind speed (10 m elevation)		
1 min mean (m/s)	29.4	32.6
3 s gust (m/s)	37.3	41.3
Waves		
Significant wave height (m)	2.1	2.1
Peak spectral period	7.0	7.0
Currents		
Speed (m/s)	0.30	0.30
Depth (m)	75	75

H.9.2.6 Loop and Eddy Currents

H.9.2.6.1 General

Two sets of Loop Current and eddy current conditions are provided: one set assuming maximum Loop current/eddy surface current and background wind and wave conditions, and the other set considering the joint occurrence of Loop Current/eddy events and storms at a site. The Loop Current conditions have been developed based on extrapolations from the GEM database [107, 114]. The nominal joint loop-storm cases have been estimated from the joint statistics [115] of winter storms, hurricanes, and Loop Current eddies for a location near Walker Ridge, supplemented by studies [116, 117] on the interaction of storm-generated waves and currents with the loop current.

H.9.2.6.2 Maximum Surface Current

Contours of 10- and 100-year Loop Current surface speeds are shown in Figure H.24 and Figure H.25 respectively, applicable to locations in water depths of 300 m or greater. Table H.16 shows associated winds, waves, and surge to apply in concert with the loop current, along with a normalized loop current profile. The profile should be scaled by the surface speeds provided in the two figures to develop a 10- or 100-year Loop Current profile, with the speeds never below 0.2 m/s. At and below 1000 m depth, a speed of 0.2 m/s should be applied regardless of return period. The currents, along with the associated winds and waves, should be treated as omni-directional. The duration associated with the Loop Current event can be represented as follows:

- ramp from 0.4 to 0.9 of n -year profile over 14 days;
- ramp from 0.9 of n -year profile to n -year profile over 24 h;
- n -year profile for 3 h;
- ramp from n -year profile to 0.75 of n -year profile over 48 h;
- ramp from 0.75 to 0.45 of n -year profile over 14 days.

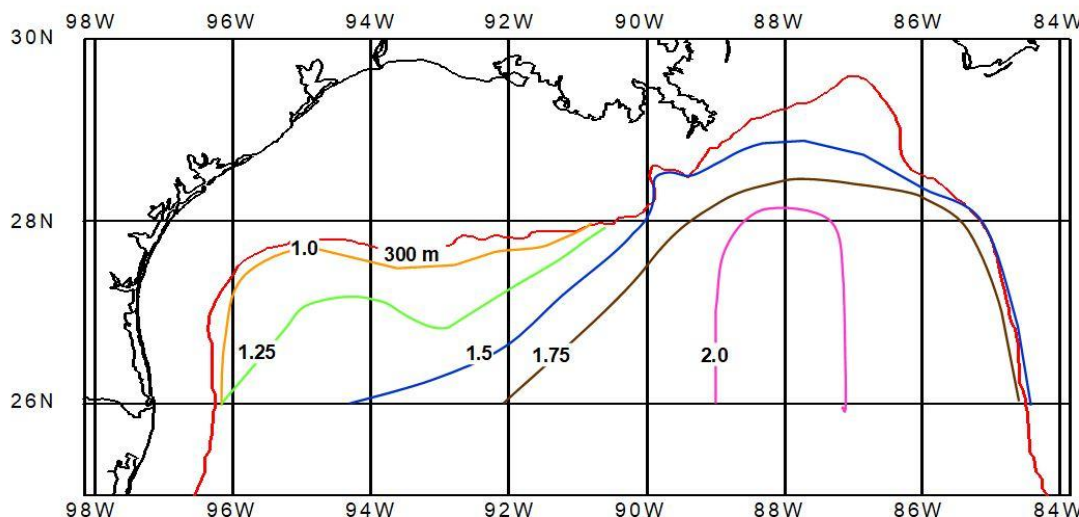


Figure H.24—10-year Loop Current/Eddy Surface Speeds (m/s)

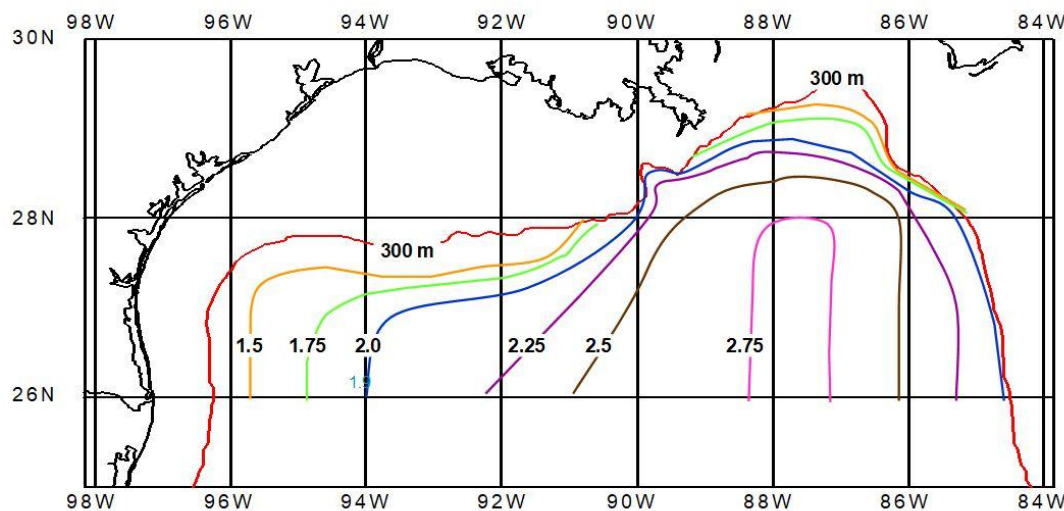


Figure H.25—100-year Loop Current/Eddy Surface Speeds (m/s)

Table H.16—Loop Current Profile and Associated Wind, Waves, and Surge

Wind (10 m elevation)	
1 h mean (m/s)	7.6
10 min mean (m/s)	8.0
1 min mean (m/s)	8.6
3 s gust (m/s)	9.4
Waves	
Significant wave height (m)	2.0
Maximum wave height (m)	3.0
Extreme water level (m)	1.8
Peak spectral period (s)	6.0
Period of maximum wave (s)	6.0
Water level	
Storm surge (m)	0.20
Tidal amplitude (m)	0.42
Normalized current profile	
Depth below surface (m)	Scale
0	1.00
50	0.99
150	0.66
300	0.35
600	0.20
1000+	0.20 m/s

H.9.2.6.3 Loop Current and Storms

The joint occurrence of Loop Current/eddy currents and winds and waves from tropical or winter storms at a site should be considered. These joint occurrences may be more frequent at some sites than at others; for example, sites in the southern Gulf of Mexico such as Walker Ridge would be expected to have more frequent joint occurrences due to a higher frequency of Loop Current/eddy encounters. Indicative joint cases and procedures for estimating them are available in industry literature^[136].

H.9.2.6.4 Topographic Rossby Waves

The deepwater areas between 89.5° and 92° W along the Sigsbee Escarpment and toward Green Knoll are frequently subject to very strong bottom currents due to the interaction of TRWs with the steep local bathymetry. Table H.17 provides nominal 10- and 100-year values of bottom current speeds due to TRWs along this area. The conditions have been developed from very limited measurement records^[114] and hence have a high level of uncertainty. The following guidance applies.

- a) TRWs should be considered along the Sigsbee Escarpment towards Green Knoll (1500 to 3000 m, from 89.5° to 92° W). To the north (shallow side) of the Escarpment, the current should decay as e^{-x} where x the distance in km from the Escarpment base. To the south (deeper) direction, assume the current should decrease as $e^{-x/50}$.
- b) The current profile should be constant from the bottom to the top of the Escarpment, and then decay linearly to background surface values (may assume 0.25 m/s).
- c) The current heading should be toward a westerly direction but aligned with the local isobaths averaged over roughly a 30 km along-slope section.
- d) Currents generated by TRWs often appear as a series of two pulses each 7 to 14 days in duration, with the duration dependent on the location along the Escarpment. The increase and decay of the pulses can be characterized by $\sin(\pi t/D)$ for $0 \leq t \leq D$, with t in days, and D is the duration (7 to 14 days).
- e) The potential for simultaneous occurrence of TRW and Loop Current/eddy currents at a site should be considered.

Table H.17—N-Year Current from TRW, 3 m above Bottom

Return Period (years)	Current (m/s)
10	1.00
100	1.25

H.9.2.7 Air and Sea Temperatures

Table H.18—Indicative Extreme Air and Sea Temperatures

Parameter	Factors
Sea water temperature	
Minimum near-surface	8.5 C
Maximum near-surface	32.5 C
Minimum near-bottom (2000 m)	3.2 C
Maximum near-bottom (2000 m)	4.8 C
Air temperature	
Minimum	0.0 C
Maximum	39.0 C

H.9.3 Long-term Distribution of Metocean Parameters

A wave scatter diagram for the deepwater areas of the northern Gulf of Mexico, showing the total significant wave height and associated spectral peak periods, is provided in Table H.19. This table is applicable to exposed deep water areas. For shallower areas, there can be site- and depth-dependent effects in the long-term distributions as well as in the extreme criteria. The information in the table was generated from data from National Data Buoy Center Buoy No. 42001, located in the central Gulf at 25.92 °N, 89.68 °W.

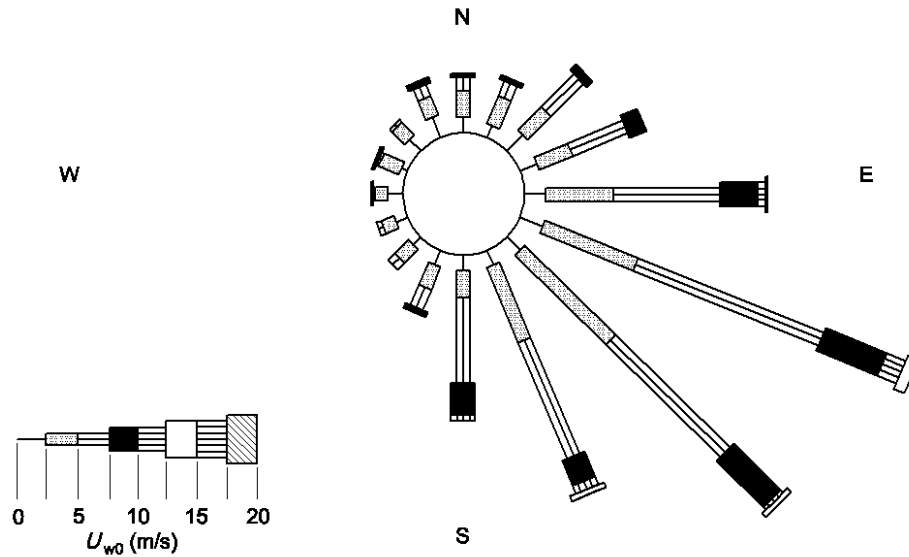
Figure H.26 shows wind roses for a location in the northwest Gulf of Mexico, for the summer and winter periods.

It is emphasized that the long-term distribution of currents, particularly for sites in deepwater, is of critical importance in the design of offshore facilities. The long-term distribution of currents should be determined through site-specific studies.

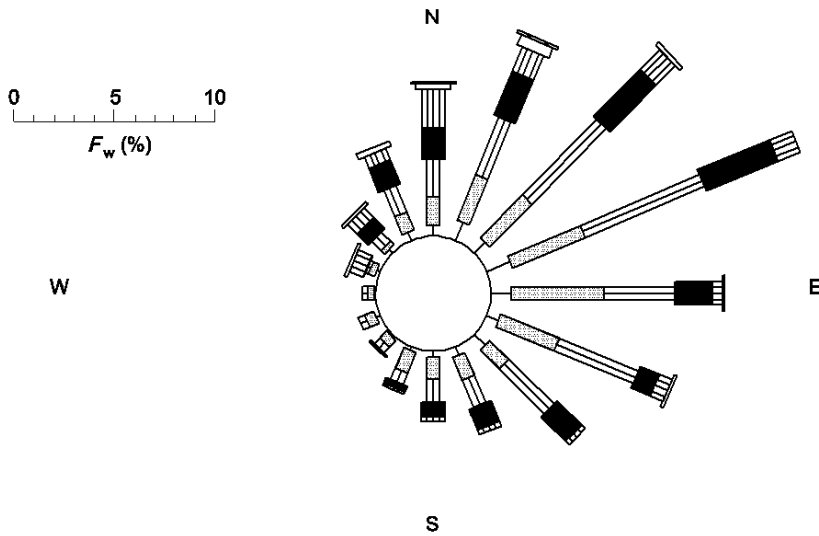
Table H.19—Percentage Occurrence of Total Significant Wave Height and Spectral Peak Period Combinations—Deep Water Location—Gulf of Mexico

Significant Wave Height (m)	Peak Period (s)												
	0.5 to 1.5	1.5 to 2.5	2.5 to 3.5	3.5 to 4.5	4.5 to 5.5	5.5 to 6.5	6.5 to 7.5	7.5 to 8.5	8.5 to 9.5	9.5 to 10.5	10.5 to 11.5	11.5 to 12.5	Total for 0.5 to 12.5
0.2 to 0.5	0	0.16	1.99	4.26	5.67	2.74	1.05	0.67	0.05	0.01	0.02	0	16.62
0.5 to 0.8	0	0.04	1.22	3.39	7.78	6.62	1.84	0.53	0.13	0.01	0.00	0	21.56
0.8 to 1.1	0	0.01	0.35	1.41	4.80	7.84	3.14	0.61	0.08	0.03	0.00	0	18.27
1.1 to 1.4	0	0	0.07	0.27	1.97	5.89	4.78	1.50	0.08	0.01	0.01	0	14.58
1.4 to 1.7	0	0	0.01	0.05	0.49	3.02	4.28	2.32	0.14	0.03	0.01	0	10.35
1.7 to 2.0	0	0	0	0	0.13	1.16	2.87	2.37	0.23	0.03	0.01	0	6.80
2.0 to 2.3	0	0	0	0	0.03	0.36	1.54	2.05	0.39	0.08	0.02	0	4.47
2.3 to 2.6	0	0	0	0	0	0.11	0.62	1.46	0.39	0.10	0.02	0	2.70
2.6 to 2.9	0	0	0	0	0	0.02	0.20	0.88	0.37	0.11	0.02	0	1.60
2.9 to 3.2	0	0	0	0	0	0	0.06	0.46	0.42	0.08	0.02	0	1.04
3.2 to 3.5	0	0	0	0	0	0	0.02	0.20	0.25	0.10	0.03	0	0.60
3.5 to 3.8	0	0	0	0	0	0	0.01	0.12	0.17	0.13	0.03	0	0.46
3.8 to 4.1	0	0	0	0	0	0	0	0.08	0.12	0.13	0.04	0	0.37
4.1 to 4.4	0	0	0	0	0	0	0	0.02	0.05	0.08	0.03	0	0.18
4.4 to 4.7	0	0	0	0	0	0	0	0.01	0.03	0.04	0.05	0	0.13
4.7 to 5.0	0	0	0	0	0	0	0	0	0.01	0.03	0.05	0	0.09
5.0 to 5.3	0	0	0	0	0	0	0	0	0	0.01	0.05	0	0.06
5.3 to 5.6	0	0	0	0	0	0	0	0	0	0.00	0.04	0	0.04
5.6 to 5.9	0	0	0	0	0	0	0	0	0	0.01	0.04	0	0.05
5.9 to 6.3	0	0	0	0	0	0	0	0	0	0.01	0.02	0	0.03
Total for 0.2 to 6.3	0	0.21	3.64	9.38	20.87	27.76	20.41	13.28	2.91	1.03	0.51	0	100.00

NOTE The table does not adequately represent extreme hurricane or extratropical storm events.



a) Typical June wind rose



b) Typical December wind rose

Directions are "from"

Shading indicates wind speed, U_{w0}

Length indicates percentage of month (F_w) at that direction and wind speed

Figure H.26—June/December Wind Roses—Northwest Gulf of Mexico [75]

H.10 Guidelines for Site-specific Metocean Studies in the US Gulf of Mexico

H.10.1 General

Performance of a site-specific metocean study is the only way of ensuring that regional variations in storm climate and local topographic and bathymetric effects are properly accounted for, as well as ensuring sufficient data is available to properly identify the phasing between wind, wave, current, and surge and to serve as inputs to response-based analyses aimed at determining n -year forces. It is emphasized that the goal of a site-specific study is more accurate information on the metocean conditions at a site; site-specific studies should not be performed with the sole goal of rationalizing the lowest set of design conditions possible.

Site-specific studies should be performed in conformance with the guidelines provided in A.5, with additional guidance on specific Gulf of Mexico phenomena provided below. In general, metocean conditions in the Gulf of Mexico are developed from statistical extrapolation of historical data, either measured directly or estimated through the use of hindcast models; hence, most of the guidance is related to this approach. For phenomena of limited spatial scale as compared to the size of the Gulf, such as tropical cyclones and Loop Current eddies, site pooling or averaging [128, 129, 132] is generally invoked in order to account for track variability that would occur in a longer record. Comparisons [131] between the pooling method and other site data handling methods using typical Gulf of Mexico extremal distributions has shown the pooling method works reasonably well for return periods of several hundred years and less. Industry is also evaluating the use of deductive [131] and synthetic [137, 138] models, to better estimate return periods in excess of several hundred years.

H.10.2 Hurricanes

H.10.2.1 Annual Conditions

A site-specific study of hurricane metocean conditions should be based on a hindcast database of winds, waves, currents, and surge derived from models that have been validated against severe historical storms from 1950 to 2008 including Opal (1995), Ivan (2004), Katrina (2005), and Ike (2008). Validation should show that the wind, wave, and surge models have a coefficient of variation no more than 15 % when comparing model peak wind speed, wave height, or surge height to their respective measured peak values. An acceptable coefficient of variation for the current model validations can be as high as 30 %. Any bias between the model and data should be removed with at least a simple linear fitting process. Use of numerical wave, current, and surge models based on discrete finite element or finite difference solutions of the governing partial differential equations is preferred; grid resolution for models should be equal to or finer than 15 km and the overall domain should be sufficient to prevent boundary conditions from affecting the solution. Parametric models of wave, current, and surge should only be used if they have been extensively calibrated against major severe storms.

Data used for storm wind field characterization should use as a starting point the National Hurricane Center “best track” data set. Additional storm parameters such as radius to maximum winds should be determined from surface measurements, aviation reconnaissance, and satellite observations. The hindcast period used should initially consider all storms from 1900 to the present date. It is strongly recommended that more weight be given to the post-1950 period, as storm observations prior to this time generally are fewer in quantity and of lower quality due to the lack of aircraft and satellite observations; however, caution and good judgement shall be used, as it cannot be denied that some areas of the Gulf, particularly the western areas, saw more frequent severe cyclone activity in the 1900–1949 period than 1950–2010. A prudent approach to hurricane extremes is using both the 1900–present and 1950–present data sets to develop criteria, and adopting the higher results from both sets; early storm data should not be used if it results in extremes lower than using the post-1950 set of data.

Because of the low frequency of occurrence and relatively small diameter of hurricanes, estimates of extremes made from a limited (in this case, 50- to 100-year) database can vary substantially over relatively small distances, even within a region that would be expected on the basis of physical arguments to be statistically homogeneous. Specifically, sites that are very near the tracks of one or more of the few historical severe hurricanes will have much greater estimates of 100-year winds, waves, current, and surge than sites that are not near one of those tracks. It is not reasonable to expect that extreme

hurricanes in the next few centuries will have exactly the same tracks as historical hurricanes. Therefore, some means of smoothing site-specific conditions estimated from a limited database, accounting for track variability, should be used. Commonly used methods include simple spatial smoothing of site-specific estimates, track shifting, and grid point pooling. With regard to site pooling there is no uniquely "correct" way to do it. However, using data from three or more sites, all lying within the region that is expected to be homogeneous on the basis of physical arguments, arranged in a curvilinear array oriented more or less perpendicular to the tracks of the most severe hurricanes in deep water, or oriented along a bathymetric contour in shallow water, with a spacing of at least 75 km between grid points to reduce the correlation among grid point statistics, generally provides reasonable results. Some deepwater locations may need a south-north and east-west arrangement of grid points (such as a five-point "cross" centered on the site) to capture the influence of both south-to-north and east-to-west tracking storms near the site. The distance over which pooling is performed should generally not be less than 150 km or greater than 400 km wide, and should be selected with attention to local water depth, fetch limitations, proximity to the Loop Current or areas with frequency warm-core eddies, and orientation of major storm tracks.

For return periods greater than 100 years, extremes may be derived either using the methods above or through the use of deductive models or Monte Carlo simulations of synthetic storms.

H.10.2.2 Sudden Hurricane Conditions

Development of sudden storm conditions, used to assess risks to platforms when manned, requires definition of the timing and environment limits associated with removing personnel from a facility at a given site. The arrival of tropical storm force winds at a site within 24 h of a system becoming a named storm has commonly been used as a screening criterion for identifying those storms considered sudden; however, this criterion is by no means universal. Platforms located farther south in the Gulf of Mexico, and possibly having large crews requiring more time to evacuate, may have sudden storm populations quite different from those associated with smaller platforms close to shore.

Once the timing and environment limits have been established, the historical storm record can be scanned and those storms identified as being "sudden" for the site will be those from which sudden storm conditions are derived. The guidelines associated with storm hindcasts, data set length, and pooling extents described in H.10.2.1 also apply to sudden storms.

H.10.2.3 Seasonal Conditions

The following guidelines are recommended for the derivation of seasonal hurricane conditions in the Gulf of Mexico, and should be followed when a site-specific study is performed.

- a) Studies of seasonal conditions should at a minimum consider the distinction between the peak and nonpeak periods of cyclone activity. The peak period of cyclone activity is that period from early August through mid-October; extremes derived for this period should be essentially identical to the annual extremes for the location in question, due to the concentration in this time period of severe storms which control the annual extremes.
- b) Conditions outside of the peak period of hurricane season can be defined by considering those storms occurring between May and late July/early August to define an early season period, and those occurring after mid-October through December to define a late season period.
- c) When defining seasonal hurricane conditions, extreme conditions associated with other storm phenomena such as frontal or extra-tropical storms should also be evaluated, taking care to keep the tropical and nontropical storm populations separate. For periods outside of the peak of hurricane season, particularly in the late season period after mid-October, wind and wave extremes may be controlled by winter storms instead of tropical cyclones. The total risk to an operation is the combined risk from tropical and nontropical storms through the period of the operation.

H.10.3 Winter Storms

Perhaps the best source of data for winter storm winds and waves is that recorded by the NOAA buoys in the Gulf of Mexico. Several of these stations have nearly 25 years of data. Another source of information is the WINX [67] hindcast; however, users of WINX are cautioned that the hindcast has a known low bias, has

insufficient events to derive statistics for conditions more frequent than 10 years, and also does not include the most severe extratropical event to affect the Gulf of Mexico, the "Storm of the Century" in March 1993. The GOMOS [68] hindcast includes a winter storm hindcast starting in 1950 and a continuous hindcast period from 1980 onward. An additional source of data is the continuous WaveWatch III hindcast being archived by NOAA [118].

As the scale of these storms is quite large compared to tropical cyclones there is comparatively less east-to-west regional variation in extremes across the Gulf. In this Annex, deepwater extremes were represented with a single set of values (see Table H.13) for the entire US portion of the Gulf. It should be noted, however, that the winter storm climate on the Florida shelf is significantly more severe than in the western and central Gulf as is reflected in both NOAA buoy data and the above noted hindcasts.

H.10.4 Loop Currents and Eddies

The GEM database [107] maintained by CASE-EJIP is generally applied to the derivation of Loop Current conditions in the Gulf of Mexico. The database consists of eddy events from the early 1970s through 2013; however, users are generally cautioned to avoid relying on the pre-1985 data due to the sparse nature of eddy observations prior to this time. In addition, starting in 2001 the Gulf of Mexico has seen a large increase in the generation of eddies by the Loop Current; statistics developed prior to that time will appear biased low without the addition of the last 7 years. As with hurricane conditions, there is no unique way to generate *n*-year conditions from historical data. A typical approach is to develop eddy statistics at a location by pooling five sites in a cross pattern, with the sites separated by approximately 30 km.

The issue of Loop-hurricane interaction has begun to receive more attention in recent years, as a number of sites have been subjected to both eddy currents and hurricanes in the 2004 and 2005 hurricane seasons. While most deepwater design bases generally include a Loop-winter storm condition for assessment, few include a joint Loop-hurricane condition. Recent examination of both hurricane and Loop Current/eddy site statistics will show that with the increase in both eddy activity, and the more frequent occurrence of large hurricanes in the Gulf of Mexico, the likelihood of having joint Loop-hurricane events has correspondingly increased. However, even with the increased number of events, there are still at most 20 years with useful data on hurricane-Loop Current/eddy encounters.

Studies sponsored by CASE-EJIP [116, 117] have revealed the potential for hurricane inertial currents to become trapped and enhanced near Loop Current Eddy fronts, leading to strong currents at depth. The interaction is highly nonlinear, and cannot be resolved by simply superimposing the individual Loop and hurricane current components. This case could be significant for deepwater risers. In addition, the presence of eddy currents may result in focusing the waves from hurricanes, leading to increases in wave height in certain areas of the hurricane wave field that would depend on the relative geometry of the eddy and the hurricane during the passage of the hurricane. A further effect is that the passage of a large hurricane can cause large displacements in the Loop Current front, causing it to otherwise encroach on sites that the GEM model would indicate are free of Loop Current/eddy effects.

One approach that has been applied to the problem is to develop an extended time series of Loop-hurricane encounters affecting a site, and then model the joint encounters in such a way that the nonlinear interaction is properly represented. Final design statistics are then developed from the hindcast interaction events. At present the CASE-EJIP is exploring the development of a parametric model to represent the coupling between inertial and Loop Current/eddy currents. Additionally, some wave hindcast models allow for the explicit consideration of the effects of surface current fields on waves; use of these models should be considered for sites where Loop-hurricane encounters are relatively frequent.

H.10.5 Topographic Rossby Waves

The deepwater areas between 89.5° and 92° W along the Sigsbee Escarpment and towards Green Knoll are frequently subject to very strong bottom currents due to the interaction of TRWs with the steep local bathymetry. At present, the mechanism for TRWs is not well understood. The best approach for development of design statistics is to utilize existing industry and government measurements made in close proximity to the site in question, or to undertake a site-specific measurement program. It should be noted that there is some evidence that generation of TRWs is linked to the presence of the Loop Current, and that joint Loop Current/eddy-TRW may be relatively frequent [136].

Annex I (informative)

US Coast of California

I.1 Description of Region

The geographical extent of the region is the waters off the coast of California in the United States, the hydrocarbon producing area being shown in Figure I.1.

The region is primarily the Southern California Bight, which stretches from Point Arguello to San Diego and contains all but one of the offshore oil-producing blocks on the west coast of the lower 48 states of the United States. The northern portion of the bight contains an important sub-region, the Santa Barbara Channel, where the majority of offshore production lies. The bight is bounded to the north and east by the California coast and offshore to the west by the Santa Rosa-Cortes ridge (see Figure I.1). There are numerous submarine valleys and mountains within the bight. The peaks of some of the mountains pierce the surface and form the Channel Islands.

I.2 Data Sources

A comprehensive summary of the available oceanographic (excluding waves) and meteorological data is provided in Reference [83]. In addition, the US Bureau of Ocean Energy Management, Regulation, and Enforcement (BOEMRE) has published the proceedings of a workshop on oceanography of the Southern California Bight [84]. Most of this clause focuses on the bight and the Santa Barbara Channel.

An extensive study [85, 86] of the Santa Barbara Channel included nine current moorings and a similar number of wind stations deployed for three years. Data were collected between 1992 and 1995, and the analysis was completed in 1997.

Extensive wind and wave data sets now exist at several sites along the California coast. There are many years of wind and wave data available at the National Data Buoy Center from five data buoys lying between 5 and 50 km off the coast in the bight. Some of these buoys have been equipped with acoustic doppler current profilers (ADCP) in recent years. In addition, the Scripps Institution of Oceanography has maintained roughly 17 wave stations along the coast in the bight [85]. Some of the stations have operated almost continuously since 1978 and include directional wave information.

A cooperative study between BOEMRE and the state of California, the “Santa Barbara Channel–Santa Maria Basin Circulation Study,” was completed in the late 1990s, with the objectives of determining the frequency, the timing of occurrence and the short-term variability of the major circulation processes of importance in the Santa Barbara Channel–Santa Maria Basin Circulation. Pertinent publications arising from this study include References [87] to [92].

I.3 Overview of Regional Climatology

The climate of the bight is Mediterranean, characterized by partly cloudy, cool summers, with little precipitation. Thunderstorms are infrequent. Winters are mostly clear and mild. Precipitation in winter is associated with winter seasonal storms. Fog and low clouds are common along the coast during the night and early morning hours in late spring and early summer. Afternoons are usually clear with sea breezes. The persistent Pacific High over the ocean to the west, combined with thermal contrasts between the land and the adjacent ocean and with effects of the coastal mountain range, result in mild temperatures throughout the year [93].

During the winter season, three weather regimes are common [93]:

- periods of low clouds and fog;
- periods of clear skies, cool nights, and warm days;
- periods of variable cloudiness, shifting and gusty winds, and precipitation.

An atmospheric low, sometimes referred to as the Catalina Eddy, is often present in the Southern California Bight. When this eddy expands northward, short-duration south-easterly sea breezes develop in the Santa Barbara Channel in the afternoon. When the eddy is well developed, the sea breezes can persist all day [93].

I.4 Water Depth, Tides, and Storm Surges

Tides are mixed, with the semi-diurnal constituent dominating the diurnal constituent. Tidal ranges are small, with mean ranges of about 1 m. Maximum water depths within the Santa Barbara Channel are approximately 1000 m. Water depths increase rapidly west of the Channel Islands. Storm surge is not a major design consideration offshore California.

I.5 Winds

Winds tend to be steady all along the California coast and are primarily driven by the subtropical anticyclone over the eastern Pacific. The anticyclone is strongest during the summer months, when it occupies its most northerly position near 30 °N to 40 °N and 140 °W to 150 °W. During the winter, the airflow over the open ocean is generally westerly off northern California and northwesterly off southern California. In the spring, the speed increases and becomes uniformly northwesterly over the entire region. This continues throughout the summer with mean speeds reaching 9 m/s to 10 m/s near points such as Point Conception/Point Arguello. In the autumn, winds weaken somewhat and slowly return to the two-region winter flow pattern.

The strongest wind forcing during the winter comes from strong fronts moving through the bight toward the east. Winds reach 20 m/s to 25 m/s and become much more intense around points such as Point Conception. Between fronts, the surface pressure gradient sometimes reverses and this can cause strong low-level offshore flows known as Santa Anas, characterized by easterly flow of dry desert air with speeds of 10 m/s to 15 m/s.

Tropical storms can occasionally reach the southern portions of the bight in late summer to early fall; however, as they reach the bight, the storms are rapidly eroded by the bight's cold surface waters.

I.6 Waves

The wave environment of the Southern California Bight area is the result of local wind-driven waves and swell from distant storms. The Channel Islands and the ridges shelter the Santa Barbara Channel from much of the offshore wave energy. This effect is dramatically illustrated by the fact that wave spectral energy is an order of magnitude lower at Sunset Beach (south of Los Angeles) than it is at San Nicholas Island. The restricted fetches in the bight result in relatively small amplitude, short period wind seas. The short durations of the sea breezes also tend to keep wave amplitudes low. High waves form in the region only when gale-force winds blow from the west. Individual wave heights as high as 7.6 m have been reported in the San Pedro Channel as a result of these winds. Locally generated waves are characterized by their choppiness and are always accompanied by high winds. Sheltering effects of the shoreline are reduced because these waves and swell are locally generated.

Long period swell can come from north, west, or south, but most is generated by winter storms in the North Pacific Ocean. To the north of Los Angeles and south of the Santa Barbara Channel, the extreme waves are driven by the large extratropical winter storms of the eastern Pacific, between Hawaii and the California coast. The dominant swell period is 16 s.

Extreme wave conditions in the southern part of the bight are dominated by swell from the occasional eastern Pacific hurricane.

I.7 Currents

Currents in the bight are complex and poorly understood. Tidal currents are weak and less than 0.1 m/s except near narrow passages like the southern Santa Barbara Channel where velocities can reach 0.1 m/s to 0.2 m/s due to an internal tide. To the north of the bight, the mean flow is dominated by the California Current flowing south with mean speeds of 0.1 to 0.2 m/s. To the south of the Santa Barbara Channel, there is evidence of weak northerly flow that sometimes displays a large cyclonic motion. The Santa Barbara Channel is a mixing zone of the California Current and the northerly flowing warm bight waters. As a result, large water temperature gradients are often evident with unusually complex flows that are independent of local wind.

Extreme currents are generally mild, reaching perhaps 0.5 m/s to 1.0 m/s. They are weakly correlated with the local wind except in shallow water less than 50 m deep. Extreme currents in deeper water (greater than 50 m) are probably driven by nonlocal, large-scale processes originating from the California Current. Vertical temperature stratification is mild, with a weak thermocline evident between 60 m to 100 m below the surface. Extreme flows tend to be uniform with depth, much as in the North Sea.

I.8 Other Environmental Factors

I.8.1 Marine Growth

Offshore southern and central California, marine growth thicknesses of 200 mm are common. Site-specific studies should be conducted to establish the thickness variation with depth.

I.8.2 Snow and Ice Accretion

Snowfall and ice accumulations on structures are not design or operational considerations offshore California.

I.8.3 Tsunamis

The highest water level increases (1.5 m to 4.5 m) along the California coast are caused by tsunamis. Fortunately, tsunamis occur only infrequently and should not cause serious damage to properly designed offshore structures in deep water.

I.9 Estimates of Metocean Parameters

Indicative extreme values of metocean parameters for two areas offshore California are provided in Tables I.1 and I.2.

Indicative values of operational metocean parameters offshore California are provided in Table I.3.

Table I.1—Indicative Independent Extreme Values for Winds, Waves, and Hurricane-driven Currents for Southern California (Santa Barbara and San Pedro Channels)

Metocen Parameter	Return Period (years)				
	1	5	10	50	100
Wind speed (m/s)					
10 min mean wind speed	18	22	24	27	28
3 s gust wind speed	22	27	30	34	35
Wave height (m)					
Maximum	6.3	9.4	10.6	13.5	14.6
Significant	3.5	5.2	5.9	7.5	8.1
Wave direction (from)	W-NW	W-NW	W-NW	W-NW	W-NW
Spectral peak period (s)	14–17	14–17	14–17	14–17	14–17
Current speed (m/s)					
Surface current speed	1.2	1.2	1.3	1.4	1.5
90 m depth current speed ^a	0.5	0.5	0.6	0.6	0.7
1 m above sea floor current speed	0.5	0.5	0.6	0.6	0.7

^a For water depths less than 90 m, the seabed current should be calculated from a linear distribution between the surface current and that at 90 m depth in this table.

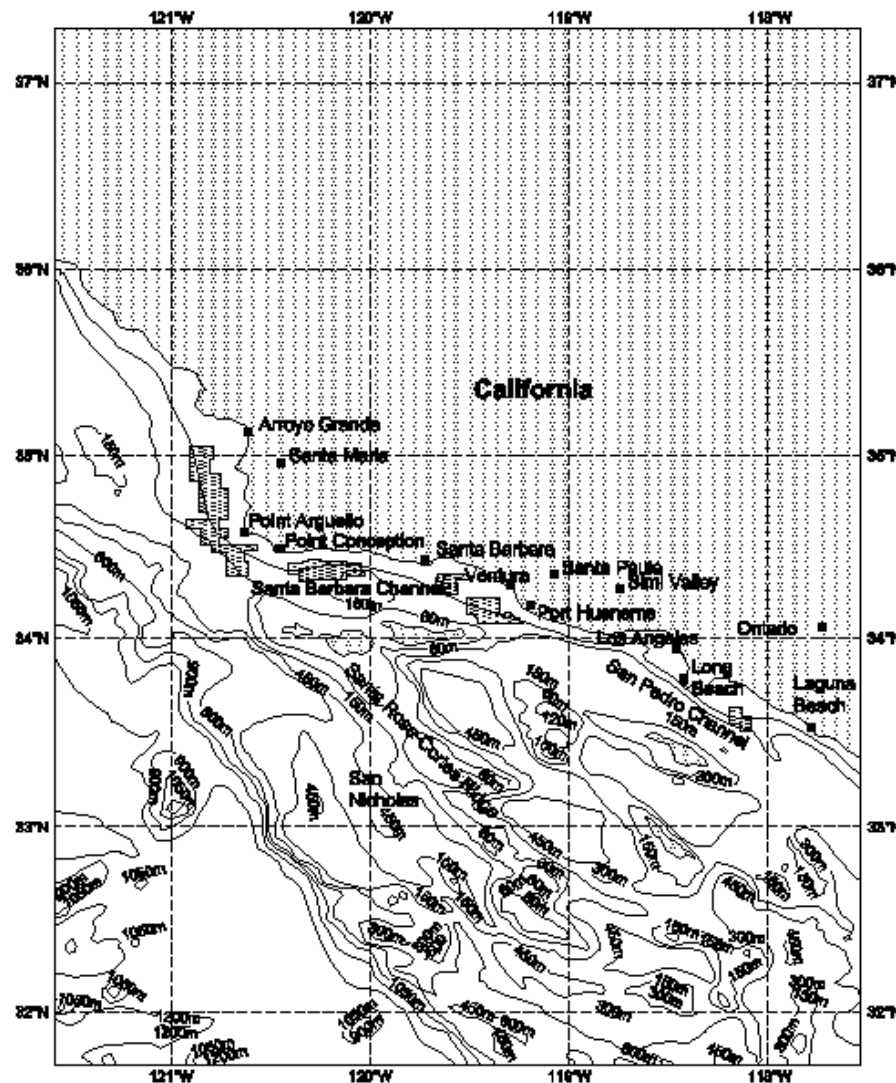
Table I.2—Indicative Independent Extreme Values for Central California

Metocen Parameter	Return Period (years)				
	1	5	10	50	100
Wind speed (m/s)					
10 min mean wind speed	14	18	19	21	22
3 s gust wind speed	17	22	23	26	27
Wave height (m)					
Maximum	9.4	13.5	14.2	15.8	16.4
Significant	5.2	7.5	7.9	8.8	9.1
Wave direction (from)	NW-N	NW-N	NW-N	NW-N	NW-N
Spectral peak period (s)	10–17	12–17	12–17	12–17	12–17
Current speed (m/s)					
Surface	0.6	0.7	0.7	0.8	0.8
90 m depth ^a	0.5	0.6	0.6	0.7	0.7
1 m above sea floor	0.5	0.6	0.6	0.7	0.7

^a For water depths less than 90 m, the seabed current should be calculated from a linear distribution between the surface current and that at 90 m depth in this table.

Table I.3—Indicative Extreme Values for Other Metocean Parameters

Mean spring tidal range (m)	1.0 m
Sea water temperature (°C)	
Min. near surface	12.5
Max. near surface	20.0
Swell	
Maximum height (m)	2.5 (spring)
Period (s)	16 to 18 (winter) 5 to 10 (summer)
Direction (from)	S to W
Air temperature (°C)	
Minimum	10.0
Maximum	21.8

**Figure I.1—Map of California Offshore Region**

Annex J (informative)

Other US Waters

J.1 Overview of Regions Excluding Gulf of Mexico and California

Guideline omni-directional metocean conditions with a nominal return period of 100 years are provided in Table J.1 and Table J.2 for the areas of US waters outside of the Gulf of Mexico (Zones 1 and 2) and California (Zones 3, 4, and 5) shown in Figure J.1. Except as noted, the guideline waves and storm tides are applicable to water depths greater than 90 m. The conditions have been compiled from a variety of sources [139 to 163], many of which are quite dated. The numbers provided have a high degree of uncertainty and should not be relied on for design purposes.

The ranges of wave heights, currents, and surge reflect variations in interpretation of the data in the references cited, quality rating, and the spatial variability within the areas shown. The ranges in wave steepness reflect the variability in wave period associated with a given wave height. Significant wave height H_s can be estimated from the relationship $H_{max}/H_s = 1.7$ to 1.9. Peak spectral period T_p can be estimated from the relationship $T_p/T_{H_{max}} = 1.05$ to 1.20. The wave heights are generalized to apply to open, broad continental shelf areas. Coastal configurations, exposure to wave generation by severe storms, and bottom topography may cause variations in wave heights for different sites within an area, especially for areas 9, 10, and 13 through 18.

Areas 6 through 17 are dominated by extratropical storms; a wave kinematics factor of 1.0 should be used unless a lower factor can be justified on the basis of reliable and applicable measured data. Areas 18 through 20 are affected by both extratropical storms and hurricanes; consequently the wave kinematics factor varies between 0.88 and 1.0.

Two wind speed values are provided in Table J.2; the first is the wind speed associated with the maximum wave height, while the second is the independent extreme. The reference elevation is 10 m and the averaging interval is 1 h.

The currents provided are near-surface values, in line with the wave direction. The currents should be considered uniform to a depth of 70 m, with a speed defined by the value in Table J.1 less than 1 m/s for depths below 70 m.

Site-specific studies should be conducted to establish the thickness variation of marine growth with depth.

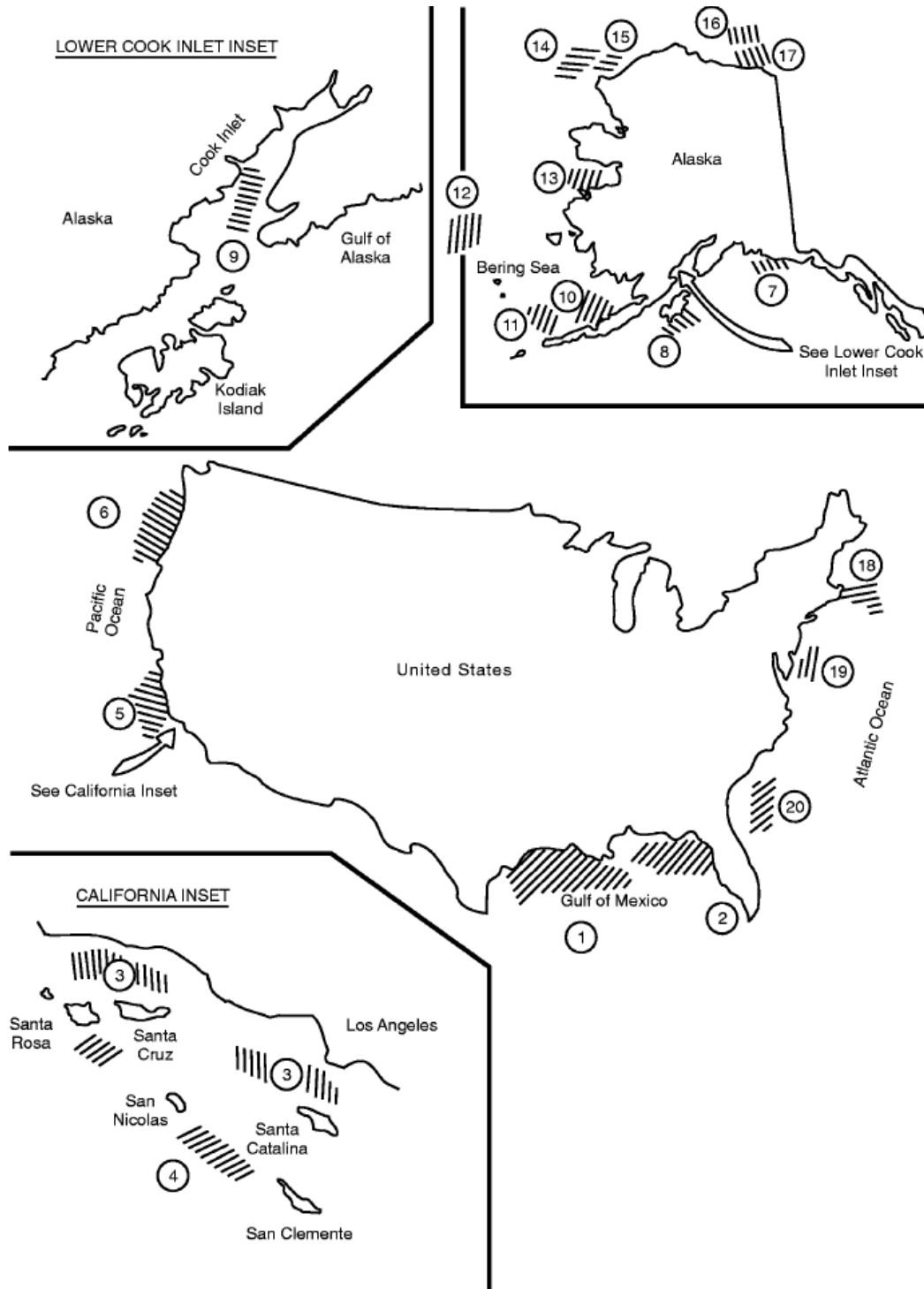


Figure J.1—Other US Waters

Table J.1—Nominal 100-year Extreme Wave with Associated Current and Storm Tide for Other US Waters (Depths > 90 m Unless Otherwise Noted)

Zone	Location	100-Year H_{\max} (m)		Wave Steepness	Current (m/s)		Storm Tide (m)		Basis
		Mean	Range		Range	Mean	Range	Mean	
6	Washington/Oregon	26	21–31	1/13–1/19	1.0	0.5–2.0	2.4	2.1–3.0	3
7	Gulf of Alaska (Icy Bay)	31	27–37	1/13–1/17	1.5	1.0–2.0	3.4	3.0–4.0	2
8	Gulf of Alaska (Kodiak)	28	24–34	1/13–1/17	1.5	1.0–2.0	3.0	2.7–3.7	2
9	Lower Cook Inlet	18	14–21	1/10–1/11	2.0	1.5–3.0	4.9	4.0–6.1	2
10	Northern Aleutian Shelf	21	18–27	1/12–1/16	1.5	1.0–2.0	2.4	1.8–3.7	1
11	St. George Basin	26	23–29	1/12–1/16	1.5	1.0–2.0	1.5	0.9–2.1	1
12	Navarin Basin	26	23–29	1/12–1/16	1.0	0.5–1.5	1.2	0.9–1.5	1
13	Norton Sound (depth = 18 m)	14	11–15	1/11–1/18	1.5	0.5–2.0	3.4	2.4–4.3	2
14	Chukchi Sea (depth > 18 m)	15	12–18	1/11–1/15	1.0	0.5–1.5	1.8	1.2–2.4	3
15	Chukchi Sea (depth ≤ 18 m)	Depth limited	Depth limited	1/11–1/15	1.5	1.0–2.5	2.7	1.8–3.7	3
16	Beaufort Sea (depth > 15 m)	12	11–15	1/13–1/17	1.0	0.5–1.5	1.2	0.6–2.1	2
17	Beaufort Sea (depth ≤ 15 m)	Depth limited	Depth limited	1/13–1/17	2.0	1.5–3.0	2.4	-0.6–3.7	2
18	Georges Bank	26	23–29	1/10–1/16	1.0	0.5–1.5	1.5	1.2–1.5	2
19	Baltimore Canyon	28	24–31	1/10–1/14	1.5	1.0–2.0	1.5	1.2–1.5	2
20	Georgia Embayment	23	20–26	1/11–1/15	2.5	1.0–4.0	1.5	0.9–2.1	2
NOTE 1 $T_{H_{\max}}$ associated with H_{\max} should be calculated from the wave steepness (S) according to $T_{H_{\max}} = [2\pi H_{\max}/gS]^{0.5}$, with $g = 9.81 \text{ m/s}^2$.									
NOTE 2 The current is in-line with the wave, uniform to 70 m, and then uniform from 70 m to the bottom with speed reduced by 1 m/s (never less than 0.1 m/s).									
NOTE 3 The storm tide includes both storm surge and tide, i.e. reference is to MLLW.									
NOTE 4 Where waves are depth-limited, calculate H_{\max} according to $H_{\max} = 0.78(\text{depth} + \text{storm tide})$.									
NOTE 5 Basis: (1) = based on comprehensive hindcast study verified against measurements, (2) = based on hindcasts and/or measurements, (3) = preliminary estimates.									

Table J.2—100-year Extreme Wind Speeds for Other US Waters

Zone	Location	Wind Speed (10 m 60 min), m/s	
		With Wave	Maximum
6	Washington/Oregon	31	41
7	Gulf of Alaska (Icy Bay)	31	46
8	Gulf of Alaska (Kodiak)	31	46
9	Lower Cook Inlet	31	46
10	Northern Aleutian Shelf	31	46
11	St. George Basin	31	46
12	Navarin Basin	31	46
13	Norton Sound (depth = 18 m)	31	46
14	Chukchi Sea (depth > 18 m)	31	41
15	Chukchi Sea (depth ≤ 18 m)	31	41
16	Beaufort Sea (depth > 15 m)	31	36
17	Beaufort Sea (depth ≤ 15 m)	31	36
18	Georges Bank	31	41
19	Baltimore Canyon	46	51
20	Georgia Embayment	46	51

Annex K (informative)

Identification and Explanation of Deviations

K.1 Introduction

The Metocean and Hydrodynamics resource group of the API Subcommittee on Offshore Structures that voted to adopt ISO-19901-1:2015 as Revision 2 of API 2MET determined that the following modifications were necessary. These deviations from the ISO standard have been incorporated directly into the text.

K.2 List of Modifications

Modifications to ISO-19901-1:2015 made during its adoption as the Second Edition of API 2MET are shown as follows.

Clause/Subclause	Modifications
A.7.3 Wind Profile and Time-averaged Wind Speed	<p>This subclause recommended using the Frøya wind profile and time-averaging relations for all storm types. This subclause now has four subsections:</p> <ul style="list-style-type: none">• (A.7.3.1) Explains which relations are appropriate to which storm type.• (A.7.3.2) Present the Frøya equations as appropriate for extratropical storms. The text and equations in this subsection are unchanged from the original description.• (A.7.3.3) Present simplified ESDU equations as appropriate for tropical cyclones.• (A.7.3.4) Present equations appropriate for squall events that are based on a measurement program that was specifically designed to measure squall profiles and gusts. <p>Explanation: Extensive validation of differing wind relations against wind measurements in tropical cyclone events demonstrated that the ESDU relations as presented in the annex are a more appropriate basis for tropical cyclones than the Frøya-based relations (based on wind measurements made offshore Norway). A joint industry program developed specifically to examine wind profiles and gusts in offshore wind squalls recommended a new set of relations appropriate to that storm type.</p>

Clause/Subclause	Modifications
A.7.4 Wind Spectra	<p>This subclause recommended using the Frøya wind spectra for all storm types. This subclause now has three subsections:</p> <ul style="list-style-type: none"> • (A.7.4.1) Explains which relations are appropriate to which storm type. Clarifies that squalls are inherently transient phenomena more appropriately treated in the time domain than by a spectral representation. Adds a figure showing a comparison of extratropical and tropical storm wind spectra at two elevations for two representative wind speeds. • (A.7.4.2) Presents the Frøya equations as appropriate for extratropical storms. The text and equations in this subsection are unchanged from the original description except that the figure showing sample wind spectra is deleted in light of the figure added in A.7.4.1. • (A.7.4.3) Presents simplified ESDU spectra as appropriate from tropical cyclones.
	<p>Explanation: Comparison of the Frøya-based relations and ESDU wind spectra against measurements in tropical cyclone events demonstrated that the ESDU relations as presented in A.7.4.3 are a more appropriate basis for tropical cyclones than the Frøya-based relations (based on wind measurements made offshore Norway).</p>
Annex H	<p>Added regional annex for the US Gulf of Mexico.</p>
	<p>Explanation: ISO-19901-1:2015 does not have an annex for the US Gulf of Mexico. This annex has updated information relative to the First Edition of API 2MET.</p>
Annex I	<p>Added regional annex for the US Coast of California.</p>
	<p>Explanation: ISO-19901-1:2015 does not have an annex for the US Coast of California. This annex presents precisely the same information as the First Edition of API 2MET.</p>
Annex J	<p>Added regional annex for the Other US Waters.</p>
	<p>Explanation: ISO-19901-1:2015 does not have an annex for the Other US Waters (areas outside Gulf of Mexico and California offshore region). This annex presents precisely the same information as the First Edition of API 2MET.</p>

Bibliography

- [1] Shaw C.J., *Offshore Industry Requirements and Recent Metocean Technology Developments*, Proc. of the CLIMAR 99: WMO Workshop on Advances in Marine Climatology, Vancouver, September 1999, pp. 324–329
- [2] Tromans P.S. and Vanderschuren L., *Response Based Design Conditions in the North Sea: Application of a New Method*, Proc. of the 27th Offshore Technology Conference, OTC 7683, Houston, May 1995
- [3] Heideman J.C.H., Hagen O., Cooper C.K. and Dahl F.E., *Joint Probability of Extreme Waves and Currents*, J. Waterw., Port, Coast., Ocean Eng., 1989, 115, p. 534
- [4] Winterstein S.R., Ude T.C., Cornell C.A., Bjerager P. and Haver S., *Environmental Parameters for Extreme Response: Inverse FORM with Omission Factors*, Proc. of the 6th Intl. Conference on Structural Safety and Reliability, Innsbruck, August 1993
- [5] The International Association of Oil & Gas Producers ³, *HS&E Guidelines for Metocean and Arctic Surveys*, Report no. 447, October 2011
- [6] Cox A.T., et al., *Case Studies of Tropical to Extra-Tropical Cyclone Conversion in the Western North Atlantic: Wind Field Kinematics and Wave Response*, 7th Intl. Workshop on Wave Forecasting and Hindcasting, Banff, 2002
- [7] Forristall G.Z., *On the Use of Directional Wave Criteria*, J. Waterw., Port, Coast., Ocean Eng., 2004
- [8] Tucker M.J. and Pitt E.G., *Waves in Ocean Engineering*, Elsevier Ocean Engineering Book Series, Amsterdam, Vol. 5, 2001
- [9] Grant C.K. and Shaw C.J., *Operational Oceanographic Needs for the Oil and Gas Industry*, UNESCO Global Ocean Observing System (GOOS) Bulletin #1, March 2001
- [10] Barltrop N.D.P. (Ed.), *Floating Structures: A Guide for Design and Analysis*, Centre for Marine and Petroleum Technology (CMPT), OPL Pub. 101/98, Ledbury, 1998
- [11] John A., Woodworth P.L., Aarup T. and Wilson W.S. (Eds.), *Understanding Sea-level Rise and Variability Church*, 2010, Wiley-Blackwell, ISBN: 978-1-4443-3451-7
- [12] World Meteorological Organization ⁴, *Guide to Meteorological Instruments and Methods of Observation*, Publication WMO-No. 8, 7th Edition, 2008
- [13] Andersen O.J. and Løvseth J., *The Maritime Turbulent Wind Field*, Measurements and Models, Phase 2-Ext 1-Task 4, Extended Analyses of the Frøya Database, Final Report, December 1992
- [14] Coastal Engineering Research Center, *Shore Protection Manual*, US Army Corps of Engineers, Washington, DC, Vol. 1, 1984

³ International Association of Oil & Gas Producers (IOGP), City Tower, 40 Basinghall Street, 14th Floor, London, EC2V 5DE, United Kingdom.

⁴ World Meteorological Organization, 7bis, Avenue de la Paix, Case Postale 2300, CH-1211 Geneva 2, Switzerland.

- [15] Forristall G.Z. and Davies A.M. (Eds.), *Verification of a Soil-Wave Interaction Model in Modelling Marine Systems*, Vol. II, CRC Press, Florida, 1990
- [16] Bouws E.H., Gunther H., Rosenthal W. and Vincent C.L., *Similarity of the Wind Wave Spectrum for Finite Depth Water: Part 1 Spectral Form*, J. Geophys. Res., 1983, 90 (C1), pp. 975–986
- [17] Reece A.M. and Cardone V.J., *Test of Wave Hindcast Model Results against Measurements during Four Different Meteorological Systems*, Proc. of the 14th Offshore Technology Conference, OTC 4323, Houston, May 1982
- [18] *Recommended Standard for Wave Data Sampling and Near Real-Time Processing*, E & P Forum, Report 3.4/186, 1992
- [19] Goda Y., *Random Seas and Design of Maritime Structures*, University of Tokyo Press, Tokyo, 1985
- [20] Ochi M.K. and Hubble E.N., *Six-Parameter Wave Spectrum*, Coastal Engineering, Chapter 18, 1976, pp. 301–28
- [21] Torsethaugen K., *A Two Peak Wave Spectral Model*, Proceedings OMAE, Glasgow, 1993
- [22] Kirby J.T. and Chen T.S., *Surface Waves on Vertically Sheared Flows: Approximate Dispersion Relations*, J. Geophys. Res., 1989, January 15, 94 (no. C1), pp. 1013–1027
- [23] Haring R.E., Osborne A.R. and Spencer L.P., *Extreme Wave Parameters Based on Continental Shelf Storm Wave Records*, Coastal Engineering, Chapter 10, 1976, pp. 151–170
- [24] Fenton J.D., *A Fifth Order Stokes Theory for Steady Waves*, J. Waterw., Port, Coast., Ocean Eng., 1985, 1111, pp. 216–233
- [25] Chappellear J.E., *Direct Numerical Calculation of Wave Properties*, J. Geophys. Res., 1961, 66 (2)
- [26] Lambrakos K.F., *Extended Velocity Potential Wave Kinematics*, J. Waterw., Port, Coast., Ocean Div., Vol. 17, no. WW3, August 1981
- [27] Dean R.G., *Stream Function Representation of Non-linear Ocean Waves*, J. Geophys. Res., 1965, 70 (18), pp. 4561–4572
- [28] Tromans P.S., Anatürk A.R. and Hagemeijer P.M., *A New Model for the Kinematics of Large Ocean Waves—Application as a Design Wave*, 1st Intl. Offshore and Polar Engineering Conference, Edinburgh, International Society of Offshore and Polar Engineers, 1991
- [29] Rodenbusch G. and Forristall G.Z., *An Empirical Model for Random Directional Wave Kinematics Near the Free Surface*, Proc. of the 18th Offshore Technology Conference, OTC 5097, Houston, May 1986
- [30] Tucker M.J., *An Improved Battjes Method for Predicting the Probability of Extreme Waves*, Appl. Ocean Res., 1989, 4, pp. 212–213
- [31] Forristall G.Z., *On the Statistical Distribution of Wave Heights in a Storm*, J. Geophys. Res., May 1978, pp. 2353–2358

- [32] Longuet-Higgins M.S., *On the Statistical Distribution of the Heights of Sea Waves*, J. Mar. Res., 1952, 11, pp. 245–266
- [33] Krogstad H.E., Addendum to: *Height and Period Distributions of Extreme Waves*, Appl. Ocean Res., 1985, 7 (3), pp. 158–165
- [34] Bateman W.J.D., Swan C. and Taylor P.H., *On the Efficient Numerical Simulation of Directionally Spread Water Waves*, J. Comput. Phys., 2001, 174, pp. 277–305
- [35] Bateman W.J.D., Swan C. and Taylor P.H., *On the Calculation of the Water Particle Kinematics in a Directionally Spread Wave Field*, J. Comput. Phys., 2001, 186, pp. 70–92
- [36] Hague C.H. and Swan C., *A Multiple-Flux Boundary Element Method Applied to the Description of Water Surface Waves*, J. Comput. Phys., 2009, 228, pp. 5111–5128
- [37] Chalikov D. and Sheinin D., *Modelling of Extreme Waves Based on Equations of Potential Flow With a Free Surface*, J. Comput. Phys., 2005, 210, p. 247
- [38] Zakharov V.E., *Stability of Periodic Waves of Finite Amplitude on the Surface of a Deep Fluid*, J. App. Math. and Tech. Phys., 1968, 9, pp. 190–194
- [39] Krasitskii V.P., *On Reduced Equations in the Hamiltonian Theory of Weakly Non-linear Surface Waves*, J. Fluid Mech., 1994, 272, pp. 1–20
- [40] Zeitoun H., Tornes K., Oldfield S., Cumming G., Pearce A., Sabavala H., et al., *Effect of Applying 2nd Order Wave Theory on Pipeline Dynamic Response*, ASME Conf. Proc., 2010, 323, DOI: 10.1115/OMAE2010-20311
- [41] Forristall G.Z. and Ewans K.C., *World-Wide Measurements of Directional Wave Spreading*, J. Atmos. Ocean. Technol., 1998, 15, pp. 440–469
- [42] Forristall G.Z., *Wave Crest Distributions: Observations and Second Order Theory*, J. Phys. Oceanogr., 2000, August, 30, pp. 1931–1948
- [43] Forristall G.Z. and Cooper C.K., *Design Current Profiles Using Empirical Orthogonal Functions (EOF) and Inverse FORM Methods*, Proc. of the 29th Offshore Technology Conference, OTC 8267, Houston, May 1997
- [44] Dalrymple R.A. and Heideman J.C., *Non-linear Water Waves on a Vertically-Sheared Current*, E & P Forum Workshop on Wave and Current Kinematics and Loading, Paris, October 1989
- [45] Eastwood J.W. and Watson C.J.H., *Implications of Wave-Current Interactions for Offshore Design*, E & P Forum Workshop on Wave and Current Kinematics and Loading, Paris, October 1989
- [46] Wheeler J.D., *Method for Calculating Force Produced by Irregular Waves*, J. Pet. Technol., 1970, 22, pp. 473–486
- [47] *Appraisal of Marine Growth on Offshore Installations*, MTD Ltd. Publication, ISBN 1 870553 128, 1992
- [48] International Oceanographic Data and Information Exchange
- [49] Peters D.J., et al., *Modelling the North Sea through the North European Storm Study*, Proc. of the 25th Offshore Technology Conference, OTC 7130, Houston, May 1993

- [50] Reistad M. and Iden K.A., *Updating, Correction and Evaluation of a Hindcast Data Base of Air Pressure, Winds and Waves for the North Sea, Norwegian Sea and the Barents Sea*, Technical Report 9, Det Norske Meteorologiske Institut, Oslo, 1995
- [51] Fugro G.E.O.S., *Wind and Wave Frequency Distributions for Sites Around the British Isles*, Offshore Technology Report 2001/030, Health and Safety Executive, London, 2001
- [52] Grant C.K., et al., *Development of a New Metocean Design Basis for the NW Shelf of Europe*, Proc. of the 27th Offshore Technology Conference, OTC 7685, Houston, May 1995
- [53] Bomel Ltd., *Environmental Considerations*, Offshore Technology Report 2001/010, Health and Safety Executive, London, 2001
- [54] Norwegian Technology Centre, *Actions and Action Effects*, NORSO_K N-003, Revision 1, February 1999
- [55] Vefsnmo S., Mathiesen M. and Løvås S., *IDAP 90—Statistical Analysis of Sea Ice Data*, Norges H. Hydrodynamiske Laboratorier, Trondheim, 1990
- [56] Oceanweather Inc.⁵, *WANE: West Africa Normals and Extremes*
- [57] Fugro G.E.O.S., *West Africa Regional Environmental Study*, CD-ROM, UK Hydrographic Office, 2001
- [58] *Africa Pilot*, Vol. 1 and Vol. 2, Hydrographer of the Navy, Taunton, 1978
- [59] Cardone V.J., Cooper C.K. and Szabo D., *A Hindcast Study of the Extreme Wave Climate of Offshore West Africa (WAX)*, Proc. of the 27th Offshore Technology Conference, OTC 7687, Houston, May 1995
- [60] Cooper C.K., *Metocean Criteria for the Coast of W. Africa*, Chevron Petroleum Technology Report, February 1994
- [61] Evensen G.A., *Circulation Model for the West African Coast: Current Simulations for the WAX Project*, Nansen Environmental and Remote Sensing Center, Technical Report 154, 1998
- [62] *International Station Meteorological Climate Summary*, CD-ROM, Version 4, United States Federal Climate Complex, Asheville, 1996
- [63] Tsunami Database, United States National Oceanic and Atmospheric Administration, National Geophysical Data Center
- [64] Dowdy M.J., Hoyle M.J.R. and Stiff J.J., *Environmental Actions in the New ISO for the Site-Specific Assessment of Mobile Jack-up Units*, Offshore Technology Conference, OTC 23342, May 2012
- [65] National Data Buoy Center⁶
- [66] Oceanweather Inc., GUMSHOE: Gulf of Mexico Storm Hindcast of Oceanographic Extremes, 1990
- [67] Oceanweather Inc., WINX: Winter Extremes—Gulf of Mexico, 1992

⁵ Oceanweather Inc., 350 Bedford Street, Suite 404, Stamford, Connecticut 06901.

⁶ National Data Buoy Center, Bldg. 3205, Stennis Space Center, Mississippi 39529.

- [68] Oceanweather Inc., GOMOS: Gulf of Mexico Oceanographic Study, 2014
- [69] Nowlin W.D., Jochens A.E., Reid R.O. and Dimarco S.F., OCS Study MMS 98-0035 and MMS 98-0036, US Dept. of the Interior, Minerals Management Service, Gulf of Mexico OCS Regional Office, *Texas-Louisiana Shelf Circulation and Transport Process Study: Synthesis Report LATEX A*, Appendices, New Orleans, Vol. I and II, 1998, p. 492
- [70] Minerals Management Service, *Texas-Louisiana Shelf Circulation and Transport Processes Study*, CD-ROM NODC-88 through -92, Texas A&M University, Data and Reports, 1992–1994
- [71] Murray S.P., *An Observational Study of the Mississippi-Atchafalaya Coastal Plume*, OCS Study MMS 98-0040, US Dept. of the Interior, Minerals Management Service, New Orleans, 1997
- [72] Science Applications International Corporation ⁷, *Gulf of Mexico Physical Oceanography Program, Final Report: Year 5*, Vol. II: Technical Report, 1989, OCS Study MMS-89-0068, US Dept. of the Interior, Minerals Management Service, Gulf of Mexico OCS Regional Office, New Orleans, p. 333
- [73] Nowlin W.D. Jr., Jochens A.E., DiMarco S.F., Reid R.O. and Howard M.K., *Deep Water Physical Oceanography Reanalysis and Synthesis of Historical Data: Synthesis Report*, OCS Study MMS 2001-064, US Dept. of the Interior, Minerals Management Service, Gulf of Mexico OCS Regional Office, New Orleans, p. 528
- [74] Cooper C., Forristall G., Hamilton P. and Ebbesmeyer C., *Utilisation of Offshore Oil Platforms for Meteorological and Oceanographic Measurements*, Mar. Technol. Soc. J., 1993, 27 (2) pp. 10–23
- [75] Fugro GEOS, Technical Reference: Gulf of Mexico, 2003
- [76] Rosendal H.E., *Northers of the Gulf of Mexico and Central American Waters*, Internet Document from Mariners Weather Log, 1965
- [77] Teague W.J., Hwang P.A., Jacobs G.A., et al., *A Three-Year Climatology of Waves and Winds in the Gulf of Mexico*, Naval Research Laboratory Report No. NRL/MR/7332-97-8068, 1997
- [78] Met Office ⁸, *Meteorology for Mariners*, 1990
- [79] Vukovich F.M., *An Updated Evaluation of the Loop Current's Eddy-Shedding Frequency*, J. Geophys. Res., 1995, 100 (C5), pp. 8655–8659
- [80] Nowlin W.D., Reid R.O., et al., *Overview of Classes of Currents in the Deep Water Region of the Gulf of Mexico*, Proc. of the 34th Offshore Technology Conference, OTC 12991, Houston, May 2001
- [81] World Ocean Database
- [82] Bureau of Ocean Energy Management (formerly Bureau of Ocean Energy Management, Regulation, and Enforcement) ⁹

⁷ Science Applications International Corporation (SAIC), 12010 Sunset Hills Road Reston, Virginia 20190.

⁸ Met Office, FitzRoy Road, Exeter, Devon, EX1 3PB, United Kingdom.

⁹ Bureau of Ocean Energy Management (formerly Bureau of Ocean Energy Management, Regulation, and Enforcement), 1849 C Street, NW, Washington, DC 20240.

- [83] National Oceanic and Atmospheric Administration¹⁰, *A Climatology and Oceanographic Analysis of the California Pacific Outer Continental Shelf Region*, US Dept. of Commerce, Washington, DC, 1981
- [84] Minerals Management Service, *Southern California Bight Physical Oceanography*, Proc. of a Workshop, OCS Study MMS 91-0033, US Dept. of the Interior, Washington, DC, 1991
- [85] Scripps Institution of Oceanography¹¹, *Analysis and Acquisition of Observations of the Circulation on the California Continental Shelf*, Minutes of the Quality Review Board, Meeting 4, Dec. Centre for Coastal Studies, La Jolla, 1994
- [86] Scripps Institution of Oceanography, Coastal Data Information Program, SIO Ref. 91-32, La Jolla, 1992
- [87] Harms S. and Winant C.D., *Characteristic Patterns of the Circulation in the Santa Barbara Channel*, J. Geophys. Res., 2/1998
- [88] Dever E.P., Hendershott M.C. and Winant C.D., *Statistical Aspects of Surface Drifter Observations of Circulation in the Santa Barbara Channel*, J. Geophys. Res., 2/1998
- [89] Winant C.D., Alden D.J., Edwards K.A. and Hendershott M.C., *Near-Surface Trajectories off Central and Southern California*, J. Geophys. Res., 7/1999
- [90] Dorman C.E. and Winant C.D., *The Structure and Variability of the Marine Atmosphere Around the Santa Barbara Channel*, Monthly Weather Review, 2/2000
- [91] Dever R.P. and Winant C.D., *The Evolution and Depth Structure of Shelf and Slope Temperatures and Velocities during the 1997–1998 El Niño near Point Conception, California*, J. Geophys. Res., 2002, 54, pp. 77–103
- [92] Winant C.D., Dever E.P. and Hendershott M.C., *Characteristic Patterns of Shelf Circulation at the Boundary between Central and Southern California*, J. Geophys. Res., 2003, 108 (C2), p. 3021, DOI: 10.1029/2001JC001302
- [93] Minerals Management Service, Pacific OCS Region, *Delineation Drilling Activities in Federal Waters Offshore Santa Barbara County, California*, US Dept. of the Interior, Camarillo, 2001
- [94] Swail V.R., Ceccacci E.A. and Cox A.T., *The AES40 North Atlantic Wave Reanalysis; Validation and Climate Assessment*, 6th Int. Workshop on Wave Hindcasting and Forecasting, Monterey, November 6–10, 2000
- [95] PanCanadian Energy¹², *Cohasset/Panuke Development Project—Environmental Assessment*, Section 6&8, 1990
- [96] PanCanadian Energy, *Deep Panuke Offshore Gas Development—Environmental Impact Statement*, Vol. 4, 2002

¹⁰ National Oceanic and Atmospheric Administration, 1401 Constitution Avenue NW, Room 5128, Washington, DC 20230.

¹¹ Scripps Institution of Oceanography, 9500 Gilman Drive, La Jolla, California 92093.

¹² PanCanadian Energy Corporation (now Encana), 500 Centre Street SE, PO Box 2850, Calgary, T2P 2S5, Canada.

- [97] MacLaren Plansearch Limited, *Sable Offshore Energy Project—Environmental Impact Statement*, Vol. 3, Sable Offshore Energy Project, 1996
- [98] World Meteorological Organization, *Sea Ice Nomenclature*, Publication 259, Geneva
- [99] Canadian Ice Service ¹³, *Sea Ice Climatic Atlas, East Coast of Canada, 1971–2000*, 2001
- [100] Markham W.E., *Ice Atlas, Eastern Canadian Seaboard*, Atmospheric Environment Service, Cat. No. EN56-55, 1981 E, 1980
- [101] Petro-Canada ¹⁴, *Development Application for Terra Nova Development—Environmental Impact Statement*, 1996
- [102] Campbell, *Modifications to the Grand Banks Scour Catalogue (GBSC) 1999–2004*, Canadian Seabed Research Ltd. for the Geological Survey of Canada Atlantic, 2004
- [103] Forristall G.Z., *Wave Crest Heights and Deck Damage in Hurricanes Ivan, Rita and Katrina*, OTC 18620, Proc. of the 2007 Offshore Technology Conference, Houston, May 2007
- [104] National Hurricane Center Archives
- [105] Hansen J., Resio D., Smith J. and Wallace R., *MORPHOS: Advancing Coastal Process Research and Modeling*, 10th Int. Workshop on Wave Hindcasting and Forecasting and Coastal Hazard Symposium, Oahu, November 2007
- [106] Minerals Management Service, Technology Assessment and Research Program, Projects 193, 467, and 580
- [107] Forristall Ocean Engineering, *Gulf Eddy Model—GEM 4.1*, Proprietary Report to CASE-EJIP Members, June 2007
- [108] Horizon Marine, Inc. ¹⁵, EddyWatch Program Gulf of Mexico
- [109] Minerals Management Service, Gulf of Mexico Region Environmental Studies Program
- [110] DeepStar ¹⁶, Technology Development for Deepwater Research
- [111] Research Partnership to Secure Energy for America (RPSEA) ¹⁷, Ultra-Deepwater Program
- [112] Knabb R.D., Rhome J.R. and Brown D.P., *Tropical Cyclone Report: Hurricane Katrina, 23–30 August 2005*, Report by the National Hurricane Center, August 10, 2006

¹³ Canadian Ice Service.

¹⁴ Petro-Canada Lubricants Inc., 2310 Lakeshore Road West, Mississauga, Ontario, L5J 1K2, Canada.

¹⁵ Horizon Marine, Inc. (now Woods Hole Group, Inc.), 107 Waterhouse Road, Bourne, Massachusetts 02532.

¹⁶ DeepStar, 1201 Lake Robbins Drive, United States Allison Tower Suite 9051, The Woodlands, Texas 77380.

¹⁷ Research Partnership to Secure Energy for America (RPSEA), 2211 Norfolk Street, Suite 410, Houston, Texas 77098.

- [113] Lott N., *The Big One! A Review of the March 12–14, 1993 “Storm of the Century,”* Technical Report 93-01, National Climate Data Center, Research Customer Service Group, May 14, 1993
- [114] Cooper C.K., Stear J.D., Mitchell D.A., Wang W., Driver D.B., Heideman J., et al., *Development of Gulf of Mexico Deepwater Currents for Reference by API Recommended Practices*, OMA E2007-29588, Proc. of the 26th Int. Conference on Offshore Mechanics and Arctic Engineering, San Diego, June 2007
- [115] Cornell A., *Reliability of Marine Structures Program*, Stanford University, 1994–1996
- [116] Accurate Environmental Forecasting, Inc., *Ocean Response to Hurricanes in Presence of the Loop Current, Final Report, Part 1: Hurricane-generated Currents*, Proprietary Report to CASE-EJIP Members, April 2007
- [117] Accurate Environmental Forecasting, Inc., *Ocean Response to Hurricanes in Presence of the Loop Current, Final Report, Part 2: Hurricane-generated Waves*, Proprietary Report to CASE-EJIP Members, April 2007
- [118] National Oceanic and Atmospheric Administration, National Weather Service Environment Modeling Center, NOAA WaveWatch III
- [119] Cooper C., Stear J., Frolov S., Gordon L., Jeans G., Symonds D., et al., *The Case Against Severe Cold Eddies*, OTC 19618, Proc. of the Offshore Technology Conference, Houston, May 2008
- [120] Berek E.P., *Deepwater Gulf of Mexico Metocean Extremes*, Report to ABS Consulting as Part of MODU JIP, ABSC/1514096/GB-01, December 2006
- [121] Berek E.P., Cooper C.K., Driver D.B., Heideman J.C., Mitchell D.A., Stear J.D., et al., *Development of Revised Gulf of Mexico Metocean Hurricane Conditions for Reference by API Recommended Practices*, OTC 18903, Proc. of the 2007 Offshore Technology Conference, May 2007
- [122] Cooper C.K., *A Preliminary Case for the Existence of Hurricane Alleys in the Gulf of Mexico*, OTC 6831, 1992
- [123] Cooper C.K., Stear J., Heideman J., Santala M., Forristall G., Driver D., et al., *Implications of Hurricane Ivan on Deepwater Gulf of Mexico Metocean Design Criteria*, OTC 17740, Proc. of the 2005 Offshore Technology Conference, Houston, May 2005
- [124] Chouinard L.E., Liu C. and Cooper C.K., *Model for Severity of Hurricanes in Gulf of Mexico*, J. Waterw., Port, Coast., Ocean Eng., 1997 May/June
- [125] Shay L.K., Goni G.J. and Black P.G., *Effects of a Warm Oceanic Feature on Hurricane Opal*, *Monthly Weather Review*, American Meteorological Society, Vol. 128, 2000
- [126] Cooper C.K. and Stear J.D., *Hurricane Climate in the Gulf of Mexico*, OTC 18418, Proc. of the 2006 Offshore Technology Conference, Houston, May 2006
- [127] Landsea C.W., Anderson C., Charles N., Clark G., Dunion J., Fernandez-Partagas J., et al., The Atlantic Hurricane Database Re-analysis Project: Documentation for 1851–1910 Alterations and Additions to the HURDAT Database, *Hurricanes and Typhoons, Past, Present and Future*, Murnane R. J. and Liu K.B. (Eds.), Columbia Press, 2004

- [128] Haring R.E. and Heideman J.C., *Gulf of Mexico Rare Return Periods*, OTC 3230, Proc. of the 10th Annual Offshore Technology Conference, Houston, May 1978
- [129] Heideman J.C. and Mitchell D.A., *Grid Point Pooling in Extreme Value Analysis of Hurricane Hindcast Data*, J. Waterw., Port, Coast., Ocean Eng., February 2007
- [130] Heideman J.C. and George R.Y., *Biological and Engineering Parameters for Macrofouling Growth on Platforms Offshore Louisiana*, IEEE Conference, MIT, 1981
- [131] Toro G.R., Cornell C.A., Cardone V.J. and Driver D., *Comparison of Historical and Deductive Methods for the Calculation of Low-Probability Seastates in the Gulf of Mexico*, OMAE 2004–51634, 2004
- [132] Ward E.G., Borgman L.E., and Cardone V.J., *Statistics of Hurricane Waves in the Gulf of Mexico*, OTC 3229, Proc. of the 10th Annual Offshore Technology Conference, Houston, May 1978
- [133] Pielke R.A. Jr., Landsea C., Mayfield M., Laver J. and Pasch R., *Hurricanes and Global Warming*, Bull. Am. Meteorol. Soc., November 2005
- [134] Webster P.J., Holland G.J., Curry J.A. and Chang H.R., *Changes in Tropical Cyclone Number, Duration, and Intensity in a Warming Environment*, Science 2005 (September), p. 16
- [135] Jacob S.D. and Shay L.K., *The Role of Oceanic Mesoscale Features on the Tropical Cyclone-Induced Mixed Layer Response: A Case Study*, J. Phys. Oceanogr., 2003, Vol. 33, Issue 4
- [136] Cooper C. and Stear J., *Estimating Design Currents During Joint Eddy-TRWs and Joint Eddy-Hurricanes*, OTC 19985, Proc. of the 2009 Offshore Technology Conference, Houston, May 2009
- [137] Forristall Ocean Engineering¹⁸, *Development of Synthetic Time Series for the Loop Current and Associated Eddies, Phase 1: Isolated Eddy Simulations*, Report to CASE-EJIP, February 2008
- [138] Applied Research Associates¹⁹, *A Synthetic Cyclone Track and Intensity Model for the Gulf of Mexico Region*, Report to API, ARA Final Report 18736, May 2009
- [139] Marine Advisors, Inc., *Group Oceanographic Survey—Gulf of Alaska*, 1970
- [140] Intersea Research Corporation, *Gulf of Alaska Wave and Wind Measurement Program*, 1974–1976
- [141] Intersea Research Corporation, *A Data Collection, Analysis and Simulation Program to Investigate Ocean Currents, North-East Gulf of Alaska*, 1975
- [142] Brower W.A., et al., *Climate Atlas of the Outer Continental Shelf Waters and Coastal Regions of Alaska, Vol. I, Gulf of Alaska*, National Oceanic and Atmospheric Administration, 1977
- [143] Intersea Research Corporation, *Gulf of Alaska Hindcast Evaluation*, 1975–1976

¹⁸ Forristall Ocean Engineering, 101 Chestnut Street, Camden, Maine 04843.

¹⁹ Applied Research Associates, 4300 San Mateo Blvd. NE, Suite A-220, Albuquerque, New Mexico 87110.

- [144] Evans-Hamilton, Inc., *A Meteorological and Oceanographic Study of Extreme and Operational Criteria in Lower Cook Inlet*, 1977
- [145] Intersea Research Corporation, *Oceanographic Conditions and Extreme Factors in Lower Cook Inlet*, Alaska, 1976
- [146] Intersea Research Corporation, *Oceanographic Conditions for Offshore Operations in Lower Cook Inlet*, Alaska, 1975
- [147] Brower W.A., et al., *Climatic Atlas of the Outer Continental Shelf Waters and Coastal Regions of Alaska*, Vol. II, Bering Sea, National Oceanic and Atmospheric Administration, 1977
- [148] Oceanweather Inc., *Bering Sea Phase 1 Oceanographic Study—Bering Sea Storm Specification Study*, 1980
- [149] Brown and Caldwell, *Bering Sea Comprehensive Oceanographic Measurement Program*, 1981–1983
- [150] Intersea Research Corporation, *Bering Sea Oceanographic Measurement Program*, 1976–1978
- [151] Ocean Science and Engineering, Inc., *Bristol Bay*, Environ. Rep., 1970
- [152] Oceanweather Inc., *St. George Basin Extreme Wave Climate Study*, 1983
- [153] Brower W.A., et al., *Climate Atlas of the Outer Continental Shelf Waters and Coastal Regions of Alaska*, Vol. III, Chukchi-Beaufort Seas, National Oceanic and Atmospheric Administration, 1977
- [154] Oceanweather Inc., *Beaufort Sea Wave Hindcast Study: Prudoe Bay/Sag Delta and Harrison Bay*, 1982
- [155] Ward E.G. and Reece A.M., *Arctic Development Project, Task 1/10, Part I, Meteorological and Oceanographic Conditions, Part II, Summary of Beaufort Sea Storm Wave Study*, Shell Development Company, 1979
- [156] Ocean Science and Engineering, Inc., *Reconnaissance Environmental Study of Chukchi Sea*, 1970
- [157] Exxon Company, *Alaska Beaufort Sea Gravel Island Design*, 1979
- [158] Oceanographic Services Inc., *Beaufort Sea Summer Oceanographic Measurement Programs*, 1979–1983
- [159] Evans-Hamilton, Inc., *A Preliminary Environmental Study for the East Coast of the United States*, 1976
- [160] Ward E.G., Evans D.J. and Pompa J.A., *Extreme Wave Heights along the Atlantic Coast of the United States*, OTC 2846, Proc. of the 1977 Offshore Technology Conference, Houston, May 1977
- [161] Science Applications, Inc., *Characterization of Currents over Chevron Tract #510 off Cape Hatteras, North Carolina*, 1982
- [162] Evans-Hamilton, Inc., *An Interpretation of Measured Gulf Stream Current Velocities off Cape Hatteras, North Carolina*, 1982

- [163] Oceanweather Inc., *Final Report—Manteo Block 510 Hurricane Hindcast Study*, 1983
- [164] *Atlas of Tidal Currents, St. Lawrence Estuary from Cap Bon-Désir to Trois-Rivières*, Catalogue No. Fs 72-33/1997, Minister of Fisheries and Oceans, Canada, 1997
- [165] Burns B.M., *The Climate of the Mackenzie Valley—Beaufort Sea*, 1973, Vol. 1, Climatological Studies Number 25, Environment Canada, p. 239
- [166] Canadian Ice Service, *Sea Ice Climatic Atlas, East Coast of Canada 1971–2000*, Report GB2429.S42, Environment Canada, 2001, pp vi+189
- [167] Canadian Ice Centre, *Ice Thickness Climatology, 1961–1990 Normals, Report: Ice 2–91*, Environment Canada, 1992
- [168] Campbell, *Modifications to the Grand Banks Scour Catalogue (GBSC) 1999–2004*, Contract Report and Database Prepared by Canadian Seabed Research Ltd. for the Geological Survey of Canada, Atlantic, 2004, p. 15
- [169] Canadian Ice Service, *Sea Ice Climatic Atlas, East Coast of Canada, 1981–2010*, Environment Canada
- [170] *Cohasset/Panuke Development Project—Environmental Assessment*, Sections 6&8, PanCanadian Energy for the Cohasset/Panuke Development Project, 1990
- [171] *Deep Panuke Offshore Gas Development—Environmental Impact Statement*, PanCanadian Energy for the Deep Panuke Offshore Gas Development, Vol. 4, 2002
- [172] Devon Energy Corporation²⁰, *Devon Canada Corporation Beaufort Sea Exploration Drilling Program Baseline Reports*, Devon Canada Corp., Beaufort Sea Drilling Program, Calgary, 2004
- [173] *Environmental Impact Statement (EIS), Beaufort Sea—Mackenzie Delta*, Vol. 3a, Beaufort Sea—Delta Setting, Dome Petroleum, Esso Resources Canada Ltd. and Gulf Canada Resources Inc., Calgary, 1982
- [174] Fissel D.B., *On the Ocean Current Measurements at Offshore Drill Sites in the SE Beaufort Sea, 1976 to 1979*, Report to Dome Petroleum, Arctic Sciences, Ltd., Sidney, 1981
- [175] Gregory D.N., Nadeau O.C. and Lefavre D., *Current Statistics of the Gulf St. Lawrence and Estuary*, Canadian Technical Report of Hydrography and Ocean Sciences, No. 120, November 1989, p. 178
- [176] *2003 Ice Season Report for the Grand Banks of Newfoundland*, Prepared by Provincial Airlines Environmental Services Ltd. for Petro-Canada as Operator of the Terra Nova Project, 2003
- [177] Lewis C.F.M. and Blasco S.M., *Character and Distribution of Sea-Ice and Iceberg Scours*, Workshop on Ice Scouring and the Design of Offshore Pipelines, Calgary, 1990, pp. 57–102
- [178] Markham W.E., *Ice Atlas, Eastern Canadian Seaboard*, Atmospheric Environment Service, Cat. No. EN56-55/1981 E, 1980, p. 66

²⁰ Devon Energy Corporation, 333 West Sheridan Avenue, Oklahoma City, Oklahoma 73102.

- [179] McNeill M. and Garrett J.R., *Open Water Surface Currents*, Beaufort Sea Project Technical Report 17, Institute of Ocean Sciences, Patricia Bay, Sidney, 1975
- [180] Newton J.L., *The Canada Basin: Mean Circulation and Intermediate Scale Flow Features*, Ph.D. Thesis, University of Washington, Seattle, 1973
- [181] *Monthly Wind and Wave Extreme Estimates for Flemish Pass*, Contract Report Prepared by Oceans Ltd. for Terra Nova, March, 2001
- [182] O'Connor M.J., *Development of a Proposed Model to Account for the Surficial Geology of the South-eastern Beaufort Sea*, Geological Survey of Canada Contract Report OSC 79-000212, 1980
- [183] Provincial Airlines "Bay Nord Ice Environment," Contract Report Prepared for Petro-Canada, March 2001
- [184] Saucier F.J., Chassé J., Couture M., D'Astous A., Dorais R., Lefaivre D., et al., *The Making of a Surface Current Atlas of the St. Lawrence*, Wessex Institute of Technology, Proc. of the Conference on Coastal Engineering, 1999, Lemnos, J. Computational Mechanics, 1999, pp. 87–97
- [185] *Sable Offshore Energy Project—Environmental Impact Statement*, Vol. 3, Prepared for the Sable Offshore Energy Project (SOEP) by MacLaren Plansearch Ltd., 1996
- [186] Spedding L.G., *Statistics of Beaufort Sea Summer Ice Cover for Ice/Structure Interaction Collision Assessment*, Esso Resources Internal Report IPRT-2ME-78, Calgary, 1978
- [187] Swail V.R., Ceccacci E.A. and Cox A.T., *The AES40 North Atlantic Wave Reanalysis; Validation and Climate Assessment*, 6th Int. Workshop on Wave Hindcasting and Forecasting, Monterey, November 6–10, 2000
- [188] *Development Application for Terra Nova Development—Environmental Impact Statement*, Prepared by Petro-Canada on behalf of the Terra Nova Proponents, 1996
- [189] Timco G.W. and Burden R.P., *An Analysis of the Shapes of Sea Ice Ridges*, Cold Reg. Sci. Technol., 1997, 25, pp. 65–77
- [190] Xu Z., Saucier F.J. and Lefaivre D., *Water Level Variations in the Estuary and Gulf of St. Lawrence*, 2006
- [191] Milne A.R. and Childerhouse R.J. (Eds.), *Oil, Ice and Climate Change: The Beaufort Sea and the Search for Oil*, Beaufort Sea Project, Department of Fisheries and Oceans, Canada, 1977, p. 103 (Beaufort Sea Project Overview Report Series)
- [192] Wadhams P. and Horne R.T., *An Analysis of the Ice Profiles obtained by Submarine Sonar in the AIDJEX Area of the Beaufort Sea*, SPRI Tech. Report 78-1, 1978
- [193] Oceanweather Inc., *Sakhalin Island Meteorological and Oceanographic Study Update (SIMOS-3)*, July 2004 (Joint Industry Project, Participants: BP, ExxonMobil, and Shell)
- [194] Shevchenko G.V., Rabinovich A.B. and Thomson R.E., *Sea-Ice Drift on the North-Eastern Shelf of Sakhalin Island*, J. Phys. Oceanogr., 2004, 34, pp. 2470–2491

- [195] Kowalik Z. and Polyakov I., *Tides in the Sea of Okhotsk*, J. Phys. Oceanogr., 1998, 28, pp. 1389–1409
- [196] Mizuta G., Fukamachi Y., Ohshima I.K. and Wakatsuchi M., *Structure and Seasonal Variability of the East Sakhalin Current*, J. Phys. Oceanogr., 2003, 33, pp. 2430–2445
- [197] Kowalik Z. and Polyakov I., *Diurnal Tides over Kashevarov Bank, Okhotsk Sea*, J. Geophys. Res., 1999, 104, pp. 5361–5380
- [198] Parkinson C.L. and Gratz A.J., *On the Seasonal Ice Cover of the Sea of Okhotsk*, J. Geophys. Res., 1983, 88, pp. 2793–2802
- [199] Yakunin L.P., *Hydrometeorology and Hydrochemistry of Seas*, Vol. IX, Okhotsk Sea, Issue 1, Hydrology, St. Petersburg, Chapter 9.3, 1998
- [200] Yakunin L.P., *Atlas of Edges of Large Forms of Ice in the Far Eastern Seas*, Russian Academy of Sciences, Far East Department, Pacific Institute of Oceanology, Vladivostok, 1995
- [201] Marko J.R., *Observations and Analysis of an Intense Waves-In-Ice Event in the Sea of Okhotsk*, J. Geophys. Res., 2003, 108, pp. 3296–3309
- [202] Caspian Environment Programme, Baku, Azerbaijan, 1999–2002
- [203] Federal Emergency Management Agency²¹, *Coastal Flooding Hurricane Storm Surge Model: Methodology*, Vol. 1, Federal Insurance Administration, Washington, DC, August 1988
- [204] Cooper C.K., *Estimates of Storm Surge and Associated Dike Design Levels*, Proprietary Report, Chevron Petroleum Technology Company, September 1994
- [205] Cooper C.K. and Thompson J.D., *Hurricane-Generated Currents on the Outer Continental Shelf, 1. Model Formulation and Verification*, J. Geophys. Res., 1989, 94 (No. C9)
- [206] *Hydrometeorology and Hydrochemistry of the Seas*, Vol. IV: Caspian Sea, Edition 1: Hydrometeorological Conditions, Gidrometeoizdat, St. Petersburg, 1992
- [207] Kantha L.H. and Clayson C.A., *An Improved Mixed-Layer Model for Geophysical Applications*, J. Geophys. Res., 1994, 99 (No. C12)
- [208] Kosarev A.N. and Yablonskaya E.A., *The Caspian Sea*, SPB Academic Publishing, the Hague, 1994
- [209] Atlas M, In: *Atlas of the Seas of the World*, Denim L.A. (Ed.), Moscow, 1950
- [210] Oceanweather Inc., *Caspian Sea Meteorological and Oceanographic Study (CASMOS)*, December 2002
- [211] Schwab D.J. and Muhr G.C., *Caspian Sea Project Report*, Great Lakes Environmental Research Laboratory, National Oceanic and Atmospheric Administration, US Department of Commerce, Ann Arbor, December 1989

²¹ Federal Emergency Management Agency, 500 C Street SW, Washington, DC 20472.

- [212] Sovintervod, *The Caspian Sea: Natural Environment, Forecast of Level Fluctuations and Surge Phenomena*, Proprietary Report to CPTC, 1993
- [213] Woodward-Clyde, *Environmental Issues in the AIOC Contract Area*, Literature Review, 1995
- [214] Zenkevitch L., *Biology of the Seas of the USSR*, The Caspian Sea, Chapter 11, Wiley and Sons, New York, 1963
- [215] Graham C., Cardone V.J., Ceccacci E.A., Parsons M.J., Cooper C. and Stear J., *Challenges to Wave Hindcasting in the Caspian Sea*, 7th Int. Workshop on Wave Hindcasting and Forecasting, Banff, October 21–25, 2002
- [216] Kara B., Wallcraft A. and Metzger J., *HYCOM Caspian Sea Modeling. Part I: An Overview of the Model and Coastal Upwelling*, Naval Research Laboratory, Stennis Space Center, United States, and Gunduz M., Institute of Marine Sciences, Erdemli, Icel, April 2007
- [217] Kravets L.M., *Sea Ice Conditions in the Caspian Sea during Severe Winters and Their Influence on Fleet Operations*, *Problems of the Arctic and Antarctic*, 1977, 50, pp. 136–137
- [218] Energy Information Administration, *Caspian Sea Region*, US Department of Energy, 2001 [online]
- [219] *The Azerbaijan International Operating Company (AIOC)*, Azerbaijan International, 1995 [online]
- [220] Eni (2008), *Eni in Kazakhstan* [online], EniComunicazione, Italy
- [221] Ochi M., Hatanaka M., Oikawa N. and Hoshi T., *Generation of Bathymetric Map in the North Caspian Sea Using Multi-Temporal Satellite Images*, 1998 [online], Republic of Kazakhstan, GIS Development, Noida, India
- [222] Geology Institute of the Azerbaijan National Academy of Sciences, *The Caspian Sea*, 1999 [online], Penki Kontinentai, Baku, Azerbaijan
- [223] Evers K., Spring W., Foulkes K., Kuehnlein W. and Jochmann P., *Ice Model Testing of an Exploration Platform for Shallow Waters in the Caspian Sea*, 16th POAC Conference, Ottawa, 2001
- [224] Dotsenko S.F., Kuzin I.P., Levin B.V. and Solovieva O.N., *Tsunamis in the Caspian Sea: Historical Events, Regional Seismicity and Numerical Modelling*, September 2002
- [225] Arpe K., Bengtsson L., Golitsyn G.S., Mokhov I.I., Semenov V.A. and Sporyshev P.V., *Connection between Caspian Sea Level Variability and ENSO*, *Geophys. Res. Lett.*, 2000, 27, pp. 2693–2696
- [226] Dotsenko S.F., Kuzin I.P., Levin B.V. and Solovieva O.N., *Tsunamis in the Caspian Sea: Historical Events, Regional Seismicity and Numerical Modeling*, September 2002
- [227] US Naval Research Laboratory, HYCOM Caspian Sea Model, 2007
- [228] CASPINFO, *Caspian Sea Facts*, 2007
- [229] Oceanweather Inc., *Final Report: Caspian Sea Meteorological and Oceanographic Hindcast Study 2 (CASMOS-2)*, June 2007
- [230] Fissel D.B., Martínez de Saavedra Álvarez M., Ross E., Marko J.R. and Slonimer A., *Long Term Changes in Metocean-Ice Conditions in the Canadian Beaufort Sea*, Proc. of the Annual Meeting of the International Society of Offshore and Polar Engineers, Anchorage, June 2013, p. 8

- [231] Swail V.R., Cardone V.J., Ferguson M., Gummer D.J., Harris E.L., Orelup E.A., et al., *The MSC50 Wind and Wave Reanalysis*, Proc. of the 9th Int. Workshop on Wave Hindcasting and Forecasting, September 24–29, 2006, Victoria, JCOMM-TR-034, WMO/TD-NO.1368, World Meteorological Organization, Geneva
- [232] Timco G.W. and Frederking R., *Overview of Historical Canadian Beaufort Sea Information*, NRC Canadian Hydraulics Centre Technical Report CHC-TR-057, 2009, p. 99
- [233] Swail V.R., Cardone V.J., Ferguson M., Gummer D.J. and Cox A.T., *The MSC Beaufort Sea Wind and Wave Reanalysis*, Proc. of the 10th Int. Workshop on Wave Hindcasting and Forecasting and Coastal Hazards Symposium, November 11–16, 2007, Oahu, JCOMM-TR-044, WMO/TD-No.1442, World Meteorological Organization, Geneva
- [234] Vickery P.J., *Analysis of Hurricane Winds*, OTC 25244, Proc. of the 2014 Offshore Technology Conference, Houston, May 2014
- [235] Vickery P.J., *Analysis of the Characteristics of Hurricane and Non-Hurricane Marine Winds for the Development of Design Standard Recommendations for Modeling the Near Surface Marine Atmospheric Boundary Layer*, Final Report Version 1.0 Submitted to Participants of the DeepStar JIP by Applied Research Associates, Inc., June 2015
- [236] Santala M.J., Calverley M., Taws S., Grant H., Watson A. and Jeans G., *Squall Wind Elevation/Gust Factors and Squall Coherence*, OTC 25249, Proc. of the 2014 Offshore Technology Conference, Houston, May 2014
- [237] Jeans G., Cooper C. and Yetsko C., *New Squall Wind Criteria for the Gulf of Mexico*, OTC 27204, Proc. of the 2016 Offshore Technology Conference, Houston, May 2016
- [238] Santala M.J., *Resolving the API RP 2MET “Crest Conundrum” for Wave-in-Deck Loading*, OTC 27640, Proc. of the 2017 Offshore Technology Conference, Houston, May 2017
- [239] API Recommended Practice 2A-WSD, *Planning, Designing, and Constructing Fixed Offshore Platforms—Working Stress Design*
- [240] API Recommended Practice 2SIM, *Structural Integrity Management of Fixed Offshore Structures*
- [241] API Recommended Practice 2SK, *Design and Analysis of Stationkeeping Systems for Floating Structures*



AMERICAN PETROLEUM INSTITUTE

200 Massachusetts Avenue, NW
Suite 1100
Washington, DC 20001-5571
USA

202-682-8000

Additional copies are available online at www.api.org/pubs

Phone Orders: 1-800-854-7179 (Toll-free in the U.S. and Canada)
303-397-7956 (Local and International)
Fax Orders: 303-397-2740

Information about API publications, programs and services is available
on the web at www.api.org.

Product No. GG2MET02